ANL-75-75

ANL-75-75

INL Technical Library
072272

PLEASE RETURN TO
MFC BRANCH LIBRARY

PHYSICS DIVISION

ANNUAL REVIEW

1 April 1974—31 March 1975

U of C-AUA-USERDA

ARGONNE NATIONAL LABORATORY, ARGONNE, ILLINOIS

Prepared for the U. S. ENERGY RESEARCH
AND DEVELOPMENT ADMINISTRATION
under Contract W-31-109-Eng-38

The facilities of Argonne National Laboratory are owned by the United States Government. Under the terms of a contract (W-31-109-Eng-38) between the U. S. Energy Research and Development Administration, Argonne Universities Association and The University of Chicago, the University employs the staff and operates the Laboratory in accordance with policies and programs formulated, approved and reviewed by the Association.

MEMBERS OF ARGONNE UNIVERSITIES ASSOCIATION

The University of Arizona
Carnegie-Mellon University
Case Western Reserve University
The University of Chicago
University of Cincinnati
Illinois Institute of Technology
University of Illinois
Indiana University
Iowa State University
The University of Iowa
Kansas State University
The University of Kansas
Loyola University
Marquette University
Michigan State University
The University of Michigan
University of Minnesota
University of Missouri
Northwestern University
University of Notre Dame
The Ohio State University
Ohio University
The Pennsylvania State University
Purdue University
Saint Louis University
Southern Illinois University
The University of Texas at Austin
Washington University
Wayne State University
The University of Wisconsin

NOTICE

This report was prepared as an account of work sponsored by the United States Government. Neither the United States nor the United States Energy Research and Development Administration, nor any of their employees, nor any of their contractors, subcontractors, or their employees, makes any warranty, express or implied, or assumes any legal liability or responsibility for the accuracy, completeness or usefulness of any information, apparatus, product or process disclosed, or represents that its use would not infringe privately-owned rights. Mention of commercial products, their manufacturers, or their suppliers in this publication does not imply or connote approval or disapproval of the product by Argonne National Laboratory or the U. S. Energy Research and Development Administration.

Printed in the United States of America
Available from
National Technical Information Service
U. S. Department of Commerce
5285 Port Royal Road
Springfield, Virginia 22161
Price: Printed Copy $10.75; Microfiche $2.25

Distribution Category:
Physics (UC-34)

ANL-75-75

ARGONNE NATIONAL LABORATORY
9700 South Cass Avenue
Argonne, Illinois 60439

PHYSICS DIVISION ANNUAL REVIEW

1 April 1974–31 March 1975

Lowell M. Bollinger, Division Director

Preceding Annual Reviews:

ANL-7848, Annual Review 1970—1971
ANL-7971, Annual Review 1971—1972
ANL-8035, Annual Review 1972—1973

FOREWORD

The Physics Division Annual Review presents a comprehensive picture of the work of the Division in the year ending in the spring of 1975. In addition, the papers published in the 1-year period from 1 April 1974 through 31 March 1975 are listed immediately after the reports on the research.

Another picture of the relative emphases on the different programs of the Division is supplied by the roster of personnel, in which the staff members are grouped by program. (It must be understood, however, that staff members frequently do part of their work in another program.) This roster forms the last section of the report.

TABLE OF CONTENTS

Page

I. INTERMEDIATE-ENERGY PHYSICS 1

Introduction 1

A. Experiments at ZGS 2

1. Multinucleon Removal from Nuclei by High-Energy Pions 2
(P. T. Debevec, L. R. Greenwood, H. E. Jackson, D. G. Kovar, L. Meyer-Schützmeister, J. P. Schiffer, R. E. Segel, T. P. Wangler, W. R. Wharton, and B. Zeidman)

2. Study of the Feasibility of an Intense Kaon Beam 3

B. Experiments at LAMPF 4

1. Meson-Induced Nuclear Reactions 4

a. Nuclear γ Rays Arising from the Interaction of Pions with Nuclei-Alpha Removal (H. E. Jackson, D. G. Kovar, L. Meyer-Schützmeister, J. P. Schiffer, R. E. Segel, S. E. Vigdor, T. P. Wangler, V. G. Lind, E. N. Hatch, O. H. Otteson, R. E. McAdams, R. L. Burman, P. A. M. Gram, D. M. Drake, R. B. Clark, and B. C. Cook) 4

b. Nuclear γ Rays Arising from the Interaction of Pions with Nuclei - ^{58}Ni and ^{60}Ni (H. E. Jackson, D. G. Kovar, L. Meyer-Schützmeister, J. P. Schiffer, R. E. Segel, S. E. Vigdor, T. P. Wangler, V. G. Lind, E. N. Hatch, O. H. Otteson, R. E. McAdams, R. L. Burman, P. A. M. Gram, D. M. Drake, R. B. Clark, and B. C. Cook) 5

c. Nuclear γ Rays Arising from the Interaction of Pions with Nuclei - ^{51}V and ^{27}Al (H. E. Jackson, D. G. Kovar, L. Meyer-Schützmeister, J. E. Monahan, J. P. Schiffer, R. E. Segel, S. E. Vigdor, T. P. Wangler, V. G. Lind, E. N. Hatch, O. H. Otteson, R. E. McAdams, R. L. Burman, P. A. M. Gram, D. M. Drake, R. B. Clark, and B. C. Cook) 6

Page

d. Nuclear γ Rays Arising from the Interaction of Pions with Nuclei - ^{93}Nb and ^{138}Ba (H. E. Jackson, D. G. Kovar, L. Meyer-Schützmeister, J. P. Schiffer, R. E. Segel, S. E. Vigdor, T. P. Wangler, V. G. Lind, E. N. Hatch, O. H. Otteson, R. E. McAdams, R. L. Burman, P. A. M. Gram, D. M. Drake, R. B. Clark, and B. C. Cook) 6

e. Neutron Components of Inelastic Pion Excitations (J. P. Schiffer, H. E. Jackson, D. G. Kovar, R. D. Lawson, L. Meyer-Schützmeister, R. E. Segel, S. E. Vigdor, and T. P. Wangler) 7

2. Pion Scattering 7

Pion Scattering from Complex Nuclei (T. H. Braid, H. E. Jackson, J. P. Schiffer, T. P. Wangler, B. Zeidman, H. A. Thiessen, J. S. McCarthy, S. E. Sobottka, G. C. Morrison, R. H. Siemssen, S. I. Baker, K. K. Seth, and H. Plendl) 8

3. Channeling Experiments 9

a. Electron Channeling Measurements at the Argonne Electron Linac (D. S. Gemmell, J. Remillieux, T. P. Wangler, and J. N. Worthington) 9

b. Pion Channeling (D. S. Gemmell, T. H. Braid, R. E. Holland, J.-C. Poizat, J. Remillieux, J. P. Schiffer, J. W. Tippie, T. P. Wangler, J. N. Worthington, B. Zeidman, D. M. Lee, and H. A. Thiessen) 10

4. Instrumentation 11

a. Design, Construction and Performance of a Scintillator-Beam-Monitor System for High-Intensity Secondary Charged-Particle Beams (T. P. Wangler, S. E. Vigdor, and J. N. Worthington) 11

b. Position-Sensitive Proportional Counters (T. H. Braid) 12

c. Design of a Charged-Pion Detector for ZGS and LAMPF Experiments (T. P. Wangler) 13

Page

II. HEAVY-ION PHYSICS 15

Introduction 15

A. Basic Research 17

1. Transfer Reactions and Spectroscopy 17

a. Study of Single-Nucleon Transfer Systematics in Heavy-Ion-Induced Reactions (Y. Eisen, H. T. Fortune, W. Henning, D. G. Kovar, S. E. Vigdor, and B. Zeidman) 18

b. j Determination from Angular Structure of $p_{1/2}$ Proton Transfer (J. R. Erskine, L. R. Greenwood, W. Henning, and D. G. Kovar) 20

c. Studies of ^{16}O-Induced "α-Particle" Transfer on Calcium Isotopes (Y. Eisen, J. R. Erskine, H. T. Fortune, L. R. Greenwood, W. Henning, D. G. Kovar, S. E. Vigdor, and B. Zeidman) 20

d. Studies of Two-Nucleon Transfer Reactions in the Scattering of ^{16}O from ^{48}Ca and ^{42}Ca (Y. Eisen, H. T. Fortune, W. Henning, D. G. Kovar, S. E. Vigdor, and B. Zeidman) 22

e. Studies of Sub-Coulomb Neutron Transfers in the Region of Ca, Sr, and Zr Isotopes (Y. Eisen, J. R. Erskine, J. P. Schiffer, and P. Sperr) 27

f. L Dependence in Angular Distributions of the Two-Proton Transfer Reaction $^{48}Ca(^{16}O,^{14}C)^{50}Ti$ (J. R. Erskine, W. Henning, D. G. Kovar, and B. Zeidman) 27

g. The Reaction $^{48}Ca(^{16}O,^{15}C)^{49}Ti$ (Y. Eisen, H. T. Fortune, W. Henning, D. G. Kovar, and B. Zeidman) 29

h. The $^{40}Ca(^{16}O,^{12}C)^{44}Ti$ Reaction (J. R. Erskine, W. Henning, D. G. Kovar, and L. R. Greenwood) 32

i. Li-Induced Reactions (C. L. Fink, A. M. Friedman, D. S. Gale, and B. Zeidman) 33

Page

2. Reaction Systematics and Cross Sections 34

a. The Optical Potential in Heavy-Ion Transfer Reactions (Y. Eisen, J. R. Erskine, W. Henning, D. G. Kovar, and B. Zeidman) 35

b. ^{16}O and ^{18}O Induced Reactions on ^{118}Sn at the Coulomb Barrier (Y. Eisen, W. Henning, H.-J. Körner, D. G. Kovar, J. P. Schiffer, S. E. Vigdor, and B. Zeidman) 37

c. Cross Sections for Reactions Induced by ^{16}O on Ca Isotopes (Y. Eisen, H. T. Fortune, W. Henning, D. G. Kovar, S. E. Vigdor, and B. Zeidman) 37

3. Resonance Phenomena 41

a. $^{12}C(^{12}C,\alpha)^{20}Ne$ Excitation Functions and Angular Distributions (L. R. Greenwood, R. E. Segel, K. Raghunathan, M. A. Lee, H. T. Fortune, and J. R. Erskine) 41

b. Inelastic Scattering of $^{16}O + ^{12}C$ Around $E_{c.m.} = 19.7$ MeV (J. R. Erskine, W. Henning, and P. Sperr) 42

c. The $^{24}Mg(^{16}O,^{12}C)^{28}Si$ Reaction (J. R. Erskine, W. Henning, D. G. Kovar, L. R. Greenwood, and R. M. DeVries) 44

d. "$^{12}C + ^{16}O$" States in ^{28}Si (J. P. Schiffer, W. R. Wharton, and P. T. Debevec) 44

e. Spin of the 23.85-MeV State in ^{28}Si (R. L. Boudrie, F. W. Prosser, and P. T. Debevec) 46

B. Instrumentation 48

Page

a. Time-of-Flight Mass Identification System (Y. Eisen, W. Henning, D. G. Kovar, S. E. Vigdor, and B. Zeidman) 48

b. A New Heavy-Ion Focal Plane Detector for the Magnetic Spectrograph (J. R. Erskine, T. H. Braid, and J. C. Stoltzfus) 51

c. Conversion of the Broad-Range Spectrograph (R. L. Boudrie and F. W. Prosser) 51

d. Workshop on Fast Timing in Heavy-Ion Physics, Argonne National Laboratory, June 7—8, 1974 (B. Zeidman, L. M. Bollinger, W. Henning, D. G. Kovar, M. H. Macfarlane, and J. P. Unik) 53

III. LIGHT-ION PHYSICS 55

Introduction 55

A. Charged-Particle Research at the Tandem 57

1. States of Intermediate-Mass Nuclides 57

a. Studies of ^{39}Ar (R. E. Segel, P. T. Debevec, W. C. Corwin, and J. F. Tonn) 57

b. Study of ^{44,46}Sc by the ^{42,44}Ca(α, d)^{44}Sc Reaction (T. H. Braid, J. Manthuruthil, and C. P. Poirier) 58

c. (^{3}He, p) Reaction on $f_{7/2}$-Shell Nuclei (Gerald Hardie, David Gloeckner, L. Meyer-Schützmeister, and T. H. Braid) 59

d. Level Structure of ^{76}As (J. F. Lemming, J. Rapaport, and A. J. Elwyn) 59

e. Experimental Investigation of ^{92}Tc by the ^{92}Mo(^{3}He, t) Reaction (T. H. Braid, H. T. Fortune, and F. J. D. Serduke) 61

f. Investigation of the Nucleus $^{89}_{41}$Nb$_{48}$ by the $^{92}_{42}$Mo$_{50}$ (p, α) Reaction (W. Henning and F. J. D. Serduke) 61

Page

2. Structure of Actinide Nuclides 62

Single-Particle States in Actinide Nuclei (J. R. Erskine, A. M. Friedman, R. R. Chasman, T. H. Braid, and D. S. Gale) 62

3. Reaction Mechanisms 64

a. Back-Angle Excitation Functions of $\alpha + {}^{39}K$ and $\alpha + {}^{40,44}Ca$ Scattering Between 20 and 27 MeV (K. A. Eberhard, T. H. Braid, T. Renner, J. P. Schiffer, and S. E. Vigdor) 64

b. Anomalies in the ${}^{72}Ge(\alpha, n){}^{75}Se$ Reaction Near Isobaric Analog Resonances in ${}^{76}Se$ (A. J. Elwyn, J. E. Monahan, J. F. Lemming, J. Rapaport, and M. Sample) 64

4. Effective Residual Interaction 66

Effective Interactions from Nuclear Spectra Near Closed Shells (J. P. Schiffer) 66

5. Electromagnetic Properties 67

a. Nuclear g Factor of the $d_{3/2}$ Hole State in ${}^{43}Sc$ (R. P. Scharenberg, R. Mitchell, T. V. Ragland, R. E. Holland, and F. J. Lynch) 67

b. Measurement of the g Factor of the 6^+, 88-μsec Isomeric State of ${}^{90}Nb$ (R. J. Mitchell, T. V. Ragland, R. P. Scharenberg, R. E. Holland, and F. J. Lynch) 68

c. Isomerism in ${}^{194}Au$ (S. W. Yates and F. J. Lynch) 68

d. Decay of the $t_{1/2}$ = 22 μs Isomeric State of ${}^{38}K$ (S. W. Yates, F. J. Lynch, R. E. Holland, I. Ahmad, and A. M. Friedman) 70

e. Lifetimes of the $\frac{1}{2}^+[631]$ to $\frac{5}{2}^+[622]$ E2 Transitions in Some Actinide Nuclei (S. W. Yates, F. J. Lynch, R. E. Holland, A. M. Friedman, and I. Ahmad) 72

f. Measurement of the g Factor of the 10-μsec Isomeric State of ${}^{115}Te$ (R. J. Mitchell, T. V. Ragland, R. P. Scharenberg, F. J. Lynch, and R. E. Holland) 74

Page

g. The Gamma Decay of High-Spin States in ^{47}Ti (L. Meyer-Schützmeister, Terrence Sjoreen, and Gerald Hardie) 76

h. Study of the ^{54}Fe(α, γ)^{58}Ni Reaction (L. Meyer-Schützmeister, W. Wharton, P. Debevec, R. E. Segel, and K. Raghunathan) 78

6. Measurements of Astrophysical Interest 78

a. Facility for Observing Decay Properties of Isotopes Far from β Stability (C. N. Davids, R. C. Pardo, and L. A. Parks) 78

b. New Isotopes of Interest to Explosive Nucleosynthesis (C. Davids, R. Pardo, and L. Parks) 79

c. Radiative De-excitation of the 7.655-MeV State of ^{12}C—Helium Burning in Stars (C. N. Davids, R. C. Pardo, and A. W. Obst) 80

B. Charged-Particle Work at the Cyclotron 82

a. Deuteron-Induced Nucleon Pickup (T. H. Braid, J. L. Yntema, H. T. Fortune, and L. R. Medsker) 82

b. The ^{16}O(α, p)^{19}F Reaction and Three-Particle Cluster Transfer Spectroscopic Factors (T. H. Braid, H. T. Fortune, and W. Henning) 82

C. Light-Ion Physics at the Dynamitron 84

1. Low-Energy Cross Sections 84

a. Cross Sections for Neutrons from ^{6}Li+d Reactions at Low Energies (A. J. Elwyn, R. E. Holland, F. J. Lynch, J. E. Monahan, and F. P. Mooring) 85

b. Cross Sections for Charged Particles from ^{6}Li+d Reactions at Low Energies (C. N. Davids, A. J. Elwyn, R. E. Holland, L. Meyer-Schützmeister, and F. P. Mooring) 87

c. Search for Direct Radiative α Capture. The ^{16}O(α, γ)^{20}Ne Reaction (A. J. Elwyn, L. Meyer-Schützmeister, G. Hardie, F. P. Mooring, and J. E. Monahan) 87

Page

d. Neutron Polarization in Isospin-Forbidden (p, n) Reactions (J. E. Monahan and A. J. Elwyn) 88

e. Short-Lived Spontaneously Fissioning Isomers in Neutron-Induced Reactions (A. J. Elwyn, F. J. Lynch, F. P. Mooring, and M. J. Fluss) 90

2. Channeling 90

Channeling of Particles Injected As Members of Molecular Ions (D. S. Gemmell, J. M. Remillieux, and R. E. Holland) 91

IV. ACCELERATOR OPERATIONS 93

A. The FN Tandem Van de Graaff Accelerator 93

a. The Pelletron Chain and Closed-Corona Voltage-Distribution System 93

b. Ion-Source Development 94

c. Control System for the Tandem 95

d. Physics Division On-Line Computer System 95

e. Planned Upgrading of the Tandem 95

f. University Use of the Tandem Accelerator 96

B. Operation of the Dynamitron 99

Operational Experience (F. P. Mooring, A. Langsdorf, Jr., and R. L. Amrein) 99

V. SUPERCONDUCTING LINAC DEVELOPMENT 103
(L. M. Bollinger, J. Aron, R. Benaroya, B. E. Clifft, A. H. Jaffey, K. W. Johnson, T. K. Khoe, J. J. Livingood, F. J. Lynch, P. Markovich, J. M. Nixon, G. W. Parker, and B. Zeidman)

Page

Introduction 103

A. Concept and Component Development 104

λ/2 Helix Performance 104

Beam-Line Use of a λ/2 Resonator 104

5λ/2 Resonator 104

Fabrication Techniques 107

Split-Ring Resonator 107

Theory 109

Tandem-Linac-Accelerator Concept 109

B. Bunching of Heavy-Ion Beams 111

C. Heavy-Ion Energy Booster 114

VI. NEUTRON PHYSICS 119

Introduction 119

A. Threshold Photoneutron Experiments at the ANL Linac 121

a. Photodisintegration of the Deuteron Near Threshold (H. E. Jackson, R. J. Holt, and W. M. Wilson) 122

b. Nonresonant (γ,n) Reactions in the Mass Region $A \approx 60$ (H. E. Jackson, R. J. Holt, and W. M. Wilson) 123

c. Ground-State Radiation Widths Near Photoneutron Threshold for the A=140 Mass Region (R. J. Holt and H. E. Jackson) 124

d. Valence Transitions in $^{91}Zr(\gamma,n)^{90}Zr$ (R. E. Toohey and H. E. Jackson) 126

Page

e. Giant M1 Resonance in ^{207}Pb (L. R. Medsker and H. E. Jackson) 127

f. Background (γ,n) Cross Section in ^{208}Pb (H. E. Jackson) 127

g. Threshold Photoneutron Polarization in the ^{208}Pb($\gamma,\vec{n}_0$)^{207}Pb Reaction: A New Method for Threshold Photoneutron Spectroscopy (R. J. Holt, H. E. Jackson, and W. M. Wilson) 129

B. Research at the CP-5 Reactor 131

1. Fundamental Phenomena 132

a. Measurements of Spacial Asymmetries in the Decay of Polarized Neutrons (V. E. Krohn and G. R. Ringo) 132

b. The Electron-Neutron Interaction (V. E. Krohn and G. R. Ringo) 132

c. Search for Collapsed Nuclei (L. M. Bollinger, A. M. Friedman, S. M. Fried, J. P. Schiffer, J. R. Specht, G. E. Thomas, and A. Turkevich) 133

d. Rotational Invariance in Nuclei (R. J. Holt and W. M. Wilson) 134

2. Photon Scattering Studies 134

a. Delbrück and Nuclear Raman Scattering of 10.83-MeV Photons by Deformed and Spherical Heavy Nuclei (H. E. Jackson, K. J. Wetzel, and G. E. Thomas) 134

b. Nuclear Raman Scattering of 11.4-MeV Photons (H. E. Jackson, G. E. Thomas, and K. J. Wetzel) 135

3. Neutron-Capture γ Rays 137

a. A Comparison of the γ-Ray Spectra from Thermal-Neutron Capture and 2.8-keV Neutron Capture in ^{23}Na (W. M. Wilson, G. E. Thomas, and H. E. Jackson) 137

b. Gamma Rays from Thermal-Neutron Capture in ^{59}Ni and ^{63}Ni (W. M. Wilson, G. E. Thomas, and H. E. Jackson) 138

Page

c. Average Resonance Method for Neutron-Capture γ-Ray Spectroscopy: ^{176}Lu and ^{177}Lu (W. M. Wilson, G. E. Thomas, and H. E. Jackson) 140

d. Absolute (n, γ) Cross Sections in the ^{113}Cd(n, γ)^{114}Cd and ^{149}Sm(n, γ)^{150}Sm Reactions (R. K. Smither and G. E. Thomas) 142

e. Nuclear Structure of ^{148}Sm, ^{150}Sm, and ^{152}Sm (R. K. Smither and D. L. Bushnell) 143

f. Nuclear Structure of ^{114}Cd (R. K. Smither) 145

g. Neutron Capture in Isomeric States in Te Isotopes (R. K. Smither and B. Hamermesh) 145

h. Nuclear Structure in ^{144}Nd and ^{146}Nd (R. K. Smither, D. L. Bushnell, G. Tassotto, S. Ledvina, and J. Hawkins) 146

i. Studies of the Excited States of ^{160}Tb Populated in the Reactions ^{159}Tb(n, γ) and ^{159}Tb($\bar{n}$, γ)^{160}Tb (S. B. Burson, F. J. Zehr, J. R. Champion, and C. H. Batson) 147

j. Nuclear Structure of ^{178}Hf and ^{180}Hf (R. K. Smither, D. L. Bushnell, and D. J. Buss) 148

k. Nuclear Structure of ^{184}W (R. K. Smither, D. L. Bushnell, J. Hawkins, and R. Goebbert) 150

ℓ. Statefit: A Computer Program to Facilitate the Interpretation of Spectroscopic Data (S. B. Burson, G. T. Wood, and C. H. Batson) 150

C. Fast-Neutron Research 153

Experimental and Theoretical Studies of Neutron Elastic Scattering from ^{12}C Below 5 MeV (R. J. Holt, A. B. Smith, and J. F. Whalen) 153

Page

VII. THEORETICAL PHYSICS 155

A. Heavy-Ion Reaction Theory 155

1. Peripheral or Quasi-elastic Collisions 156

a. Calculational Techniques and Methods (D. H. Gloeckner, M. H. Macfarlane, and S. C. Pieper) 156

b. Partial-Wave Structure of Heavy-Ion-Transfer Amplitudes (M. H. Macfarlane and S. C. Pieper) 156

c. Structure Amplitudes for Three-Nucleon Transfer with 1p-Shell Targets (D. Kurath and D. J. Millener) 157

2. Head-on Collisions, Fusion, and Viscosity 157

a. Microscopic Calculations of Viscosity in Heavy-Ion Collisions (D. Glas and U. Mosel) 157

b. Critical Distances in Fusion Reactions (D. Glas and U. Mosel) 158

3. Electromagnetic Effects in Heavy-Ion Reactions 159

Vacuum Polarization- and Molecular-Potential Effects in Heavy-Ion Scattering (Johann Rafelski)

B. Nuclear Matter and Nuclear Forces 162

1. Relativistic Effects in Phenomenological Nucleon-Nucleon Potentials and Nuclear Matter (F. Coester, Steven C. Pieper, and F. J. D. Serduke) 163

2. Three-Body Correlations in Nuclear Matter (B. Day and F. Coester) 165

3. Isobar Configurations in Nuclear Matter (B. Day and F. Coester) 166

4. Approximately Relativistic Particle Interactions (F. Coester and P. Havas) 167

5. Elastic Electron-Deuteron Scattering As a Probe of the Deuteron Wave Function (F. Coester and A. Ostebee) 167

C. Collapsed Nuclei and Dense Nuclear Matter 169

1. Phenomenology of Collapsed Nuclei (A. R. Bodmer) 169

Page

2. Surface Properties of Abnormal Nuclear Matter (A. R. Bodmer and J. Boguta) 170

D. Nuclear Structure Theory 171

1. Non-normal Parity States in Light Nuclei (D. Kurath and D. J. Millener) 171

2. Direct Radiative Capture (J. E. Monahan, A. J. Elwyn, and F. J. D. Serduke) 172

3. Hartree-Fock Calculations for Light Nuclei Using the Skyrme Interaction (B. D. Chang, M. H. Macfarlane, U. Mosel, and K.-H. Passler) 173

4. Spurious Center-of-Mass Motion (D. H. Gloeckner and R. D. Lawson) 174

5. Isospin-Forbidden E1 Transitions (D. H. Gloeckner and R. D. Lawson) 174

6. The E6 Gamma Transition in ^{53}Fe (D. H. Gloeckner and R. D. Lawson) 175

7. Beta Decay of ^{209}Tl (R. D. Lawson) 176

8. Shell-Model Study of Nuclei with $Z < 38$ and $N \leq 50$ (D. H. Gloeckner and F. J. D. Serduke) 176

9. Shell-Model Study of N=48 Nuclei (D. H. Gloeckner and F. J. D. Serduke) 177

10. Shell-Model Study of N=49 Nuclei (D. H. Gloeckner, R. D. Lawson, and F. J. D. Serduke) 177

11. An Extended Shell-Model Description of $^{88}_{39}Y_{49}$ (D. H. Gloeckner and F. J. D. Serduke) 178

E. Other Theoretical Physics 179

1. The Pion-Nucleus Interaction (J. E. Monahan, L. Meyer-Schützmeister, and F. J. D. Serduke) 179

2. Boundary Perturbations (J. E. Monahan and Norbert Rosenzweig) 180

3. Grouped-Sample Modifications of the Cramèr-Smirnov Test for Goodness of Fit (J. E. Monahan and Norbert Rosenzweig) 180

4. A Statistical Analysis of Counting Data (J. E. Monahan) 181

Page

5. The Hartree-Fock Approximation and Quantum Electrodynamics (J. Rafelski and Berndt Müller) 181

6. Spurious Contact Divergences in the S-Matrix Formulation of Field Theory (Johann Rafelski and Michael Danos) 182

7. Stabilization of the Charged Vacuum Created by Very Strong Electrical Fields in Nuclear Matter (Johann Rafelski) 183

8. General Formulation of Pionic Decays in the Quark Model (Harry J. Lipkin) 186

9. Einstein's Equivalence Principle. An Explicit Statement and Its Derivation from Special Relativistic Presymmetry (Y. Avishai and H. Ekstein) 187

F. Speakeasy Development 188

1. The Kappa Release of Speakeasy (S. Cohen, Steven C. Pieper, and M. J. Stob) 188

2. The Speakeasy Center (S. Cohen) 188

VIII. ATOMIC AND MOLECULAR PHYSICS 191

Introduction 191

A. Photoionization and Photoelectron Physics and Chemistry 192

1. Photoionization Mass Spectrometric Study of Several Molecules in the Extreme Ultraviolet (Paula L. Kronebusch and J. Berkowitz) 192

a. Photodissociative Ionization of CO_2 193

b. Photodissociative Ionization of H_2O 197

2. Photoelectron Spectroscopy of High-Temperature Vapors (D. G. Streets and J. Berkowitz) 201

a. Thallium Fluoride Dimer 201

b. Group VI Homonuclear Diatomic Molecules 202

Page

c. Laser Vaporization 205

3. High-Resolution Photoionization Studies 206

a. High-Resolution Study of Photoionization in H_2, HD, and D_2 (W. A. Chupka, P. M. Dehmer, and W. T. Jivery) 206

b. High-Resolution Photoionization Study of Ion-Pair Formation in H_2, HD, and D_2 (W. A. Chupka, P. M. Dehmer, and W. T. Jivery) 209

c. High-Resolution Study of Photoionization and Photoemission from Metastable Autoionizing States of OI (P. M. Dehmer, W. A. Chupka, and W. T. Jivery) 212

d. Photoionization Study of the Reaction of $O_2^+(a^4\Pi_u)$ with O_2 (P. M. Dehmer, W. A. Chupka, and W. T. Jivery) 213

B. Interactions of Energetic Particles and Photons with Surfaces of Solids 217

1. Blistering of Surfaces of Solids by Charged-Particle Irradiation 217

a. Effect of Irradiation Temperature on Erosion by Blistering (M. Kaminsky and S. K. Das) 217

b. Irradiation of Nb by He^+ Ions of Different Energies (M. Kaminsky and S. K. Das) 219

c. Effect of He^+ and D^+ Ion Beam Flux on Blister Formation in Niobium and Vanadium (S. K. Das and M. Kaminsky) 220

d. Threshold Dose for Helium Blister Appearance in Nb (S. K. Das and M. Kaminsky) 222

e. Correlation Between Blister-Skin Thickness and Projected Ranges of He^+ Ions in Nb and V (G. Fenske, S. K. Das, and M. Kaminsky) 222

f. Helium Blistering in Nb Damaged by 14-MeV Neutron Irradiation (M. Kaminsky and S. K. Das) 223

Page

g. Effect of Irradiation Temperature on Blister Morphology in Nickel (M. K. Sinha, S. K. Das, and M. Kaminsky) 223

h. Helium Blistering of Silicon Carbide (M. Kaminsky and S. K. Das) 224

i. Studies of the Reduction of Surface Erosion Due to Helium Blistering (S. K. Das, M. Kaminsky, and T. Rossing) 224

2. 14-MeV Neutron Sputtering 225

a. 14-MeV Neutron Sputtering of Nb (M. Kaminsky and S. K. Das) 225

b. 14-MeV Neutron Sputtering of Silicon Carbide (M. Kaminsky and S. K. Das) 227

c. Effect of Irradiation Temperature on 14-MeV Neutron Sputtering of Nb (M. Kaminsky and S. K. Das) 228

d. Chunk Emission from V, Stainless Steel, Monocrystalline Si (M. Kaminsky and S. K. Das) 228

e. Neutron Sputtering of Surfaces Prestressed with Helium-Ion Implantation (M. Kaminsky and S. K. Das) 228

f. Dependence of Neutron Sputtering on Incident Neutron Energy (M. Kaminsky and S. K. Das) 228

3. Ion Sputtering (P. Dusza and M. Kaminsky) 229

4. Surface Phenomena Induced by Photon Impact (S. Brumbach, M. Kaminsky, and S. K. Das) 230

5. Development of Techniques for Measuring Surface Contamination in Very Small Concentrations (10^{-1} — 10^{-4} Monolayers) (M. Kaminsky and P. Dusza) 231

6. Design of a Two-Component Ion-Accelerator System (R. Ekern, D. C. Hess, and M. Kaminsky) 233

C. Optical and Radiofrequency Spectrometry of Free Atoms and Molecules 234

1. Atomic-Beam Magnetic Resonance of the Actinides (W. J. Childs, H. Diamond, L. S. Goodman, and T. Waech) 234

Page

2. Experiments with ^{221}Fr (W. J. Childs, H. Diamond, L. S. Goodman, and B. Greenebaum) 235

3. Laser Spectroscopy of Actinide Molecules (W. J. Childs and L. S. Goodman) 237

D. Mössbauer Effect Research 241

1. Mössbauer Measurements with the 93.26-keV Transition in ^{67}Zn (G. J. Perlow, W. Potzel, R. M. Kash, and H. DeWaard) 241

2. Study of Lake Michigan Sediments by ^{57}Fe Mössbauer Spectroscopy (G. J. Perlow, W. Potzel, and D. Edgington) 242

3. Atomic Motions in Liquids and Glasses (S. L. Ruby, B. J. Zabransky, J. C. Love, and P. A. Flinn) 243

4. Radiation Damage Effects (R. S. Preston and B. J. Zabransky) 243

5. x-Ray Mirrors (S. L. Ruby) 244

6. Mössbauer Spectroscopy of ^{129}I in Thyroxin-like Compounds (S. L. Ruby, R. S. Preston, and B. J. Zabransky) 245

7. Carbonic Anhydrase Studies Using Mössbauer Spectroscopy (A. M. Friedman and S. L. Ruby) 246

E. Scanning Secondary-Ion Microprobe 247

Microscopic Location of Stable Tracer Isotopes (V. E. Krohn, W. E. Kisieleski, and G. R. Ringo) 247

F. Radiative Spectra, Decay Times, and Collision Dynamics of Heavy Ions 250

1. Okorokov Effect in Channeling (D. S. Gemmell, R. E. Holland, J. M. Remillieux, and H. G. Berry) 250

2. Light Polarization of Channeled Ions (H. G. Berry and J. M. Remillieux) 250

3. Orientation of Fast Heavy-Ion Beams (H. G. Berry and C. H. Batson) 250

Page

4. Circularly Polarized Quantum Beats (H. G. Berry, R. M. Schectman, and L. J. Curtis) 251

5. Electric Field Quantum Beats (H. G. Berry, G. Gabrielse, R. M. Schectman, and L. J. Curtis) 252

6. Heavy-Ion Spectroscopy and Lifetimes (H. G. Berry and C. H. Batson) 252

IX. PUBLICATIONS FROM 1 APRIL 1974 THROUGH 31 MARCH 1975 255

X. STAFF MEMBERS OF THE PHYSICS DIVISION 281

I. INTERMEDIATE-ENERGY PHYSICS

INTRODUCTION

In its Medium-Energy Research program, the Argonne Physics Division applies the techniques and accumulated knowledge of low-energy nuclear physics to intermediate-energy problems. The experimental part of the program is carried out primarily at LAMPF but, when advantageous, other accelerators are used for exploratory experiments or to make use of particle beams that are not provided by LAMPF. The ZGS is especially useful for such auxiliary experiments because of its kaon beam and because it provides pions of higher energy than are available from LAMPF.

Following exploratory measurements at the ZGS, an extensive study of pion-induced nuclear reactions has been started at LAMPF. The technique of on-line high-resolution measurements of nuclear gamma rays has been systematically applied to studies of the products of pion-induced reactions. Taking advantage of the unique facility available at LAMPF, it has been possible in several cases to accumulate spectra where more than half of the total reaction cross section is accounted for by final nuclides identified by their gamma rays. Thus, this technique may provide the best overall tool for exploring the bulk of the pion-induced reactions. From a very successful first run at LAMPF, a number of new qualitative features have emerged. Earlier evidence pointing toward multiple α-particle removal is seen in a somewhat different light with the new improved data, and the dependence of exit channel on projectile, target, and energy has been studied. For the first time, reliable absolute cross sections have been obtained. A request for additional running time has been submitted.

When the EPICS channel becomes operational in late 1975, one of the first experiments will be one on pion channeling. Equipment for this study is almost complete. Experiments on pion scattering await the completion of the EPICS spectrometer.

Because its "strangeness" quantum number is different from that of the pion, investigations with kaon projectiles could open up entirely new aspects of nuclear physics. However, the possibilities are severely limited by the low intensities of existing kaon beams. In an effort to improve on this situation, we have initiated an investigation of the feasibility of obtaining a more intense kaon beam from the ZGS.

A. EXPERIMENTS AT ZGS

No experiments were carried out at ZGS during the past year. Also, no experiments at ZGS are planned for the coming year unless LAMPF turns out to be unavailable or unless there are unforeseen scientific developments that make the special capabilities of the ZGS especially attractive.

The experimental results reported below in Sec. 1 were obtained from a set of measurements carried out in the spring of 1974.

1. MULTINUCLEON REMOVAL FROM NUCLEI BY HIGH-ENERGY PIONS

P. T. Debevec, L. R. Greenwood,* H. E. Jackson, D. G. Kovar, L. Meyer-Schützmeister, J. P. Schiffer, R. E. Segel, T. P. Wangler, W. R. Wharton, and B. Zeidman

Early measurements at ANL of nuclear reactions with fast charged mesons have suggested that, for medium-weight nuclei, multinucleon removal is dominated by removal of single and multiple alpha particles. The gross characteristics of the spectra of residual nuclei are qualitatively different than those commonly associated with spallation reactions and suggest the possibility of a nuclear interaction unique to meson reactions. In an effort to explore these phenomena further, and to determine the importance of nuclear-structure features, a new series of runs were undertaken at the ZGS. The γ-ray spectra were measured for the interactions of 350-MeV pions with nuclei covering a range of mass from 32 to 75. The γ-ray spectra were observed with a Ge(Li) detector with very much improved conditions of signal to background. A preliminary analysis indicates that nuclear-structure effects can greatly alter the degree of alpha removal. A comparison of spectra show significant single and multiple alpha removal for interactions with ^{40}Ca and no observable

*Northwestern University, Evanston, Illinois.

corresponding removal in ^{40}Ar. Calculations using a nuclear-cascade evaporation model for these and other targets studied in these measurements are in progress. Detailed comparison of these results with the experimental data is expected to provide information on the nature of the reaction mechanism for transfer of pionic energy to the nucleus.

2. STUDY OF THE FEASIBILITY OF AN INTENSE KAON BEAM

The feasibility of obtaining an intense beam of kaons at the ZGS is being investigated.

The success of the studies of pion-induced nuclear reactions prompts an interest in making similar studies with kaons. Furthermore, since kaons are strangeness 1 (S=1) particles, as against S = 0 for the pion, new areas of nuclear, and perhaps particle, physics are accessible when kaon-induced nuclear reactions are studied. In the pion work we have shown that with beams averaging about 3×10^5 particles per sec nuclear reaction studies become quite feasible. We have therefore been investigating whether low momentum ($\approx$ 500 MeV/c) kaon beams of sufficient intensity might be obtainable at the ZGS.

From discussions with ZGS personnel, it has been learned that they expect to be targetting 3×10^{12} protons per pulse in the fall of 1976. Experience with a kaon beam which has been built at Berkeley indicates that, with this proton intensity, a beam delivering 3×10^5 K^+/sec could be built at the ZGS. About one contaminant particle would be present for each K^+.

A high-intensity kaon beam at the ZGS would add a new dimension to nuclear physics at Argonne and would significantly expand the capabilities of the national program in Medium-Energy Science.

B. EXPERIMENTS AT LAMPF

1. MESON-INDUCED NUCLEAR REACTIONS

Experiments done at the ZGS with kaonic atoms showed that a great deal of information about the interaction of mesons with nuclei can be deduced by measuring the resultant nuclear gamma-ray spectrum. These experiments, and subsequent studies of the spectra accompanying fast-pion bombardment, showed that qualitatively new nuclear phenomena may be manifested when mesons interact with nuclei. Opportunities for meson-nucleus studies have become much greater now that LAMPF has become operational since, not only are the pion fluxes much greater, but the experimental conditions are far superior for nuclear-physics experiments. A run at LAMPF in late 1974 produced what is easily the best data on the gamma-ray spectra from pion-induced reactions and justified our faith that nuclear physics could be fruitfully pursued in this manner.

a. Nuclear γ Rays Arising from the Interaction of Pions with Nuclei-Alpha Removal

H. E. Jackson, D. G. Kovar, L. Meyer-Schützmeister, J. P. Schiffer, R. E. Segel, S. E. Vigdor, T. P. Wangler, V. G. Lind,* E. N. Hatch,* O. H. Otteson,* R. E. McAdams,* R. L. Burman,† P. A. M. Gram,† D. M. Drake,† R. B. Clark,‡ and B. C. Cook§

Experimental data of prompt gamma rays induced by pions on a variety of targets from ^{27}Al to ^{138}Ba have been examined for evidence of alpha-particle removal as a dominant mechanism. Earlier work with stopped kaons at the ZGS and with pions at SREL indicated this to be a strong effect. While alpha removal induced by 220-MeV π^- on ^{40}Ca is observed, the cross section was found to be at least a factor of three lower than reported in the SREL experiment. For Al, V, and Ni targets, nuclei which would be left after the removal of one or more alpha particles, or

---

*Utah State University, Logan, Utah.

†Los Alamos Scientific Laboratory, Los Alamos, New Mexico.

‡Texas A & M University, College Station, Texas.

§Iowa State University, Ames, Iowa.

tritons + alpha particles for the odd nuclei, account for about 15—30% of the total cross section. With heavier targets alpha removal was not evident, although the data were not as definitive.

b. Nuclear γ Rays Arising from the Interaction of Pions with Nuclei - ^{58}Ni and ^{60}Ni

H. E. Jackson, D. G. Kovar, L. Meyer-Schützmeister, J. P. Schiffer, R. E. Segel, S. E. Vigdor, T. P. Wangler, V. G. Lind,* E. N. Hatch,* O. H. Otteson,* R. E. McAdams,* R. L. Burman,† P. A. M. Gram,† D. M. Drake,† R. B. Clark,‡ and B. C. Cook§

Prompt gamma rays induced by fast pions on ^{58}Ni have been studied with a Ge(Li) counter. These measurements provide a unique picture of the interaction between pions and complex nuclei; it is the only technique which allows a gross identification of the dominant final channels. In continuation of earlier Argonne work at the ZGS with kaons and pions, a successful experiment was carried out at LAMPF. Isotopically enriched Ni targets were used. For each isotope it was possible to assign about half the total cross section to specific final nuclides. Measurements on ^{58}Ni show virtually no dependence of the distribution of final nuclides on the pion's charge or energy (100 and 220 MeV). This is contrary to simple expectations and unlike the behavior with protons. Limited data on other nuclides have also been obtained. Future measurements are planned to explore these systematics in more detail; the energy dependence needs to be extended to lower energies and the charge dependence checked with other targets. We also plan to look at some gross charged-particle spectra in attempting to gain additional information of the reaction mechanisms.

---

*Utah State University, Logan, Utah.

†Los Alamos Scientific Laboratory, Los Alamos, New Mexico.

‡Texas A & M University, College Station, Texas.

§Iowa State University, Ames, Iowa.

c. Nuclear γ Rays Arising from the Interaction of Pions with Nuclei - ^{51}V and ^{27}Al

H. E. Jackson, D. G. Kovar, L. Meyer-Schützmeister, J. E. Monahan, J. P. Schiffer, R. E. Segel, S. E. Vigdor, T. P. Wangler, V. G. Lind,* E. N. Hatch,* O. H. Otteson,* R. E. McAdams,* R. L. Burman,† P. A. M. Gram,† D. M. Drake,† R. B. Clark,‡ and B. C. Cook§

Prompt gammas from fast pion bombardment of ^{27}Al and ^{51}V indicate rather large cross sections for the production of final nuclei removed by one triton or 1 triton + 1 alpha from the target nucleus. This result is quite different from those obtained in even-even target nuclei of the same mass region, where the yields of the nuclei with 1α or 2α removed from the target nucleus are most prominent. In ^{51}V, for example, 25% of the total observed reaction cross section leads to ^{48}Ti (^{51}V triton or 2n + 1p). Some exploratory calculations have been carried out using a particle evaporation model.

d. Nuclear γ Rays Arising from the Interaction of Pions with Nuclei - ^{93}Nb and ^{138}Ba

H. E. Jackson, D. G. Kovar, L. Meyer-Schützmeister, J. P. Schiffer, R. E. Segel, S. E. Vigdor, T. P. Wangler, V. G. Lind,* E. N. Hatch,* O. H. Otteson,* R. E. McAdams,* R. L. Burman,† P. A. M. Gram,† D. M. Drake,† R. B. Clark,‡ and B. C. Cook§

Gamma rays from fast pion interactions with ^{138}Ba and ^{93}Nb have been studied at the LAMPF-LEP pion channel. For ^{138}Ba, ^{126}Xe, and ^{128}Xe lines corresponding to 2-proton + 8 or 10 neutron removal dominate the spectrum. With a ^{93}Nb target, γ rays corresponding to ^{88}Zr and ^{84}Sr are the strongest; again the number of neutrons removed is more than double the number of protons. The mechanism of fast pion interactions

---

*Utah State University, Logan, Utah.

†Los Alamos Scientific Laboratory, Los Alamos, New Mexico.

‡Texas A & M University, College Station, Texas.

§Iowa State University, Ames, Iowa.

with these heavy targets seems to be qualitatively different from that with lighter ones.

e. Neutron Components of Inelastic Pion Excitations

J. P. Schiffer, H. E. Jackson, D. G. Kovar, R. D. Lawson, L. Meyer-Schützmeister, R. E. Segel, S. E. Vigdor, and T. P. Wangler

When inelastic scattering of both π^+ and π^- is measured to a given state at the same incident pion energy, if it is assumed that such scattering is due to a direct process, one may extract rather unique information from the data. The normal experimental quantities for (E2) inelastic excitations are the B(E2)'s which represent electromagnetic (i.e., charge or proton) transitions. If the pion interaction is by way of the 3,3 resonance, the corresponding quantity for neutrons may be extracted through the relation $"B(E2)_n"/B(E2) = [(3-\rho)/(3\rho-1)]^2$, where $\rho \equiv (\sigma_{\pi^+}/\sigma_{\pi^-})^{1/2}$. Under the assumption that the ground-state gamma-ray transitions in the target nuclei studied in our LAMPF experiment are caused by direct inelastic excitations and not cascades, this ratio of matrix elements was extracted from the ^{58}Ni data and is in accord with a theoretical estimate based on the phenomenology of the nickel isotopes. Encouragement can be drawn from the results obtained to date that direct experimental access to this important nuclear quantity is possible through the study of pion-induced reactions.

2. PION SCATTERING

The intense (the order of nanoamps are expected soon) pion beams at LAMPF present the opportunity to carefully and systematically study the interaction of nuclei with pions. The spectrometer EPICS is an auxiliary facility being built that will greatly facilitate nuclear studies.

Pion Scattering from Complex Nuclei

T. H. Braid, H. E. Jackson, J. P. Schiffer, T. P. Wangler, B. Zeidman, H. A. Thiessen,* J. S. McCarthy,† S. E. Sobottka,† G. C. Morrison,‡ R. H. Siemssen,§ S. I. Baker,‖ K. K. Seth,¶ and H. Plendl**

Two experiments have been planned and approved for the EPICS system at LAMPF.

(1) Survey of π scattering by complex nuclei, using targets of ^{28}Si, ^{60}Ni, ^{88}Sr, ^{208}Pb, and ^{238}U. This will provide the first information on the average pion-nucleus potential (for both π^+ and π^-) and its description in terms of an optical-model potential for a wide range of masses. The distorted-wave functions derived from this will be required in the analysis of other pion-induced reactions.

(2) Elastic and inelastic scattering of π^+ and π^- from ^6Li, ^{10}B, and ^{14}N at $E \approx 200$ MeV, with emphasis on populating the low-lying T=0 and T=1 levels and the (π^+,π^0)-charge-exchange reaction. Since the levels of the targets chosen have been studied extensively, and since the inelastic scattering to the T=1 levels is equivalent to the single-charge-exchange reaction to other members of the same isospin triplet, the data obtained will make possible an internally consistent test of our knowledge of pion-nucleus scattering.

Neither experiment has yet been performed since the EPICS channel is not yet ready; it is likely to be available for the experiments in the next fiscal year.

---

*Los Alamos Scientific Laboratory, Los Alamos, New Mexico.

†University of Virginia, Charlottesville, Virginia.

‡University of Birmingham, Birmingham, England.

§University of Groningen, Groningen, Netherlands.

‖National Accelerator Laboratory, Batavia, Illinois.

¶Northwestern University, Evanston, Illinois.

**Florida State University, Tallahassee, Florida.

3. CHANNELING EXPERIMENTS

Almost all channeling work to date has been done with positive ions. With the advent of LAMPF, it becomes possible to study this process with heavy negative particles and an experiment is planned for 1975—76. Since the channeling process is governed by Coulomb forces, qualitative differences are expected. As part of the preparation for the experiment and testing the apparatus, some electron-channeling measurements have been carried out.

a. Electron Channeling Measurements at the Argonne Electron Linac

D. S. Gemmell, J. Remillieux, T. P. Wangler, and J. N. Worthington

In order to simulate conditions at LAMPF prior to Argonne's pion-channeling experiment, some channeling measurements were attempted at the electron linac at Argonne. In this experiment a thin silicon crystal was used both as a channeling medium and as a detector, since if channeling effects are important, the output pulse generated when a pion passes through the detector should depend upon the detector orientation.

One question being investigated is whether there would be experimental problems associated with the small pulse expected when minimum ionizing pions deposit energy in the thin silicon. The electron linac was used as a source of minimum ionizing particles in order to study these problems. Among the problems encountered were: (1) pickup noise pulses in the silicon which were of greater magnitude than the signal, (2) pileup of pulses due to the low duty factor of the Linac, and (3) pulse distortion arising from thermal noise or other background radiation.

Some significant progress was made towards solving the pickup noise and pileup problems and work is continuing in an effort to solve the remaining problems before the first experimental run, which should be in August 1975.

b. Pion Channeling

D. S. Gemmell, T. H. Braid, R. E. Holland, J.-C. Poizat, J. Remillieux, J. P. Schiffer, J. W. Tippie,* T. P. Wangler, J. N. Worthington, B. Zeidman, D. M. Lee,† and H. A. Thiessen‡

The pion-channeling experiments proposed at LAMPF will proceed in two stages. The first will consist of a measurement in which a thin (110) planar Si crystal will constitute both a target for channeling and a detector to measure energy loss. The second will use the EPICS spectrometer to measure the momentum and spatial distributions for pions transmitted through a variety of thin target crystals. The channeling effect has been investigated mostly with positive ion beams, and to a much lesser extent, with beams of electrons and positrons. The use of pion beams will provide data for an incident particle mass that is intermediate between the extremes of the electron and proton masses. This is expected to prove useful in relating the different theoretical descriptions applicable to positive ion channeling on the one hand (usually a classical theory suffices) and electron and positron channeling on the other (often, but by no means always, a quantum mechanical description is required). The experiments will be done both with beams of π^+ and π^-, so that a comparison will be possible between channeling effects for particles identical except for the sign of their charge.

The apparatus required for the first experiment has all been assembled, and it has been tried out with protons at the ANL tandem. We successfully measured the energy loss in the Si target counter and correlated that energy loss with the direction of the individual protons as determined by a pair of helical counters, and demonstrated the decrease in energy loss for the channeling direction.

---

*Applied Mathematics Division, ANL.

†University of Virginia, Charlottesville, Virginia.

‡Los Alamos Scientific Laboratory, Los Alamos, New Mexico.

The EPICS channel has not been available for an experimental run, but it is scheduled to be available early in the next fiscal year and the experiment will be performed then.

4. INSTRUMENTATION

The challenges of medium-energy research demand the development of novel instrumentation to meet the needs and insure the success of the program. Members of the Argonne medium-energy group have been in the forefront of these efforts. They have solved the problem that arises at LAMPF of measuring beams that are too intense for the counting of individual particles, and yet too weak for conventional high-precision current integration. A novel position-sensitive detector that is necessary to determine pion position in the upcoming channeling experiments has been built and tested. The success of this instrument under test suggests that it may very well have other valuable uses in particle research. An advanced detection system for studying the charged-particle products of pion-induced reactions is being developed.

a. Design, Construction and Performance of a Scintillator-Beam-Monitor System for High-Intensity Secondary Charged-Particle Beams

T. P. Wangler, S. E. Vigdor, and J. N. Worthington

An important problem for Argonne's recent experiment #121 at LAMPF was the need for a means to monitor the incident pion beam in which the instantaneous rate was $10^7 - 10^9$ particles/sec. A detector was constructed consisting of a thin plastic scintillator in the beam, which was viewed by a photomultiplier. The photomultiplier current was integrated by a charge-balancing A/D converter whose output was scaled. Tests with a pulsed light-emitting diode showed that the detector was linear to about ±1% over more than four orders of magnitude in light intensity. The integrated current was calibrated at low-beam intensity against the number of particles counted in a coincidence telescope which included a second photomultiplier viewing the beam monitor scintillator. The average photomultiplier currents from two

additional scintillation counters placed in the periphery of the beam were used to monitor changes in beam position or focussing.

This beam-monitor system was successfully used at LAMPF for both pion and proton beams. Calibrations which were made several days apart were consistent in all cases within 1% accuracy.

An important part of monitoring the beam was the construction of a rigid mechanical frame upon which the scintillation counters and targets could be mounted in close relative proximity. The basic frame was attached with roller bearings to an external frame bolted into the experimental floor. This allowed for easy access into a geometrically-confined region for the necessary changes of target in the experiment.

b. Position-Sensitive Proportional Counters

T. H. Braid

A position-sensitive counter with a helical cathode has been built for the pion-channeling experiment at LAMPF, and has been tested in a model channeling experiment with protons at the tandem. Extensive use is made of printed circuit and modular plug-in techniques so as to make a highly convenient system with rapidly interchangeable parts, which can rapidly be reproduced. A number of these counters will be used in the channeling experiment in the next fiscal year.

A fast analog computer circuit has been developed for particle identification with a position-sensitive and dE counter pair in the magnetic spectrograph. The dE pulse varies in magnitude as position varies and is therefore not by itself satisfactory for particle identification. From the outputs of the two counters, x and dE, the pulse computer derived the quantity

$$[(x + k)^2 \Delta E]^{1/2} \propto m(z/q)$$

z = charge in vacuum
q = charge in counter gas
k = adjustable constant

which does not vary with x, and depends only on the charge of the particle and its mass.

Systems such as this can be made to evaluate more complex functions of pulses from counters. More elaborate counter systems may be built for the purpose of identifying heavy-ion species incident at the detector.

c. Design of a Charged-Pion Detector for ZGS and LAMPF Experiments

T. P. Wangler

A scintillation counter detector has been designed whose purpose is to select π^+ mesons with a wide spectrum of energies in the presence of a background of other charged and neutral particles. The detector consists of alternate layers of scintillator and brass and identifies the pions (after bringing them to rest by means of their attenuation in the brass) by detecting the electron from the delayed π-μ-e decay. The design of the large-area scintillation counter features the use of Winston light collectors which improve light collection efficiency and should give a more uniform response across the area of the scintillator.

II. HEAVY-ION PHYSICS

INTRODUCTION

The heavy-ion research program at the Argonne tandem accelerator is a multifaceted attempt to investigate the mechanisms involved in the interaction of heavy ions with light- and medium-mass nuclei and to explore the ways in which heavy-ion reactions enlarge our understanding of nuclear structure.

Coupled with the basic-physics studies are efforts to develop advanced instrumentation for heavy-ion research. This work includes the development of a sophisticated heavy-ion beam-bunching system to provide the ultra-short pulses needed for a full exploitation of the time-of-flight method in heavy-ion research. This same bunching system is also essential for the superconducting linac that will be installed as an energy booster at the output of the tandem, as described in Sec. V.C of this document.

The scope and effectiveness of the program of heavy-ion experiments at the tandem is closely linked to several technical efforts now in progress. Already well underway is a long-term effort to enhance the heavy-ion capability of the tandem itself. As described in Sec. IV.A, the machine has been substantially improved during the past year, and the upgrading planned for the next two years will result in even greater research capabilities.

The advanced ion-bunching techniques described in Sec. V.B are now ready for application in ion time-of-flight experiments and, although further technical development is needed, pulsed-beam methods will soon begin to open up new experimental possibilities.

On a somewhat longer time scale, the planned addition of a superconducting energy booster (see Sec. V.C) will have a major impact on our research capabilities. The program of research at the tandem is evolving along lines that will enable the new research tools to be used with full effectiveness.

Most of the recent basic-physics experiments at the tandem have been based on an important technical development started at Argonne in early 1974, namely, the development of charged-particle time-of-flight measurements with exceedingly good time resolution. This technique has allowed experimentalists to carry out over the past year whole

classes of measurements which were previously inconceivable. The systematics of simple transfer reactions to individual levels have been explored in considerable detail. Many complex reactions were also investigated, and their general importance is now clearly established. Focal-plane detectors for the magnetic spectrograph have also undergone significant improvement. The high-resolution capabilities of this instrument have been utilized in a number of studies.

The installation of a Pelletron charging system and a corona voltage divider at the Tandem (see Sec. IV.A.a) has been an unqualified success after solution of some initial problems. The accelerator now produces beams much more stable than those prior to the change, and operates at higher terminal voltages. As a result, the new system has improved both the efficiency and reliability of the facility and the quality of the experimental data.

A. BASIC RESEARCH

1. TRANSFER REACTIONS AND SPECTROSCOPY

Transfer reactions have long been used as spectroscopic tools in the investigation of nuclear structure. With the advent of heavy-ion beams and high-resolution detection systems, transfer reactions become a powerful probe of those nuclei that can be formed only via multinucleon transfers.

In order to investigate these phenomena, a substantial portion of the Argonne heavy-ion program is concerned with investigation of transfers of one, two, and four nucleons. Studies with both the time-of-flight telescope and the magnetic spectrograph have shown that, at far forward angles, the shapes of the angular distributions exhibit a structure characteristic of the total angular-momentum transfer. As a result, comparisons based upon known spins, parities, and other results from light-ion experiments have provided a means for calibration of the measured angular-distribution shapes and the assignment of new spins. The high degree of localization in heavy-ion transfers allows sub-Coulomb transfer to provide a sensitive probe of the neutron wave function. Above the Coulomb barrier, data obtained with the time-of-flight telescope have shown that even the analysis of simple single-nucleon transfer is beset with difficulties for those reactions that are badly matched with respect to the dominant partial waves.

Multinucleon transfers involve correlations between transferred nucleons. To the extent that these correlations may be considered as representing clusters of nucleons with specific quantum numbers, the theoretical analysis of data for multinucleon-transfer reactions is feasible with existing calculational techniques. However, in our work it has been demonstrated that there are substantial disagreements between measured and theoretical cross sections in all cases, though the ratios of measured cross sections to states in a given nucleus can provide useful spectroscopic information. Pioneering studies with the time-of-flight telescope show angular distributions for many multinucleon transfers that oscillate markedly and are characteristic of the angular-momentum transfer. These data therefore provide a starting point for detailed "α" and "cluster" spectroscopy.

a. Study of Single-Nucleon Transfer Systematics in Heavy-Ion-Induced Reactions

Y. Eisen, H. T. Fortune, W. Henning, D. G. Kovar, S. E. Vigdor, and B. Zeidman

The single-nucleon transfer reactions induced by bombardment of ^{40,42,44,48}Ca targets by 56-MeV ^{16}O ions were measured using a ΔE-E time-of-flight system. The measured angular distributions for the transfers observed to low-lying single-particle (hole) states establish the systematics of the reactions as function of Q value and L transfer, and provide a stringent test for reaction-model calculations in a mass region where the structure is well known. While outgoing projectiles of ^{15}O, ^{15}N, ^{17}O, and ^{17}F were detected, the most complete data were obtained for ^{15}N. Shown in Fig. 1 are the angular distributions measured for the (^{16}O, ^{15}N) reactions leading to the $f_{7/2}$ ground state and lowest $p_{3/2}$ states in the respective residual scandium nuclei. From this figure it is obvious that (1) the angular distributions become more forward peaked as the Q value becomes more negative, and (2) the change in shape is more rapid for the smaller L transfer (L = 2, 3 for the $p_{3/2}$) than for the larger L transfer (L = 3, 4 for the $f_{7/2}$). The curves in the figure are exact finite-range DWBA calculations using optical-model potentials which fit elastic scattering. As can be seen, except for the well matched L=4(3) transfer of the ^{48}Ca(^{16}O, ^{15}N)^{49}Sc (g. s.) reaction, DWBA is not able to reproduce the shapes of the angular distributions. Our studies (see previous report) show that optical-model ambiguities are apparently not the reason for the failure. Studies are underway to see whether a more sophisticated reaction model, such as a coupled-channels treatment, will be able to reproduce the experimental data.

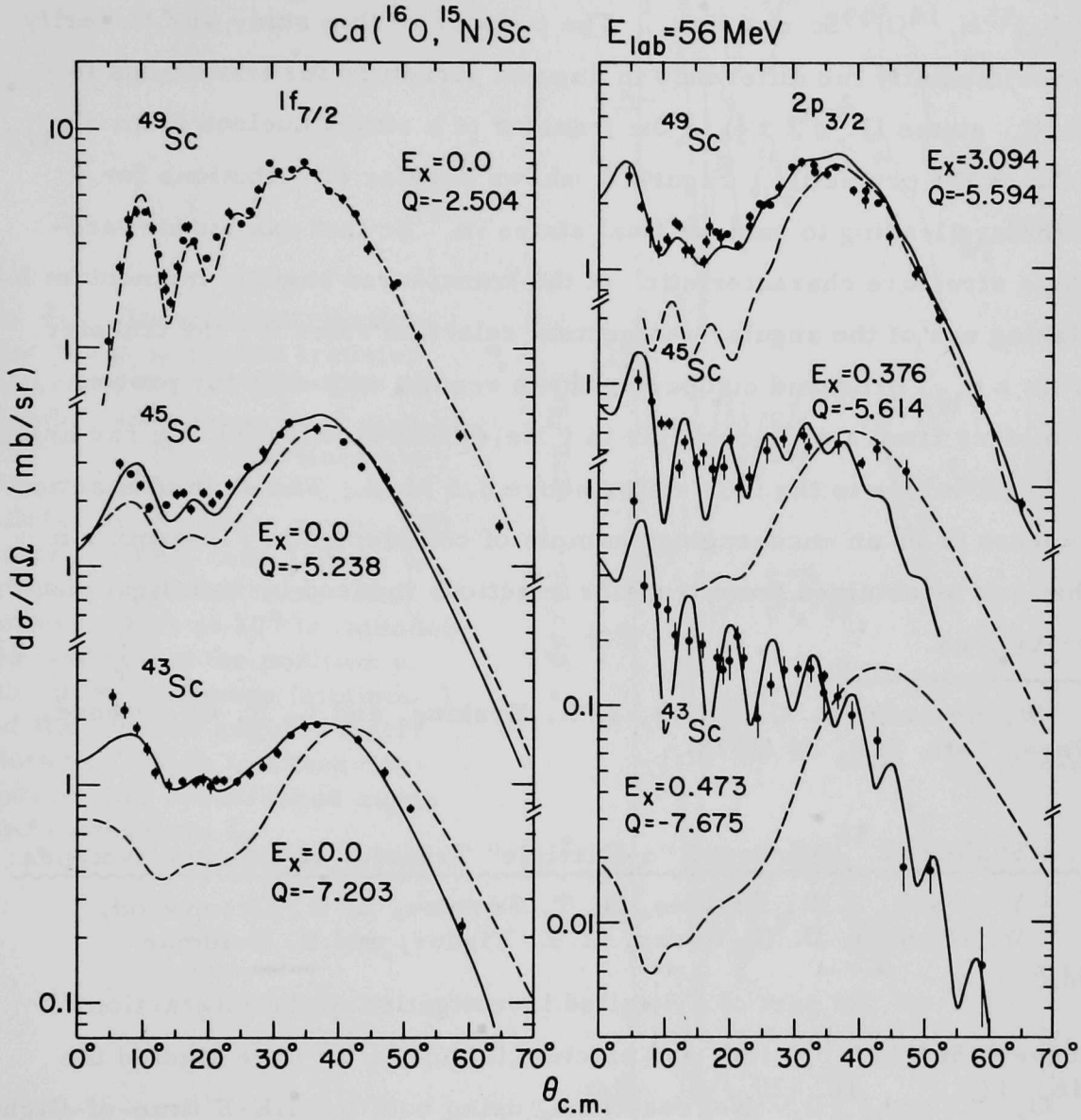

Fig. 1. Angular distributions measured for the (^{16}O,^{15}N) reaction on ^{42,44,48}Ca. The curves are DWBA cross sections calculated by the code LOLA.

b. j Determination from Angular Structure of $p_{1/2}$ Proton Transfer

J. R. Erskine, L. R. Greenwood, W. Henning, and D. G. Kovar

Detailed angular distributions extending to forward angles ($\theta_{lab} = 3^{o}$) have been measured for various transitions in the $^{48}Ca(^{15}N, ^{14}C)^{49}Sc$ reaction.[1] The purpose of this study was to verify experimentally the difference in angular structure for transitions to $j_{>}$ and $j_{<}$ states ($j_{\gtrless} = \ell \pm \frac{1}{2}$) in the transfer of a single nucleon from a $p_{1/2}$ orbit in the projectile. Figure 2 shows angular distributions for transfers leading to various final states in ^{49}Sc that exhibit forward-angle structure characteristic of the transferred angular momentum L. Making use of the angular-momentum selection rules for the transfer from a $p_{1/2}$ orbit and comparing these results with data for proton transfers from a $s_{1/2}$ orbit [as in (^{3}He,d) measurements], we can assign $j_{\gtrless}$ spin values to the four states above 3.5 MeV. The studied reaction appears to be an encouraging example of complementary information that can be obtained from transfer reactions induced by both light and heavy ions.

---

[1] W. Henning, D. G. Kovar, J. R. Erskine, and L. R. Greenwood, Phys. Lett. 55B, 49 (1975).

c. Studies of ^{16}O-Induced "α-Particle" Transfer on Calcium Isotopes

Y. Eisen, J. R. Erskine, H. T. Fortune, L. R. Greenwood, W. Henning, D. G. Kovar, S. E. Vigdor, and B. Zeidman

As part of a detailed investigation of the interaction between 56-MeV ^{16}O ions and calcium isotopes, we have studied the (^{16}O, ^{12}C) and (^{16}O, ^{20}Ne) reactions, using both the ΔE-E time-of-flight telescope and the split-pole spectrograph. It is of interest to determine whether these processes can be described simply as a single-step transfer of an α-particle or α-like cluster.

These reactions proceed strongly (relative to other transfer-reaction channels) for $^{40,42}Ca$ but are very weak for ^{48}Ca,

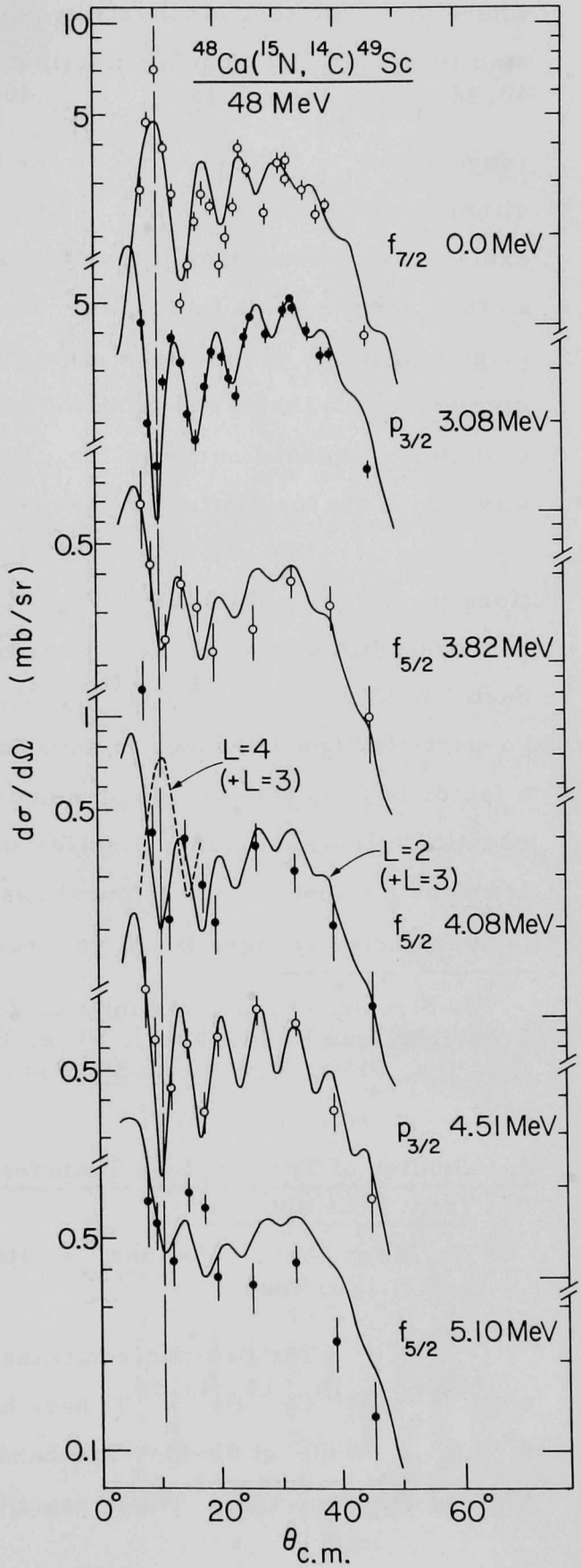

Fig. 2. Angular distributions for the $p_{1/2}$ proton transfer reaction $^{48}Ca(^{15}N,^{14}C)^{49}Sc$ leading to various final states in ^{49}Sc. The solid lines are the theoretical curves predicted by the finite range, full recoil DWBA code LOLA, as discussed in the text. The vertical line at 10° is intended to emphasize the position of the first maximum (minimum) of the various angular distributions, which is characteristic of the transferred angular momentum L.

where they lead to neutron-rich residual nuclei far from the line of stability. Detailed angular distributions have been obtained for $^{40,42}Ca(^{16}O, ^{12}C)^{44,46}Ti$ and for $^{40}Ca(^{16}O, ^{20}Ne)^{36}Ar$ over the angular range $4^{\circ} \leq \theta_{lab} \leq 40^{\circ}$. In each case the angular distributions for transitions leading to low-lying 0^{+} states of the residual nucleus (see Fig. 3) exhibit very strong oscillations and a rapid decrease in overall magnitude as the reaction angle increases. These features, along with the relatively large magnitude of the peak cross sections, are suggestive of a single-step cluster-transfer mechanism, but are not well explained by calculations (e.g., dashed curve in Fig. 3) using the conventional distorted-wave Born approximation and assuming α-particle transfer.

One can obtain DWBA fits to the observed angular distributions (e.g., see solid curve, Fig. 3) by arbitrarily readjusting the real-well diffuseness of the optical-model potential in the exit channel. Such DWBA fits to the $^{40}Ca(^{16}O, ^{12}C)$ measurements yield relative "α-particle" spectroscopic factors for states in ^{44}Ti which agree within a factor of 2—3 with values obtained in a study[1] of the $^{40}Ca(^{6}Li, d)$ reaction. However, the reliability of spectroscopic information extracted from the present results is questionable since the physical meaning of the parameter changes is not yet understood.

---

[1] U. Strohbusch, C. L. Fink, B. Zeidman, R. N. Horoshko, H. W. Fulbright, and R. Markham, Phys. Rev. Lett. 29, 735 (1972); R. M. DeVries, Phys. Rev. Lett. 30, 666 (1973).

d. Studies of Two-Nucleon Transfer Reactions in the Scattering of ^{16}O from ^{48}Ca and ^{42}Ca

Y. Eisen, H. T. Fortune, W. Henning, D. G. Kovar, S. E. Vigdor, and B. Zeidman

The two-nucleon transfer reactions $^{42,48}Ca(^{16}O, ^{18}O)^{40,46}Ca$ and $^{42,48}Ca(^{16}O, ^{14}C)^{44,50}Ti$ have been studied in the angular range $6^{\circ} \leq \theta_{c.m.} \leq 60^{\circ}$ at 56-MeV bombarding energy utilizing a ΔE-E time-of-flight system. These reactions complement studies of light-ion

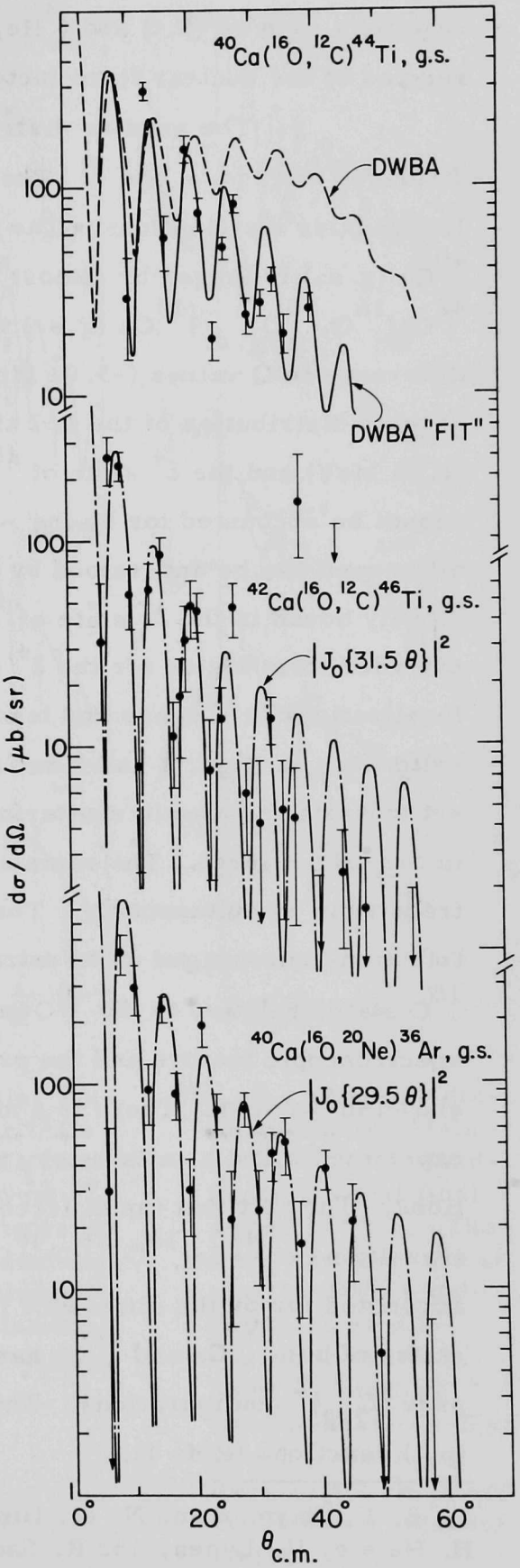

Fig. 3. Angular distributions for the L=0 ground-state transitions ^{40,42}Ca(^{16}O,^{12}C)^{44,46}Ti and ^{40}Ca(^{16}O,^{20}Ne)^{36}Ar at 56-MeV bombarding energy. The simple oscillatory behavior of the measurements is emphasized by the dot-dashed curves, which are generated from spherical Bessel functions $J_0[(\ell + \frac{1}{2})\theta]$ corresponding to a single ℓ value. The solid and dashed DWBA curves are discussed in the text.

reactions such as (p,t) and (^{3}He,n) because they are sensitive to different regions of the nuclear form factors.

The angular distributions of the (^{16}O, ^{18}O) reactions are displayed in Figs. 4 and 5. The ground-state transitions show typical L=0 angular distributions. The peak cross section of the ^{48}Ca(^{16}O, ^{18}O$_{g.s.}$) ^{46}Ca (g.s.) is larger by almost a factor of 4 than that observed for the ^{42}Ca(^{16}O, ^{18}O$_{g.s.}$)^{40}Ca (g.s.) which can be understood as a result of the difference in Q values (-5.04 MeV and -7.6 MeV, respectively). The angular distribution of the L=2 transitions leading to the 2^+ state of ^{46}Ca (1.35 MeV) and the 2^+ state of ^{18}O (1.98 MeV) are markedly different and cannot be accounted for by the ~0.6 MeV difference in Q value. This difference can be understood by the fact that the two neutrons are more loosely bound in the 2^+ state of ^{18}O than in the 2^+ state of ^{46}Ca; the more extended form factor for the 2^+ of ^{18}O reduces the effect of the strong localizations in L space and leads to a smoother angular distribution. The solid lines in Figs. 4 and 5 are cluster-DWBA fits obtained with a parameter set that fits the elastic scattering in entrance channels, but is modified in the exit channel. The same set of parameters was used for fitting all transitions simultaneously. The good reproductions of the angular distributions encouraged us to extract spectroscopic factors for the excited ^{18}O states relative to the ^{18}O ground state. A comparison of the extracted spectroscopic factors and the predictions of shell-model calculations is shown in Table I. There is a nice consistency between the two (^{16}O, ^{18}O) experiments and a satisfactory agreement with the shell-model calculations. The fact that the difference in magnitude between the ground-state transitions of ^{48}Ca(^{16}O, ^{18}O)^{46}Ca and ^{42}Ca(^{16}O, ^{18}O)^{40}Ca can be accounted for by the difference in Q values suggests that the ground states of both ^{42}Ca and ^{46}Ca have very similar descriptions not far from pure $(f_{7/2})^2$ configurations. This is consistent with what was found in (p,t) reactions (Ref. 1).

---

[1] B. F. Bayman and N. M. Hintz, Phys. Rev. 172, 1113 (1968); H. Hefele, U. Lynen, and R. Santo, Nucl. Phys. A157, 93 (1970).

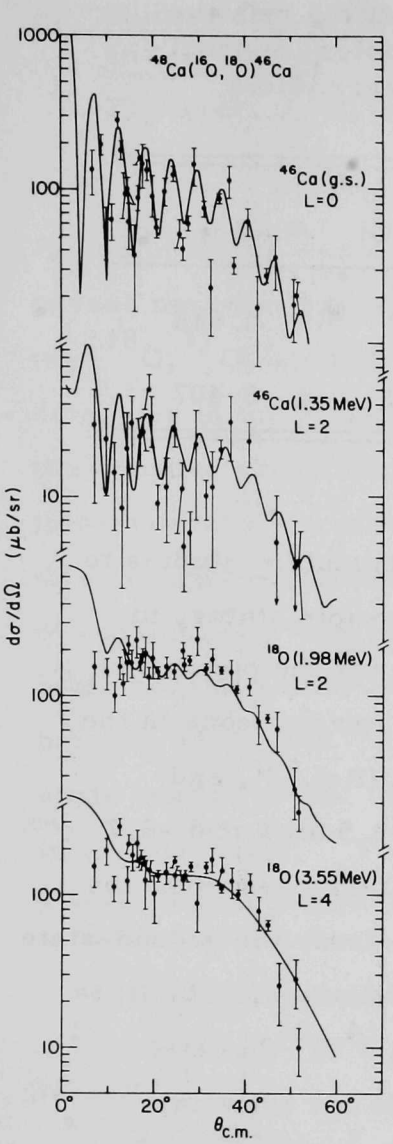

Fig. 4. Angular distributions for ^{48}Ca (^{16}O,^{18}O)^{46}Ca leading to the lowest 0^+, 2^+, and 4^+ states in ^{18}O and to the lowest 2^+ state in ^{46}Ca. The lines are theoretical cluster DWBA calculations as discussed in the text.

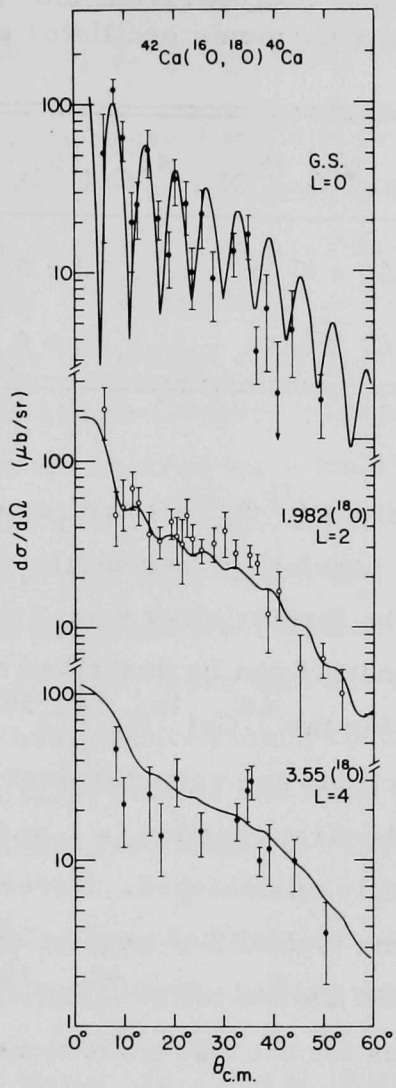

Fig. 5. Angular distributions for ^{42}Ca (^{16}O,^{18}O)^{40}Ca leading to the lowest 0^+, 2^+, and 4^+ states in ^{18}O. The lines are theoretical cluster DWBA calculations as discussed in the text.

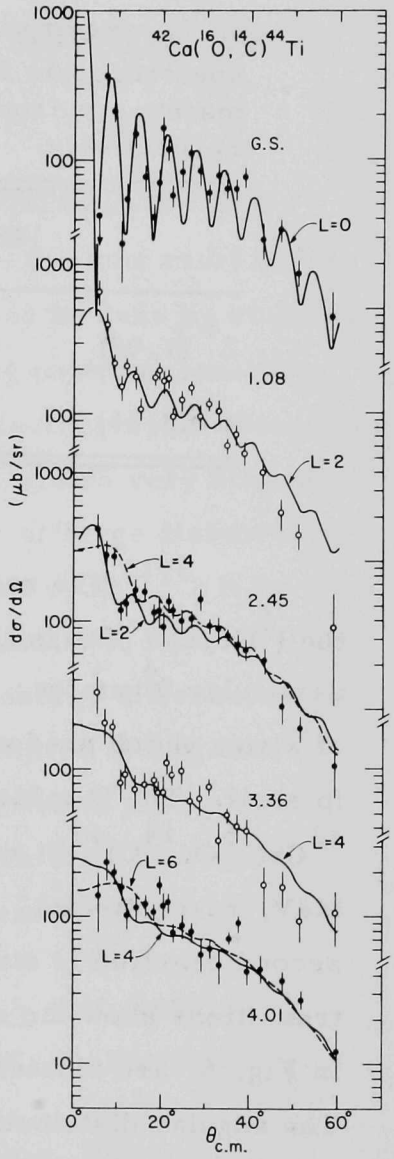

Fig. 6. Angular distributions for ^{42}Ca (^{16}O,^{14}C)^{44}Ti leading to several final states in ^{44}Ti. The lines are theoretical cluster-DWBA calculations as discussed in the text. Solid and dashed lines appear together in cases where experiment could not resolve two adjacent states.

TABLE I. Experimental and theoretical relative spectroscopic factors obtained from the "cluster" approximation and from the harmonic oscillator prescription, respectively.

	$^{48}Ca(^{16}O, ^{18}O)$	$^{42}Ca(^{16}O, ^{18}O)$	Shell model
2^+ (1.98)	0.60 ± 0.06	0.70 ± 0.12	0.646
4^+ (3.55)	1.67 ± 0.17	1.48 ± 0.29	0.407

The reactions $(^{16}O, ^{14}C)$ are complementary studies to the $(^3He,n)$. The latter populate preferentially low-spin states, in particular 0^+ states. The former show selectivity for the population of states which predominantly can be described as few nucleons in the fp shell. The Q values for the $^{48}Ca(^{16}O, ^{14}C)^{50}Ti$ (Ref. 2), and $^{42}Ca(^{16}O, ^{14}C)^{44}Ti$ reactions are very different (-0.5 MeV and -8.7 MeV, respectively). The first reaction is L and Q matched while the second reaction is strongly mismatched. Nevertheless, the ground-state transitions show the same typical L=0 angular distribution. The lines in Fig. 6 are cluster-DWBA fits to the $^{42}Ca(^{16}O, ^{14}C)^{44}Ti$ data. The angular distributions for the $L \neq 0$ transitions do not show any oscillatory behavior, which might be the result of the mixing of the different M amplitudes that contribute incoherently to the transfer cross sections. Assuming $(f_{7/2})^2 \otimes {}^{42}Ca$ configurations for the ground state and the first 2^+ (1.08 MeV) excited state of ^{44}Ti, one can calculate that the ratio of the spectroscopic factors for these states is 0.22. The experimental value is 0.39 ± 0.10. This discrepancy might result from a larger mixing of the $p_{3/2}$ into the $f_{7/2}$ configuration.

---

[2] W. Henning, D. G. Kovar, B. Zeidman, and J. R. Erskine, Phys. Rev. Lett. 32, 1015 (1974).

e. Studies of Sub-Coulomb Neutron Transfers in the Region of Ca, Sr, and Zr Isotopes

Y. Eisen, J. R. Erskine, J. P. Schiffer, and P. Sperr

The aim of the present study is to determine the rms radius of the excess neutrons in the Ca isotopes and the rms radii of the excess neutrons in the Sr and Zr isotopes. This may be done by studying the (^{18}O, ^{17}O) and the (^{14}N, ^{15}N) reactions, utilizing position-sensitive detectors in the focal plane of an Enge split-pole spectrograph. Measuring the transfer cross section at sub-Coulomb energies yields very accurate information on the size of the neutron wave function at large distances; this in turn determines the rms radius of the neutron orbit.[1,2] It is of considerable current interest to compare this quantity to the rms radius of the excess neutrons found from Coulomb energy differences between nuclei and their analogs, work that was initiated at Argonne some years ago and that has produced much controversial discussion in the literature.[3] Feasibility studies and tests have been carried out and the actual measurements are planned for the near future.

---

[1] J. P. Schiffer and H. J. Körner, Phys. Rev. C 8, 841 (1973).

[2] G. D. Jones, J. L. Durell, J. S. Lilley, and W. R. Phillips, preprint.

[3] J. P. Schiffer, J. A. Nolen, Jr., and N. Williams, Phys. Lett. 29B, 399 (1969).

f. L Dependence in Angular Distributions of the Two-Proton Transfer Reaction $^{48}Ca(^{16}O,^{14}C)^{50}Ti$

J. R. Erskine, W. Henning, D. G. Kovar, and B. Zeidman

The reaction $^{48}Ca(^{16}O,^{14}C)^{50}Ti$ was measured over the angular range $\theta_L = 3.6-37.5^{\circ}$ using a ΔE-E time-of-flight telescope and $\theta_L = 3-15^{\circ}$ using a split-pole magnetic spectrograph. A time resolution of 84 psec was obtained for the time-of-flight system. The use of analog electronic circuits for $\Delta E \times E$ and $E \times t^2$ multiplications

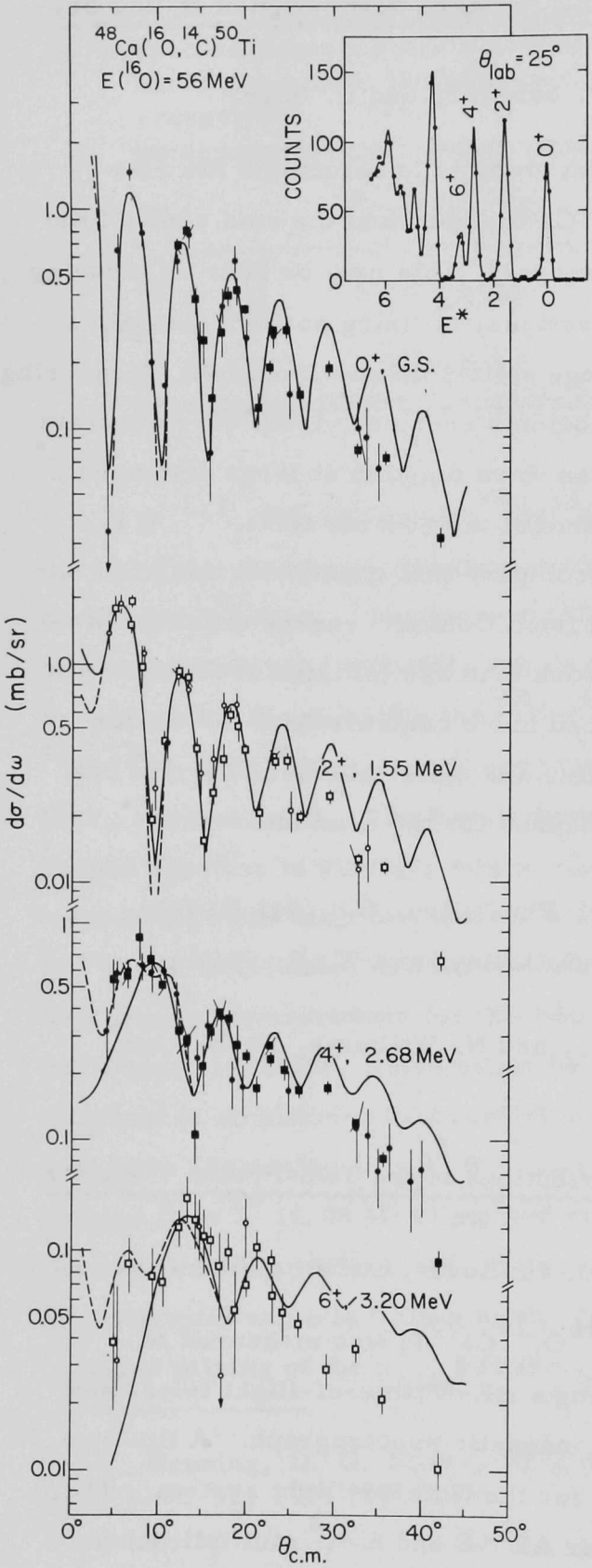

Fig. 7. Angular distributions for the two-proton transfer reaction $^{48}Ca(^{16}O,^{14}C)^{50}Ti$ leading to the lowest 0^+, 2^+, 4^+, and 6^+ final states in ^{50}Ti as obtained with the time-of-flight system (squares) and the split-pole spectrograph (circles). The solid lines are the theoretical curves predicted by the exact DWBA code LOLA, as discussed in the text. The inset shows an energy spectrum of the ^{14}C ions measured with the time-of-flight telescope.

in order to determine charze Z and mass m of the emerging ions, together with an antipileup circuit, allowed data accumulation rates in excess of 10 kHz. The focal-plane detector in the magnetic spectrograph was a 50-cm-long proportional counter with a high-resistance wire. Position and energy-loss signals from the detector made possible the separation of ion species.

Figure 7 shows the measured angular distributions of the (^{16}O, ^{14}C) reaction proceeding to the $J^{\pi} = 0^+$, 2^+, 4^+, and 6^+ final states in ^{50}Ti. Strong oscillations are observed for all transitions, with different patterns at extreme forward angles. With increasing final-state spin, the dominant first maximum shifts to larger angles; at even larger angles all angular distributions oscillate nearly in phase independent of spin. The extreme-forward-angle structure is characteristic of the transferred angular momentum L. At larger angles, the period of oscillation depends upon the dominant partial-wave angular momenta in the elastic entrance and exit channels. The angular distributions are well reproduced by finite-range, distorted-wave Born-approximation (DWBA) calculations. Consideration of the transfer amplitude suggests that the observed forward-angle L dependence can be a feature of a wider class of heavy-ion—induced transfer reactions under conditions of good ℓ matching between entrance and exit channels.

g. The Reaction $^{48}Ca(^{16}O, ^{15}C)^{49}Ti$

Y. Eisen, H. T. Fortune, W. Henning, D. G. Kovar, and B. Zeidman

To provide information relevant to the question of multistep processes in heavy-ion-induced transfer reactions, we have studied[1] the reaction $^{48}Ca(^{16}O, ^{15}C)^{49}Ti$, a reaction which involves the transfer of two units of charge, but only a single unit of mass. Since the transfer cannot proceed via the simple one-step process conventionally considered,

---

[1] D. G. Kovar, W. Henning, B. Zeidman, Y. Eisen, and H. T. Fortune, Phys. Rev. Lett. 33, 1611 (1974).

our measurements provide information about the magnitude and character of a more complex transfer process.

The experiment was performed with 56-MeV ^{16}O ions incident on enriched ^{48}Ca targets. The outgoing ions produced were detected with a ΔE-E time-of-flight telescope[2] which allowed for unambiguous particle identification. An energy spectrum for ^{15}C, obtained by summing the kinematically corrected spectra measured at 15 angles between 9.4° and 25°, is shown in Fig. 8. The four lowest levels in the spectrum could be identified on the basis of their observed energies. The first two levels correspond to the ^{49}Ti ground state with ^{15}C in its ground state and first excited state, respectively. The third and fourth levels are identified as the known $J^{\pi} = \frac{3}{2}^-$ and $(\frac{5}{2}^-, \frac{7}{2}^-)$ states in ^{49}Ti at excitation energies of 1.382 MeV and 2.262 MeV, respectively, both with ^{15}C in its ground state. The angular distributions, measured for three of the transitions mentioned above, are all observed to be forward peaked (see Fig. 9). The curves drawn in Fig. 9 are meant to guide the eye, showing that the data are consistent with either a smooth or an oscillatory behavior. (The oscillations shown have a period of about 6°, approximately the period of partial waves corresponding to a grazing collision.)

The magnitudes of the differential cross sections observed at forward angles are of the order of 5—50 μb/sr. These are comparable in magnitude (within a factor of 2—5) to the cross sections observed in the experiment for the few-nucleon transfers which are generally regarded as simple one-step cluster transfers [e.g., (^{16}O, ^{13}C), (^{16}O, ^{14}N), and (^{16}O, ^{18}O)]. Despite the uncertainties of such a comparison, which ignores structure effects, it appears clear that the cross sections for the noncluster transfer (^{16}O, ^{15}C) are comparable to those observed for conventional cluster transfers. Hence our results indicate the potential importance of multistep processes in reactions where both direct one-step and multistep processes are possible.

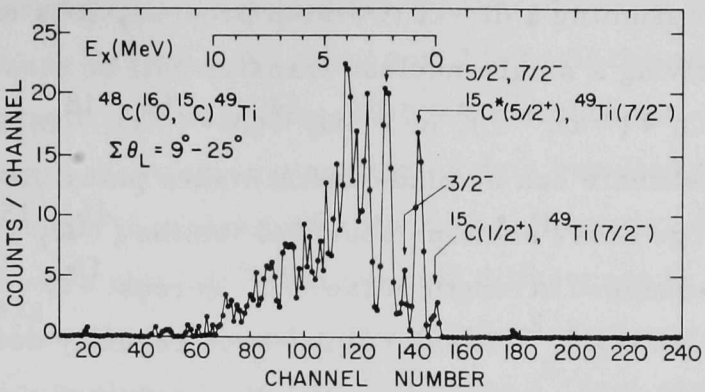

Fig. 8. Angle-integrated ^{15}C spectrum observed in the ^{16}O+^{48}Ca reaction at 56 MeV.

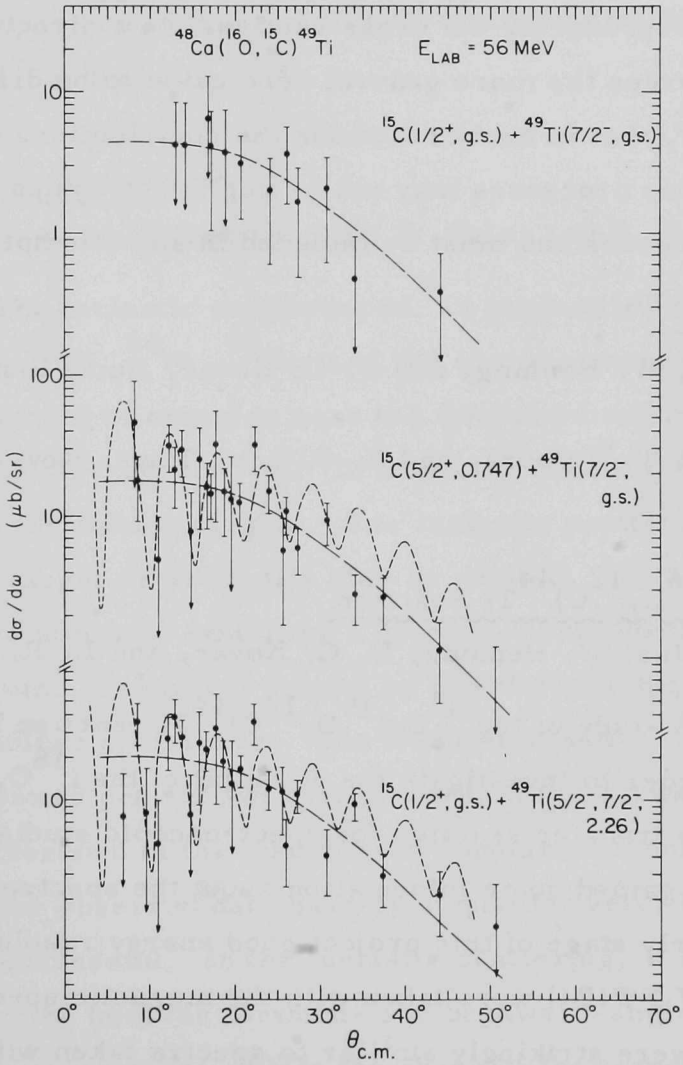

Fig. 9. Angular distributions observed in the (^{16}O,^{15}C) reaction. The curves are to guide the eye (see text).

Assuming a direct two-step process, it is expected that transitions involving a single-nucleon transfer will be most probable [e.g., (^{16}O, ^{17}O) → (^{17}O, ^{15}C), or (^{16}O, ^{14}C) → (^{14}C, ^{15}C)]. A crude cross section estimate can be made which makes plausible the somewhat surprizingly large cross sections observed for the (^{16}O, ^{15}C) reaction, as well as the enhanced strength of the ^{15}C* versus ^{15}C$_{g.s.}$ transition to the ^{49}Ti ground state.[2] These results have recently been confirmed by more sophisticated calculations in which an assumed sequential two-step reaction process is able to reproduce both the strengths and the shapes of the measured angular distributions.[3] The success of the calculations in reproducing the cross sections via a direct two-step process re-enforces the more general conclusion to be drawn from our results, namely, that in many reactions the contributions of the more complex multistep processes may not be negligible compared to the single-step processes and must be included in any attempt to predict the total cross section.

---

[2] B. Zeidman, W. Henning, and D. G. Kovar, Nucl. Instrum. Methods 118, 361 (1974).

[3] T. Udagawa, T. Tamura, and K. S. Low, Phys. Rev. Lett. 34, 30 (1975).

h. The ^{40}Ca(^{16}O, ^{12}C)^{44}Ti Reaction

J. R. Erskine, W. Henning, D. G. Kovar, and L. R. Greenwood*

A study of the ^{40}Ca(^{16}O, ^{12}C)^{44}Ti reaction has been performed in order to investigate the potential of the (^{16}O, ^{12}C) reaction as an α-particle transfer reaction for spectroscopic studies in the fp shell. We also gained some information about the spectroscopy of ^{44}Ti. At an early stage of this project good energy resolution spectra (75-keV FWHM) were taken with the magnetic spectrograph. These spectra were strikingly similar to spectra taken with the ^{40}Ca(^{6}Li, d)^{44}Ti reaction. In order to make a better test of this

---

* Northwestern University, Evanston, Illinois.

reaction, angular distribution data were measured $8^{\circ} \leq \theta_L \leq 33^{\circ}$ and 56-MeV bombarding energy. We were not able to fit the angular distribution data with the conventional DWBA calculations. Optical-model potentials which fit elastic-scattering data resulted in DWBA curves which strongly disagreed with the data. However, fairly good DWBA fits were obtained when the real diffuseness in the outgoing channel was arbitrarily increased. The relative spectroscopic factors obtained agreed to within a factor of 2—3 of the (^{6}Li,d) spectroscopic factors. However, the (^{6}Li,d) analysis did not use a full recoil, DWBA code and consequently the spectroscopic factors may not be trustworthy. A definitive comparison of these reactions awaits a new DWBA analysis of the (^{6}Li,d) data.

i. Li-Induced Reactions

C. L. Fink, A. M. Friedman,* D. S. Gale, and B. Zeidman

The inelastic scattering of ^{7}Li projectiles incident upon targets of ^{58}Fe, ^{58}Ni, ^{64}Ni, ^{64}Sn, and the even-neodymium isotopes has been investigated at energies near the Coulomb barrier (18—24 MeV for A ≈ 60 and 32 MeV for the Nd). In addition, the (^{7}Li,^{6}Li) reactions were studied on the lighter targets. For inelastic scattering at these energies either target or projectile may be excited, but the angular distributions are similar, exhibiting a grazing-bump shape with a dip near the maximum. The dip is caused by interference between Coulomb and nuclear excitations. The transfer reactions, however, are strongly forward peaked and oscillate with a far-forward-angle behavior characteristic of the transferred angular momentum. Attempts to fit the observed data have been qualitatively, but not quantitatively, successful. In the inelastic scattering, it has not been possible to describe both the forward- and backward-angle data with the same set of parameters. While the shape of the transfers is

---

*Chemistry Division, ANL.

reproduced by DWBA calculations, there is a definite angular shift between the data and calculation. Attempts to resolve these discrepancies with more complete calculations have not as yet been successful.

2. REACTION SYSTEMATICS AND CROSS SECTIONS

The interaction between a heavy-ion projectile and a complex-nucleus target generates a system with many degrees of freedom that cannot be explicitly considered in a theoretical description. In order to understand the relationships between the degrees of freedom and reaction mechanisms, systematic studies of reactions and cross sections have been undertaken with the use of the newly-developed time-of-flight telescope system.

The optical-model formalism provides a method for describing elastic scattering by an equivalent central potential which includes absorption, i. e., removal of flux from the incident channel. There has been considerable effort expended in studying elastic scattering and transfer reactions for poorly matched cases. Such interactions have been measured with both our magnetic spectrograph and with the time-of-flight telescope. These experiments have now demonstrated that simple optical-model descriptions are doomed to failure. More elaborate methods, such as coupled-channels calculations, have been suggested and applied in a few cases. These calculations require considerably more effort and, at present, the efficacy of these approaches is undetermined. In order to examine transfer reactions and scattering under conditions where the reaction is well understood, our time-of-flight telescope has been used in a systematic study of oxygen-induced reactions at energies below and near the Coulomb barrier, where the semiclassical appraoch is valid. A major conclusion of this study is that some of the basic assumptions of DWBA are not justified in heavy-ion reactions.

While significant progress has been made by considering the simplified aspects of heavy-ion reactions, the complexity inherent in the interaction between two complex nuclei precludes full understanding on the basis of simple known models. The artificial separation of simple and complex direct reactions requires highly speculative models and assumptions and has generated considerable discussion regarding the relative importance of complex or multistep reactions. In a unique experimental study of a reaction that can proceed only through complex processes, our measurements with the time-of-flight telescope have shown that these complex transfers are comparable in intensity to simple

transfer processes. Accordingly, the importance of complex transfer mechanisms has been established.

a. The Optical Potential in Heavy-Ion Transfer Reactions

Y. Eisen, J. R. Erskine, W. Henning, D. G. Kovar, and B. Zeidman

Elastic scattering in the nuclear systems $^{42,48}Ca + ^{16}O$ and $^{45}Sc + ^{15}N$, and single proton transfer reactions induced by ^{15}N, ^{16}O, and ^{19}F on ^{48}Ca have been measured at projectile energies around 56 MeV and compared to optical model and DWBA calculations. The purpose of this investigation was to study the role of the optical potential in heavy-ion-induced transfer reactions. We find that the ambiguities that exist in the optical-model parameters for the elastic scattering predictions persist for the DWBA transfer calculations. This is demonstrated in Fig. 10. The elastic scattering angular distribution for the $^{48}Ca + ^{16}O$ system has been fitted by various optical potential parameter sets yielding equivalent results (Fig. 10a). Transfer predictions for the $^{48}Ca(^{16}O, ^{15}N)^{49}Sc$ reaction as calculated with the DWBA using the same potential sets also show a great similarity in the angular distribution (Fig. 10b). If we compare the transfer predictions to the experimental results, we find that angular distributions are well reproduced by DWBA under conditions of well-matched channels, i.e., cases where the dominant partial waves in the ingoing and outgoing channels overlap strongly. Under conditions of mismatch, deviations occur that cannot be accounted for by the same optical parameter sets that are required to reproduce elastic scattering. Whether these discrepancies can be removed by extending the DWBA formalism or by introducing new reaction mechanisms is subject to further studies.

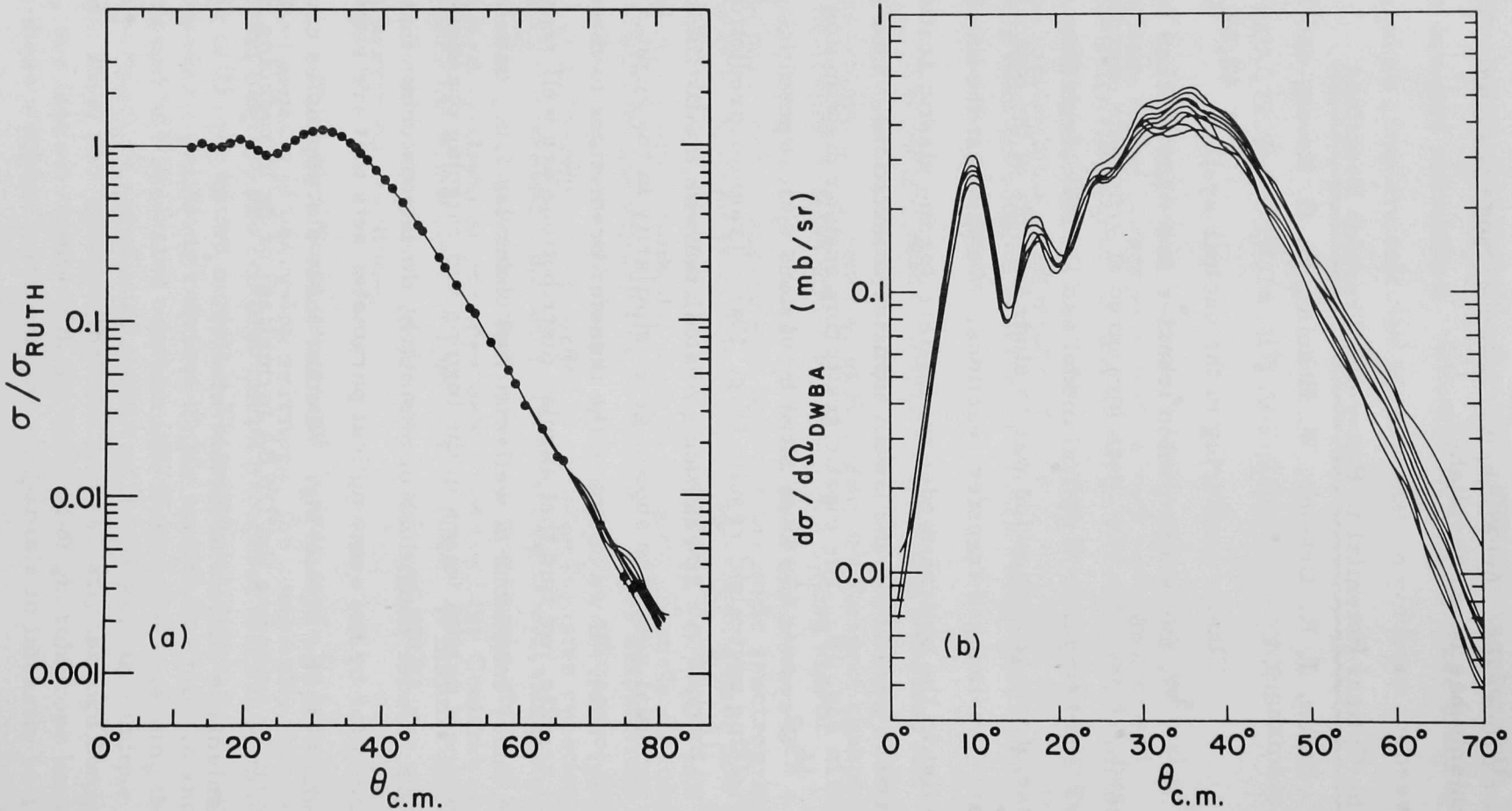

Fig. 10. (a) Optical-model fits to the elastic scattering angular distribution of the system $^{48}Ca + ^{16}O$ at 56 MeV for various parameter sets. (b) DWBA predictions with code LOLA by R. De Vries for the $^{48}Ca(^{16}O,^{15}N)^{49}Sc$ reaction using the various optical potential sets from the elastic scattering fits in (a).

b. ^{16}O and ^{18}O Induced Reactions on ^{118}Sn at the Coulomb Barrier

Y. Eisen, W. Henning, H.-J. Körner, D. G. Kovar, J. P. Schiffer, S. E. Vigdor, and B. Zeidman

All transfer channels and inelastic scattering have been measured for ^{16}O and ^{18}O induced reactions on ^{118}Sn in the energy range $50 \leq E_{lab} \leq 62$ MeV (energies below and slightly above the Coulomb barrier). The objective was the determination of the fraction of the total cross section that goes by direct channels. Separation of the various reaction channels was achieved through the use of a ΔE-E surface-barrier detector time-of-flight telescope. The differential cross sections of the various single- and multinucleon transfers show an exponential fall-off as a function of the distance of closest approach. Summation of the transfer and inelastic cross sections yields the total quasi-elastic cross section; this is a large fraction ($\geq 50\%$) of the total cross section over the energy range studied. The quasi-elastic cross section is also comparable to the elastic cross section for values of the distance of closest approach D, where most of the transfer cross sections originate. This is illustrated in Fig. 11. The results imply that some of the basic assumptions made in the usual DWBA analyses of heavy-ion reactions are incorrect. Further measurements are planned to explore the quantitative validity of these results for different heavy-ion projectiles, and over as large a range of energy and target nuclei as is practical.

c. Cross Sections for Reactions Induced by ^{16}O on Ca Isotopes

Y. Eisen, H. T. Fortune, W. Henning, D. G. Kovar, S. E. Vigdor, and B. Zeidman

The reaction cross sections for a large number of exit channels resulting from the interaction of ^{16}O with Ca isotopes have been measured at $E(^{16}O) = 56$ MeV using the ΔE-E time-of-flight system. This kind of information is important for a complete understanding of the complex interaction between two heavy ions. We have measured

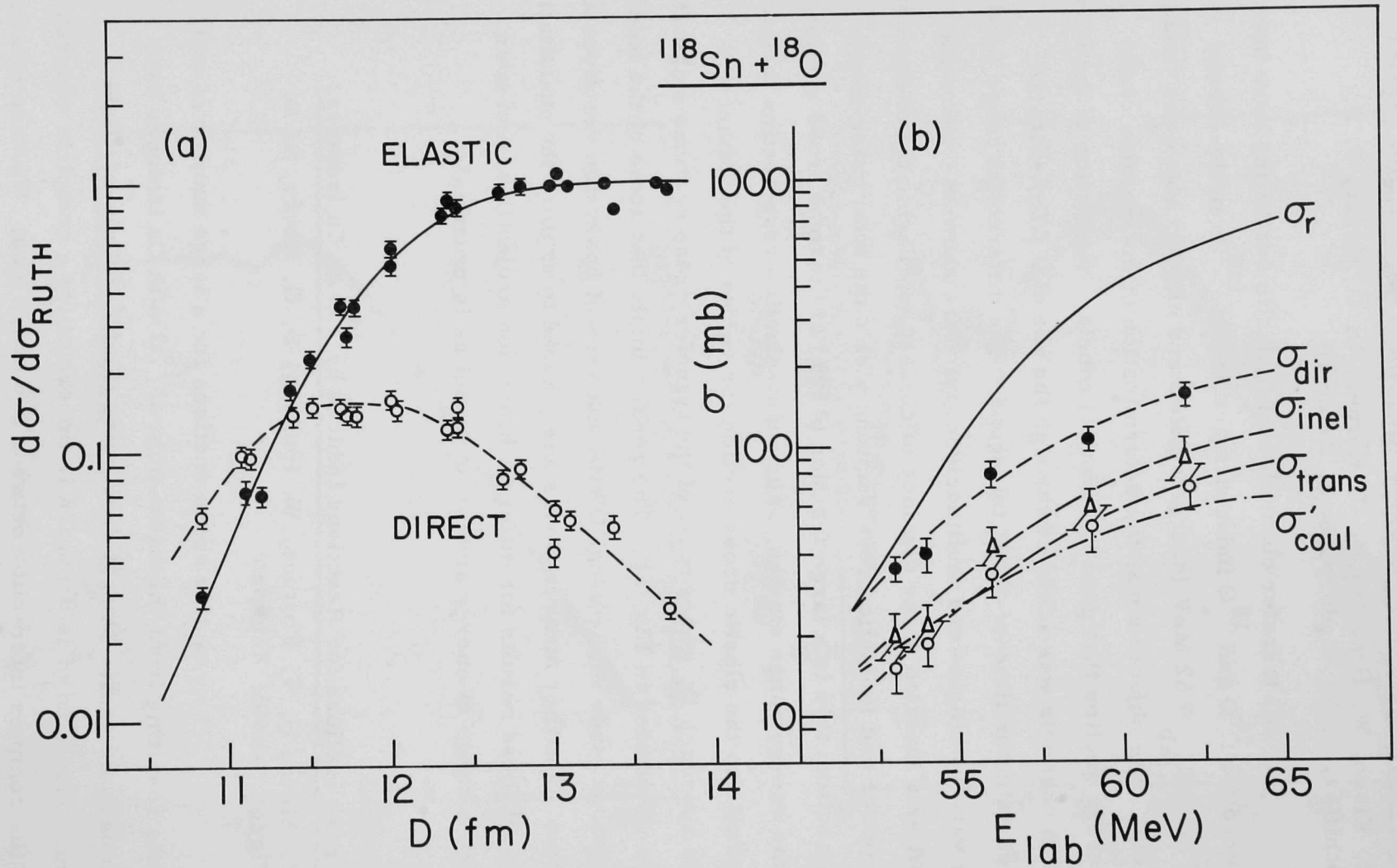

Fig. 11. Ratio of elastic and quasi-elastic cross section to Rutherford cross section for the reaction $^{118}Sn + ^{18}O$ as a function of distance of closest approach D.

energy spectra for outgoing particles from B through Mg over a large angular range. The cross sections integrated over excitation energy show forward peaked angular distributions for all transfer channels as is shown in Fig. 12. Integration over all angles and summation over all channels yields the total transfer cross section which is approximately 10% of the total reaction cross section. The balance is presumed to result in compound nucleus formation followed by boil-off. In order to check these expectations, preliminary studies of compound nucleus cross sections have been performed. Within errors, the measured cross sections are in agreement with calculations. Direct measurements of the masses of the compound products using a pulsed beam and TOF are planned shortly.

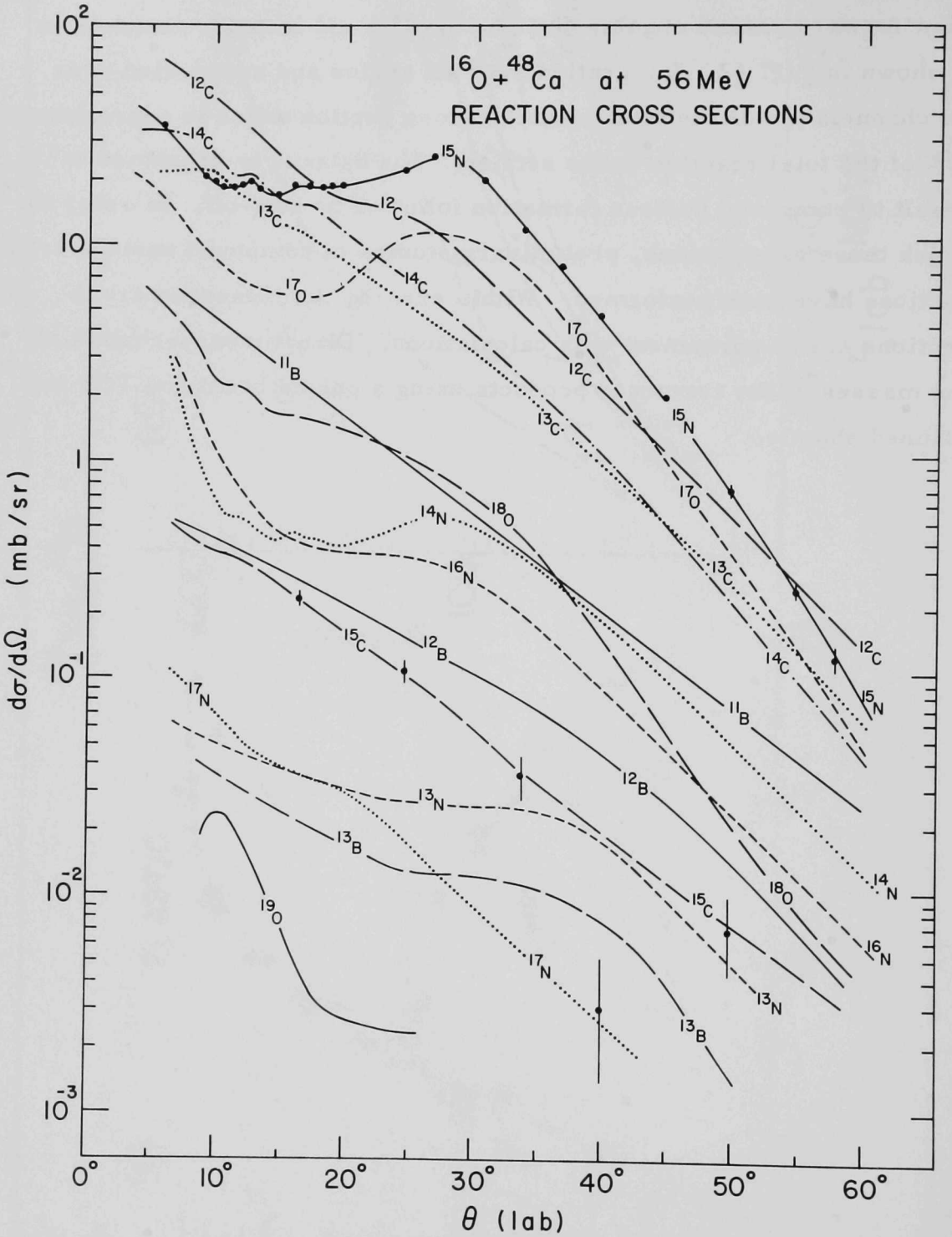

Fig. 12. Angular dependence of transfer cross sections for $^{16}O + ^{48}Ca$ at $E(^{16}O) = 56$ MeV.

3. RESONANCE PHENOMENA

The complexity of heavy-ion interactions is nowhere more evident than in studies of resonance effects. The observation of strong resonances, frequently dominated by a single partial wave at very high excitation energies in the compound nuclear system, is clear evidence for the existence of highly correlated structures involving many nucleons. These structures are, accordingly, best investigated through the use of heavy-ion probes.

Recent studies at Argonne of excitation functions for the $^{12}C(^{12}C,\alpha)^{20}Ne$ reaction reveal that both direct and compound processes contribute to the population of most levels. Statistical fluctuations are primarily responsible for the strong resonant behavior of the cross sections. At 19.7 MeV in the $^{16}O+^{12}C$ system, there is a strong nonstatistical resonance that was originally observed in this Laboratory during the course of studies of elastic-scattering systematics. The structure of this J=14 resonance has been probed by time-of-flight telescope measurements of all final states of this nuclear system. A study is also under way to measure the spins of states in ^{28}Si, with large $^{16}O+^{12}C$ parentage, at lower excitation energies via the $^{16}O(^{16}O,\alpha)^{28}Si$ reaction.

a. $^{12}C(^{12}C,\alpha)^{20}Ne$ Excitation Functions and Angular Distributions

L. R. Greenwood,* R. E. Segel, K. Raghunathan, M. A. Lee, H. T. Fortune, and J. R. Erskine

Excitation functions have been measured at a laboratory angle of 5° over an incident energy range of 18—25.5 MeV (c.m.) for the $^{12}C(^{12}C,\alpha)$ reaction leading to about 30 levels in ^{20}Ne (E_x = 0—20 MeV). Angular distributions were measured at 5 energies. An Ericson fluctuation analysis yields the result that most levels are populated by a large nonstatistical reaction component. A significant compound-nuclear component is also present, with correlation widths on the order of 150—250 keV (c.m.). The energy-averaged cross sections have been compared with statistical compound-nuclear (Hauser-Feshbach) calculations. This comparison shows clearly the presence of a strong

*Northwestern University, Evanston, Illinois.

direct-reaction mechanism, especially for the members of the proposed 8p-4h band (at 7.196, 7.834, 9.040, and 12.16 MeV). A pronounced minimum in the excitation functions is evident at $E_{c.m.} = 19.2$ MeV, near the recently-reported strong resonance in the $^{12}C(^{12}C,p)^{23}Na$ channel. Other correlated effects also appear to be present at specific energies, but the cross correlations, calculated for the entire energy range, are largely statistical.

b. Inelastic Scattering of $^{16}O + ^{12}C$ Around $E_{c.m.} = 19.7$ MeV

J. R. Erskine, W. Henning, and P. Sperr

The inelastic scattering to various excited states has been measured for $^{16}O + ^{12}C$ around $E_{c.m.} = 19.7$ MeV with high resolution using the split-pole magnetic spectrograph. Figure 13 shows part of the excitation-energy spectrum taken with a proportional counter at $E_{c.m.} = 19.27$ and 19.70 MeV at $\theta_{lab}(^{12}C) = 7^{o}$. The main purpose of the measurement was to resolve the 6.050-MeV (0^{+}) and 6.131-MeV (3^{-}) states and study which of these states shows a correlation with the nonstatistical resonant behavior of the elastic scattering at $E_{c.m.} = 19.7$ MeV. From these measurements we find that at $\theta_{lab}(^{12}C) = 7^{o}$ the 3^{-} state resonates strongly, whereas the 0^{+} state shows smooth behavior over the resonance region. These results do not support an explanation for the $E_{c.m.} = 19.7$-MeV resonance, which involves an α-particle exchange mechanism.

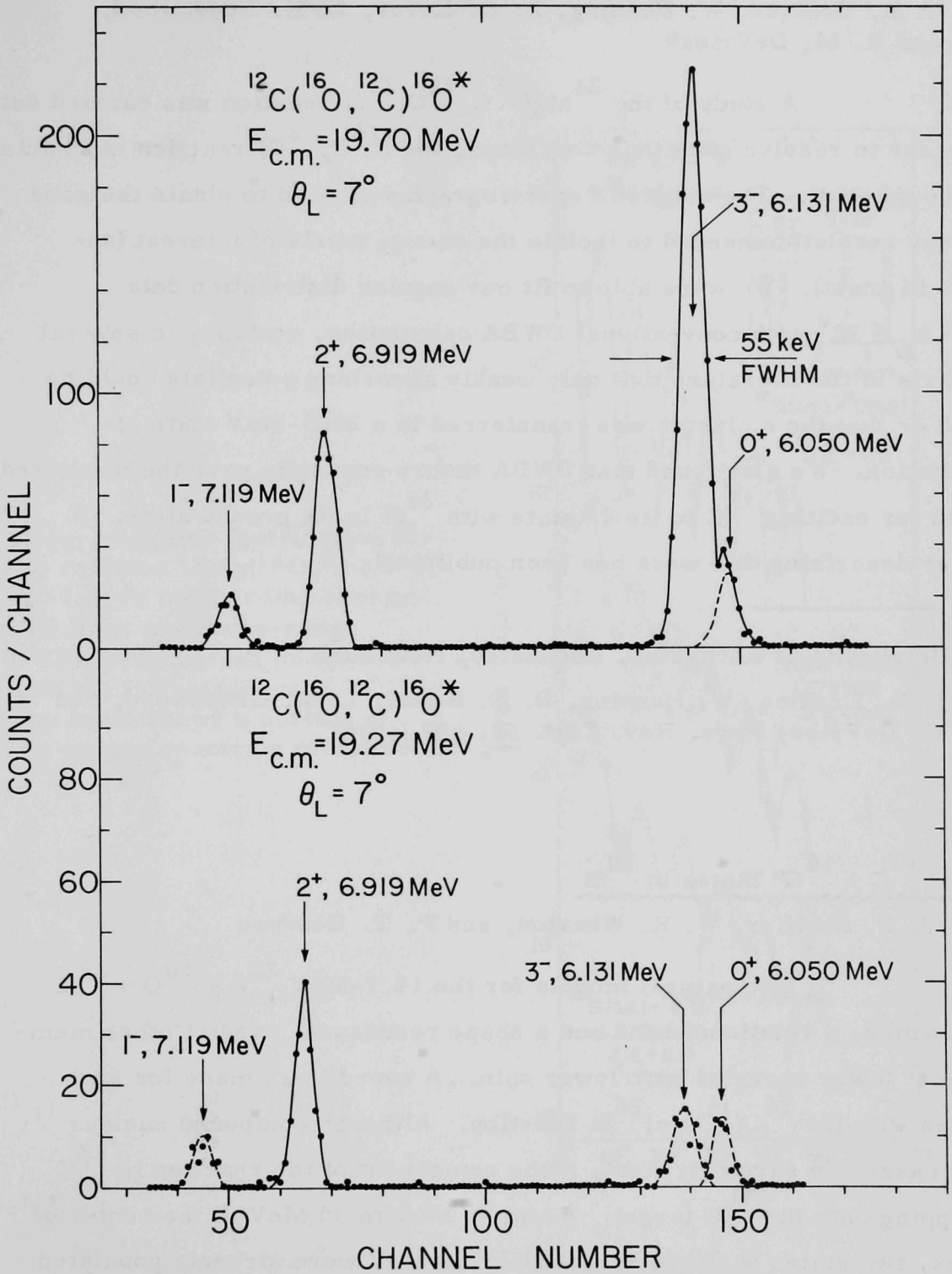

Fig. 13. Part of the energy spectrum of outgoing ^{12}C ions observed in the reaction $^{16}O + ^{12}C$ at θ_{lab} (^{12}C) = 7° for two bombarding energies on and off the 19.70-MeV resonance.

c. The $^{24}Mg(^{16}O, ^{12}C)^{28}Si$ Reaction

J. R. Erskine, W. Henning, D. G. Kovar, L. R. Greenwood, and R. M. DeVries*

A study of the $^{24}Mg(^{16}O, ^{12}C)^{28}Si$ reaction was carried out in order to resolve questions concerning the $(^{16}O, ^{12}C)$ reaction mechanism in the sd shell. The magnetic spectrograph was used to obtain the good energy resolution needed to isolate the energy levels of interest (see Fig. 14 inset). We were able to fit our angular distribution data $4^{\circ} \leq \theta_L \leq 32^{\circ}$ with conventional DWBA calculation, contrary to several reports in the literature that only weakly absorbing potentials could be used or that the α cluster was transferred in a 28.5-MeV state of excitation. We also found that DWBA theory correctly gave the measured yield for exciting ^{12}C to its 2^+ state with ^{28}Si in its ground state. A letter describing this work has been published.[1]

---

*University of Rochester, Rochester, New York.

[1] J. R. Erskine, W. Henning, D. G. Kovar, L. R. Greenwood, and R. M. DeVries, Phys. Rev. Lett. 34, 680 (1975).

d. "$^{12}C + ^{16}O$" States in ^{28}Si

J. P. Schiffer, W. R. Wharton, and P. T. Debevec

Two natural models for the 19.7-MeV $^{12}C + ^{16}O \rightarrow ^{28}Si$ resonance, a rotational band and a shape resonance, predict other members at lower energies with lower spin. A search was made for such states with the $^{16}O(^{16}O, \alpha)^{28}Si$ reaction. Although compound nuclear processes are surely present, some component of the reaction is ^{12}C stripping onto the ^{16}O target. From 26 MeV to 30 MeV in the center of mass, two states at 21.64 MeV and 23.85 MeV were strongly populated. The yields of these states fluctuated with bombarding energy; however, they were by far the strongest states seen over the entire region.

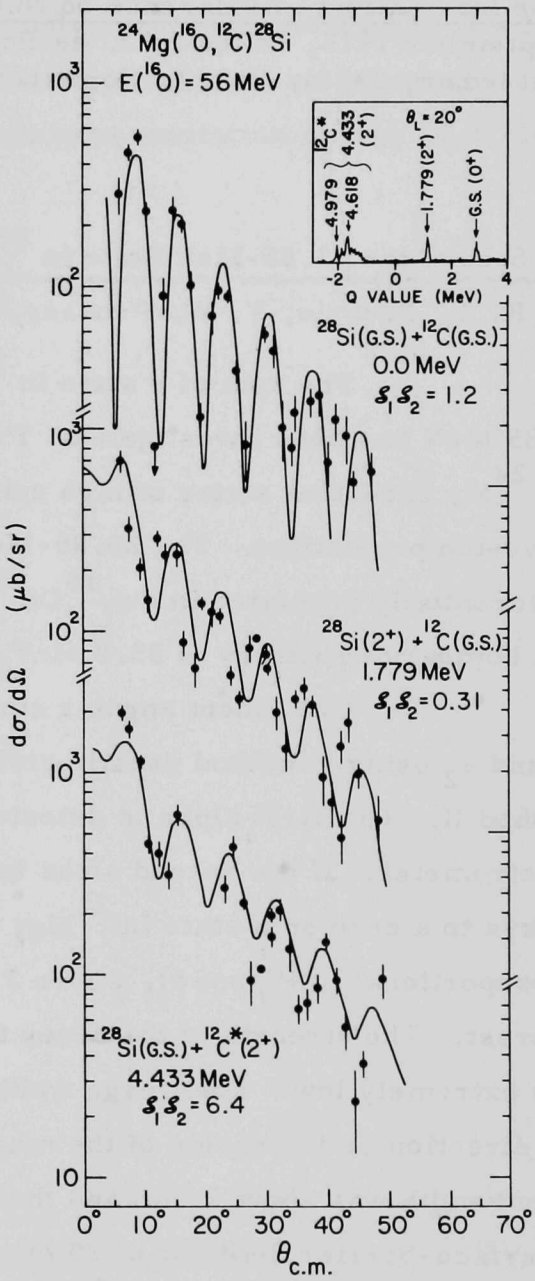

Fig. 14. Angular distribution for the reaction $^{24}Mg(^{16}O,^{12}C)^{28}Si$ at 56-MeV bombarding energy. The lines are finite-range DWBA calculations computed with the full-recoil code LOLA. The inset shows a portion of the energy spectrum measured at $\theta_L = 20^o$.

Angular distributions were consistent with $1/\sin\theta$. A report of this work was given at the International Conference on Nuclear Structure.[1]

[1] W. R. Wharton, P. T. Debevec, and J. P. Schiffer, in Proceedings of the International Conference on Nuclear Physics, Munich, 27 August-1 September 1973, edited by J. de Boer and H. J. Mang (North-Holland, Amsterdam, 1973), Vol. 1, Contributed Papers, p. 541.

e. Spin of the 23.85-MeV State in ^{28}Si

R. L. Boudrie, F. W. Prosser,* and P. T. Debevec

The spin of a state in ^{28}Si at an excitation energy of 23.85 MeV has been investigated. Previous studies by others in ^{20}Ne and ^{24}Mg show that states of high spin are preferentially populated with heavy-ion projectiles. The 23.85-MeV state has been seen here to be preferentially populated in the $^{16}O(^{16}O,\alpha_1)^{28}Si^* \rightarrow {}^{24}Mg + \alpha_2$ reaction at a bombarding energy of 53.8 MeV.

Coincident angular correlations are obtained between α_1 and α_2 using a method usually referred to as Litherland and Ferguson Method II. The first alpha is detected at 0° with the recently converted 0° spectrometer. If the second alpha in coincidence with the first alpha decays to a zero spin state in ^{24}Mg, the resulting angular distribution is proportional to $P_J^2(\cos\theta)$, where J is the spin of the state in ^{28}Si of interest. The strength of the decay to a zero-spin state in our case was extremely low. The image width in the direction perpendicular to the direction of dispersion of the magnet was about 16 mm since the object width was about 2 mm and the magnification in that direction is 8. A surface-barrier detector of 20 mm diameter had to be used at a predetermined position along the focal plane in order to accept this large width. Two position-sensitive detectors in the target chamber, each covering an angular range of 50° in the lab, are used to determine the

*University of Kansas, Lawrence, Kansas.

angular distribution of the second alpha. Four parameter event-by-event data was recorded on magnetic tape.

Least-squares fits to a constant plus $P_J^2(\cos\theta)$, integrated over the finite solid angle of slices of the position detector, were made to the data for various values of J. The only reasonable fit was for J = 5. Work is continuing to assure that the background from neighboring states in ^{28}Si is isotropic. Another strong state at excitation energy 21.6 MeV in ^{28}Si will be investigated.

B. INSTRUMENTATION

The development of improved techniques form the basis for continued progress in heavy-ion research. The large number of reaction channels coupled to an enormous range of cross sections demands detection techniques capable of high selectivity over a wide dynamic range. Improvements in two major experimental systems, the magnetic spectrograph and the ΔE-E time-of-flight telescope, have recently resulted in increased performance capabilities.

a. Time-of-Flight Mass Identification System

Y. Eisen, W. Henning, D. G. Kovar, S. E. Vigdor, and B. Zeidman

We have developed a time-of-flight (TOF) mass identification system that retains all the virtues of the conventional ΔE-E surface-barrier detector telescope while providing excellent mass resolution over a wide range of mass and energy.[1]

In the TOF system, the ΔE detector and the E detector are physically separated by 25 cm. The ΔE and E signals are processed with conventional analog circuitry. In order to obtain sufficient precision in the time measurement, specially built fast circuits which process the E and ΔE pulse information are used to generate start and stop signals for a commercial time-to-amplitude converter. A time resolution of 70 picoseconds has been obtained for 55-MeV ^{16}O ions whose time of flight is $\approx$14 ns between the detectors.

The raw signals ΔE, E, and t are processed with analog circuitry to yield the energy (E_{total}), charge (Z), and mass (M) of the detected particle which are stored directly in the computer memory. The energy E_{total} is given by $\Delta E + E$. The charge Z is determined by performing a multiplication of the form $\Delta E \times E$, where the product is approximately proportional to MZ^2. The mass spectrum results from analog multiplications to form the product $t^2 \times E$ which is proportional

[1] B. Zeidman, W. Henning, and D. G. Kovar, Nucl. Instrum. Methods 118, 361 (1974).

to M. The data are stored in an external computer memory in a 3-parameter matrix of dimensions 4 (Z) $\times$ 64 (M) $\times$ 256 (E_{total}). The selection of a mass peak in one of the Z groups yields a 256 channel display of the energy spectrum for a single isotopic species.

The use of direct memory access, together with pileup rejection, allows data to be taken at rates in excess of 10^4 events/s with no degradation in quality. These high data rates permit the study of low cross-section reactions within reasonable running times.

Compared to conventional detector telescopes, this new TOF system has equivalent solid angle and efficiency, equal or better energy resolution, and vastly better mass resolution.

During the past year the time-of-flight mass identification system has been used extensively for the investigations of heavy-ion-induced reactions. In experiments already performed, it was found that the high selectivity and low background of the system allows for investigation of nuclei far from the line of stability produced through transfer of many nucleons. Although MZ^2 provides excellent Z separation near the line of stability, ambiguities may arise for exotic low-cross-section reactions when attempting to distinguish, for example, ^{18}N from ^{14}O. To solve this problem, new arithmetic units have been constructed to perform the operation $(MZ^2 \times 1/M)^{1/2} = Z$. In addition to yielding unambiguous Z selection, the procedure also linearizes the Z scale and thereby reduces the dynamic signal range required. The dynamic range of the system has also been increased by selectively routing more than one Z into a single quadrant of the memory. This is possible when the masses of different elements do not overlap, e.g., B, F. In this way up to eight different charges may be stored. As shown in Fig. 15, for ^{16}O incident upon ^{44}Ca, data from reactions yielding B to Mg (Z = 5 to 12) and masses from 10 to 24 can be obtained concurrently during a single run.

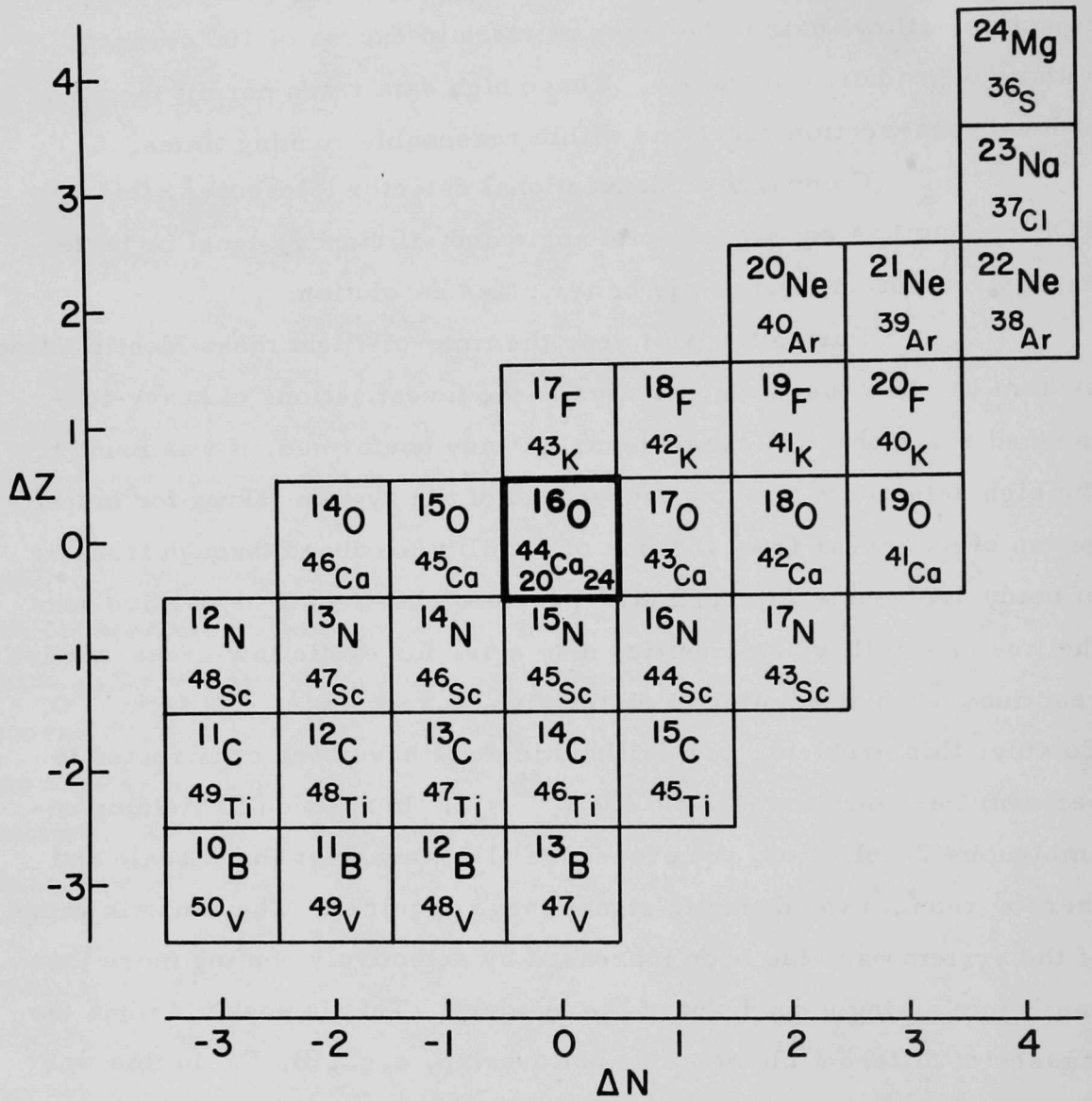

Fig. 15. Nuclei detected with the TOF telescope. The axes indicate the number of nucleons transferred to the projectile ^{16}O.

b. A New Heavy-Ion Focal Plane Detector for the Magnetic Spectrograph

J. R. Erskine, T. H. Braid, and J. C. Stoltzfus*

A new type of focal plane detector is being developed for the study of heavy ions with the split-pole magnetic spectrograph. A novel configuration of ionization chamber and resistive-wire proportional counter offers major improvements in detection capabilities, particularly in particle identification. With this new detector the excellent energy resolution and large angle capabilities of the magnetic spectrograph can be applied to heavy-ion reaction studies. In the new detector heavy ions are stopped in the gas of a 50-cm-long by 13-cm-deep gridded ionization chamber. The electron swarm drifts to a split anode plate where a resistive-wire proportional counter is used to measure position along the focal plane. A second resistive-wire proportional counter is used to determine position further along the ion trajectory and thus to measure incident angles. Two ΔE signals are also obtained from the split anode. Position resolution of 1 mm, ΔE resolution of 4% and E_{total} resolution of 1% have been measured. A cross section view of the counter is shown in Fig. 16.

*Beloit College, Beloit, Wisconsin.

c. Conversion of the Broad-Range Spectrograph

R. L. Boudrie and F. W. Prosser*

The Browne-Buechner broad-range magnetic spectrograph has been converted to a double-focussing magnetic spectrometer with the addition of a single element quadrupole lens. The spectrometer is positioned at 0° to do angular correlation experiments of the type usually referred to as Litherland and Ferguson Method II. The addition of the quadrupole between the target and main magnet increases the solid angle of acceptance by an order of magnitude. The resolution and aberration are preserved to a great extent especially at angle of deflection 90°.

*University of Kansas, Lawrence, Kansas.

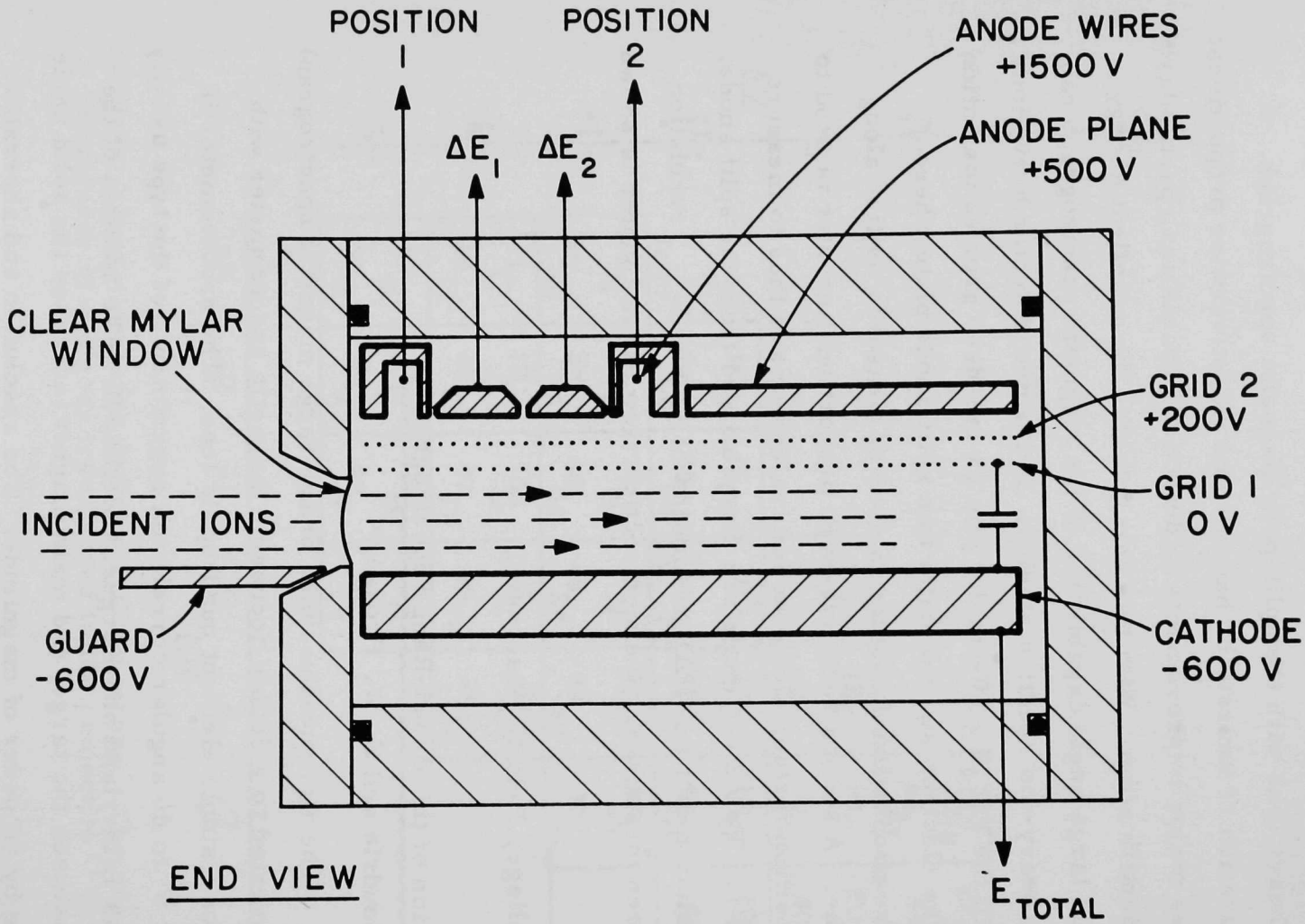

Fig. 16. Cross section of a new type of focal plane detector for heavy ions. Ions incident from the left are stopped in isobutane gas inside an ionization chamber. The resulting electron swarm drifts toward the double grid structure where total energy and ΔE signals are produced. Information about the position along the focal plane and the incident angle is measured by resistive wire proportional counters imbedded in the anode plane.

With the use of an electronic detector in the focal plane and this increase in solid angle, low-coincidence-rate experiments have been realized.

A new 10-in. diameter target chamber has been installed. One side of the cylindrical wall of the chamber is a uniform thickness of 0.125 in. to reduce γ-ray absorption. NaI detectors, 3 × 4 in. in size, can be centered anywhere between 30° and 160° with respect to the beam axis. Mounts have been made for positioning surface barrier and position-sensitive detectors inside the chamber.

A new vacuum box at the exit of the magnet has been installed. Its volume has been reduced by about $\frac{1}{3}$ since the useful distance along the focal plane is decreased. At a particular field setting double-focussing at the focal plane is possible for only one energy. Pumping is also done at the vacuum box, where vacuum of about 10^{-6} Torr are reached. A Faraday cup is positioned at the base of the vacuum box with an adjustable space to allow the particular energy range of reaction particles to reach the focal plane. Position-sensitive detectors of the solid state or gas-proportional type have been used in the focal plane.

The controls for the quadrupole and main magnet have been coupled. After selecting the current ratio of the quadrupole and main magnet, the quadrupole is made a slave to the main magnet. The magnet controls have been modified for minimum operator interaction.

d. Workshop on Fast Timing in Heavy-Ion Physics, Argonne National Laboratory, June 7—8, 1974

B. Zeidman, L. M. Bollinger, W. Henning, D. G. Kovar, M. H. Macfarlane, and J. P. Unik*

The workshop provided a bridge between purely technical aspects such as techniques, circuits, etc., and the physics results both experimental and theoretical. Of the 85 participants, more than a third came from foreign institutions. The attendance, which exceeded

*Chemistry Division, ANL.

original estimates, is indicative of the interest in the techniques and application of fast timing (1 ns or less) to studies in heavy-ion physics.

The workshop was divided into three sections: (1) State of the Art, (2) Accelerators, and (3) Prospects for Future Research. In each section, there were discussions of techniques, data, and theoretical implications. In the area of reaction studies, use of time of flight, in detector telescopes or in conjunction with magnetic spectrometers, yields unprecedented particle identification along with good energy resolution, particularly for low cross-section reactions. It was also shown that the superconducting cyclotrons and linear accelerators will generate very short beam bursts at high repetition rates with a little reduction in average beam intensity. Other talks emphasized possibilities for high-quality pulsed beams from Tandem Van de Graaffs. The final session consisted of talks on prospects for future research; new detectors, limitations in present detectors, and new developments were discussed.

There was spirited participation from many of the attendees, the format being conducive to open discussion. It was generally agreed that future research in heavy-ion physics will be strongly based upon the use of pulsed beams and timing measurements.

III. LIGHT-ION PHYSICS

INTRODUCTION

The investigations included within this experimental program are carried out mainly at the FN Tandem Van de Graaff accelerator, except that one important set of studies makes use of the 4-MV Dynamitron. The 60-in. cyclotron operated by the Chemistry Division and accelerators at other institutions are also used occasionally.

Until the advent of heavy-ion research and medium-energy research, investigations with low-energy light ions formed the core of nuclear physics. Although much of our effort has been transferred to these new areas, our light-ion program continues to include a wide range of research topics. We continue to regard low-energy charged-particle physics as an important contributor to the development of nuclear science as a whole, and we do not foresee that the balance between light-ion research and the other main areas of nuclear research in the Physics Division will change much during the next two years.

Important new activities started during the past year are the following.

(a) A program of measurements of astrophysical interest was begun. (For convenience, all of this work is described here even though some of it makes use of heavy-ion projectiles.)

(b) A program to measure low-energy charged-particle cross sections of interest in CTR applications was started with a systematic investigation of the ^{6}Li+d system.

(c) A collaboration with a group from Purdue University started on a series of measurements of magnetic moments of excited nuclear states. This work complements measurements of transition probabilities carried out at Argonne in the past.

Special note should be made of the extensive and increasing use made of our tandem accelerator by outside users during the past year. This has been a healthy feature of our program and a number of collaborative ventures between Argonne staff and outside users have been undertaken. Information about outside-user experiments is given under Sec. IV.B.

Improvements in the performance of the tandem during the past year resulted in important gains for the experimental program. The main elements of these improvements are the installation of

a Pelletron charging chain and voltage-distribution system at the tandem (see Sec. IV. A. a).

The level of activity in the various parts of the light-ion physics program at this time may be inferred from the following table of relative effort in each part.

Activity	Relative Effort (%)
Program at Tandem (Total)	(66)
States of intermediate-mass nuclides	15
Structure of actinide nuclides	4
Reaction mechanisms	15
Effective residual interaction	2
Electromagnetic properties	15
Astrophysical measurements	15
Program at Cyclotron (Total)	(5)
Program at Dynamitron (Total)	(29)
Low-energy cross sections	24
Channeling	5

A. CHARGED-PARTICLE RESEARCH AT THE TANDEM

The investigations carried out with light-ion projectiles from the tandem included a wide range of topics, and many of these investigations interact strongly with other parts of our nuclear science program. In particular, there continues to be an unusual degree of constructive interaction between the experimental and theoretical programs. Also, many of the people who are involved in light-ion research also carry out heavy-ion and medium-energy research.

Several of the research topics in light-ion physics represent continuing efforts that extend back several years. The systematic study of nuclear structure in the $f_{7/2}$ and mass-90 regions is closely tied to theoretical work on shell-model calculations carried out at Argonne in recent years. The study of two-particle spectra near closed-shell nuclei extends back at least eight years and has included at least seven detailed, precise, and careful experiments. The work reported here is on the analysis of all available experimental data in an attempt to deduce a single effective force that can explain the data for nuclides throughout the periodic table.

Less effort than formerly is being devoted to the experimental program on nuclear properties of the heaviest nuclei, but it is continuing to provide the most detailed and careful spectroscopic information available in the actinide region.

An effort has been started to understand a long outstanding anomaly in nuclear reactions, the strong backward rise in cross section for elastic alpha scattering for targets near ^{40}Ca. Qualitatively new information has been obtained which shows that this effect cannot be explained in terms of compound mechanisms, but must be due to a direct term in the alpha-nucleus interaction. The other new activities in the program were listed earlier.

1. STATES OF INTERMEDIATE-MASS NUCLIDES

a. Studies of ^{39}Ar

R. E. Segel, P. T. Debevec, W. C. Corwin, and J. F. Tonn

Several reactions leading to the nucleus ^{39}Ar have been investigated. An investigation of the ^{37}Cl(^{3}He,p) reaction revealed that, while as expected the analog of the ^{39}Cl ground state stood out clearly,

the antianalog of this state, which should be stronger, was hardly in evidence. Careful analyses of the data revealed that the antianalog state is strongly fragmented and that the center of gravity lies $\sim 1\frac{1}{2}$ MeV higher than theory predicts.

The ^{40}Ar(p, d) reaction has been studied at a bombarding energy of 35 MeV. For these data the cyclotron at Michigan State University was used. Angular distributions were taken on states up to 6 MeV in ^{39}Ar. A study has been initiated at Argonne on the ^{43}Ca(^{16}O, ^{20}Ne) reaction. The results of this study will be compared to α pickup studies on the nearby even-Ca isotopes.

b. Study of ^{44,46}Sc by the ^{42,44}Ca(α, d)^{44}Sc Reaction

T. H. Braid, J. Manthuruthil,* and C. P. Poirier*

The purpose of this study is to make definite assignments of spin and parity to a number of known levels below $E_x = 3.3$ MeV. Experimentally, the (α, d) reaction presents difficulties in distinguishing the detected deuterons from spurious background caused either by the intense flux of elastically scattered α particles which is incident on the same region of the focal plane or by knock-on protons from absorbers. We have largely overcome the problem by using 27-MeV α's which are now available from the tandem, so that there is a greater separation between the magnetic rigidity of the α particles and the deuterons, and by taking care to minimize the hydrogenous material in the absorbers. Good data have now been obtained for both targets and are being analyzed. The data will provide a test of the purity of the $(f_{7/2})^n$ wave functions since the positive-parity states excited should be of odd spin.

---

*Aerospace Research Laboratories, Wright-Patterson Air Force Base, Dayton, Ohio.

c. (^{3}He,p) Reaction on $f_{7/2}$-Shell Nuclei

Gerald Hardie, David Gloeckner, L. Meyer-Schützmeister, and T. H. Braid

Using the Argonne split-pole magnetic spectrograph, the ^{43}Ca(^{3}He,p)^{45}Sc reaction was studied at E(^{3}He) = 17 MeV and with a range of angles from 7 to 55°. From the measured proton angular distributions the orbital angular momenta transferred (L_{np}) by the n-p pair were obtained. In addition, at the same bombarding energy and at several angles, cross sections for L_{np} = 0 and 0 + 2 were measured for the (^{3}He,p) reactions with ^{46,48,50}Ti and ^{45}Sc targets. For these and other f-shell nuclei, systematics of the cross sections for L_{np} = 0 and the sum of the differential cross sections for L_{np} = 0 + 2 will be discussed. In particular, we found that for odd-A targets the L_{np} = 0 + 2 sums are significantly smaller than the average for even-even f-shell targets. Two-particle spectroscopic amplitudes are calculated for transitions to ^{44}Sc, ^{45}Sc, ^{46}Sc, ^{47}Ti, ^{48}Sc, and ^{48}V using an $(f_{7/2})^n$ model and for transitions to ^{44}Sc, ^{45}Sc, ^{46}Sc, and ^{48}Sc using an $(f_{7/2}p_{3/2})^n$ model. Both models are based on an inert ^{40}Ca core. Zero-range distorted-wave Born-approximation calculations are then performed with these amplitudes. Reasonable agreement is found for the ratio of L_{np} = 0 + 2 to L_{np} = 0 strength with both models.

d. Level Structure of ^{76}As

J. F. Lemming,* J. Rapaport,* and A. J. Elwyn

The energy-level structure of ^{76}As has been studied by the ^{75}As(d,p) reaction with 12.0-MeV incident deuterons. Investigation of the low-lying levels in such doubly-odd nuclei can provide valuable information about the residual proton-neutron interaction. Furthermore, for ^{76}As in particular there has been recent interest in the structure of

---

*Ohio University, Athens, Ohio.

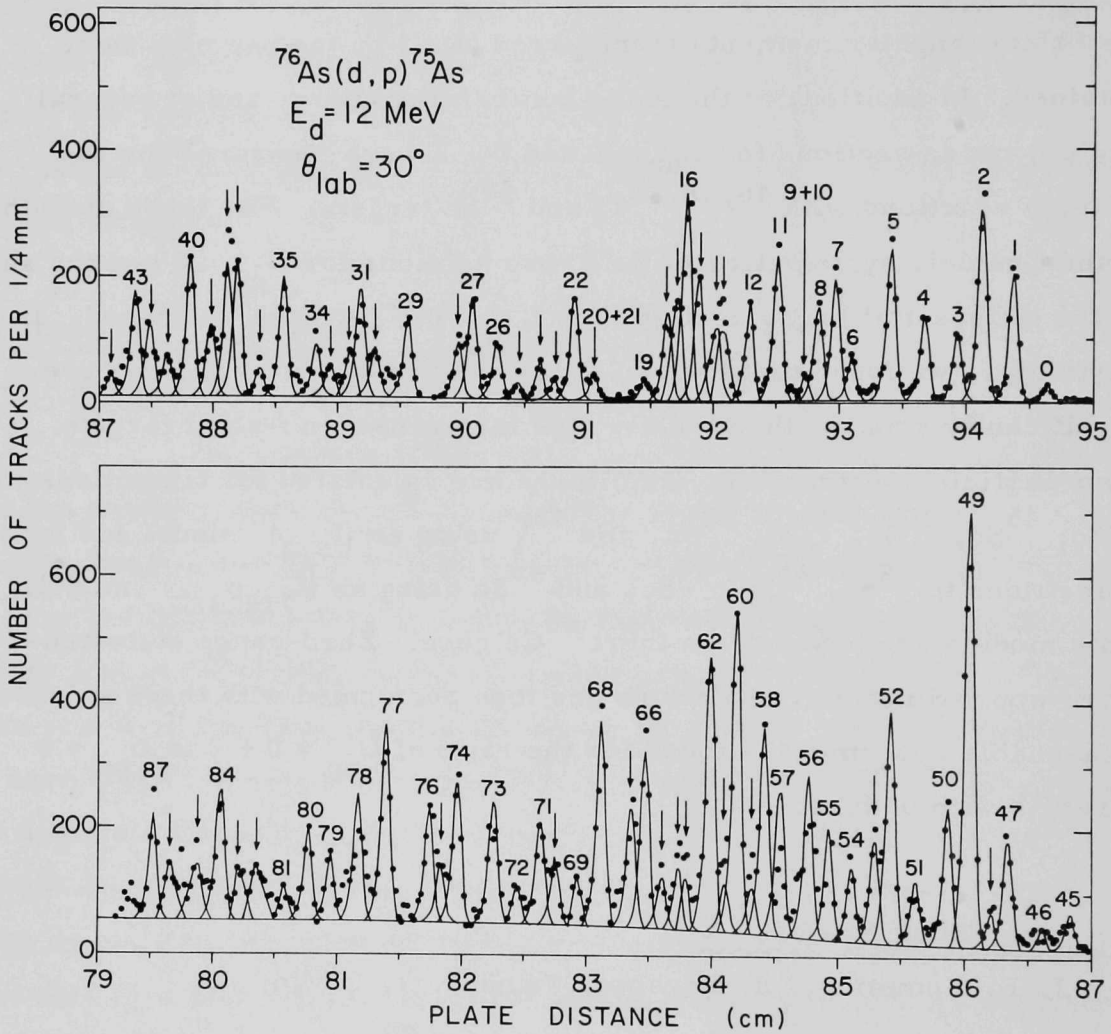

Fig. 17. The proton spectrum from the ^{75}As(d,p)^{76}As reaction.

low-lying states in connection with the interpretation[1] of isobaric analog resonances in ^{76}Sc. The outgoing protons in this reaction, initiated by deuterons accelerated in the ANL tandem, were studied by the use of photographic emulsions in the focal plane of the Enge split-pole spectrograph. The proton spectrum corresponding to states in ^{76}As is shown in Fig. 17. Eighty-seven excited energy levels up to 2.5 MeV have been identified, and the angular distributions for thirty-nine of the observed transitions have been compared with distorted-wave Born approximation calculations. Angular momentum transfers were determined and spectroscopic strengths deduced from the data. This has allowed comparisons with shell-model sum rules and with other (d,p) results on N=42 isotopes, and spin values for a number of levels in ^{76}As have been assigned.

---

[1] A. J. Elwyn, J. E. Monahan, J. F. Lemming, J. Rapaport, and M. Sample, Phys. Rev. C 10, 1939 (1974).

e. Experimental Investigation of ^{92}Tc by the ^{92}Mo(^{3}He,t) Reaction

T. H. Braid, H. T. Fortune, and F. J. D. Serduke

The odd-Z isotones of N = 49, ^{88}Y, ^{90}Nb, and ^{92}Tc have a multiplet of 10 states with spins 0^+ through 9^+ that arise from the coupling of a $\frac{9}{2}^+$ proton excitation to a $\frac{9}{2}^+$ neutron hole state. Experimental information on such multiplets in the vicinity of closed-shell nuclei is of great import to theoretical shell-model studies. A satisfactory identification of this multiplet in ^{92}Tc is as yet unavailable; in fact, the existing data on this nucleus are plagued with inconsistencies. Therefore, we have recorded data on this reaction, using an 18-MeV ^{3}He beam; the analysis is in progress.

f. Investigation of the Nucleus $^{89}_{41}$Nb$_{48}$ by the $^{92}_{42}$Mo$_{50}$(p,α) Reaction

W. Henning and F. J. D. Serduke

The nucleus $^{89}_{41}$Nb$_{48}$ is of spectroscopic interest because of its proximity to the closed shell nucleus $^{88}_{38}$Sr$_{50}$. A major shell-model

study of neutron-deficient nuclei in the mass-90 region here at Argonne stimulated this experimental investigation. Based on results of our experiment, we find that the previous, scanty data on this nucleus are incorrect. Our work has yielded a measurement of the mass of ^{89}Nb, a new identification of its ground-state spin and 25 previously unknown excited states. An account of this work will be submitted to the Physical Review.

2. STRUCTURE OF ACTINIDE NUCLIDES

Single-Particle States in Actinide Nuclei

J. R. Erskine, A. M. Friedman,* R. R. Chasman,* T. H. Braid, and D. S. Gale

A program to study single-particle excitations in actinide nuclei has been underway for some time. Magnetic spectrograph data on the (d,p), (d,t), (^{3}He,d), and (α,t) reactions for many actinide targets have resulted in extensive knowledge of single-particle states. This basic knowledge is of crucial importance for the understanding of the complex nuclear excitations in deformed nuclei in the actinide region. An article for Reviews of Modern Physics which surveys single-particle excitations in actinide nuclei is in preparation.

In the past year much effort has been focussed on data from the ^{244}Pu(d,t)^{243}Pu and ^{244}Pu(d,p)^{245}Pu reactions. Our charged-particle reaction data to states in ^{243}Pu have been combined with data on the ^{242}Pu(n,γ)^{243}Pu reaction studied at the Brookhaven High Flux Beam Reactor. This has resulted in the identification of 12 single-particle rotational bands in ^{243}Pu. This probably makes ^{243}Pu the best known of any odd-A actinide nucleus. A spectrum of the ^{244}Pu(d,p)^{245}Pu reaction together with preliminary assignments for the levels is shown in Fig. 18.

---

*Chemistry Division, ANL.

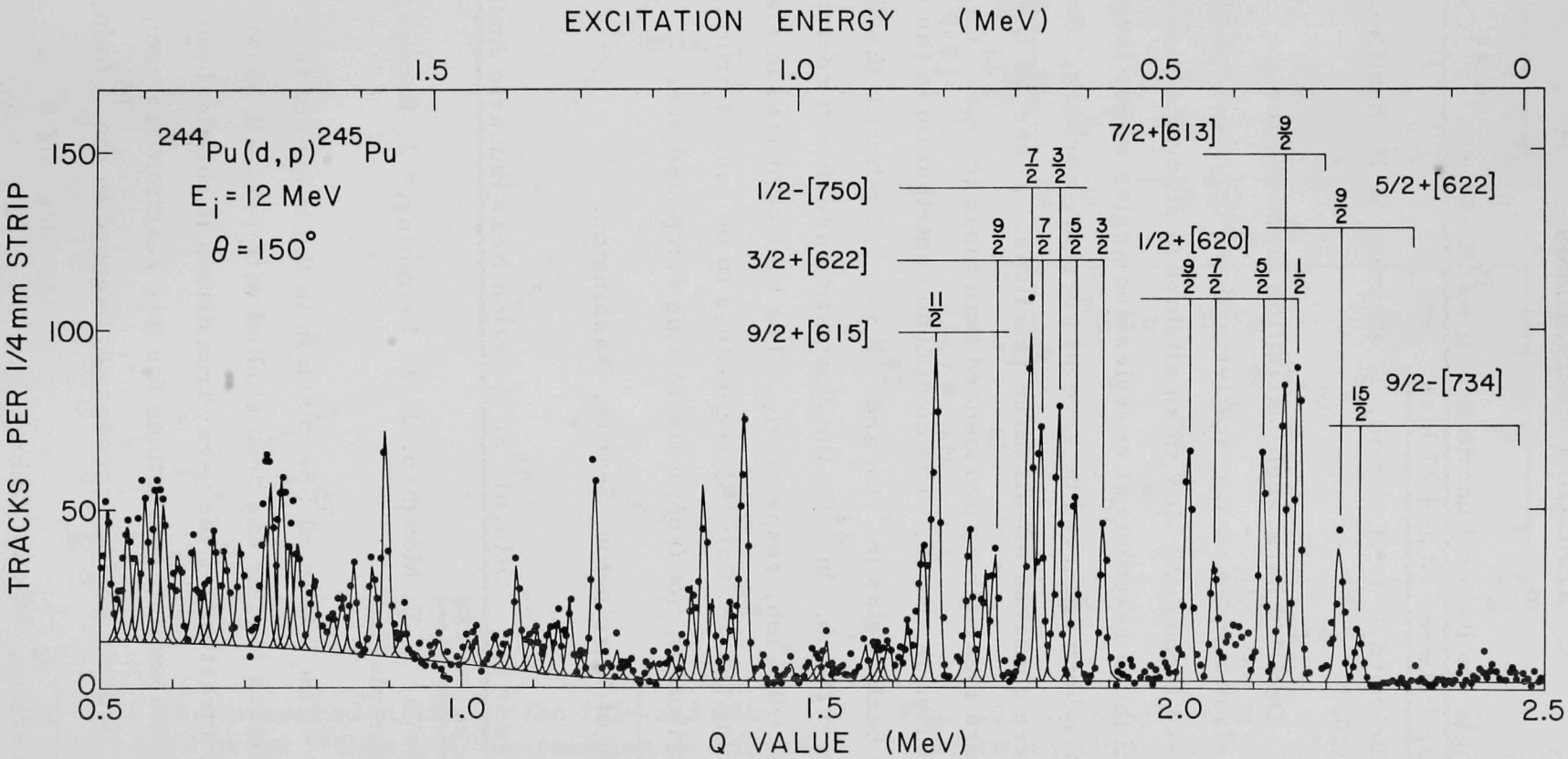

Fig. 18. Proton spectrum from the ^{244}Pu(d,p)^{245}Pu reaction. Tentative assignments for seven rotational bands are indicated. The curves through the data points were drawn by the peak fitting program AUTOFIT.

3. REACTION MECHANISMS

a. Back-Angle Excitation Functions of $\alpha + {}^{39}K$ and $\alpha + {}^{40,44}Ca$ Scattering Between 20 and 27 MeV

K. A. Eberhard,* T. H. Braid, T. Renner, J. P. Schiffer, and S. E. Vigdor

Detailed back-angle excitation functions for $\alpha + {}^{39}K$ and $\alpha + {}^{40,44}Ca$ elastic and inelastic scattering have been measured in the energy range 20 through 27 MeV in an attempt to study the reaction mechanism of these reactions at energies and angles where large anomalies have been observed by several previous workers. Statistical fluctuations are observed for all three reactions. Those for $\alpha + {}^{40}Ca$ and $\alpha + {}^{39}K$ are clearly less pronounced than those for $\alpha + {}^{44}Ca$, where the backward rise is absent. The compound contribution to the elastic scattering at back angles in ${}^{40}Ca$ and ${}^{39}K$ is ~0.2 mb with the direct cross section ~10 mb. In ${}^{44}Ca$ the fluctuating and direct contributions are ~0.1 and ~0.8 mb, respectively. The backward rise in elastic alpha scattering from ${}^{40}Ca({}^{39}K)$ seems thus to be caused primarily from a direct contribution, not from a fluctuating compound one.

*University of Washington, Seattle, Washington.

b. Anomalies in the ${}^{72}Ge(\alpha,n){}^{75}Se$ Reaction Near Isobaric Analog Resonances in ${}^{76}Se$

A. J. Elwyn, J. E. Monahan, J. F. Lemming,* J. Rapaport,* and M. Sample*

The ${}^{72}Ge(\alpha,n){}^{75}Se$ reaction in the region of isobaric analog resonances in ${}^{76}Se$ has been studied with 7.74—8.36-MeV α particles, by investigating the γ-ray transitions in the final nucleus. Anomalies in the excitation functions for this reaction are compared in Fig. 19 with isobaric analog resonances observed in the ${}^{75}As(p,n){}^{75}Se$

*Ohio University, Athens, Ohio.

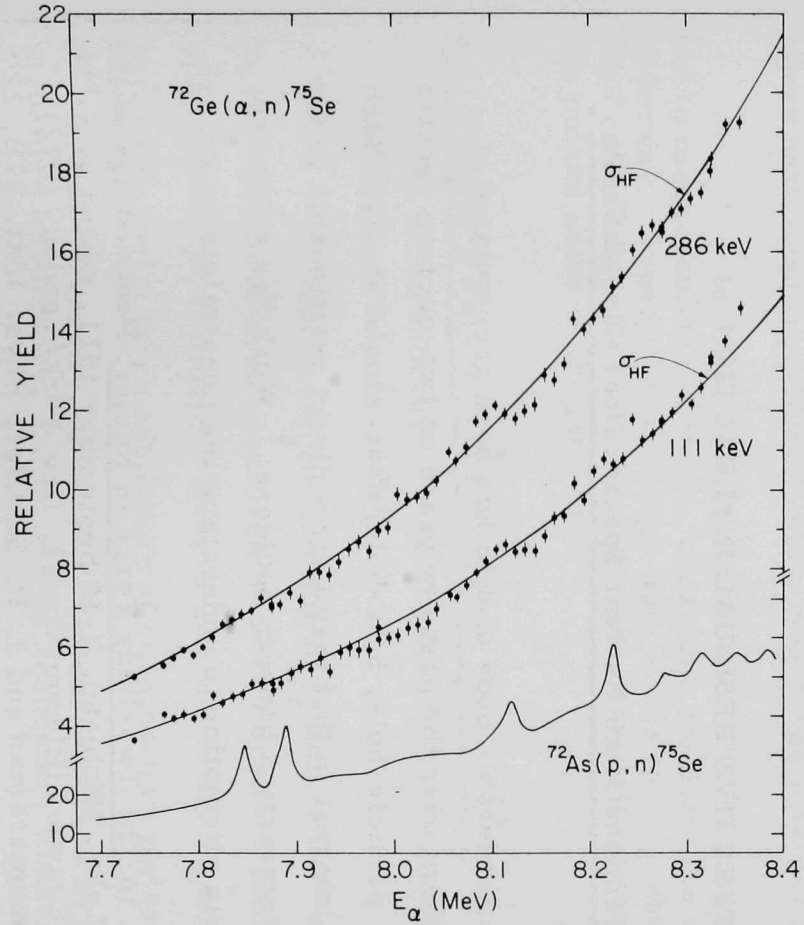

Fig. 19. The measured yields for the 111- and 286-keV γ rays in the ^{72}Ge(α,nγ)^{75}Se reaction as a function of incident α-particle energy, along with Hauser-Feshbach calculations of the (α,n) cross section. The lower smooth curve shows the measured ^{75}As(p,n)^{75}Se neutron yield plotted so that the excitation energies in ^{76}Se correspond in both reactions.

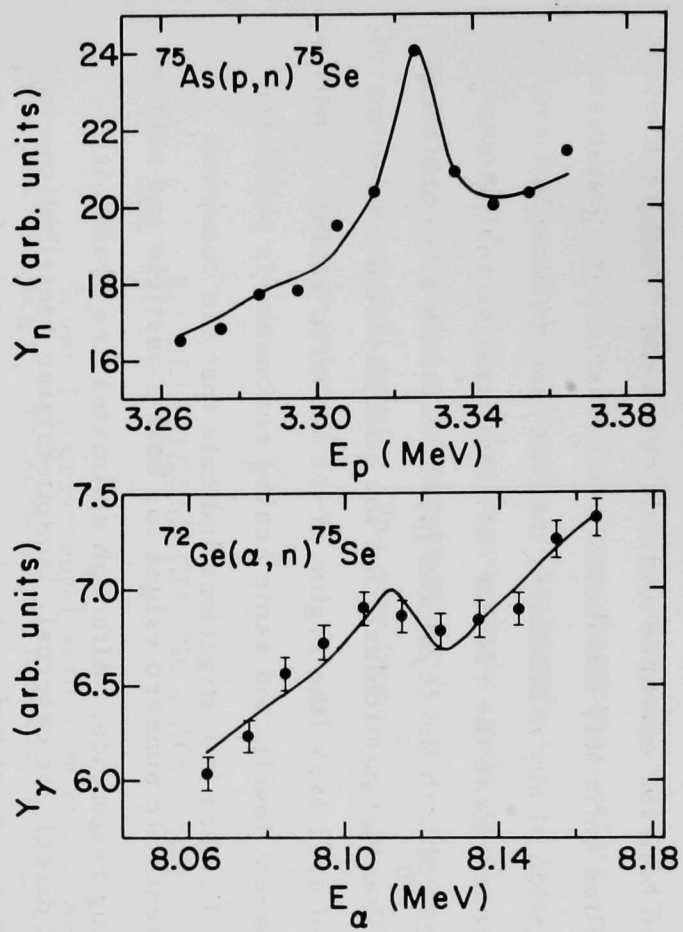

Fig. 20. Comparison of the measured 0° neutron yield in the ^{75}As(p,n)^{75}Se reaction and total γ-ray yield in ^{72}Ge(α,nγ)^{75}Se reaction with calculations (solid curve) in the region of the isobaric analog state at 3.326 MeV in the (p,n) reaction—corresponding to an α-particle energy of 8.12 MeV in the (α,nγ) reaction.

reaction. Population of isobaric analog resonances in (α,n) reactions is isospin-forbidden in both the entrance and exit channels. Thus, the existence of anomalies definitely attributable to isobaric analog states allows the investigation of any mechanism that may cause isospin mixing.[1] In the present case the results of simultaneous analyses (as shown in Fig. 20) of both the (α,n) and (p,n) reactions are consistent with the interpretation that particularly for the anomaly observed at an α-particle energy of 8.12 MeV (the region of the isobaric analog of the 0.309-MeV ^{76}As parent level), the same analog resonance is populated in both reactions. Further investigations indicate that the observed results are consistent with nonzero values for both α-particle and neutron widths for the analog resonance. Although estimates are crude, it appears likely that direct, or external, isospin-mixing contributions to the α-particle width are dominant.

[1] A. Richter, E. Grosse, J. Hüfner, and H. A. Weidenmüller, Phys. Lett. 38B, 349 (1972).

4. EFFECTIVE RESIDUAL INTERACTION

Effective Interactions from Nuclear Spectra Near Closed Shells

J. P. Schiffer

A considerable body of data has been accumulated at Argonne and elsewhere over the past few years on two-nucleon spectra (particle-particle, particle-hole, hole-hole) near closed shells. Such data are of unique interest in that they bear a direct relationship to the effective residual interaction between nucleons.[1] Work has continued over the past year in attempting to understand the constraints which are

[1] J. P. Schiffer, in The Two-Body Force in Nuclei, Proceedings of the Symposium, Gull Lake, Michigan, 7-10 September 1971, edited by S. M. Austin and G. M. Crawley (Plenum Press, New York/London, 1972), pp. 205-227; N. Anantaraman and J. P. Schiffer, Phys. Lett. 37B, 229 (1971).

set by the data. The importance of tensor and spin orbit two-body forces was explored. The least-squares fitting procedures establish clearly the need of at least a five-component central force with two ranges in the triplet odd part. The ranges are not well constrained by the energy level data. The improvement in fitting the data by including two ranges for other components of the force and by including noncentral forces is relatively small. The data from ^{12}C to ^{208}Pb are fit well with a single effective interaction.

5. ELECTROMAGNETIC PROPERTIES

Several experimental activities at the tandem are classified under this heading. The technique of measuring magnetic moments of excited nuclear states by observing the shift in an angular correlation pattern from a liquid source in a magnetic field is one of the few techniques which can allow one to obtain a reliable result. Such data are of particular interest in nuclei where transition probabilities are also studied. The measurements are by no means easy; several favorable cases have been investigated and a result was obtained for ^{90}Nb.

Interest in the properties of the E2 giant resonance have led to measurements of the (α, γ) capture reaction; the experiment is underway. Experiments on high-spin states in $f_{7/2}$-shell nuclei have also continued, as have measurements of transition probabilities using the pulsed beam of the tandem.

a. Nuclear g Factor of the $d_{3/2}$ Hole State in ^{43}Sc

R. P. Scharenberg,* R. Mitchell,† T. V. Ragland,† R. E. Holland, and F. J. Lynch

The mean lives of the $d_{3/2}$ proton hole states in the odd-A Sc isotopes have been measured to be 200 or more times longer than the single-particle estimate. Lawson and Macfarlane made theoretical estimates that a large admixture of core-excited states could account for

*Purdue University, Lafayette, Indiana; on leave at the Nuclear Structure Laboratory, University of Rochester, Rochester, New York.

†Purdue University, Lafayette, Indiana.

these hindered M2 transitions. Core excitation can also affect g factors. A preliminary measurement of the g factor of the $d_{3/2}$ proton hole state in ^{43}Sc at 150 keV (τ = 628 μsec) has been made with the ^{40}Ca(α,p)^{43}Sc reaction using a liquid calcium-tin alloy target. Further measurements will be made to improve statistics, and obtain the sign of the g factor.

b. Measurement of the g Factor of the 6^+, 88-μsec Isomeric State of ^{90}Nb

R. J. Mitchell,* T. V. Ragland,* R. P. Scharenberg,† R. E. Holland, and F. J. Lynch

The 88-μsec isomeric state in ^{90}Nb was excited by bombarding a liquid Zr-Cu alloy target with protons from the Argonne tandem by the reaction ^{90}Zr(p,n)^{90}Nb. The time distribution of the 122-keV γ rays following the beam burst was measured with an intrinsic Ge detector. The observed value for the g factor for this 6^+ first excited state is g = 0.620 ± 0.004. This agrees within error with the measurement of the g factor of the 8^+ ground state. Figure 21 shows a plot of the data.

*Purdue University, Lafayette, Indiana.

†Purdue University, Lafayette, Indiana; on leave at the Nuclear Structure Laboratory, University of Rochester, Rochester, New York.

c. Isomerism in ^{194}Au

S. W. Yates* and F. J. Lynch

In recent years long-lived $I^\pi = 12^-$ isomers have been discovered in ^{196}Au, ^{198}Au, and ^{200}Au. In the present measurements we have observed isomers in ^{194}Au with half-lives of 600 ± 8 and 420 ± 10 ms using pulsed beam techniques. These levels were excited by (d,2n) and (p,n) reactions on natural and enriched ^{194}Pt targets at various bombarding energies. Gamma-ray singles and γ-γ coincidence spectra

*Chemistry Division, ANL.

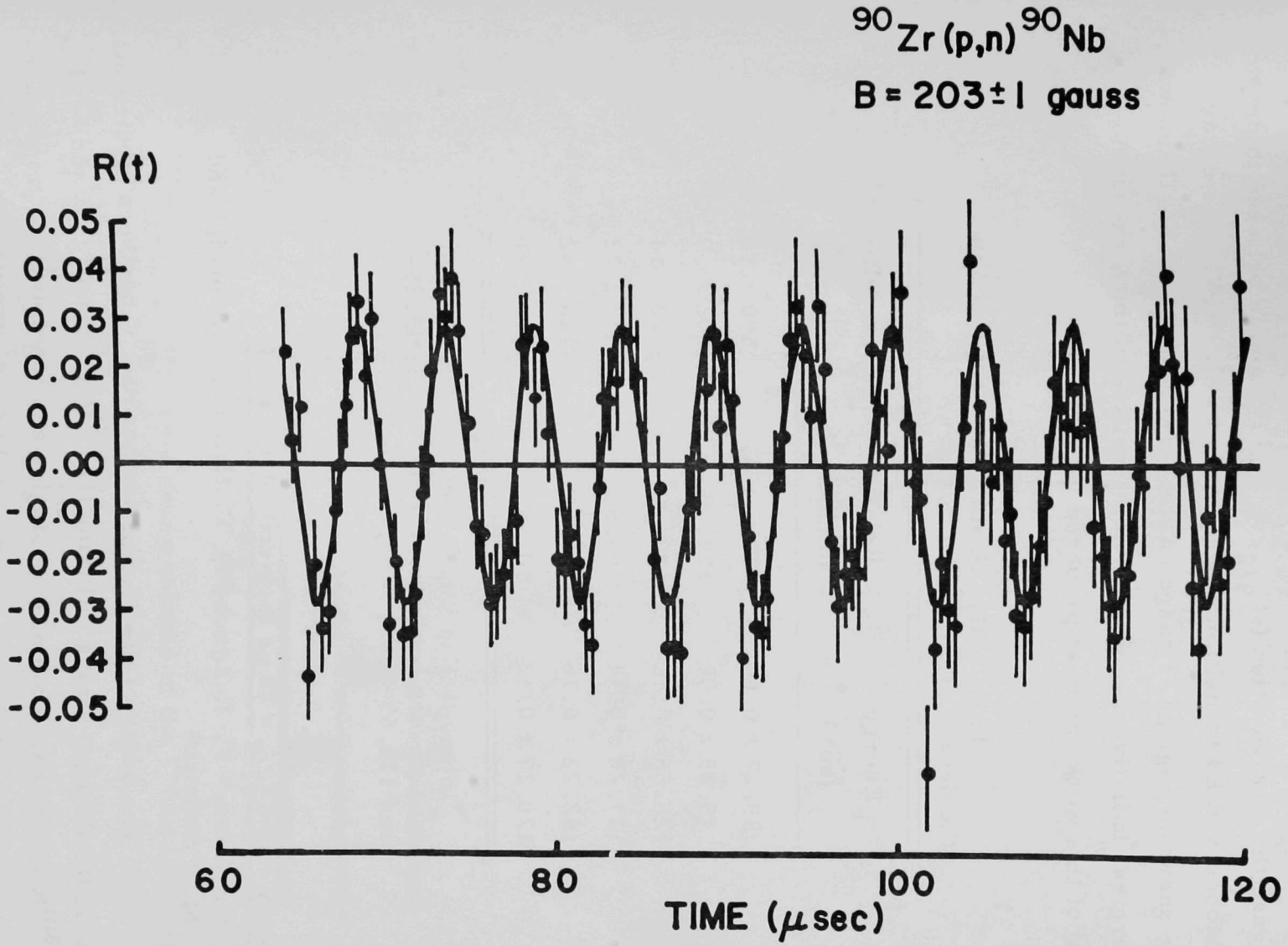

Fig. 21. Typical data from a perturbed angular distribution measurement of the g factor of ^{90}Nb. R(t) = [N(45°,t) - N(135°,t)] / [N(45°,t) + N(135°,t)] plotted as a function of time after the beam pulse. The sinusoidal curve is a least-squares fit to the data.

were measured. The longer-lived isomer at 80.5 keV is believed to have the configuration $(\pi d_{3/2}, \nu i_{13/2})\ 5^+$, while the shorter-lived isomer is assigned the configuration $(\pi h_{9/2}, \nu i_{13/2})\ 11^-$ and is believed to decay by an unobserved E3 transition to the level at 379.9 keV. The decay scheme shown in Fig. 22 is based on the present data. Table II shows the energies, half-lives, and relative intensities of the γ rays. An account of this work has been prepared for publication.

TABLE II. Gamma rays observed in the decays of the ^{194}Au isomers.

Energy (keV)	Relative intensity[a]	Half-life (ms)
35.27 ± 0.08	80 ± 23	590 ± 18
45.25 ± 0.09	100	602 ± 9
128.55 ± 0.12	100	422 ± 14
137.20 ± 0.14	64.6 ± 5.2	422 ± 22
162.22 ± 0.16	35.5 ± 4.1	420 ± 32
170.77 ± 0.12	101.8 ± 7.1	415 ± 21

[a]Intensities of γ rays from the 600 and 420 ms isomers are given relative to the 45.25- and 128.55-keV γ rays, respectively.

d. Decay of the $t_{1/2}$ = 22 μs Isomeric State of ^{38}K

S. W. Yates,* F. J. Lynch, R. E. Holland, I. Ahmad,* and A. M. Friedman*

The decay of the 22.5 μs isomer of ^{38}K has been studied by observing the delayed γ rays following the ^{24}Mg(^{16}O,pn)^{38m}K and ^{35}Cl (α,n)^{38m}K reactions. Gamma-ray singles and γ-γ coincidence measurements were made and the reaction threshold for production of the

*Chemistry Division, ANL.

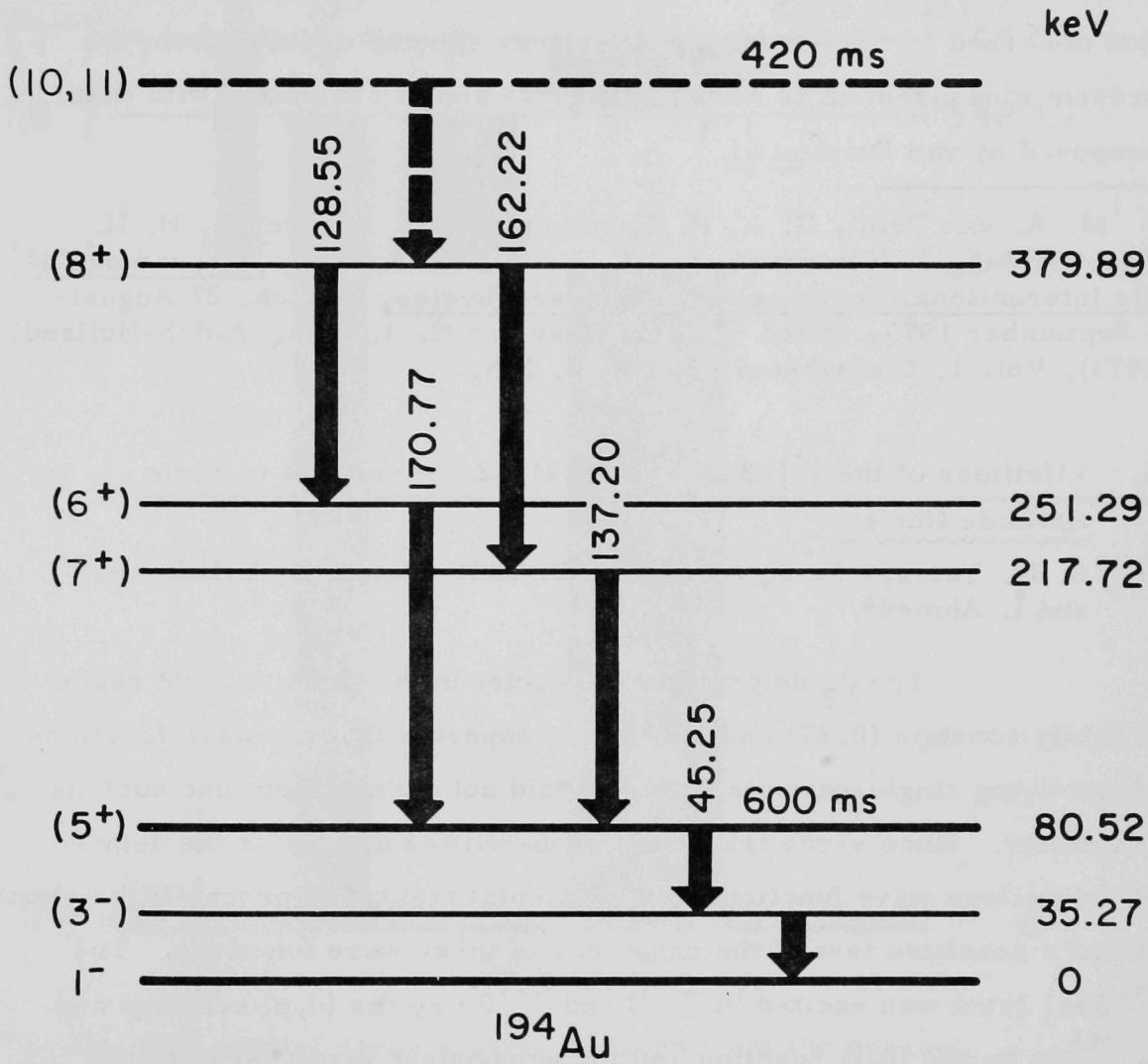

Fig. 22. The proposed decay scheme of the ^{194}Au isomers.

isomer was determined for the (α,n) reaction. The 3458-keV isomeric state decays by an apparent E1 transition (α_T = 0.58) to a level at 3420 keV and by an 812-keV transition to a level at 2646 keV. The isomerism is understood in terms of the selection rules for the decay of E1 transitions in T=0 nuclei. A weak-coupling estimate of the excitation energy of the 7^+ $(1f_{7/2})^2$ state in ^{38}K yields a value in excellent agreement with that observed for this isomer. The decay scheme deduced from the present measurement is shown in Fig. 23 and is consistent with that proposed by van Driel et al.[1]

[1] M. A. van Driel, G. A. P. Engelbertink, D. Bucurescu, H. H. Eggenhuisen, J. Konieczek, and R. L. W. van de Weg, Proceedings of the International Conference on Nuclear Physics, Munich, 27 August-1 September 1973, edited by J. de Boer and H. J. Mang (North-Holland, 1973), Vol. 1, Contributed Papers, p. 205.

e. Lifetimes of the $\frac{1}{2}^+$[631] to $\frac{5}{2}^+$[622] E2 Transitions in Some Actinide Nuclei

S. W. Yates,* F. J. Lynch, R. E. Holland, A. M. Friedman,* and I. Ahmad*

The β_2 deformation of nuclei in the Z=92 to Z=98 region is fairly constant (0.27) and hence it is expected that the wave functions of low-lying single-particle states should not change from one nucleus to another. Since γ-ray transition probabilities depend on the details of the nuclear wave functions, experimental transition probabilities should afford a sensitive test of the constancy of these wave functions. The $\frac{1}{2}^+$[631] level was excited in ^{239}U and ^{239}Pu by the (d,p) reaction and in ^{241}Pu by the (d,t) reaction and the subsequent γ-ray decay to the $\frac{5}{2}^+$[622] level was observed following a beam pulse. In the Chemistry Division, corresponding E2 transitions in ^{243}Cm and ^{245}Cm were observed in the radioactive decay of ^{243}Bk and ^{245}Bk, respectively, and the lifetimes were measured by electron-photon delayed-coincidence techniques. Partial energy-level diagrams and the half-lives of the

* Chemistry Division, ANL.

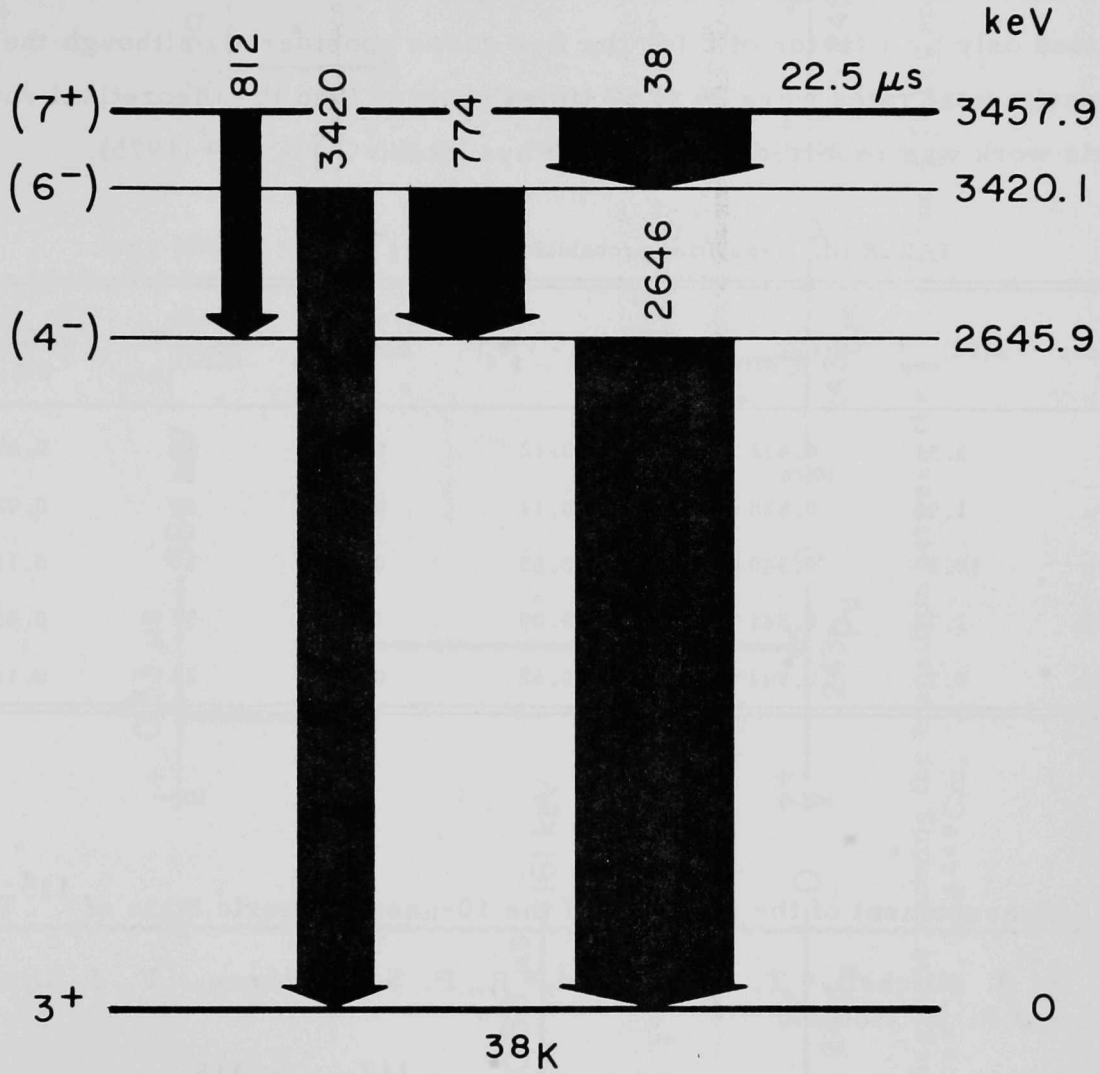

Fig. 23. ^{38}K partial decay scheme deduced from the present measurement. The widths of the arrows are proportional to the intensities of the observed gamma rays.

$\frac{1}{2}^+[631]-\frac{5}{2}^+[622]$ transitions in these nuclei are shown in Fig. 24. Reduced transition rates for these odd-neutron nuclei were calculated from a product of the Nilsson estimate and the pairing factor, and compared with rates obtained from the measured lifetimes. Results are shown in Table III. The ratios of experimental to theoretical rate varied only by a factor of 2 for the five cases considered, although the experimental rates were 26 to 57 times greater than the theoretical rates. This work was reported recently in Phys. Rev. C 11, 599 (1975).

TABLE III. Transition probabilities of the $\frac{1}{2}^+[631] \rightarrow \frac{5}{2}^+[622]$ γ ray.

Nucleus	$B(E2)_{exp}$	$B(E2)_{Nilsson}$	$(U_iU_f - V_iV_f)^2$	$B(E2)_{theo}$	$\frac{B(E2)_{exp}}{B(E2)_{theo}}$	$\frac{T_{exp}}{T_{Weisskopf}}$
^{239}U	3.51	0.538	0.12	0.065	54	0.039
^{241}Pu	1.95	0.538	0.14	0.075	26	0.022
^{243}Pu	10.2	0.540	0.63	0.34	30	0.11
^{243}Cm	2.78	0.541	0.09	0.049	57	0.031
^{245}Cm	9.7	0.544	0.62	0.34	29	0.11

f. Measurement of the g Factor of the 10-μsec Isomeric State of ^{115}Te

R. J. Mitchell,* T. V. Ragland,* R. P. Scharenberg,† F. J. Lynch, and R. E. Holland

This level was excited via the $^{112}Sn(\alpha,n)^{115}Te$ reaction. A pulsed beam of 20-MeV alpha particles bombarded an enriched liquid-tin target. The g factor was obtained by measuring the time distribution of the 280-keV γ ray from the isomer as the nuclei precessed in an

*Purdue University, Lafayette, Indiana.

†Purdue University, Lafayette, Indiana; on leave at the Nuclear Structure Laboratory, University of Rochester, Rochester, New York.

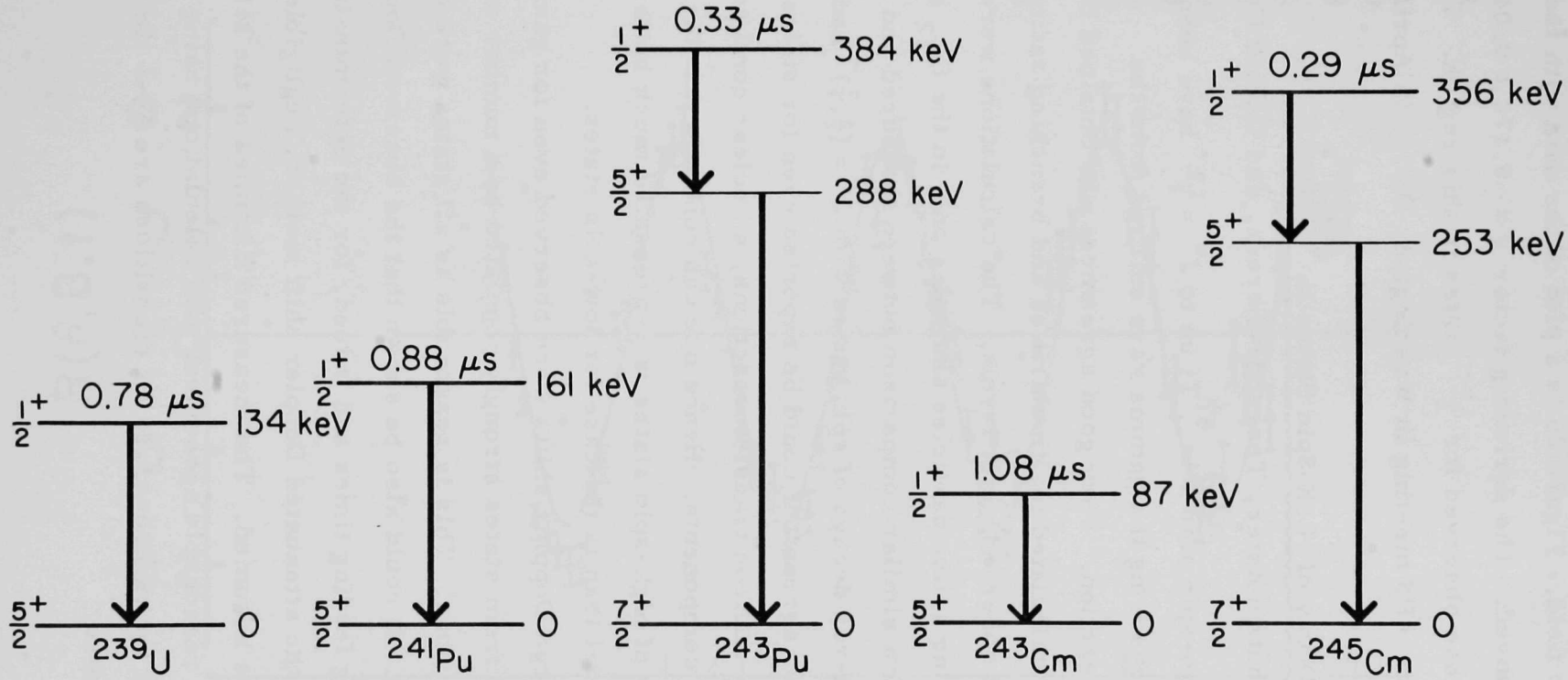

Fig. 24. Partial level diagrams showing the transition between the $\frac{1}{2}^+[631]$ and $\frac{5}{2}^+[622]$ states in ^{239}U, ^{241}Pu, ^{243}Pu, ^{243}Cm, and ^{245}Cm.

external magnetic field. Figure 25 is a plot of the data with the exponential decay removed. The derived g factor $g = -0.174 \pm 0.04$ is consistent with those observed for $\frac{11}{2}^-$ states in this region. This work was reported at the APS meeting in Washington, D.C., in April 1974.

g. The Gamma Decay of High-Spin States in ^{47}Ti

L. Meyer-Schützmeister, Terrence Sjoreen, and Gerald Hardie

High-spin states in ^{47}Ti up to $J^\pi = \frac{19}{2}^-$ have been investigated by measuring the gamma rays emitted from the ^{45}Sc(α,np)^{47}Ti* reaction. Very good agreement was obtained between the measured and calculated multipolarities and branching ratios of transitions for all observed yrast levels. The calculations were performed assuming active particles and holes only in the $f_{7/2}$ shell. In an earlier work a similar comparison between measured and calculated gamma-ray decays of spin states with $J^\pi = (\frac{5}{2},\frac{7}{2})^-$ had been made and only poor agreement could be reported even for states which showed, from one-nucleon transfer reactions, a nuclear configuration with large $(f_{7/2})^n$ components. Hence one can conclude that the gamma-ray decay of high-spin states is represented much better by a pure $(f_{7/2})^n$ model than is the case for low-spin states.

Large Doppler shifts were observed even for gamma rays which are emitted from states strongly populated by a number of preceding gamma-ray transitions. This is reasonable as all states were strongly "side-fed" (~50%). It could also be shown that the observed Doppler shifts exclude long feeding times and indeed, for the determination of the lifetimes through the attenuated Doppler shift method, negligible feeding times were assumed. The measured lifetimes of the M1 transitions are in reasonable agreement with calculations using an $(f_{7/2})^n$ model, but the two observed E2 transitions are 4—6 times faster than calculated.

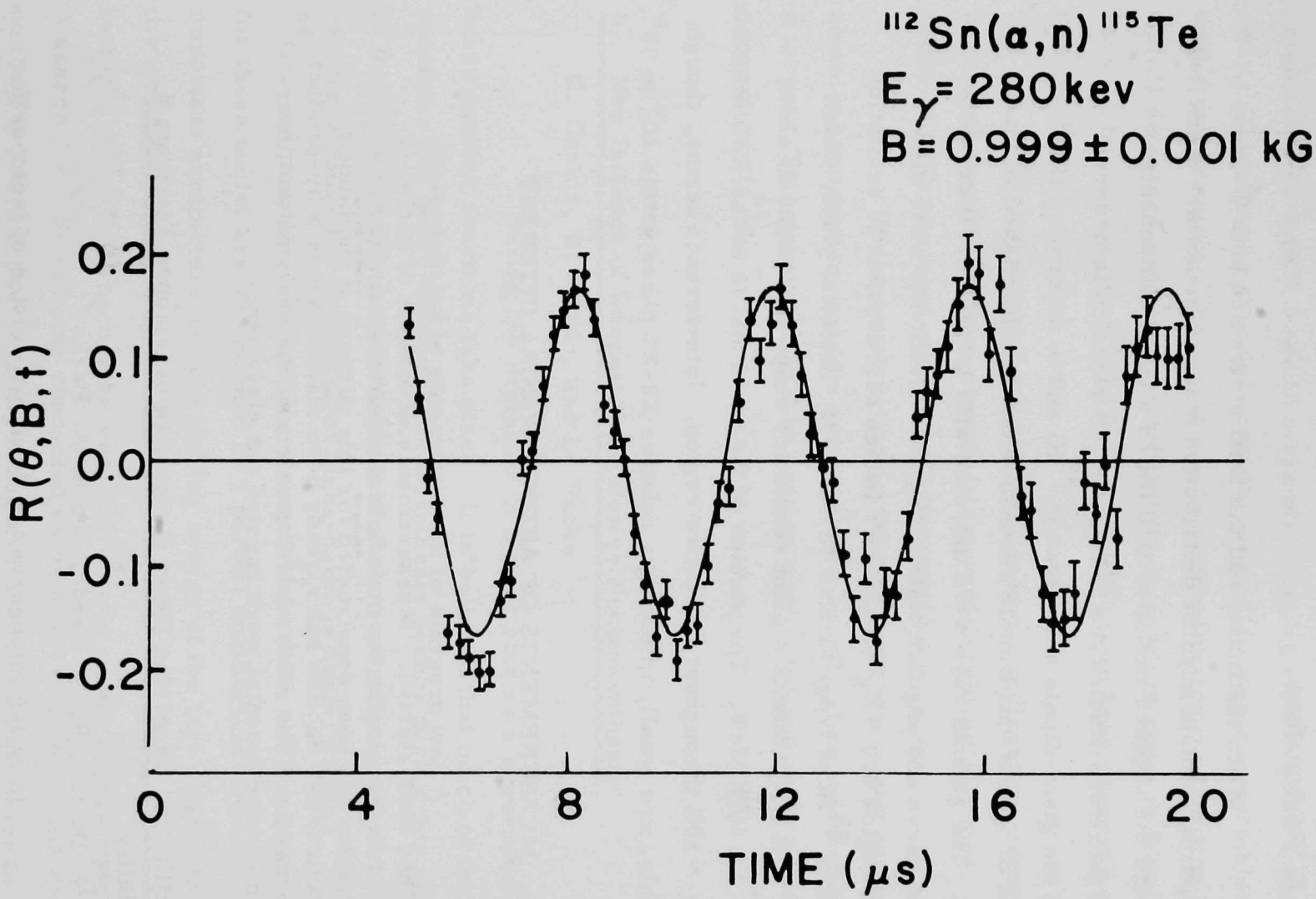

Fig. 25. Plot of $[N(t,45^\circ) - N(t,135^\circ)]/[N(t,45^\circ) + N(t,135^\circ)]$, where $N(t,\theta)$ is the time distribution in 280-keV γ rays following the beam burst with the detector at angle θ to the beam direction. The solid curve is a sine wave fitted to the data.

h. Study of the $^{54}Fe(\alpha,\gamma)^{58}Ni$ Reaction

L. Meyer-Schützmeister, W. Wharton, P. Debevec, R. E. Segel, and K. Raghunathan

When the initial and the final states are both 0^+ in an (α,γ) reaction, simple angular distribution measurements are sufficient to separate the capture radiation into its E1 and E2 components. We have therefore studied the $^{54}Fe(\alpha,\gamma)^{58}Ni$ reaction in order to examine the giant-dipole resonance in ^{58}Ni and to determine if the presence of a giant-quadrupole resonance can be established in this nucleus. The gamma rays were detected with large NaI(Tl) crystals, and yield curve and angular distribution measurements were made over the region $8.0 \leq E_\alpha \leq 13.6$ MeV (which corresponds to excitation energies in ^{58}Ni of from 13.8 to 18.3 MeV). The total yield, which is about 90% E1, exhibits a giant resonance shape that peaks at about $E_x(^{58}Ni^*) = 16.2$ MeV. The portion of the yield that is in the E2 component remains $\approx 10\%$ throughout the entire region. Interference terms, though observable, are small, implying a relative E2-E1 phase within 10° to 90°.

6. MEASUREMENTS OF ASTROPHYSICAL INTEREST

A new program of measurements of astrophysical interest has been started. Measurements of masses of nuclei of interest in He burning is the main initial experimental effort. A rabbit system has been constructed for this purpose at the tandem. A new radioactive nuclide has already been discovered as a by-product of this program. The work on ^{12}C consists of the analysis and interpretation of experimental work carried out elsewhere.

a. Facility for Observing Decay Properties of Isotopes Far from β Stability

C. N. Davids, R. C. Pardo, and L. A. Parks

In order to observe the decay properties of isotopes far from β stability, a pneumatic target-transfer system has been constructed

in the Tandem accelerator west target room. A target mounted in a delrin holder is bombarded in vacuum and transferred by a burst of helium in less than 0.5 sec to a remote counting station about 3 meters away. This area is shielded from the beam line by a concrete block wall 1 meter thick. The target can be counted with a combination of Ge(Li) detectors and plastic scintillators in order to observe γ and β rays. The new isotope ^{53}Ti ($T_{1/2}$ = 32.8 sec) has been observed using this facility.

In another configuration, gaseous radioactive atoms can be transferred in a helium stream to a remote counting chamber. The decay of ^{74}Kr has been studied with this apparatus.

Under construction is a facility whereby rapid on-line chemical separations may be accomplished shortly after irradiation of a target. This apparatus will be used to search for and study the decay properties of ^{68}Se.

b. New Isotopes of Interest to Explosive Nucleosynthesis

C. Davids, R. Pardo, and L. Parks

During the explosion of a giant star as a supernova event, many nuclear reactions take place. It is believed that much of the medium- and heavy-element nucleosynthesis occurs during this phase. In the region of the periodic table just above iron, charged-particle reactions cause the formation of alpha-particle nuclei such as ^{60}Zn, ^{64}Ge, and possible ^{68}Se. After the material cools, the final abundances for these nuclei are determined by a partial equilibrium in which the important parameters are the binding energy of the last α particle and the temperature at which the nuclear reactions cease. The first two isotopes above have been observed, but ^{68}Se is as yet unobserved. A search for ^{68}Se is being conducted using heavy-ion compound reactions on the FN Tandem accelerator, along with chemical separation techniques.

The formation of a neutron star from a supernova remnant is a process which involves the neutronization of the dense hot core of an exploding giant star. This proceeds via electron captures, since the Fermi energy of the degenerate electrons in such a dense medium can approach 10 MeV. Inside the remnant all protons are converted to neutrons, but in the outer regions there may exist neutron-rich nuclides resulting from electron captures on abundant species such as ^{56}Fe. The masses and β-decay rates for neutron-rich isotopes in the A=50—70 region are the relevant nuclear data needed for calculations of the surface properties of neutron stars. Such information can also be used to check the predictions of mass formulae as well as the nuclear systematics in this region.

New neutron-rich isotopes can be formed by heavy-ion compound reactions, as well as by multinucleon transfer processes.

A fast pneumatic transfer system has been installed at the FN Tandem accelerator, enabling the observation of delayed β and γ rays in a shielded area. Both Ge(Li) and plastic detectors are used in various combinations. The new isotope ^{53}Ti ($T_{1/2}$ = 32.7 ± 0.9s) has been observed via the reaction ^{48}Ca(^{7}Li,pn)^{53}Ti, and its decay scheme has been obtained. Work has begun on the search for ^{59}Mn.

c. Radiative De-excitation of the 7.655-MeV State of ^{12}C—Helium Burning in Stars

C. N. Davids, R. C. Pardo, and A. W. Obst*

A new measurement of the radiative branching ratio Γ_{rad}/Γ for the 7.655-MeV state of ^{12}C has been made. The quantity is needed for calculations of stellar helium burning. The 7.655-MeV state of ^{12}C was formed by inelastic scattering of 10.5-MeV protons on thin self-supporting carbon targets. Coincidences between ^{12}C recoils of the proper energy and protons inelastically scattered from ^{12}C signaled the

*Center for Nuclear Studies, University of Texas at Austin, Texas.

radiative decay of the 7.655-MeV state. A value of $(4.30 \pm 0.20) \times 10^{-4}$ was obtained for the branching ratio, compared with a recent measurement of $(4.20 \pm 0.22) \times 10^{-4}$ and the previous best value of $(2.9 \pm 0.3) \times 10^{-4}$. The experiment was carried out using the EN Tandem Van de Graaff accelerator of the University of Texas at Austin. Subsequent analysis of the data was completed at Argonne.

B. CHARGED-PARTICLE WORK AT THE CYCLOTRON

The Argonne 60-in. cyclotron is used to a limited extent for charged-particle research. It has been shut down for improvements during a large fraction of the past year. Two experiments have been carried out to complement related work at the tandem accelerator but with higher energy projectiles.

a. Deuteron-Induced Nucleon Pickup

T. H. Braid, J. L. Yntema, H. T. Fortune, and L. R. Medsker*

The study of states in K isotopes excited by proton removal from Ca isotopes has been continued by means of the (d, ^{3}He) reaction, and the data for ^{42}Ca and ^{43}Ca targets are being analyzed.

Two-nucleon pickup reaction ^{100}Mo(d, α)^{98}Nb has been used to study states in ^{98}Nb. Excitation energies were obtained for a large number of states below 2.2 MeV excitation energy. The ground state and all states below 1 MeV are very weakly populated, but a cluster of strong states is observed between 1.0 and 2.2 MeV excitation. These data are consistent with the interpretation that the lowest states in ^{98}Nb are of the $\pi(g_{9/2})\nu(g_{7/2})$ configuration, which should be populated only weakly in pickup from ^{100}Mo.

*University of Pennsylvania, Philadelphia, Pennsylvania.

b. The ^{16}O(α,p)^{19}F Reaction and Three-Particle Cluster Transfer Spectroscopic Factors

T. H. Braid, H. T. Fortune, and W. Henning

The ^{16}O(α, p)^{19}F reaction has been measured at 43.9 MeV using the Argonne 60-in. cyclotron and the split-pole magnetic spectrograph. Interest in these studies was stimulated through recent theoretical calculations within the SU(3)-labelling scheme[1] that led to a first approximation in cluster-transfer spectroscopic factors. The energy

[1] J. B. McGrory, Phys. Lett. 47B, 481 (1973).

resolution obtained in the measurements was about 30 keV which allows for the identification and extraction of the population strengths of all members of the $K=\frac{1}{2}^+$ and $K=\frac{1}{2}^-$ rotational bands up to spin $\frac{13}{2}$. A preliminary analysis for the $K=\frac{1}{2}$ positive-parity band yields relative strengths in agreement with the theoretical predictions; in particular, the $\frac{11}{2}^+$ member of the $K=\frac{1}{2}^+$ band is populated weakly compared to the other band members. A similar behavior is found for the $\frac{11}{2}^-$ member of the $K=\frac{1}{2}^-$ rotational band. Further analysis is underway. The preliminary results encourage the idea of using the (α, p) reaction for studies of three-particle cluster-transfer spectroscopic factors.

C. LIGHT-ION PHYSICS AT THE DYNAMITRON

The 4-MV Dynamitron is a general-purpose accelerator facility used for a wide variety of research activities that are supported by several research programs. The accelerator is operated by the Physics Division, and costs are shared on the basis of the fraction of time devoted to each program. The main programs involved in the use of the facility during the past year are Nuclear Sciences, Molecular Sciences, and Materials Sciences.

Because of the diversity of the research activities supported by the Dynamitron, it has been necessary to provide it with a wide range of capabilities. The installation of a new kind of accelerator tube in 1974 was another major step forward.

In the Charged-Particle Research program, the Dynamitron is used primarily for the measurement of low-energy cross sections of interest for CTR applications. The low energy, good beam quality, and pulsed source of the accelerator make it ideal for these measurements. The availability of the facility made it feasible to be effective in this new program with very little delay.

The Dynamitron is also used to some extent for channeling measurements.

1. LOW-ENERGY CROSS SECTIONS

Except for the reactions between the hydrogen isotopes, the most promising reaction for thermonuclear purposes is the one involving $^{6}Li + d$. Yet the low-energy cross sections for this process have not been well known; large discrepancies exist in the published literature. Measurements on the Dynamitron have been carried out in order to determine the cross sections for this process with good accuracy. These measurements are very demanding technically and require large amounts of accelerator-beam time. The work in this new program has gotten off to a fast start because of the availability of a good experimental system and the fact that the staff members involved were experienced in closely related investigations formerly carried out in the Neutron Physics program.

a. Cross Sections for Neutrons from ^{6}Li+d Reactions at Low Energies

A. J. Elwyn, R. E. Holland, F. J. Lynch, J. E. Monahan, and F. P. Mooring

As part of a program for determining absolute cross sections for various nuclear particles emitted in charged-particle-induced reactions on light nuclei, we have measured the differential and total cross sections for the outgoing neutrons in the bombardment of ^{6}Li by 0.2 to 0.9-MeV deuterons accelerated in the ANL Dynamitron. Knowledge of the properties of nuclear reactions of deuterons with ^{6}Li is of importance to the needs of the controlled thermonuclear research program in connection with the evaluation of advanced fusion fuels and the concept of fusion chain reactions.[1] At the same time such measurements can contribute to the understanding of the nuclear structure of light nuclei and also of the relative importance of the various reaction mechanisms that could produce a neutron in the final state. Differential and total cross sections for the neutrons corresponding to the excitation of the final ^{7}Be nucleus in its ground and 0.431-MeV excited state [in the ^{6}Li(d,n) reaction] and for the continuum neutrons that are associated with the breakup of ^{7}Be into ^{3}He and ^{4}He have been determined by the use of stilbene scintillator detectors and standard time-of-flight techniques. Target thickness and detector efficiencies have been obtained with sufficient accuracy to allow absolute cross-section measurements to ~16%. The total cross sections are displayed in Table IV. An attempt to interpret the measured neutron spectra associated with three-body breakup in terms of a consistent reaction mechanism is in progress. Preliminary results are shown in Fig. 26. As observed, the data are qualitatively different from the spectra expected from direct breakup. On the other hand, the preliminary calculation based on a sequential decay mechanism in which the s-wave Coulomb interaction between ^{3}He and ^{4}He in the final state is taken into account, appears quite promising.

---

[1] See, e.g., J. Rand McNally, Jr., "Fusion Chain Reactor Prospects and Problems," USAEC Report ORNL-TM-4575 (1974).

TABLE IV. Total cross sections (in mb) for neutrons emitted in d + ^{6}Li reactions.

E_d (MeV) (±0.005)	σ_t (g. s.) (±16%)	σ_t (431 keV) (±16%)	σ_t ($E_n \geq 0.5$ MeV) (±18%)
0.873	56.0	29.9	
0.779	49.9	25.5	61.7
0.578	45.0	19.5	41.2
0.482	41.2	14.6	
0.379	29.0	9.45	
0.375	30.4	10.1	22.1
0.328	24.3	7.78	
0.242	10.0	2.68	
0.238	11.8	3.12	7.64
0.204	7.67	2.16	5.29

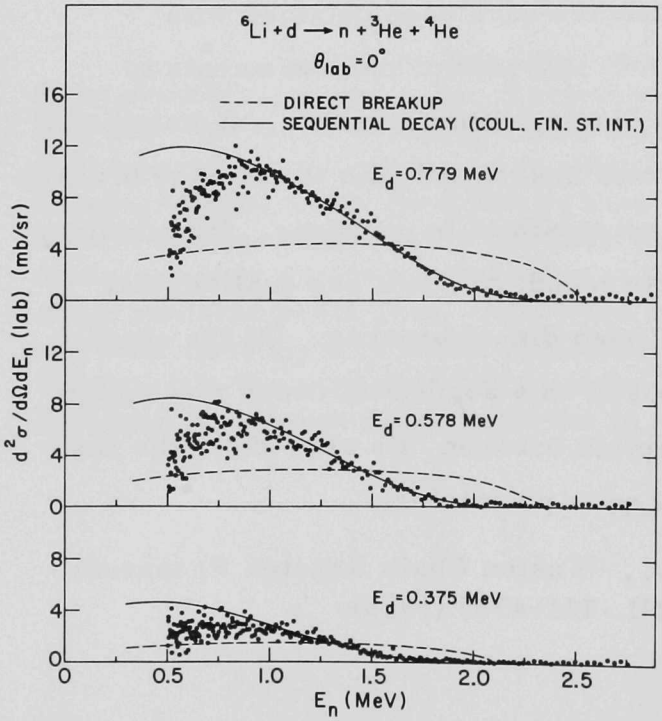

Fig. 26. Lab differential cross sections per MeV as a function of E_n at $\theta = 0^o$ for various deuteron energies, compared to preliminary calculations for direct ^{7}Be breakup (dashed) and sequential decay with a Coulomb final-state interaction between ^{3}He and ^{4}He (solid). The calculations were normalized to the data at neutron energies greater than 0.9 MeV.

b. Cross Sections for Charged Particles from ^{6}Li+d Reactions at Low Energies

C. N. Davids, A. J. Elwyn, R. E. Holland, L. Meyer-Schützmeister, and F. P. Mooring

Experiments designed to determine absolute cross sections for charged particles emitted in d + ^{6}Li reactions at low energies have been initiated. Motivation for such investigations is as presented in the previous contribution. Preliminary relative differential cross sections for the protons in the ^{6}Li(d,p)^{7}Li reaction and the α particles in the ^{6}Li(d,α)^{4}He have been obtained at angles between 15 and 165° at a number of deuteron energies between 0.2 and 0.8 MeV by use of silicon surface-barrier detectors and a 30-in.-diameter scattering chamber. Thin targets of ^{6}Li F evaporated on carbon backings are being utilized, and effects due to the energy dependence of the change of beam charge state and scattering within the target are being investigated. The study of the low-energy charged particles that arise in the breakup of ^{7}Li and ^{7}Be in the d + ^{6}Li reactions will in all likelihood require the use of time-of-flight and perhaps other more specialized techniques.

c. Search for Direct Radiative α Capture. The ^{16}O(α,γ)^{20}Ne Reaction

A. J. Elwyn, L. Meyer-Schützmeister, G. Hardie,* F. P. Mooring, and J. E. Monahan

Experiments to observe γ rays in ^{20}Ne corresponding to the direct, nonresonant alpha-particle capture in ^{16}O have been iniated. This direct capture process represents a transition for the alpha particle from an initial continuum state to a final state, which can be described as an α particle plus the target nucleus in its ground state. Since the initial state does not involve any nuclear interaction, the theory of the process is essentially model independent. Thus, a comparison of experimental and theoretical cross sections can provide α-particle spectroscopic factors for the final states that may be more reliable than such information

*Western Michigan University, Kalamazoo, Michigan.

obtained through α-particle stripping reactions, as (^{6}Li,d). Initial attempts to search for the direct capture γ rays have proved unsuccessful. In spite of the use of a 200-μA beam of 2.5-MeV α particles from the ANL Dynamitron accelerator incident on oxygen targets, no clearcut observation of nonresonant α-capture γ rays [in a 40 cc Ge(Li) detector] could be observed. For the 5.24-MeV E2 transition to the first excited (1.63-MeV) state of ^{20}Ne, an upper limit for the direct capture cross section of ~3.5 nb/sr (at 45°) is obtained from these measurements. Calculations of the direct-capture cross section for the emission of E2 radiation of this energy suggest that the cross section should be almost an order of magnitude smaller. In order that further investigations be successful, modifications of the experimental arrangement, primarily to reduce the backgrounds and eliminate beam-line contaminants, must be undertaken.

d. Neutron Polarization in Isospin-Forbidden (p,n) Reactions

J. E. Monahan and A. J. Elwyn

Most of the spectroscopic information that has been derived from isobaric-analog-resonance reactions has been based on the assumption that their fine structure (consisting of states with isospin $T_<$ that is one unit less than the isospin $T_>$ of the analog) could be treated statistically. However, the validity of this assumption has been questioned.[1] The angular distributions of the yield and of the polarization of neutrons in isospin-forbidden (p,n) reactions can be shown[2] to provide a test of this assumption.

Measurements of the yield and polarization have been made[3] for the ^{51}V(p,n)^{51}Cr reaction in the neighborhood of the analog resonance observed at a proton energy of ~2.335 MeV. The results are

[1] A. M. Lane, Phys. Lett. 29B, 263 (1969).

[2] J. E. Monahan and A. J. Elwyn, Phys. Rev. C 8, 1339 (1973).

[3] E. H. Sexton, A. J. Elwyn, F. T. Kuchnir, F. P. Mooring, J. F. Lemming, R. W. Finlay, and R. E. Benenson, Bull. Am. Phys. Soc. 16, 1432 (1971); and to be published.

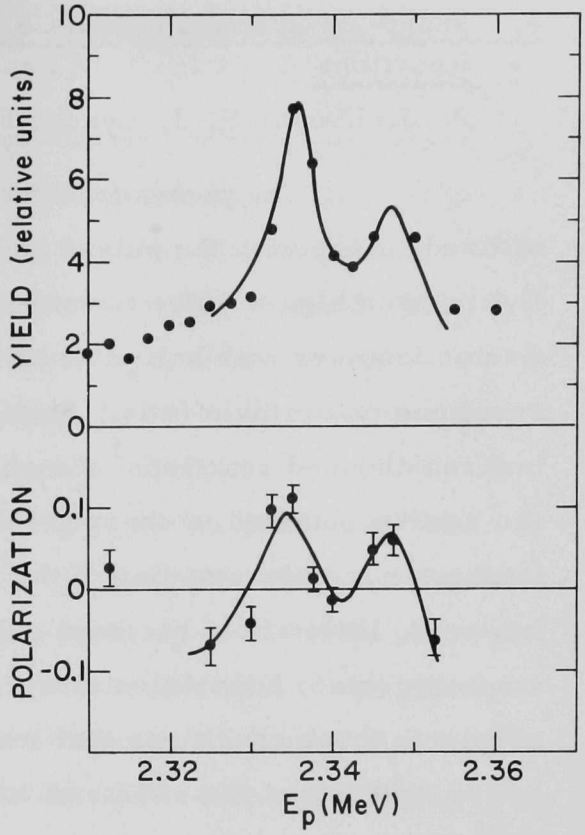

Fig. 27. The energy dependence of the neutron yield and polarization in the neighborhood of the analog resonances near 2.335 MeV. The solid curves are calculations based on the assumption of two analog resonances (at 2.335 and 2.348 MeV) plus a contribution from the inclusion of a nonresonant background in the vicinity of the resonance structure. Each analog state is treated in the single-proton-channel approximation.

shown in Fig. 27. Analysis of these data indicates the presence of two closely-spaced analog states within the energy interval of interest. Because of this complication, and also because of the apparent low density of $T_<$ states in the region of the analog, the analysis did not provide an unambiguous answer to the question about the validity of the statistical assumption. However, the results do indicate the complementary nature of differential-cross-section and polarization measurements in any investigation of the distribution of the $T_<$ states. Also, under certain specified experimental conditions, it is shown[2] that such measurements can detect any significant neutron width acquired by the analog state via Coulomb mixing with the $T_<$ background states.

e. Short-Lived Spontaneously Fissioning Isomers in Neutron-Induced Reactions

A. J. Elwyn, F. J. Lynch, F. P. Mooring, and M. J. Fluss*

The post-acceleration beam-pulsing system has been utilized, along with the pulsed and bunched proton-ion source in the Dynamitron high-voltage terminal to study the production of short-lived fission isomers with half-lives in the nanosecond range in neutron-induced reactions on uranium foils. Studies of fission-isomer formation in neutron-induced reactions[1] [such as the (n, γ) reaction] should supplement the results obtained in charged-particle reactions[2] and at the same time improve our understanding of the reaction mechanism. In the last year, however, little effort has been expended on this project due to other commitments. Experimental work has been devoted to attempts to eliminate those conditions that lead to spurious lifetime determinations, and to understand the effects of low-energy-neutron backgrounds. While some progress has been made along these lines, continuation of this project depends upon modifications of the pulsed source and accelerator optics that will improve the quality and intensity of the ion beam in the Dynamitron, and perhaps on the development of new methods of separating isomeric from prompt events.

---

*Materials Science Division, ANL.

[1] A. J. Elwyn and A. T. G. Ferguson, Nucl. Phys. A148, 337 (1970).

[2] See, e.g., H. C. Britt, At. Data and Nucl. Data Tables 12, 407 (1973).

2. CHANNELING

The channeling program at the Dynamitron has had markedly less activity recently because of the preparations for the pion-channeling experiments planned for LAMPF. The principal remaining activity has been concerned with the channeling of molecular ions. This technique is a very promising one for exploring the details of the channeling process. Possible evidence for plasma oscillations in the channeling crystals has been observed.

Channeling of Particles Injected As Members of Molecular Ions

D. S. Gemmell, J. M. Remillieux, and R. E. Holland

In the channeling of charged atomic particles the interaction between channeled particles can be disregarded since the probability of two being close enough to interact is vanishingly small. If, however, the incident particle is a molecule consisting of two or more nuclei, then the binding electrons are stripped on entrance into the crystal and members of the molecule interact via the Coulomb force and other mechanisms as they are channeled by the crystal.

We investigated the channeling of protons and deuterons introduced as H^+, H_2^+, H_3^+, and $(^4HeH)^+$. The angular spread of the transmitted protons (when the molecule was incident on the (111) plane of a 500 Å gold crystal) was measured in a direction parallel to the plane. The results for H^+ can be used to provide a "system response" function which includes the effect of angular resolution and multiple scattering from electrons in the crystal. A computer program was used to calculate the paths of channeled particles from the average planar potential and the Coulomb repulsion between the particles.

For incident molecular ions, the calculated angular spread of the protons was 40% larger than that observed. We take this to mean that additional force, such as that provided by the oscillations induced in the plasma, is operating on the protons. Calculations which include the effect of plasma oscillations do indeed provide a smaller angular spread, but the agreement is not quantitative.

We anticipate that channeling studies with molecular ions will provide an opportunity for very detailed study of the processes occurring when fast charged particles pass through condensed matter.

IV. ACCELERATOR OPERATIONS

A. THE FN TANDEM VAN DE GRAAFF ACCELERATOR

The nuclear research program at the Tandem accelerator includes ANL experiments in heavy-ion and light-ion research, as well as diverse university-user experiments.

The Tandem continues to run around the clock seven days a week. In addition to scientists from the Physics Division, members of the Chemistry Division and the Chemical Engineering Division used the facility during the past year. Outside user interest increased markedly over the previous year.

The stability of operation was significantly improved with the completion of the development work on the closed corona voltage distribution system. Changes in the control system of the tandem and its associated equipment to obtain more consistent operation were made. Both the direct-extraction duoplasmatron and the sputtering source were placed in operation.

In the period 16 March 1974 to 20 February 1975 the FN tandem operated 5110 hours. Of this time, 56% was used for the acceleration of ^{6}Li, ^{7}Li, ^{12}C, ^{13}C, ^{16}O, ^{18}O, ^{19}F, and ^{35}Cl beams. The remaining 44% was used for the acceleration of hydrogen and helium ions.

a. The Pelletron Chain and Closed-Corona Voltage-Distribution System

The operational experience with the Pelletron chain has continued to be good. The only corrective action necessary was the replacement of the idler wheels at the midsection.

The closed-corona voltage-distribution system required substantial changes in order to obtain reliable machine operation at terminal voltages in excess of 9 MV. These changes consisted of improved gas flow through the corona system, use of a single gas system through the entire length of the machine, rather than separate gas systems for the high-energy and low-energy columns, introduction of spark gaps in the corona assembly and replacement of the nichrome needles by steel.

It was necessary to use the FN tandem for this development work since an adequate test facility for the corona system did not exist. The redesigned system was installed in July 1974 and has given adequate performance since that time.

Experiments have been performed with terminal voltages as high as 9.7 MV. The machine was operated for testing with terminal voltages up to 10 MV with an analyzed $^{16}O\ 6^{+}$ beam of 200 nanoamperes. At this terminal voltage the inadequate stabilization of the ion injection system causes most of the operational difficulties. Since December 1974 the terminal voltage has been limited to about 9.4 MV due to difficulties with the TU 251 accelerator tube.

b. Ion-Source Development

All of the components to change the ion-source system configuration to allow several different sources to be on line simultaneously have been constructed.

A direct extraction source of the Wisconsin type has been built and tested on the tandem. It has successfully produced beams of ^{18}O with currents of 300 nanoamps $^{18}O\ 4^{+}$ on target. The Smith-Richards sputter PIG source is under construction. Both the good emittance and small energy spread of heavy-ion beams from this type of source are important for our future needs for bunched heavy-ion beams through the accelerator. These sources also allow the changeover of the ion-source configuration with a minimum time loss for the experimental program.

The development work on the sputtering source of the Middleton type has continued. The emittance of the source has been improved considerably without loss of useable beam current. The complexity of source changeovers needed by the requirements of the experimental program make it impractical to install the source for normal use until early July 1975.

The components necessary for single-gap bunching tests on this type of source are under construction.

c. Control System for the Tandem

A new NMR system for control of the 90° analyzing magnet as well as a new power supply for the magnet have been purchased. The control systems needed for linking the two devices are under construction. The new system will be especially useful for excitation-function type experiments, and eventually such experiments can be computer controlled. The arrangement will also reduce uncertainties due to hysteresis effects in the analyzing magnets.

d. Physics Division On-Line Computer System

The process of replacing the old ASI computers with a system based on the PDP 11/45 central processor is in progress. Peripheral devices consisting of printer/plotter, 9-track magnetic tape, ADC interfaces, storage scope display unit, 2 CAMAC crates, and 88 K of memory are now installed on the computer to be used for data acquisition at the tandem. A similar array will be available at the Dynamitron. We anticipate working programs sufficient for taking data will be available by July 1, 1975.

e. Planned Upgrading of the Tandem

A major effort to upgrade the tandem will start during the second half of 1975. The ultimate objective of this effort will be to provide intense pulsed beams of heavy ions through mass A = 70, as needed for injection into the superconducting-linac energy booster described in Sec. V.C.

In the initial phase of the work, the ion-source configuration of the tandem will be restructured in order to form a flexible multisource system. This change will include improvements in the ion-source power

supplies and the acquisition of the preacceleration system needed for reliable injection of heavy ions into the tandem. Simultaneously, the development of negative-ion sources will be continued.

The main part of the upgrading project will consist of efforts (a) to improve the vacuum in the accelerator tube, (b) to modify the terminal, and (c) to build an advanced bunching system.

f. University Use of the Tandem Accelerator

The appeal to neighboring research institutions of the Argonne tandem as an available experimental resource increased during the past year. The number of laboratories participating in the outside user program increased from eight to eleven. As in recent years, most user groups chose to collaborate with local scientists. This collaboration does facilitate the research program, as well as promote the interchange of ideas within the research community.

Most university groups tend to use existing facilities. Some, however, are pursuing fields of research for which no local specialized equipment is available. These groups have installed at the tandem equipment brought from their own institution. Generally, this equipment is complemented by a local specialized facility.

A list of those institutions whose staff members have performed experiments at the tandem during the past year together with the names of the principal investigators and the research that was done is given below. The names of the local collaborators are enclosed in parentheses.

1. East Texas State University

   Transfer Cross Sections in the Region of the Malmin Resonance

   D. S. Gale (W. Henning, D. G. Kovar, and B. Zeidman)

2. University of Kansas

   Assignment of the Spin of a State in ^{28}Si by Studying the Reaction $^{16}O(^{16}O,\alpha)^{28}Si$; $^{28}Si \rightarrow {}^{24}Mg + \alpha$

   R. W. Krone and F. W. Prosser (R. L. Boudrie)

3. Massachusetts Institute of Technology

Excitation Function of the $^{12}C(^{12}C,p)^{23}Na$ Reaction

E. R. Cosman, T. M. Cormier, K. Van Bibber, and G. Young (J. R. Erskine and L. R. Greenwood)

4. Northern Illinois University

Production of a Mössbauer source by the $^{54}Cr(\alpha,p)^{57}Mn$ Reaction

R. S. Preston (B. J. Zabransky)

5. Northwestern University

A Study of the $^{40}Ca(^{16}O,^{12}C)^{44}Ti$ Reaction

L. R. Greenwood (J. R. Erskine, W. Henning, and D. G. Kovar)

6. Ohio University

Level Structure of ^{76}As As Seen in the $^{75}As(d,p)^{76}As$ Reaction

J. F. Lemming and J. Rappaport (A. J. Elwyn)

Energy Levels of ^{108}Ag Produced by the $^{107}Ag(d,p)^{108}Ag$ Reaction

C. E. Brient and J. R. Comfort

7. University of Pennsylvania

A Study of High-Spin States in ^{20}Ne Via the $^{12}C(^{12}C,\alpha)^{20}Ne$ Reaction

H. T. Fortune (T. H. Braid, K. Raghunathan, and R. E. Segel)

8. Purdue University

Gyromagnetic Ratios of High-Spin States

R. J. Mitchell, T. V. Ragland, and R. P. Scharenberg (R. E. Holland and F. J. Lynch)

9. University of Washington

Excitation Function of Alpha Particles Elastically Scattered at Back Angles

K. A. Eberhard (J. P. Schiffer and S. E. Vigdor)

10. Western Michigan University

Lifetimes of States in fp Shell Nuclei Seen in the Gamma Decay from High-Spin States

G. Hardie (L. Meyer-Schützmeister)

11. Wright-Patterson Air Force Base

Study of the $^{42}Ca(\alpha,d)^{44}Sc$ and the $^{44}Ca(\alpha,d)^{46}Sc$ Reactions

J. C. Manthuruthil and C. P. Poirier (T. H. Braid and L. Meyer-Schützmeister)

In addition to the outside user groups which visit Argonne from their home institution to use the tandem facility, there are a number of graduate students doing their thesis problem at Argonne. These students did their course work at their sponsoring institution. For all but one, the thesis advisors are Argonne staff members. A list of the resident graduate students, their sponsoring institution, and their thesis advisors is given below.

1. R. L. Boudrie; University of Kansas
   F. W. Prosser, adv.
2. W. Corwin; Illinois Institute of Technology
   R. E. Segel, adv.
3. R. C. Pardo; University of Texas
   C. N. Davids, adv.
4. L. Parks; University of Texas
   C. N. Davids, adv.
5. K. Raghunathan; Northwestern University
   R. E. Segel, adv.
6. T. Renner; University of Chicago
   J. P. Schiffer, adv.
7. J. F. Tonn; Northwestern University
   R. E. Segel, adv.

B. OPERATION OF THE DYNAMITRON

Operational Experience

F. P. Mooring, A. Langsdorf, Jr., and R. L. Amrein

During the past year, the Dynamitron has performed well. Thirteen weeks were spent in installing the new accelerator tube and remodeling the machine. The Dynamitron was used to accelerate an ion beam for 85% of the remaining time. Among the atomic-ion beams used by the experimenters were $^{1}H^{+}$, $^{2}H^{+}$, $^{4}He^{+}$, $^{11}B^{+}$, $^{12}C^{+}$, $^{14}N^{+}$, $^{16}O^{+}$, $^{20}Ne^{+}$, $^{35}Cl^{+}$, $^{37}Cl^{+}$, $^{40}A^{+}$, $^{51}V^{+}$, $^{58}Ni^{+}$, and $^{60}Ni^{+}$. In addition, molecular-ion beams were used. They included $(^{2}H\text{-}^{2}H)^{+}$, $(^{2}H\text{-}^{2}H\text{-}^{2}H)^{+}$, $(^{4}He\text{-}^{1}H)^{+}$, $(^{4}He\text{-}^{2}H)^{+}$, $(^{16}O\text{-}^{1}H)^{+}$, and $(^{14}N\text{-}^{14}N)^{+}$.

The wide variety of experiments performed at the Dynamitron has required the use of ion beams with a great variation of intensity and energy. Ion currents from as low as a few nanoamperes to as large as 200 microamperes were used. Particle energies varied from 200 keV to slightly more than 4.5 MeV. Both dc beams and pulsed beams were used.

More than thirty scientists have used the Dynamitron in their research program. About half of its users were from the Physics Division. Investigators from two other Argonne research dividions comprised about one-third of the users. Visitors from five other laboratories were attracted by the unique capabilities of the facility, as well as visiting scientists from two foreign countries.

The machine continues to run 24 hours per day, five days per week. Actual machine failures have been minimal. The many ion-source changes required by the need to supply a great variety of ion species account for most of the lost time. A project to modify the terminal so as to make ion-source changing easier has been started. It should be completed during the coming fiscal year.

A number of improvements of the Dynamitron are planned for the coming year. The terminal will be rebuilt so as to make ion-source changes simple, safe, and efficient. Structural members within the terminal will be designed to allow easy access to the ion source. Where necessary, support structures will be hinged so that they can be moved out of the way while ion sources are being exchanged. All electronic circuits will be relocated in a logical array that takes into account their roles in the overall system. Chances of wiring errors will be practically eliminated.

If funds permit, the vacuum tube rectifiers in the Dynamitron will be replaced with solid-state rectifiers. The replacement will extend the accelerator's voltage range both upward and downward. The downward extension is of considerable importance to the program of measurements of low-energy charged-particle cross sections.

Our present switching magnet limits the angle through which energetic heavy ions can be deflected. At present most research using heavy ions is limited to the 9° ports. At this angle the mass resolution of the magnet is inadequate for many experiments. Along any other beam-line direction, the maximum available energy for heavy ions is too low for most purposes. Thus the experimental program using heavy ions has been hampered.

The ideal solution to this problem would be to replace the existing switching magnet with one having a much larger mass-energy product. This cannot reasonably be done since the space available is simply too small for a larger magnet. A satisfactory solution, though a compromise, is to install a second bending magnet along one of the 9° beam lines. This magnet will be able to bend the heavy-ion beam an additional 9° or 18°. This will add two more beam line directions to the two existing 9° lines for heavy-ion research. The new magnet will be installed during the next year.

As ion sources have become more involved and complicated, the need for knowledge of the ion source parameters has greatly increased. Previous attempts to provide a telemetering system that would provide the necessary information at the control table was not entirely successful. Tank sparks destroyed circuit components and the reliability of the system was minimal. However, new shielding techniques have been developed in recent years, and such systems at other laboratories are now dependable. Such a system will be developed and installed in the Dynamitron during the next year.

V. SUPERCONDUCTING LINAC DEVELOPMENT

L. M. Bollinger, J. Aron,* R. Benaroya,* B. E. Clifft,* A. H. Jaffey,* K. W. Johnson,* T. K. Khoe,† J. J. Livingood, F. J. Lynch, P. Markovich,* J. M. Nixon,* G. W. Parker,* and B. Zeidman

INTRODUCTION

Heavy-ion research is one of the principal activities in the Nuclear Sciences program at Argonne. As an integral part of this program, the Chemistry and Physics Divisions have for several years been jointly supporting a project aimed at the development of superconducting RF technology and its application to the acceleration of heavy ions. Beginning in mid-1975, there will be a companion project concerned with the specific task of adding a small superconducting linac as an energy booster for heavy ions from the FN tandem Van de Graaff accelerator.

Major parts of the ongoing superconducting-linac development program are: (1) the development and testing of superconducting RF accelerating structures, (2) the optimization of the fabrication techniques and component designs required for a practical accelerator, and (3) the development of the conceptual design of a tandem-linac accelerator system.

Most of the work to date has been concerned with helix accelerating structures made of niobium metal and operating at an RF frequency of about 100 MHz. The development of this structure has been pushed to the point where it is ready for practical application. Now the emphasis is shifting to the study of the split-ring structure and to the development of inexpensive techniques of fabrication. Concurrently, the concept of a tandem-linac accelerator system has evolved steadily and is now well developed. Highlights of the progress during the past year are outlined below.

---

*Chemistry Division, ANL.

†Accelerator Research Facilities Division, ANL.

A. CONCEPT AND COMPONENT DEVELOPMENT

$\lambda/2$ Helix Performance

Systematic studies of the performance of $\lambda/2$ superconducting-helix resonators such as the one illustrated in Fig. 28 have continued. In particular, tests on one resonator were carried out after each of some 37 variations in surface treatment. The results were highly reproducible, indicating that our surface-treatment techniques are reliable. Bare surfaces gave results somewhat superior to anodized surfaces but, unlike the anodized surfaces, the bare surfaces deteriorate somewhat after long exposure to air. Surface electric fields as high as 37 MV/m, magnetic fields as high as 1200 G, and surface resistances as low as 5×10^{-10} ohms have been measured. An example of experimental results is given in Fig. 29.

Beam-Line Use of a $\lambda/2$ Resonator

In connection with a beam-bunching experiment with ^{16}O projectiles (described later), a $\lambda/2$ resonator with a bare surface was maintained in a cool-down condition on a beam line at the FN tandem for a period of about 20 weeks. The performance of the system was excellent and remained unchanged during this period in spite of a series of vacuum failures. This good experience under less than ideal conditions gives us confidence that the resonators in a practical accelerator may be expected to operate well for long periods of time.

$5\lambda/2$ Resonator

A $5\lambda/2$ resonator designed for beam-line use was completed and tested under several conditions. The initial performance was adequate. However, the failure of an ion pump after this initial

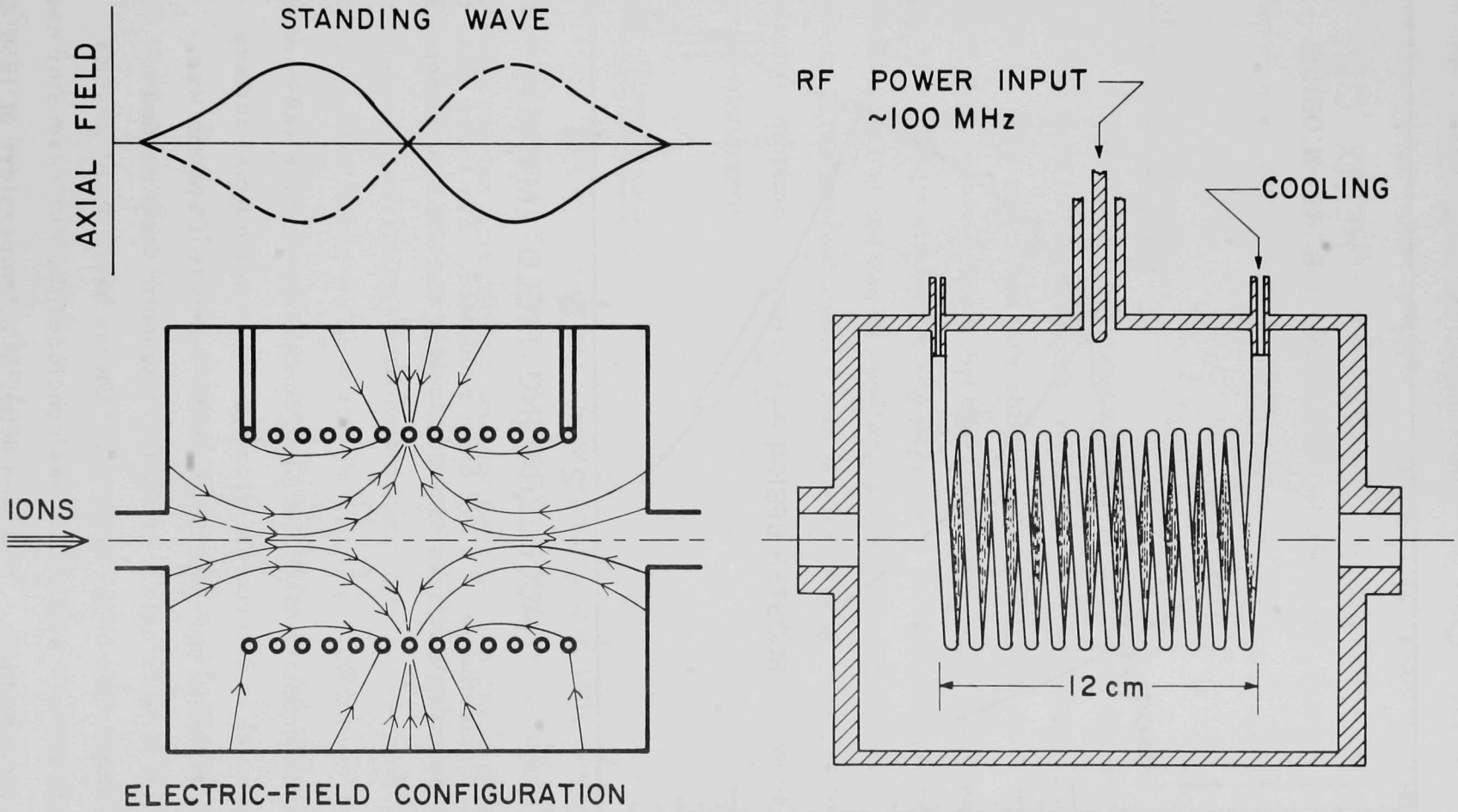

Fig. 28. Illustration of a $\lambda/2$ superconducting helix accelerating structure. The resonator is made of niobium metal and is cooled by a bath of superfluid helium.

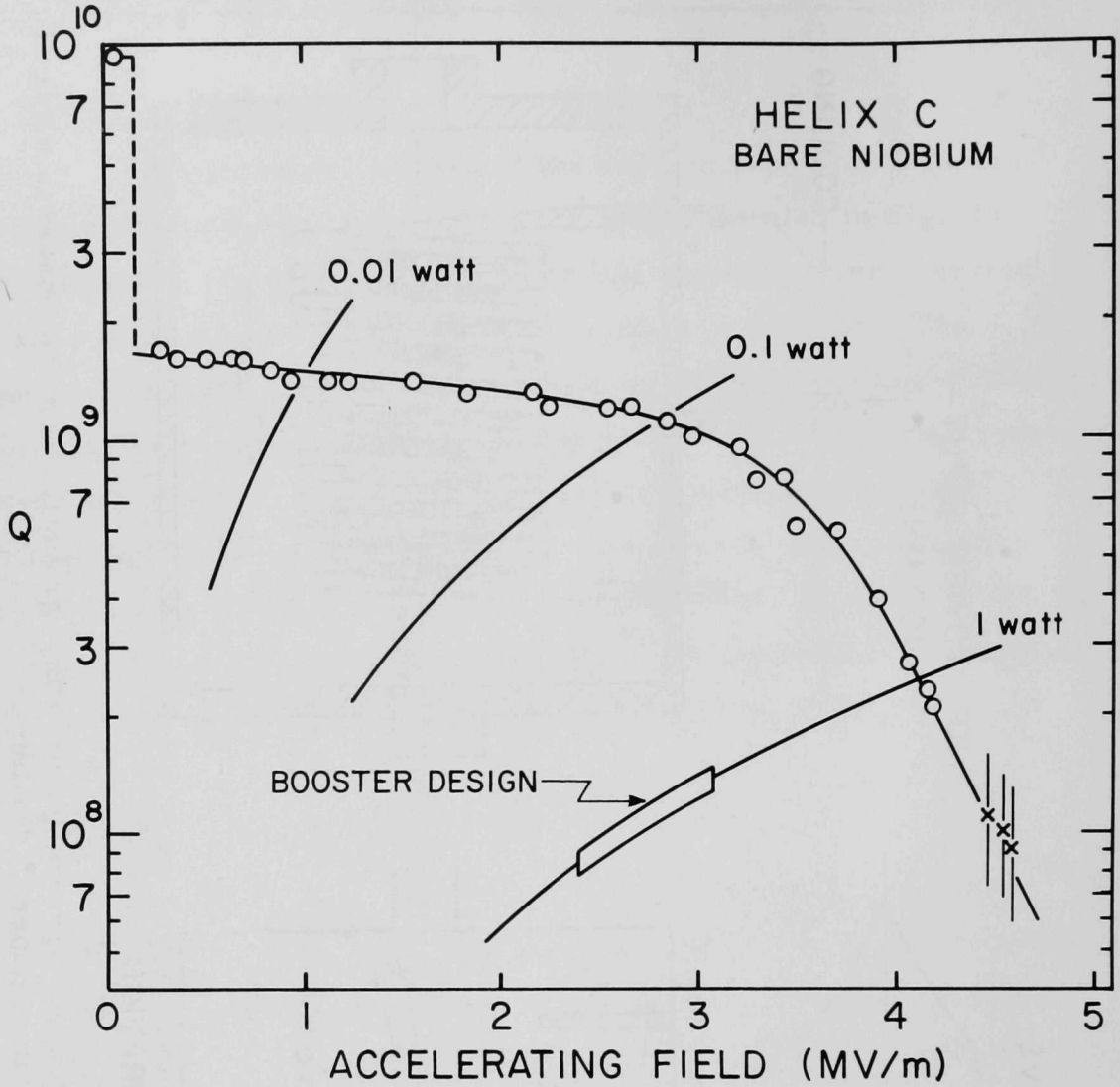

Fig. 29. Performance of a $\lambda/2$ helix resonator. For these data, the superconducting surfaces of the resonator were bare electropolished niobium.

test apparently contaminated the superconducting surface and caused the performance to deteriorate greatly. Since our normal surface treatments failed to correct the problem, a new test system was developed so as to be able to make the diagnostic tests needed to determine the nature of the difficulty. On the basis of the results of tests with the new system, it was concluded that the resonator needed to be heat treated again. This was done, at a temperature of 1250°C,

and the unit then operated up to a maximum field of 2.1 MV/m, which is above the design value. At this field level, the resonator would (for example) increase the energy of an O^{6+} ion by about 8 MeV.

Figure 30 is a photograph of the $5\lambda/2$ resonator and its beam-line cryostat prior to assembly.

Fabrication Techniques

Heretofore, the emphasis in resonator design and construction has been to optimize performance, with little attention being paid to cost. The effort has now shifted to the development of fabrication techniques that reduce costs substantially without sacrificing resonator performance. The main idea being pursued is to fabricate resonators from sheet metal by the use of bending, pressing, and extruding techniques. This approach will minimize machining, which is very expensive for niobium. Construction of the first resonator to be made in this way has started.

Split-Ring Resonator

The split-ring resonator, developed in 1974 at the California Institute of Technology, has very attractive electrical characteristics, but heretofore it has seemed impractical as a low-frequency structure made of niobium because of its large radial dimensions. The new fabrication techniques outlined above now seem to remove this objection, and hence we have started to design and construct the first such unit to be made of niobium. It will be in operation by late 1975.

If the electrical characteristics of the split-ring resonator turn out to be as good as the present evidence indicates, and if the new fabrication techniques outlined above are successful, then the split-ring superconducting resonator will be a strong contender as the optimum structure for a heavy-ion accelerator.

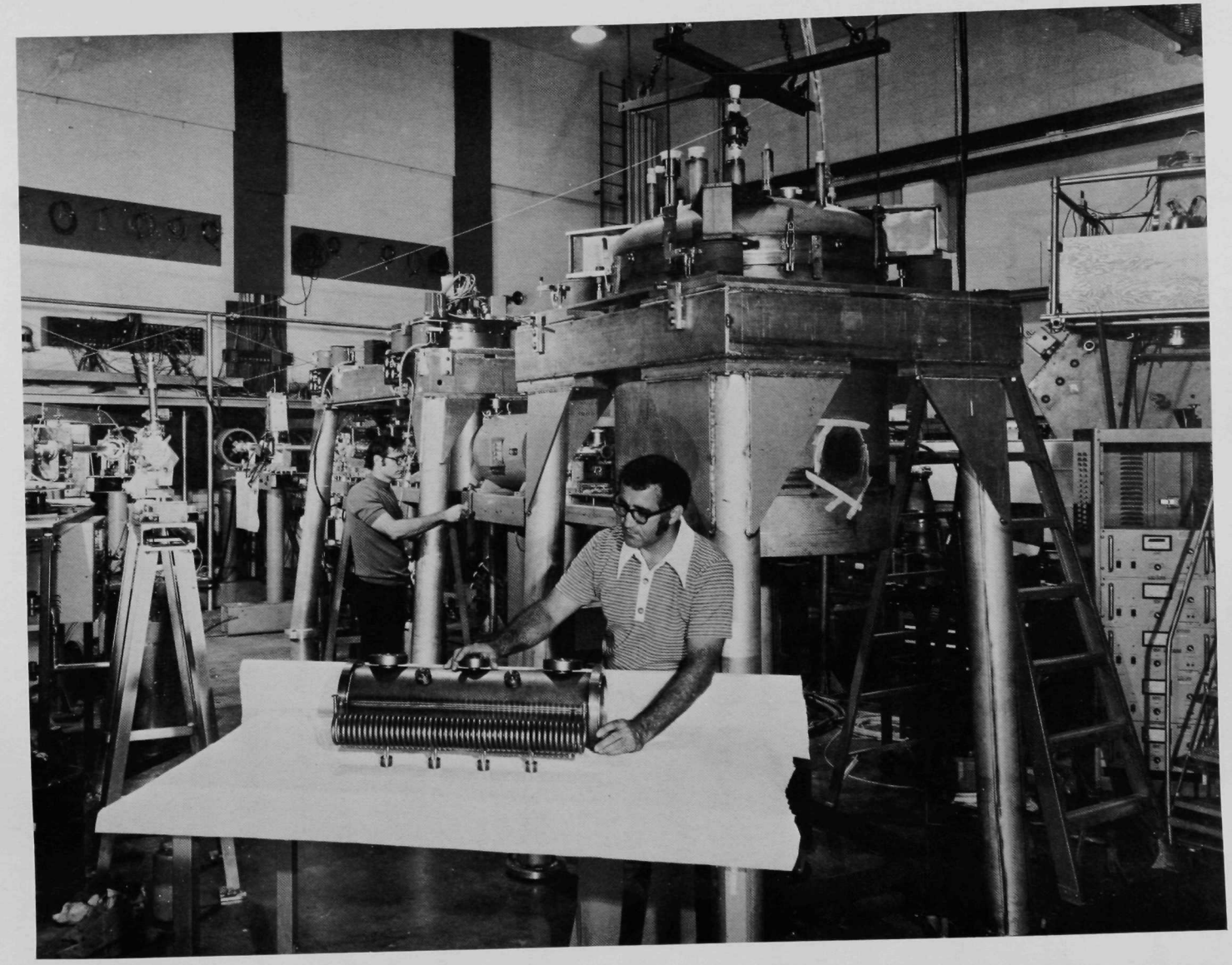

Fig. 30. Photograph of the 5λ/2 helix resonator prior to the welding of the helix into its cavity. The large apparatus behind the helix resonator is the beam-line cryostat into which the resonator was later mounted. The beam line from the tandem approaches from the left.

Theory

A thoroughgoing theoretical analysis of heavy-ion acceleration in a linac has been carried out during the past year. Various causes for loss of beam quality have been identified and described quantitatively. The analysis shows that it should be feasible to operate a linac in such a way as to provide a beam with tandem-like quality.

Tandem-Linac-Accelerator Concept

The concept of a tandem-linac accelerator system has been systematically developed for a linac with independently-phased resonators. The theoretical analysis mentioned above shows that a requirement for good performance is the injection of ultra-short beam pulses into the linac. The bunching experiments described later in this report demonstrate that the required narrow bunches can be formed. The theoretical analysis also identifies the various factors that tend to degrade the beam quality, and the relationship of these factors to component design has been examined. It has been shown that it should be feasible to reduce each of the beam degrading effects to a level such that it will cause the relative spread $\Delta E/E$ in beam energy to be substantially less than 10^{-3}.

A second requirement for good performance of a linac is a beam of small size throughout the acceleration process. The tandem provides an incident beam with the required characteristics, and radial-focusing elements may be used frequently within the linac to maintain this small size. A prototype of an inexpensive superconducting solenoid to perform this function has been designed and will be built soon.

The basic logic of how to operate a tandem-linac system for optimum performance has been developed. This study indicates that the main design objective should be to preserve the longitudinal emittance of the output beam—that is, to minimize the produce $\Delta E \Delta t$,

where ΔE is the energy spread and Δt is the time spread of the beam. Then, after leaving the linac, the phase ellipse of the beam pulse can easily be manipulated to minimize either ΔE or Δt, depending on the experimenter's requirements. In this way, the linac itself can produce a beam with $\Delta E/E < 10^{-3}$ and $\Delta t < 50$ psec and, without much complication, the beam delivered to the experimenter can be modified to have either $\Delta E/E \geqslant 2 \times 10^{-4}$ or $\Delta t \geqslant 30$ psec.

Variability of the beam energy is also achieved with ease in a linac that has independently-phased resonators.

Design studies aimed at making it feasible to implement the above ideas in a cost effective way are in progress. Our experience during the past three years indicates that, from the point of view of minimizing costs of superconducting resonators, the main problems are: (1) the difficulty of machining niobium and (2) the difficulty of making large reliable vacuum seals on the resonators. In order to eliminate these difficulties, we are developing a concept in which the liquid helium is contained in a double-walled panel that forms the resonator itself. This idea permits all large vacuum seals associated with resonator to be eliminated and hence allows the resonator to be fabricated almost entirely by bending, extruding, and welding niobium sheet metal and tubing. This approach is expected to reduce fabrication costs for resonators to about half of the cost required for conventional construction.

In addition to reducing costs substantially, the new concept for the mechanical features of the linac implies immense flexibility for future change. An attractive aspect of the linac has always been the feasibility of adding to its length, if desirable, without needing to rebuild the whole system. The new mechanical concepts that are being developed now tend to make it feasible to modify the existing structure, without great expense, at some future time in order to benefit from future technological advances.

B. BUNCHING OF HEAVY-ION BEAMS

As mentioned above, a heavy-ion linac can provide a beam of good quality only if the beam pulses injected into it are extremely short. Typically, it is desirable to have pulses less than 100 psec wide. Moreover, in a tandem-linac system, it is desirable to be able to bunch a large fraction of the beam accelerated by the tandem. These requirements of high bunching efficiency and ultra-short pulses are both an order of magnitude beyond what has been achieved previously.

We intend to meet the beam-pulsing requirements of a tandem-linac accelerator with a system in which bunching is carried out in two main steps: before and after acceleration in the tandem. The objective of the pretandem bunching is to bunch most of the DC beam from the ion source into beam pulses about 1 nsec wide (for a 10 nsec RF cycle time) at the tandem terminal. Then, following acceleration in the tandem, this relatively wide bunch is compressed to the required width of <100 psec.

By now, it is clear that the hard part of the bunching operation is the pretandem part. However, this difficulty results from well-understood effects in a regime of time that is commonplace. On the other hand, the concept of compressing a nanosecond-wide heavy ion beam pulse down to <100 psec goes well beyond reported experience. Thus, it seemed possible that some unforeseen difficulty would arise and, in order to eliminate this possibility, the bunching experiment illustrated by Fig. 31 was carried out. The DC ^{16}O beam from the tandem was first chopped into pulses about 1 nsec wide and these pulses were then compressed by a $\lambda/2$ helix resonator operating at a frequency of 92 MHz and an accelerating field of about 0.76 MV/m. The compressed beam pulse was detected about 8 meters downstream by means of a surface-barrier detector.

From the characteristics of the beam incident on the buncher and from the known time-spreading effects during the bunching

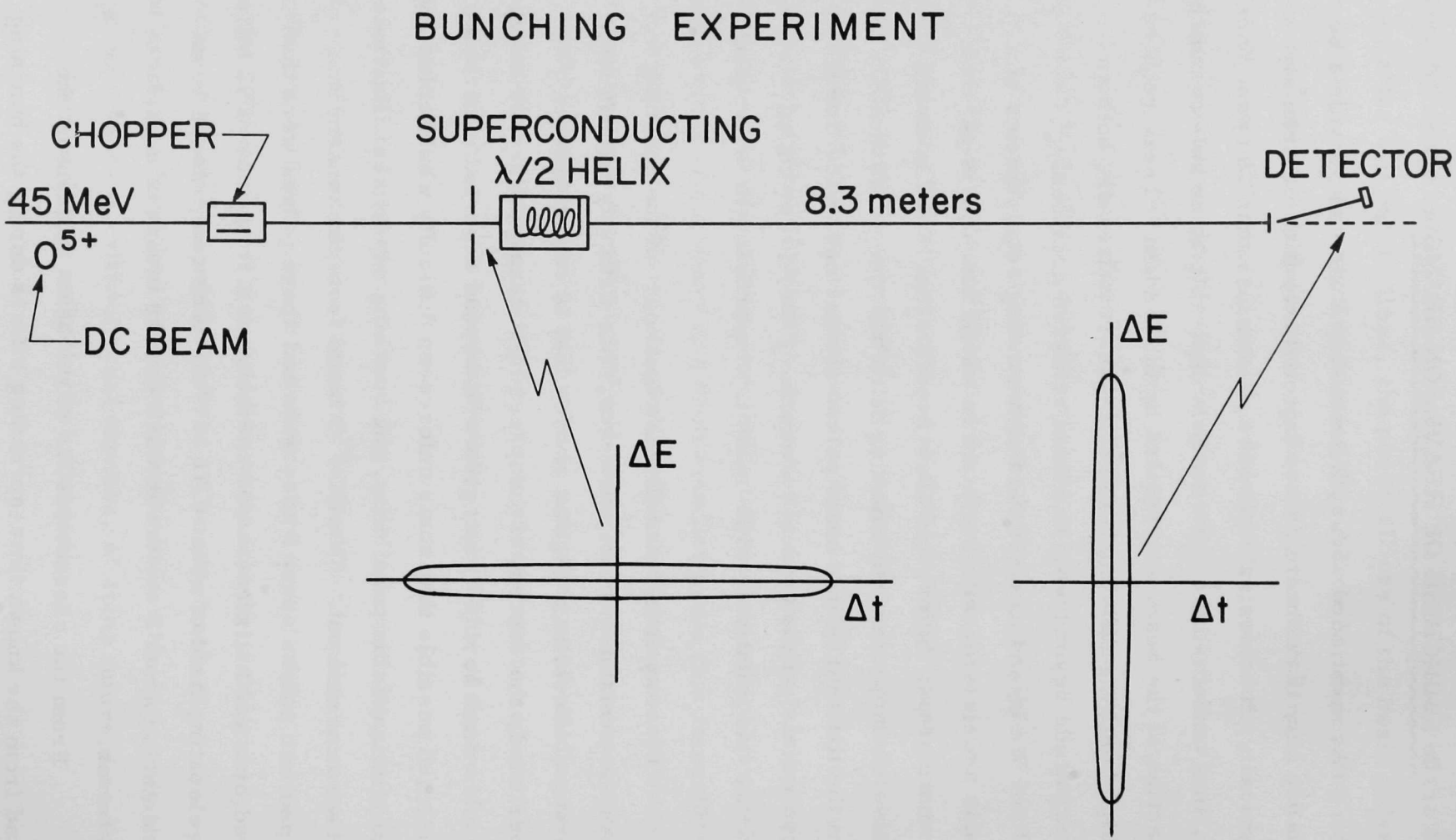

Fig. 31. Schematic representation of the experimental arrangement used to demonstrate the feasibility of bunching heavy-ion beams into ultrashort pulses. The lower part of the figure shows the phase ellipse (the dependence of energy spread ΔE on time spread Δt) at two locations.

process, it was expected that the final beam pulse would be about 20 psec wide. However, this width was expected to be largely obscured by the resolution width of the detector—a width of about 50 psec. The measured width was 57 psec (FWHM), which is consistent with what was expected and small enough to ensure that beam pulses are not seriously broadened by unforeseen effects.

The experiment outlined above indicates that the formation of ultra-short pulses of heavy ions at the energies provided by a tandem accelerator is a straightforward matter, with no barriers in principle. Thus, one can proceed with confidence to develop the concept of a tandem-linac accelerator system that operates with good beam quality. Almost as important, the availability of ultra-short pulses of heavy ions opens up many exciting new experimental possibilities, and the ease with which our bunching experiment was carried out is leading us to proceed immediately to develop a complete bunching system for this purpose.

C. HEAVY-ION ENERGY BOOSTER

In view of the success of the development program described above, in mid-1975 we intend to start on the design, construction, installation, and testing of a small superconducting linac to serve as an energy booster for heavy-ion beams from the FN tandem. The principal justification for the work is the opportunity it affords to advance the development of superconducting RF technology, but the project is also expected to result in a useful accelerator system.

Because of the developmental nature of the heavy-ion booster project, the conceptual design of the accelerator system has not yet been frozen. However, the principal design objectives are to construct a linac that (1) provides a maximum accelerating voltage of 13.5 MV and that (2) has an output beam with tandem-like beam quality. In order to achieve the second objective, we intend to use an accelerating structure with a relatively low (about 100 MHz) RF frequency. The accelerator system will consist of independently-phased resonators so as to make it useful for a wide range of projectiles. The system will be designed to be as simple and flexible as possible so that it will be feasible to make use of future improvements in a rapidly developing technology. The overall layout of the system is illustrated in Fig. 32 and its expected performance with respect to energy is shown in Fig. 33.

The first year of the project will be devoted largely to design and to other preparations for fabrication. Major parts of this initial effort are (1) the design, construction, and testing of prototype resonators, (2) the design of the mechanical system as a whole, (3) the development of specifications for a helium refrigerator, and (4) the design of the RF system. That is, most of the design decisions about the accelerator will have been made by mid-1976.

The primary decisions concerning the design of the linac involve the choice of the following: (a) accelerating structure, (b) the lengths of individual resonators, (c) the velocity profile of the linac,

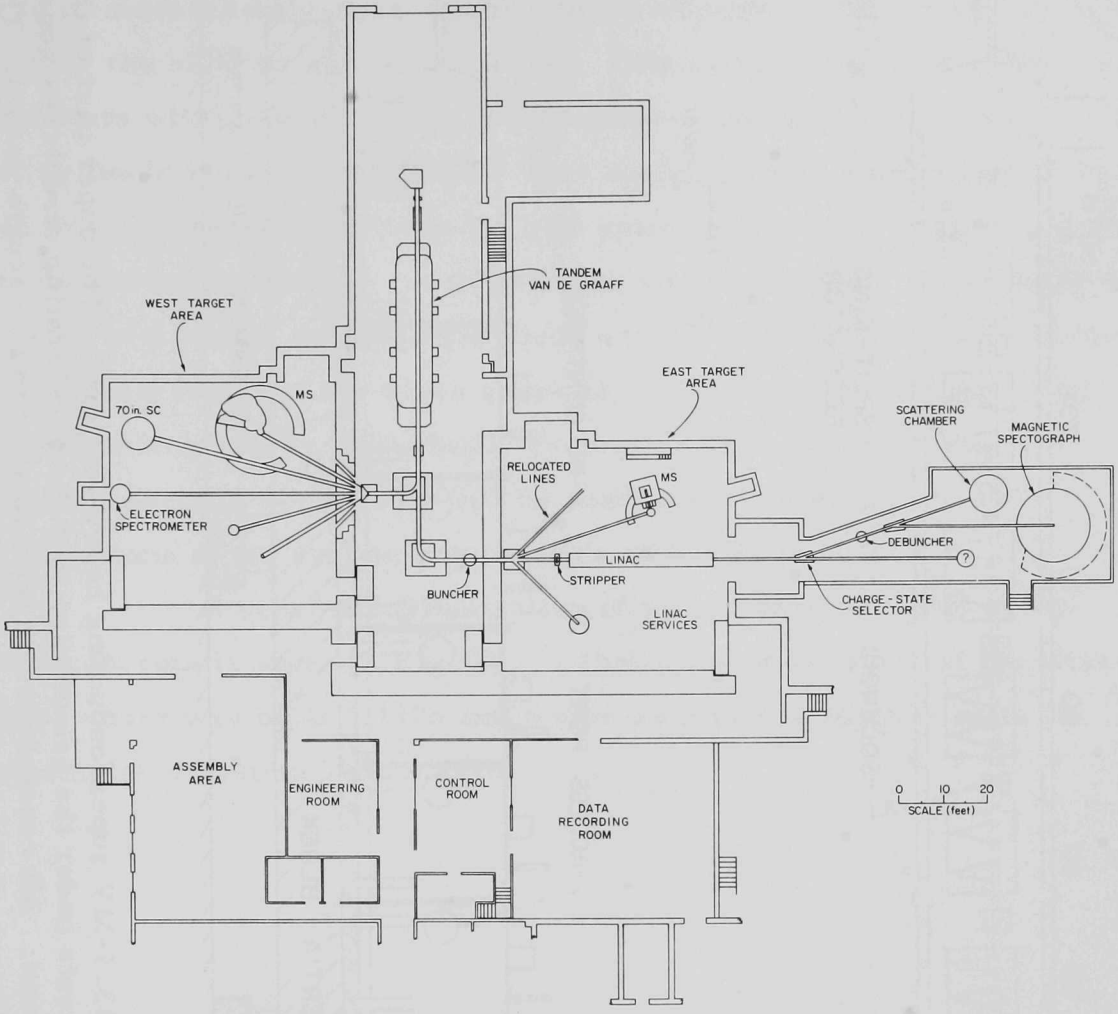

Fig. 32. Overall layout of the planned tandem-linac accelerator system. The tandem is the FN tandem in its present location.

(d) the operating temperature of the resonators and the maximum heat load of the system, (e) the technique of vibration compensation and control, and (f) the accelerating field.

Basic questions about the mode of operation and the design characteristics required to yield the desired high-quality output beam have already been answered by the investigations carried out under the general accelerator-technology development program described above.

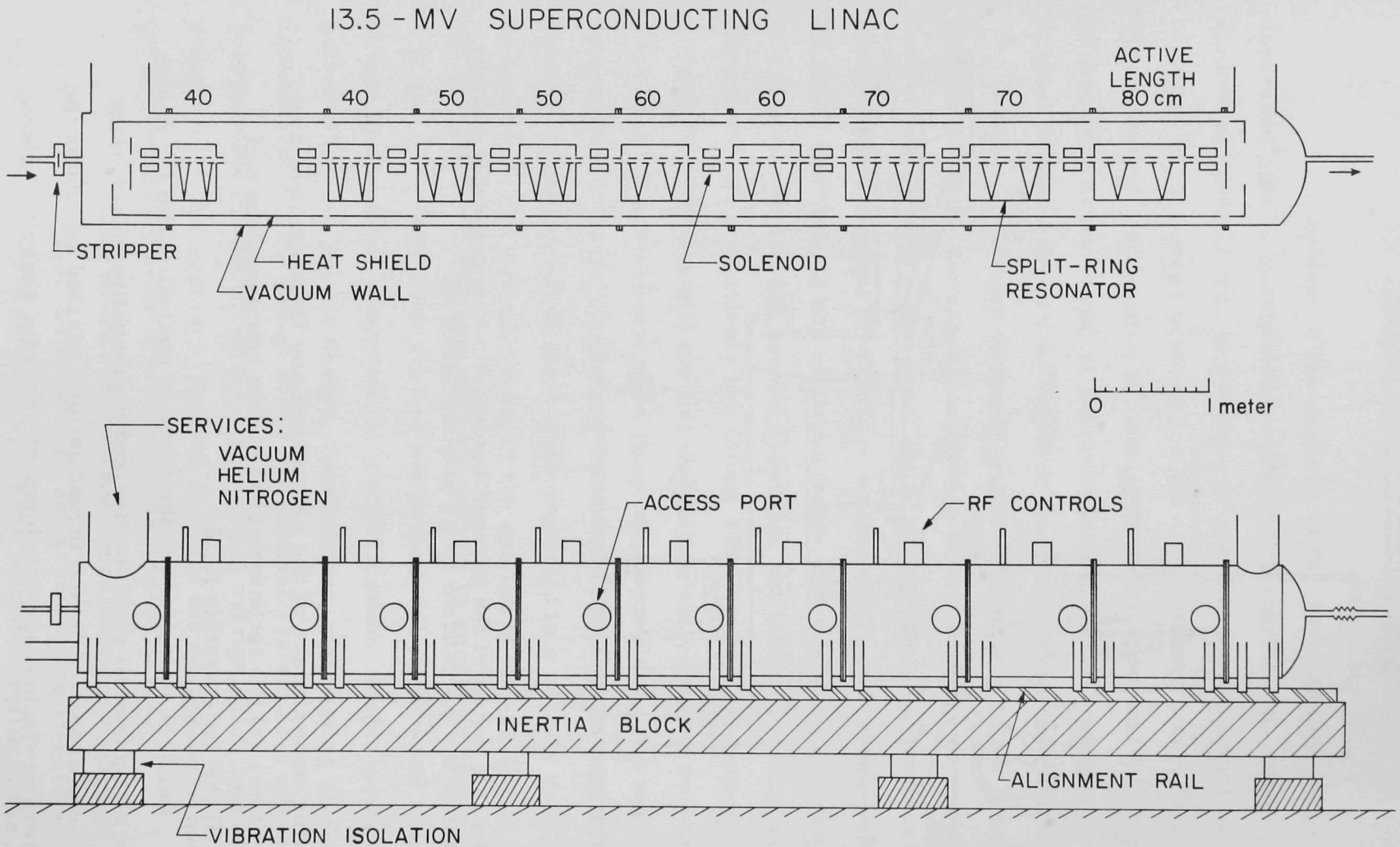

Fig. 33. Schematic representation of a 13.5-MV superconducting heavy-ion linac. The upper part of the figure shows some of the inner components under the assumption that the accelerating structures consist of two split rings within a single container. All resonators are open to a common vacuum vessel. The lower part of the figure shows outer features of the accelerator. Modules about 1 meter long can be individually removed for maintenance.

As it is now visualized, the linac will consist of a linear array of independently-phased multiple-wavelength niobium resonators of either the helix or split-ring design. The outer containers of the resonators will be formed by a double sheet-metal wall within which cooling liquid helium is confined. This design feature eliminates the need to separate the vacuum in the resonator from the insulation vacuum outside and is expected to result in major cost reductions. A cylindrical nitrogen heat shield encloses the whole array of resonators and an outer vacuum wall encloses the whole assembly. Accelerator sections about one meter long will be individually removable from the assembly. Thus, all parts of the system will be readily accessible and future modifications of the system can be made with relative ease.

A schematic illustration of an accelerator based on the above concepts is given in Fig. 34. Fabrication of all parts of the linac will be under way by late 1976 and the present aim is to start tests on the completed system before 1978.

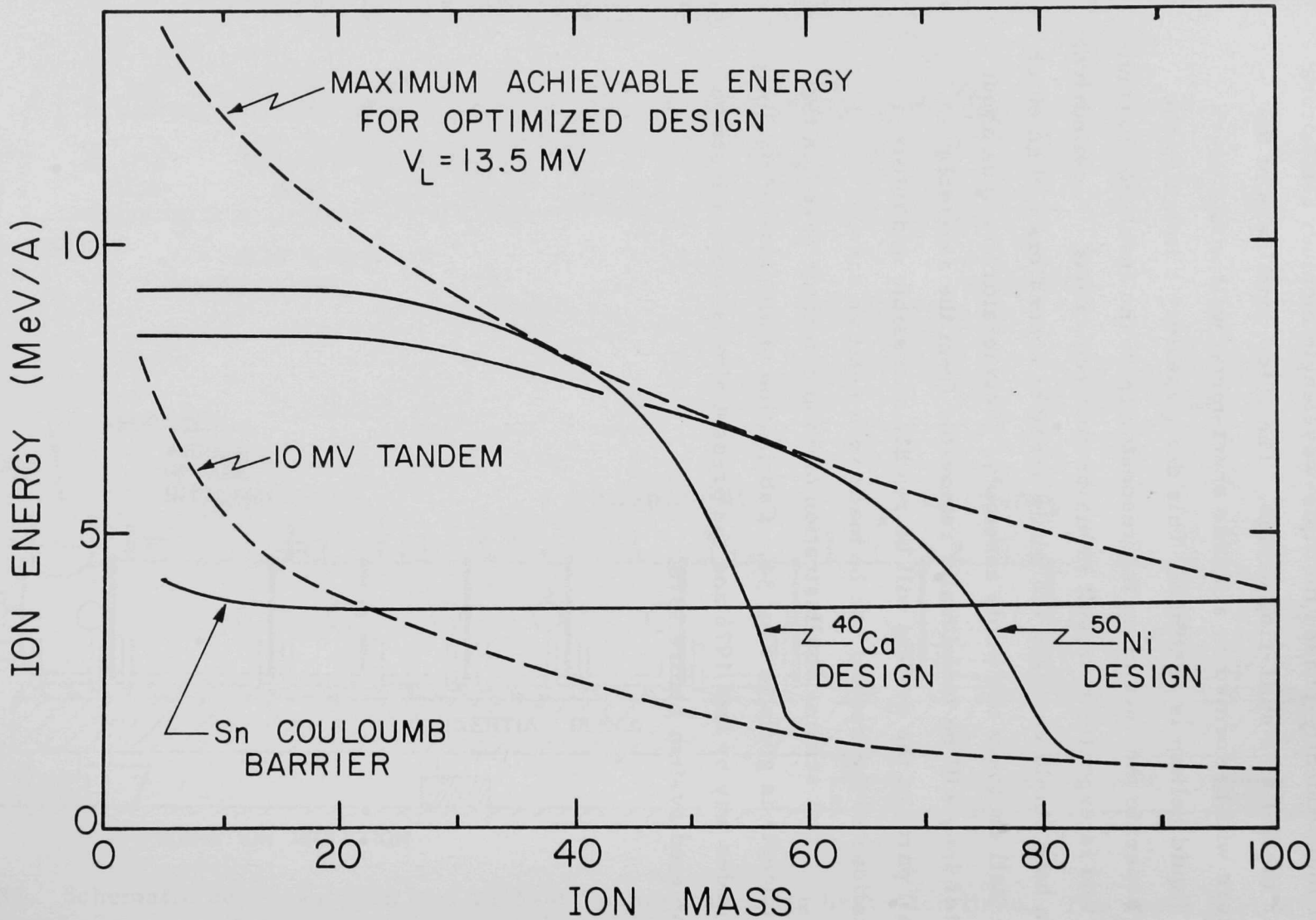

Fig. 34. Approximate calculations of the maximum ion energy as a function of ion mass for a 13.5-MV linac under the assumption that the tandem injector is operated with 10 MV on its terminal. Performance is shown for two possible designs: one optimized for ^{40}Ca and one for ^{58}Ni.

VI. NEUTRON PHYSICS

INTRODUCTION

The principal objective of the Neutron Physics program is the exploration and understanding of those features of nuclear structure for which the neutron is a useful and often unique probe. This goal sets the character of the program, a diversity of experiments spanning slow and fast neutron physics and including related photonuclear experiments. Basic nuclear studies are emphasized, but frequently results are useful in clarifying aspects of neutron physics relevant to the long-range needs of the U.S. applied energy program. Three major research facilities are utilized. Thermal- and resonance-neutron experiments are performed at the CP-5 reactor, photonuclear studies at the ANL Electron Linac, and fast-neutron measurements at the Physics Division 4-MV Dynamitron.

Threshold-photoneutron measurements at the ANL Electron Linac have become a powerful technique for exploring those aspects of radiative transitions critical to our understanding of the interaction of neutrons with complex nuclei. These studies focus on the nuclear spectroscopy of highly-excited nuclear states and radiative properties in the threshold region. The extremely high bremsstrahlung flux generated by the ANL Electron Linac has been exploited for several years in unambiguous measurements with unexcelled sensitivity and resolution of photoneutron spectra in the threshold region. Exploratory measurements completed during the past year indicate that a new dimension will be added by measuring the polarization of neutrons from (γ,n) reactions. For the moment the technical performance of the facility remains unexcelled.

At CP-5, measurements using the internal-target facility have received increasing emphasis because of their unique character, the broad classes of information which can be obtained and the ease with which this particular type of research can be supported. For certain classes of measurements in which the primary requirements are low background and high sensitivity to neutron capture, the CP-5 facility remains at the state of the art. Recent measurements include a search for "collapsed nuclei," observation of photon scattering by the giant-dipole resonance, detailed studies of nuclear level schemes and the spectroscopy of highly-excited nuclear states. Funding limitations have dictated the termination of γ-ray diffraction spectroscopy on the 7.7-m crystal spectrometer, which was shut down in January 1975. We intend to explore the possibility of continuing our nuclear-structure studies by coordinating

the average capture-spectrum measurements carried out at the high-sensitivity internal-target facility with a parallel effort at the Tandem Van de Graaff accelerator in which the same nuclei are studied by means of the charged-particle reactions.

A. THRESHOLD PHOTONEUTRON EXPERIMENTS AT THE ANL LINAC

The threshold-photoneutron experiments to study the ground-state radiative transitions of highly excited nuclear states are carried out at the high-current 20-MeV electron linac operated by the Chemistry Division.

Photoneutron experiments in which neutron spectra at threshold are observed with high resolution have become a powerful tool in the study of individual highly-excited nuclear states. They complement traditional (n, γ) measurements and in many cases extend experimentation to previously inaccessible classes of nuclei. A major factor in the success of the threshold technique has been recent advances in the performances of electron linacs and the availability of large samples of separated isotopes. This is particularly true at ANL where the characteristically high resolution and intensity which are available permit one to study large samples of materials with highly excited states which could be observed in neutron reactions only with the greatest difficulty. Very intense nanosecond-pulsed bremsstrahlung for incident electron energies of 6—14 MeV which characterize the ANL Linac make it unique for such studies and its capabilities are being extensively exploited in a program in which such measurements are being used as a probe for studying the details of nuclear interactions and nuclear structure. The exploration of the dependence of various nuclear parameters (photon strength functions, level densities) on excitation energy and spin and parity are of particular interest.

The excellent energy resolution of the time-of-flight system permits observation of level structure for a range of neutron energies much larger than is possible in neutron-capture reactions at the present time. As a result, the threshold method is an ideal technique for isolating "intermediate structure" in the distribution of reaction strength among photoneutron resonances. Those problems which have been studied in the past by neutron capture are emphasized: namely, the dependence of radiative strength on the resonance spins and parities, radiative strength functions, statistical distributions of ground-state radiation widths, and possible correlations between neutron and radiative widths. Recent results have demonstrated the power of this class of measurements and the threshold technique is making major contributions to nuclear-resonance spectroscopy.

a. Photodisintegration of the Deuteron Near Threshold

H. E. Jackson, R. J. Holt, and W. M. Wilson

Although the photodisintegration cross section of the deuteron is known to be discrepant with current theories at high photon energies, no precision absolute measurements have been made in the region near threshold. The cross section in this region is of particular interest because of its sensitivity to the relative strength of the photomagnetic and photoelectric disintegration amplitudes. The prediction of the zero-range central-force approximation is shown in Fig. 35. The only information available in this region comes from the inverse reaction, i.e., thermal capture in hydrogen. The capture cross section is observed to be enhanced over predicted values by about 10%. Recently this enhancement has been attributed to the effects of meson exchange currents. A study of deuteron photodisintegration in the threshold region $E_\gamma < 3.0$ MeV was begun in 1974. The experiments are performed by irradiating a deuterium target with pulsed bremsstrahlung and measuring

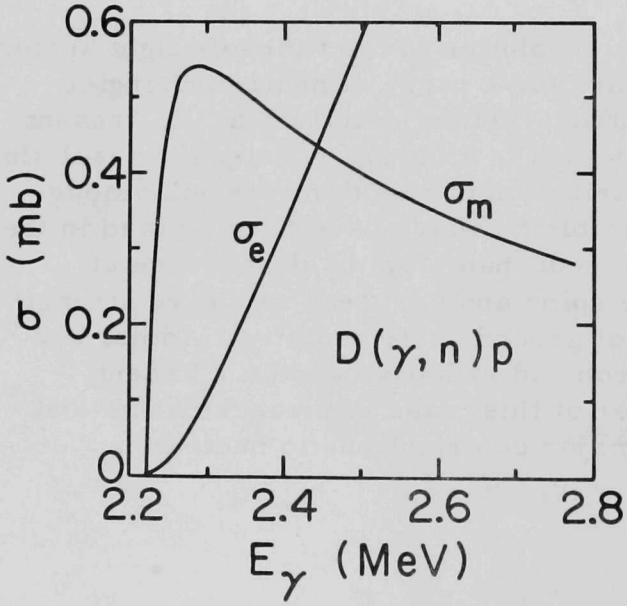

σ_m : $^3S_1 \xrightarrow{M1} {}^1S_1$

σ_e : $^3S_1 \xrightarrow{E1} {}^3P_{0,1,2}$

$d\sigma/d\omega = a + b \sin^2\theta_n$

$\sigma_m/\sigma_e = 3a/2b$

Fig. 35. Photoelectric and photomagnetic cross sections of the deuteron near threshold.

the photoneutron energy spectrum by neutron time-of-flight at 90° and 135°. The objective of the measurements in progress is to determine the angular distribution of the photoneutrons. A comparison of the observed distribution with predictions of the simple effective-range theory can be used to put limits on any final-state interaction or momentum-dependent component in the nucleon potential. Such effects would cause spin mixing and lead to an interference term in the photoneutron distribution. Such terms are absent in the predictions of the effective-range theory.

b. Nonresonant (γ, n) Reactions in the Mass Region $A \approx 60$

H. E. Jackson, R. J. Holt, and W. M. Wilson

The nuclei in the region of Cr and Ni are of particular importance in the channel theory of neutron capture. Strong nonresonant reactions which vary rapidly with changing atomic mass are predicted. The reaction amplitudes for such processes can be established in photoneutron spectra directly from the asymmetry produced by the interference between the reaction amplitude due to an isolated resonance and the underlying nonresonant amplitude. The threshold photoneutron technique is particularly well suited for measuring resonance shapes because of the absence of significant multiple scattering of the emerging neutron. Precision measurements of the line shapes for low-energy s-wave resonances in ^{53}Cr and ^{61}Ni have been performed at the ANL threshold-photoneutron facility. The time-of-flight spectrum in the energy region of the 11.7-keV resonance in ^{61}Ni is shown in Fig. 36. The initial analysis of the data indicates that a very strong nonresonant amplitude is present in the ^{53}Cr(γ, n) reaction, but almost zero within experimental error in the reaction ^{61}Ni(γ, n). This is precisely the trend predicted in the original theoretical intermediate-coupling calculations of channel capture. Efforts are continuing to explore the connection between such nonresonance reactions and correlations between the strengths for neutron and radiative decay of the resonant states.

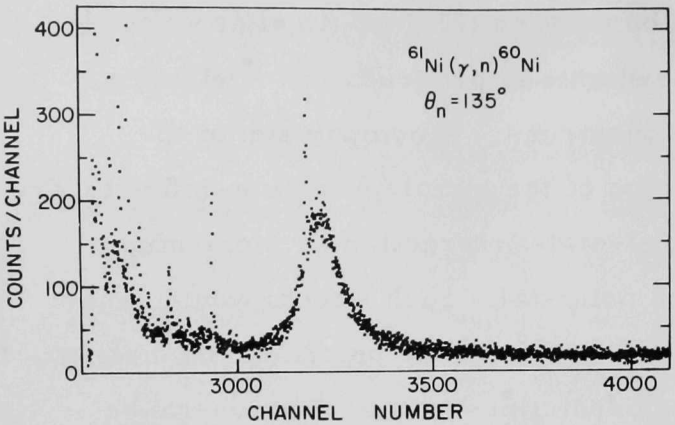

Fig. 36. Photoneutron time-of-flight spectrum in the region of the 11.7-keV resonance in the reaction ^{61}Ni(γ,n).

c. Ground-State Radiation Widths Near Photoneutron Threshold for the A=140 Mass Region

R. J. Holt and H. E. Jackson

The E1 and M1 ground-state radiation widths were measured for levels in ^{138}Ba and ^{140}Ce using the threshold-photoneutron method. The radiation widths were determined relative to the well-known 254-keV resonance in ^{208}Pb. The photoneutron spectra were measured with high resolution (0.5 ns/m) using the time-of-flight spectrometer associated with the Argonne high-current linac. The multipolarities of these states were determined by observing the photoneutron spectra simultaneously at reaction angles of 90° and 135°. The power of this method is clearly demonstrated in Fig. 37. Here, the number of observed resonances in ^{138}Ba is plotted as a function of the angular distribution ratio R. This ratio is defined as the photoneutron yield at 90° divided by that at 135°. The s- and p-wave neutrons are emitted from M1 and E1 excitations, respectively in ^{138}Ba or ^{140}Ce. Hence, R is unity for M1 resonances and 0.8 or 1.2 for E1 states. The p-wave states become enhanced above 40 keV as illustrated in Fig. 37.

The M1 ground-state radiation widths are expected to be enhanced for nuclei with A ≈ 140, since nuclei in this mass region are near a closed neutron shell ($1h_{11/2}$) and the $1h_{9/2}$ neutron orbital is vacant.

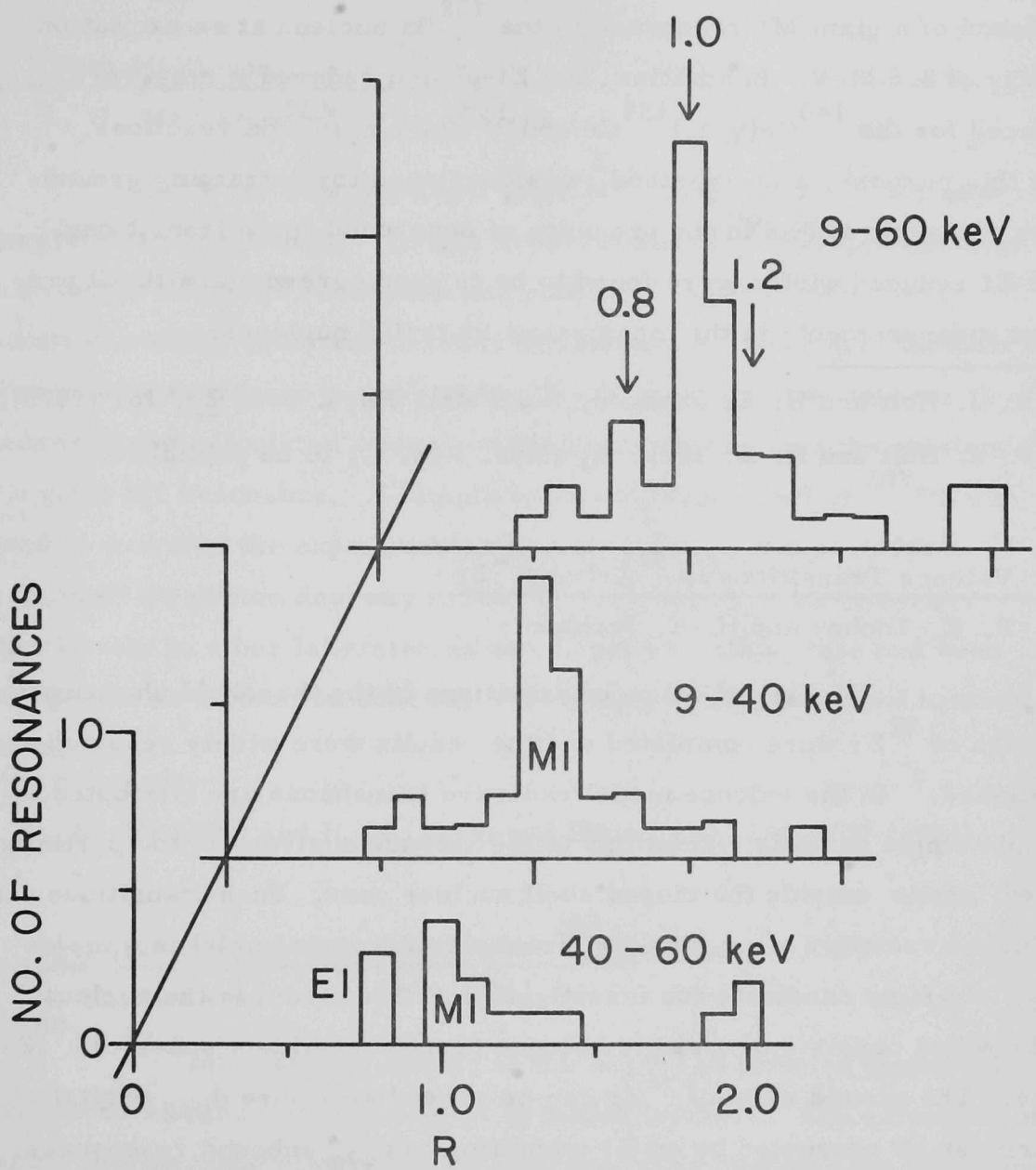

Fig. 37. The number of observed resonances plotted as a function of the angular distribution ratio.

In addition, the protons in the $1g_{9/2}$ orbital can also be excited to the vacant $1g_{7/2}$ orbital by M1 radiation. Hence, we expect a collective M1 resonance in this mass region. We have discovered and reported[1] evidence of a giant M1 resonance in the ^{138}Ba nucleus at an excitation energy of 8.6 MeV. In addition, the E1-photon reduced widths were deduced for the $^{140}Ce(\gamma,n_0)^{139}Ce$ and $^{138}Ba(\gamma,n_0)^{137}Ba$ reactions. For this purpose, a new method[2] was developed for extracting ground-state radiation widths in the presence of nonground-state transitions. The E1 reduced widths were found to be in good agreement with all previous measurements in the mass range 50 to 250 nucleons.

[1] R. J. Holt and H. E. Jackson, Bull. Am. Phys. Soc. 20, 167 (1975).

[2] R. J. Holt and H. E. Jackson, Phys. Rev. C, to be published.

d. Valence Transitions in $^{91}Zr(\gamma,n)^{90}Zr$

R. E. Toohey and H. E. Jackson

Studies of valence transitions in the threshold photoneutron spectra of ^{91}Zr were completed and the results were widely reported and published.[1] In the valence model radiative transitions are attributed to simple single particle transitions of the valence nucleons in the partially filled shells outside the closed shell nuclear core. Such transitions can influence radiative strength near threshold in certain nuclei in a major way. A prime candidate for investigation of this model is the nucleus ^{91}Zr which consists of a single valence neutron outside a spherical ^{90}Zr core. The ground state of ^{91}Zr can be viewed as a pure $d_{5/2}$ orbital which can be connected by an E1 transition to $p_{3/2}$ unbound resonances. The threshold technique was used to investigate the E1 transition strength for the nucleus by measuring the ground-state radiation widths for 35 $p_{3/2}$ resonances. A signature of the dominance of the valence reactions, a strong correlation between the ground-state radiation widths

[1] R. E. Toohey and H. E. Jackson, Phys. Rev. C 9, 346 (1974).

and the reduced neutron widths, is displayed by the threshold data. Detailed analysis of the data indicated that valence transitions account for a major portion of the E1 transition amplitude near threshold in ^{91}Zr.

e. Giant M1 Resonance in ^{207}Pb

L. R. Medsker and H. E. Jackson

Work establishing a giant M1 resonance in ^{207}Pb was completed and published.[1] In this experiment the $^{207}Pb(\gamma,n)$ reaction was studied with high resolution and photon intensity to determine radiation widths, spins and parities of resonances. The data indicate the existence of an intense p-wave strength and a comparison between the measured and calculated integrated M1 strength suggests the existence of a giant M1 resonance. A simple weak coupling model of ^{207}Pb was found to describe the experimental data very well. A search for a "common" E1 photon doorway in the $^{207}Pb(\gamma,n)$ proposed in earlier experiments in other laboratories was negative. This state had been interpreted as a common doorway occurring in both photon and neutron channels.

---

[1] L. R. Medsker and H. E. Jackson, Phys. Rev. C 9, 709 (1974).

f. Background (γ,n) Cross Section in ^{208}Pb

H. E. Jackson

Interference effects in the shapes of isolated photonuclear resonances continue to be a subject of major interest. The existence of sizable interference effects can be interpreted as evidence for anomalous reaction mechanisms such as strong direct and semidirect capture. The series of experimental estimates of the nonresonance, radiative neutron-reaction cross section in ^{208}Pb have been reported recently. Previous results from (γ,n) studies had been inconsistent with measurements of the neutron reaction. In an effort to resolve this discrepancy the shape of

TABLE V. Comparison of calculated and observed background cross sections for $^{208}Pb(\gamma,n)^{207}Pb$. The values corresponding to a $\sqrt{E_n}$ extrapolation of the thermal (γ,n) cross section are given in the fourth column. The results of a calculation mentioned in the text are given in the last column.

E_n (keV)	Experimental σ_{bg} (n,γ) (mb)	Experimental σ_{bg} (γ,n) (mb)	Calculated σ_{bg} Extrap.[a] (mb)	Calculated σ_{bg} (γ,n) (mb)
0.025×10^{-3}	709 ± 10[b]	0.0012	0.0012	0.0012
1.95	3.2 ± 1.2[c]	0.45 ± 0.16	0.34	0.41
25	0.5[d]	0.9 ± 0.2	1.2	1.01
41	. . .	$1.3^{+2.7}_{-0.7}$ [e]	1.5	1.15

[a]Cross sections extrapolated from the thermal capture cross section $\sigma_{th}(\gamma,n)$ by use of the relation

$$\sigma(\gamma,n) = \sigma_{th}(\gamma,n)[E_n/(0.025 \times 10^{-3})]^{1/2},$$

where E_n and the thermal energy are in keV.

[b]E. T. Jurney and H. T. Motz, Argonne National Laboratory Report No. ANL-6797, 1963 (unpublished), p. 236.

[c]R. C. Greenwood and C. W. Reich, Phys. Rev. C 4, 2249 (1971).

[d]O. A. Wasson and R. E. Chrien, in Proceedings of the International Conference on Photonuclear Reactions and Applications, Asilomar, 1973, edited by B. L. Berman (Lawrence Livermore Laboratory, Livermore, California, 1973), Vol. 1, p. 311.

[e]This work.

the 41-keV resonance in the reaction $^{208}Pb(\gamma,n)$ was studied in detail[1] by simultaneous measurements of the photoneutron spectra at 90° and 135°. A small asymmetry in the resonance shape was detected. Analysis of its magnitude implied a background cross section of $1.3^{+2.7}_{-0.7}$ mb. As indicated in Table V, this value can be explained in terms of contributions from neighboring resonances plus a small direct component; there is no evidence for anomalous processes.

[1]H. E. Jackson, Phys. Rev. C 9, 1148 (1974).

g. Threshold Photoneutron Polarization in the $^{208}Pb(\gamma,\vec{n}_0)^{207}Pb$ Reaction: A New Method for Threshold Photoneutron Spectroscopy

R. J. Holt, H. E. Jackson, and W. M. Wilson

Preliminary measurements of the threshold-photoneutron polarization from the $^{208}Pb(\gamma,\vec{n}_0)$ reaction have been performed. This work represents the first time that polarization of photoneutrons has been measured as a continuous function of energy near threshold. The multipolarity of photoneutron resonances cannot be determined from the neutron angular distribution alone. However, measurement of the polarization of the photoneutrons together with the angular distribution provides unambiguous determination of multipolarity. The differential polarization[1] for the $^{208}Pb(\gamma,\vec{n}_0)^{207}Pb$ reaction is given by the expression

$$\frac{d\vec{p}}{d\Omega} = \hat{k}\lambda\!\!\!^{-}_{\gamma}{}^{2}\left\{(0.38\, a_s a_{p_0} \sin\Delta_{sp_0} + 0.27\, a_s a_{p_1} \sin\Delta_{sp_1})\sin\theta + 0.20\, a_s a_d \sin\Delta_{ds} \sin 2\theta\right\},$$

where a_s, a_p, and a_d are the amplitudes for s-, p-, and d-wave neutron emission, respectively, and $\Delta_{ds} = \delta_d - \delta_s$ is the phase difference. Here $\hat{k}$ is a unit vector whose direction is perpendicular to the reaction plane and $\lambda\!\!\!^{-}_{\gamma}$ is the reduced wavelength. The E1 excited states result in s- and d-wave neutron emission while the M1 levels emit p-wave neutrons. Hence, measurements of the neutron polarization at reaction angles of 90° and 135° would uniquely define the multipolarities of the resonances.

The ^{208}Pb nucleus is particularly interesting, since the theoretical calculations[2] involving the M1 spin-flip transitions have been performed in detail. These calculations predict that an M1 giant resonance exists in ^{208}Pb at an excitation energy of 7.5 MeV. The polarization

[1] A. M. Baldin, V. I. Goldanskii, and I. L. Rozental, Kinematics of Nuclear Reactions (Oxford University Press, 1961), p. 170.

[2] J. D. Vergados, Phys. Lett. 36B, 12 (1971); T.-S. H. Lee and S. Pittel, Phys. Rev. C 11, 607 (1975).

of the photoneutrons was detected using a liquid ^{16}O polarimeter. In order to reduce systematic errors in the polarization measurement to negligible amounts, we are presently constructing a neutron spin-precession solenoid which is suitable for use with a continuous spectrum of neutrons. The preliminary polarization measurements indicate that there is considerable M1 strength in ^{208}Pb.

B. RESEARCH AT THE CP-5 REACTOR

At the present time investigations at CP-5 can be divided into three major classes: (1) measurements concerned with the reaction mechanism of neutron capture and the highly-excited states associated with the primary reaction, (2) studies of the low-lying nuclear states populated by neutron capture and subsequent γ-ray emissions, and (3) experiments in which neutron capture is used as a means of generating a monochromatic-photon source for photonuclear measurements. In the first category the primary objective is understanding the reaction mechanism for neutron capture. The "average capture-spectrum technique" which uses an internal boron-filtered target developed at ANL remains a unique and powerful tool for such studies. The energy dependence of partial radiation widths is inferred from studies of average spectra and compared with various models of radiative decay of highly excited states. Statistical analysis of partial radiation widths and corresponding parameters in related reaction data is used to determine the importance of direct and compound-nucleus reactions in describing the capture process, and features of the systematics of the photon strength functions such as mass dependence are examined in an effort to isolate giant resonances in the transition strength.

The spectroscopy of low-lying states is carried out by coordinating neutron-γ-ray measurements with related experiments which utilize nuclear reactions chosen to emphasize particular features of nuclear structure. A major objective of the program is to develop an understanding of the trends and changing character of the rotational and vibration level structure of rare-earth nuclei as one moves from the mass region corresponding to deformed nuclei toward closed shell nuclei. Such information provides insight into the character of the collective models which have been proposed to describe the level structure in this mass region.

In the measurements using monochromatic-photon beams generated by neutron capture, photon-scattering cross sections and their angular dependence are studied to understand basic photonuclear interactions such as Delbrück scattering and nuclear Raman scattering. This work is facilitated by the availability of a very intense well collimated beam of high-energy photons generated in the internal target facility at CP-5. Delbrück scattering was experimentally resolved for the first time using this beam. The high resolution characteristic of these studies permits study of inelastic and elastic scattering. An extensive program of measurements with actinide and lanthanide targets has yielded information of fundamental importance for understanding the photonuclear interaction in the region of the giant-dipole resonance.

1. FUNDAMENTAL PHENOMENA

a. Measurements of Spacial Asymmetries in the Decay of Polarized Neutrons

V. E. Krohn and G. R. Ringo

Knowledge of the asymmetry coefficients in the expression describing the decay of polarized neutrons is important to the theory of the weak interaction. We recently published[1] new results for the electron asymmetry coefficient A and the ratio of beta-decay coupling constants G_A/G_V which follows from the result for A. The values reported were $A = -0.113 \pm 0.006$ and $|G_A/G_V| = 1.258 \pm 0.015$. This result for G_A/G_V is particularly important because it is free from the complications associated with nuclear structure.

We are not planning to do further work on this project.

[1] V. E. Krohn and G. R. Ringo, Phys. Lett. 53B, 175 (1975).

b. The Electron-Neutron Interaction

V. E. Krohn and G. R. Ringo

Our value for the electron-neutron scattering length has been corrected on the basis of new measurements of some neutron scattering lengths and now is $(-1.30 \pm 0.03) \times 10^{-16}$ cm, which is 3% lower than our original result. (The equivalent figure in the Fermi convention is -3630 ± 70 eV and at $q = 0$, $dG_{En}/dq^2 = 0.0189 \pm 0.0004$ fm^2.) A check on the worrisome possibility of an H_2 impurity in the scattering gases showed that this is quite unlikely to be a significant source of error. The difference between our result and the Munich measurement and also the Foldy calculation thus continues unexplained. We have published these results[1] and do not plan further work on this project.

[1] V. E. Krohn and G. R. Ringo, Phys. Rev. D 8, 1305 (1973).

c. Search for Collapsed Nuclei

L. M. Bollinger, A. M. Friedman,* S. M. Fried,* J. P. Schiffer, J. R. Specht, G. E. Thomas, and A. Turkevich†

In 1972 A. Bodmer in the ANL Nuclear Theory program postulated the existence of "collapsed" nuclei that have properties entirely unlike normal nuclei. One such property is an extremely high binding energy for neutrons. In early 1973, a search for the possible existence of collapsed nuclei in nature was carried out by looking for neutron-capture γ rays with energies much greater than any known neutron-binding energy. The sample studied was a large cylinder of graphite bathed in an intense flux of neutrons in the through-hole facility at CP-5. The γ-ray spectrometer was an array of large NaI(Tl) scintillators, which efficiently counted γ rays in the range 25—200 MeV and effectively rejected cosmic-ray background.

No effect above background was observed. From this null result we inferred that, in the sample studied, the concentration of the hypothetical collapsed nuclei is $<10^9$ atoms/cm^3. This limit is many orders of magnitude smaller than can be inferred from other kinds of existing evidence.

The recent theory of abnormal nuclear matter by Lee and Wick has generated a renewed interest in the possibility of collapsed nuclei, and therefore we plan a new search for them in nature. To maximize the experimental sensitivity, we intend to use a sample with the following properties: (1) easily predictable geothermal behavior, (2) no stable isotopes of normal matter, and (3) atomic weight $\geqslant 200$. Of all the elements, radon most generally satisfies these criteria.

Since radon and xenon concentrate in the atmosphere, a sample of the "radon" fraction has been obtained from a commercial

---

*Chemistry Division, ANL.

†University of Chicago, Chicago, Illinois.

xenon still. This sample contains about 300 liters of residual xenon and represents the radon from about 0.2 km^3 of air. The radon is being extracted from this sample. Later this year we will attempt to detect the presence of collapsed radon nuclei in the purified sample by again looking for neutron-capture γ rays with anomalously high energy. If observed, mass spectrometric studies may be carried out.

d. Rotational Invariance in Nuclei

R. J. Holt and W. M. Wilson

We are designing an experiment which tests the fundamental principle of rotational invariance for the case of the nuclear interaction. The $^6Li(\vec{n},\vec{t})^6He$ reaction will be used in this study. This investigation will avoid the uncertainties due to isospin mixing, which are inherent in studies that involve the weak interaction, e.g., γ or β decay. The flux of thermal, polarized neutrons will be generated using the through-hole facility at the CP-5 reactor. The sensitivity of this measurement (10^{-3} to 10^{-4}) is achieved by using a null technique in which we look for a deviation from zero of the triton polarization.

2. PHOTON SCATTERING STUDIES

a. Delbrück and Nuclear Raman Scattering of 10.83-MeV Photons by Deformed and Spherical Heavy Nuclei

H. E. Jackson, K. J. Wetzel, and G. E. Thomas

Studies of the elastic and inelastic scattering of 10.8-MeV photons were completed at the internal-target facility of the CP-5 reactor, and a paper summarizing the results was published.[1] For Pb and U, extensive measurements of the angular distributions for elastic and inelastic scattering were measured. Scattered photon spectra are

[1] H. E. Jackson, K. J. Wetzel, and G. E. Thomas, Phys. Rev. C 9, 1153 (1974).

shown in Fig. 38 for a U target. For scattering angles $\theta < 45^{\circ}$ the elastic scattering is dominated by the Delbrück effect. With the possible exception of Ta, for $\theta > 90^{\circ}$ (where only nuclear resonances and Thomson scattering are important), both the magnitude and angular dependence of the elastic scattering cross section are in good agreement with the values which follow from the most recent photoabsorption cross sections in the corresponding targets. To an accuracy of $\sim$10% the elastic and inelastic (nuclear-Raman) scattering for U and Th can be deduced from the simple rotator model using the parameters implied by the photoabsorption data. A trend of Raman scattering to be 10% weaker than expected is suggested by the data. For Tb and Ta the Raman scattering is substantially weaker than expected.

b. Nuclear Raman Scattering of 11.4-MeV Photons

H. E. Jackson, G. E. Thomas, and K. J. Wetzel*

Studies of the elastic and inelastic scattering of 11.4-MeV photons were completed during the past year at the internal-target facility of the CP-5 reactor, and a paper summarizing the results will be published.[1] The beam of 11.4-MeV photons used in these measurements was generated by an internal capture target enriched in ^{59}Ni. This target was obtained by irradiating a 25-g sample of normal Ni for 90 days in the HFIR reactor at ORNL and transferring it to the CP-5 internal-target facility as shown schematically in Fig. 39. Absolute differential cross sections were measured for photon scattering by nuclei ranging from ^{141}Pr to ^{238}U. Inelastic scattering which leaves the residual nucleus in a state of the ground-state rotational band was measured relative to elastic scattering. The data confirm the trends observed in earlier ANL measurements at 10.83 MeV. The strength of inelastic scattering is systematically weaker

---

*University of Portland, Portland, Oregon.

[1] H. E. Jackson, G. E. Thomas, and K. J. Wetzel, Phys. Rev. C 11, 1664 (1975).

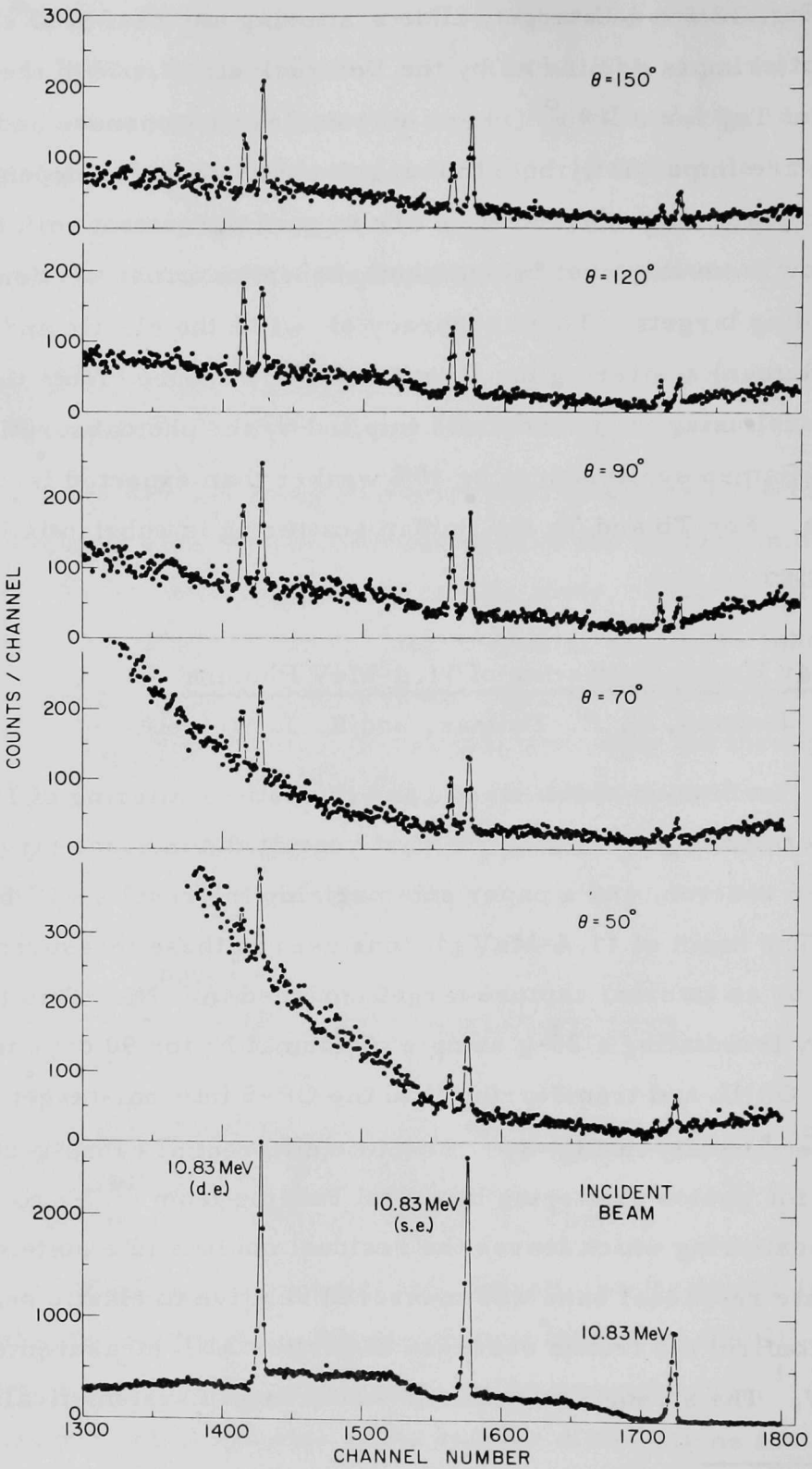

Fig. 38. High-energy portion of the spectra of 10.83-MeV radiation scattered from a U target at several angles and, at the bottom of the figure, a comparable spectrum of incident radiation.

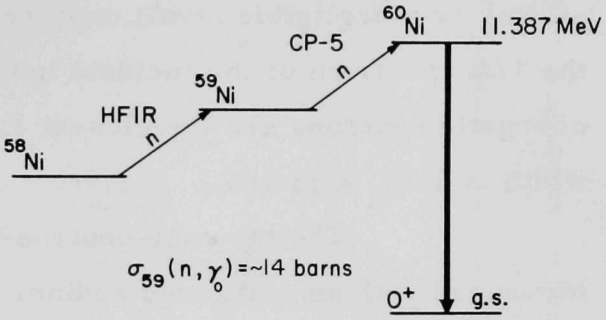

Fig. 39. Schematic of the procedure for preparing the enriched ^{59}Ni capture target used to generate the 11.387-MeV external photon beam. The initial irradiation made to enrich the natural nickel target was carried out at the HFIR at Oak Ridge National Laboratory.

than predicted by simple models of the giant-dipole resonance. The discrepancies are significant in the lanthanide region and may be viewed as evidence for the existence of a small direct nonresonant reaction component in the region of the giant-dipole state.

3. NEUTRON-CAPTURE γ RAYS

a. A Comparison of the γ-Ray Spectra from Thermal-Neutron Capture and 2.8-keV Neutron Capture in ^{23}Na

W. M. Wilson, G. E. Thomas, and H. E. Jackson

A study of the γ-ray spectra from thermal-neutron capture and 2.8-keV neutron capture was begun at the internal-target facility of the research reactor CP-5. The measurements have been made with the high-resolution annihilation-pair spectrometer and the analysis of the data is in progress. Since sodium is used as a coolant in the breeder reactor, it is important that neutron capture in the low-keV region be well understood. In particular, we are concerned here with the total radiation width of the 2.8-keV resonance. Grossly conflicting values for this width have been previously reported in the literature and this is due to the very small capture cross section. We have been able to study this resonance by using the "average resonance" technique. A $\frac{1}{4}$-in. filter of ^{10}B surrounding the Na sample reduced capture below

~2 keV to a negligible level; capture above 2.8 keV is negligible because the 1/E spectrum of the incident neutron flux assures a low intensity of energetic neutrons and the closest resonance having appreciable neutron width is at $E_n \approx 53$ keV.

The thermal-neutron-capture γ-ray spectrum was measured with an unfiltered sodium sample. Since the spectrum of neutrons from the reactor is strongly peaked at thermal energy, neutron capture (by an unfiltered sample) above thermal energies is negligible compared to thermal-neutron capture.

For each primary γ-ray transition observed in the thermal-capture spectrum, a corresponding transition was observed in the resonance spectrum. The resonance spectrum is shown in Fig. 40, where the arrows refer to primary transitions. Capture predominantly in the 2.8-keV resonance is indicated by a ~2—3-keV shift in the energies of the primary transitions relative to those observed in thermal capture. The principal feature of the analysis will be a comparison between the relative intensities of each measurement to determine the extent to which the 2.8-keV resonance contributes to the capture cross section from thermal to a few-keV neutron energy.

b. Gamma Rays from Thermal-Neutron Capture in ^{59}Ni and ^{63}Ni

W. M. Wilson, G. E. Thomas, and H. E. Jackson

The thermal-neutron capture γ-ray spectra of ^{60}Ni and ^{64}Ni were measured with the high-resolution annihilation-pair spectrometer at the internal-target facility of the research reactor CP-5. The sample, consisting of the long-lived ^{59}Ni and ^{63}Ni isotopes (as well as the stable isotopes ^{58}Ni, ^{60}Ni, ^{61}Ni, and ^{64}Ni), was prepared by irradiating natural nickel in a high neutron flux at the Oak Ridge high flux isotope reactor (HFIR). The improved precision of these data results in more accurate estimates of the neutron binding energies of ^{59}Ni, ^{60}Ni, ^{61}Ni, ^{62}Ni, and ^{64}Ni than was available earlier.

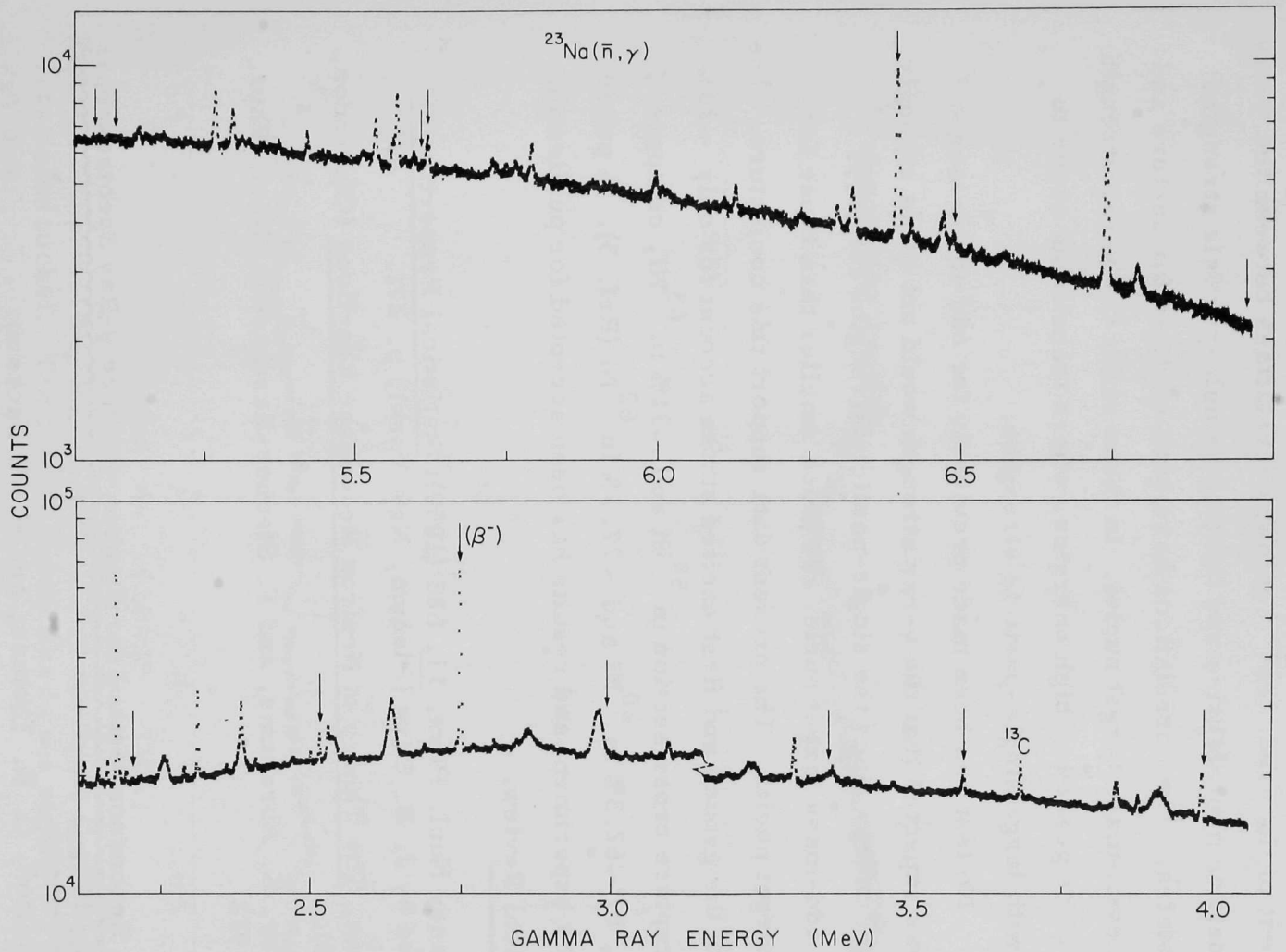

Fig. 40. The annihilation pair spectrometer spectrum for ^{23}Na($\bar{n}$, γ). The arrows refer to primary transitions observed in the present (resonance) measurement or to the energies of transitions observed by others in thermal-neutron capture. The 2.754-MeV $\beta^- \rightarrow \gamma$-ray transition is used for the absolute intensity normalization. The broken line indicates a different experimental run. A region between 4 and 5 MeV is not shown because no primary transitions are observed.

The data are plotted in Fig. 41, where the arrows indicate primary transitions in the nickel compound nuclei.

The energy distribution of the γ-ray strength provides a qualitative test of the predicted[1,2] strong correlations between the γ-ray reduced transition probabilities and the (d,p) single-particle strengths of the final states. The correlations have been verified for capture and stripping on even-mass target nuclei. In these cases the γ-ray strength is observed to be peaked at high energies, where transitions occur to final states with large single-particle strengths.

No test has been made previously for odd-mass target nuclei. It was expected that the γ-ray strength would not be as strongly peaked at high energy since the single-particle strengths for (d,p) stripping on odd-mass target nuclei are much smaller than those for even-mass target nuclei. The present data support this conjecture. The transitions to the ground and first excited states account for only ~20% of the total capture cross section in ^{59}Ni and ~31% in ^{63}Ni, compared, for example, to ~62.3% in ^{60}Ni and ~77.3% in ^{62}Ni (Ref. 3). A paper describing the experiment and results has been accepted for publication in The Physical Review.

[1] A. M. Lane, Nucl. Phys. 11, 625 (1959); Statistical Properties of Nuclei, edited by J. B. Garg (Plenum, New York), p. 271.

[2] J. E. Lynn, The Theory of Neutron Resonance Reactions (Clarendon, Oxford, 1968).

[3] J. Kopecky, K. Abrahams, and F. Stecher-Rasmussen, Nucl. Phys. A188, 535 (1972).

c. Average Resonance Method for Neutron-Capture γ-Ray Spectroscopy: ^{176}Lu and ^{177}Lu

W. M. Wilson, G. E. Thomas, and H. E. Jackson

The γ-ray spectra from neutron capture in a broad band of capture states of ^{176}Lu and ^{177}Lu have been measured at the internal target facility of the research reactor CP-5. A $\frac{1}{4}$-in. ^{10}B filter

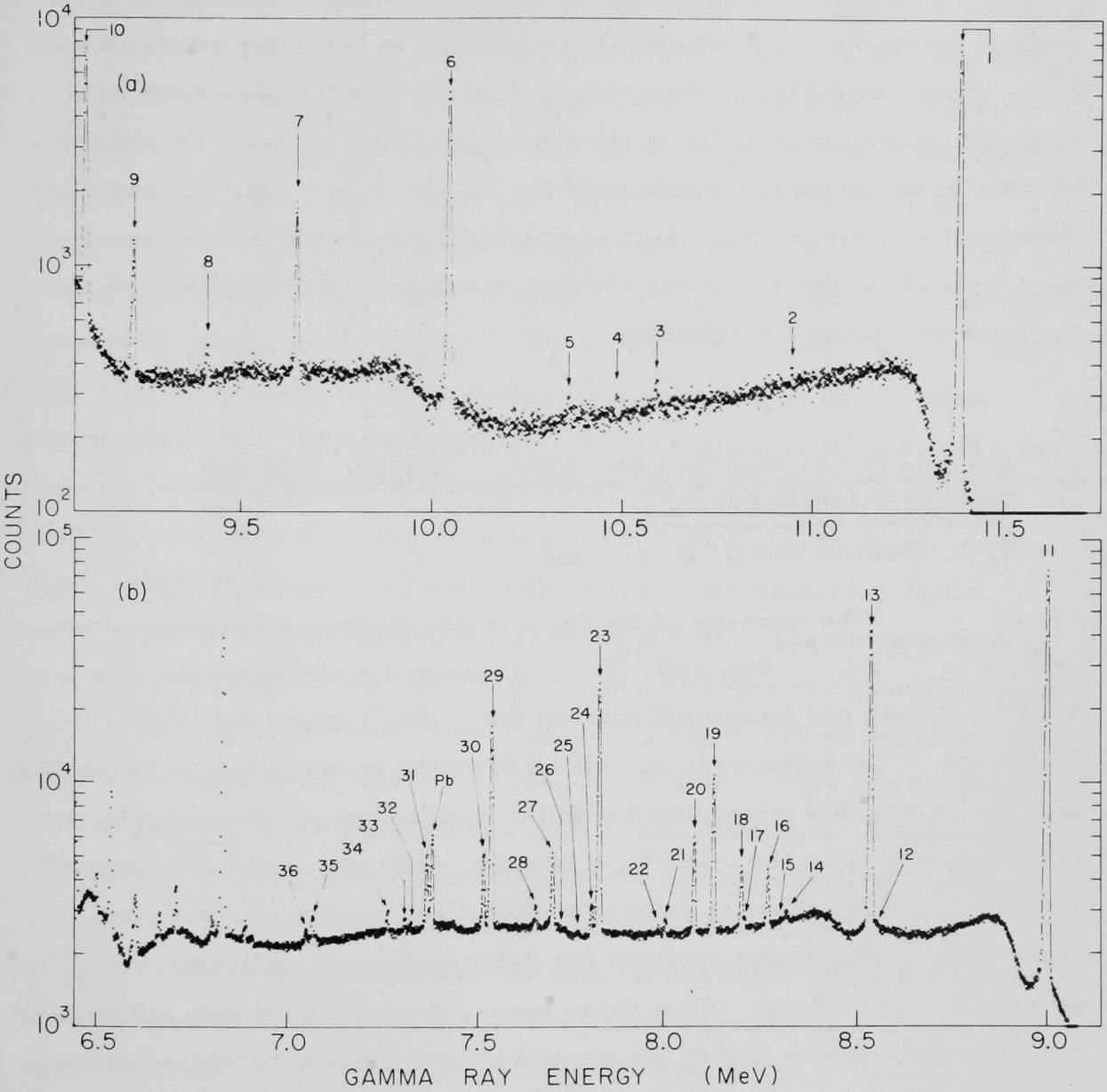

Fig. 41. Thermal-neutron capture-γ-ray spectrum above 7.0 MeV for irradiated nickel. The lead-impurity line is the strong ^{208}Pb 7381.1-keV line.

surrounding the natural lutetium target (97.4% ^{175}Lu, 2.6% ^{176}Lu) reduces thermal capture to a negligible level and thus provides an average over many capture states in the compound nuclei ^{176}Lu and ^{177}Lu. Preliminary analysis indicates a clear separation between the relative strengths of the E1 and M1 transitions to low-lying bound states of the compound nucleus. This information will enable us to determine the parities and place limits on the spins of the final states. Of greater interest is the absolute magnitude of the E1 and M1 strength functions. Additional measurements, which complement the present measurement, must be made to determine the absolute strengths. Techniques to do this are presently being investigated.

d. Absolute (n, γ) Cross Sections in the ^{113}Cd(n, γ)^{114}Cd and ^{149}Sm(n, γ)^{150}Sm Reactions

R. K. Smither and G. E. Thomas

The intensity of the (n, γ) spectrum from thermal-neutron capture in ^{113}Cd, ^{149}Sm, and ^{14}N was measured simultaneously as a function of time and integrated neutron flux. The capture rate in the ^{113}Cd and ^{149}Sm isotopes is calculated from the burn-up rate from neutron capture. When this is combined with the comparison of relative gamma-ray intensities from the three (n, γ) spectra, absolute values are obtained for the γ-ray intensities in units of gammas/100 neutron captures and in terms of partial cross sections for the production of individual gamma-ray transitions. When these results are combined with information about the neutron flux at the sample position, absolute total-capture cross sections for reactor-neutron fluxes are obtained. The previous measurements made at Argonne using this technique had errors of 2 to 5%. The new measurements of the (n, γ) spectra made this year will reduce these errors by a factor of two.

e. Nuclear Structure of ^{148}Sm, ^{150}Sm, and ^{152}Sm

R. K. Smither and D. L. Bushnell

The (n, γ) spectra from the $^{147}Sm(n,\gamma)^{148}Sm$, $^{149}Sm(n,\gamma)^{150}Sm$, and $^{151}Sm(n,\gamma)^{152}Sm$ reactions have been used to develop the level schemes of ^{148}Sm, ^{150}Sm, and ^{152}Sm and the γ-ray branching ratios between many of the levels below 3 MeV. New data were taken during the year with the Argonne 7.7-m bent-crystal γ-ray diffraction spectrometer on all three reactions. This new work improved the precision of the γ-ray energy and intensity measurements by a factor of 2 to 4 over the earlier experiments. The improvement was possible because of recent modifications to the bent-crystal spectrometer. New data were also taken for the high-energy average-resonance neutron-capture spectra. The older data suffered from poor resolution and a low signal-to-background ratio that was caused by a partial failure of the Ge(Li) γ-ray spectrometer. The new bent-crystal spectrometer work significantly improves the information about γ-ray branching ratios between the numerous excited states below 3 MeV. The new average-resonance neutron-capture data significantly improve the identification of the negative-parity levels. The most interesting result of this work is that all three level schemes are virtually identical. This can be seen in Fig. 42, where the three level schemes are compared. Furthermore, the gamma-ray branching ratios change in a smooth way from nucleus to nucleus. For some special levels the ratios do not change at all. An interesting example of this is the ratio of the B(E2) of the transition from the second 2^+ excited state to the first 0^+ excited state to the B(E2) of the transition from the second 2^+ excited state to the 0^+ ground state. This ratio remains the same to within 2% for all three nuclei even though the absolute values of the B(E2)'s change by more than an order of magnitude. These results are rather surprising since this is just the mass region where the ground-state configuration was expected to be changing quite dramatically for these nuclei.

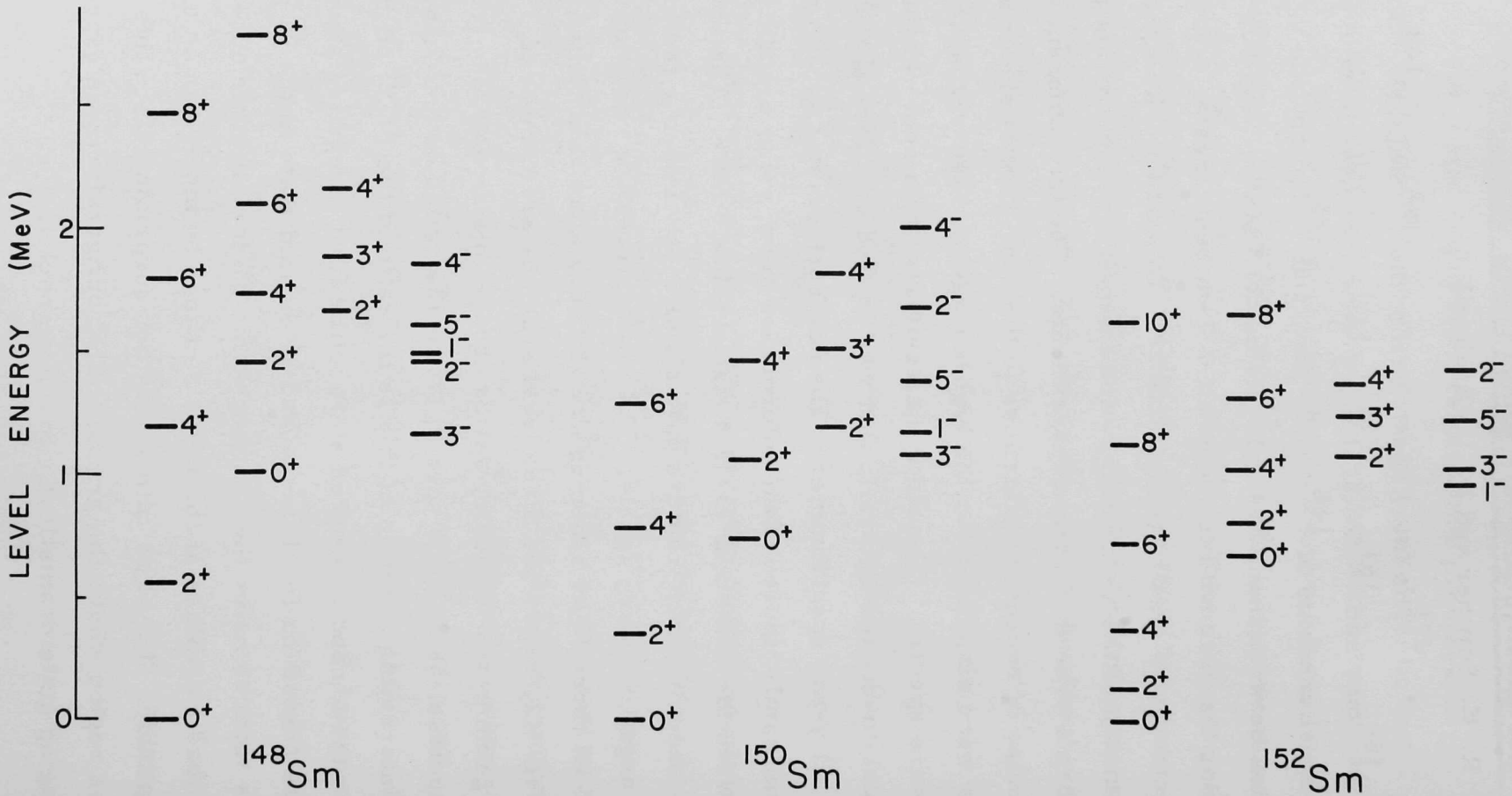

Fig. 42. Energy levels in ^{148}Sm, ^{150}Sm, and ^{152}Sm.

f. Nuclear Structure of ^{114}Cd

R. K. Smither

The average-resonance neutron-capture γ-ray spectrum of ^{113}Cd(n, γ)^{114}Cd was measured using a highly-enriched CdO sample. The new results have sufficient sensitivity and resolution for investigation of the level scheme of ^{114}Cd up to 4-MeV excitation. Of special interest are weak primary E2 transitions to 3^+ states and the strong E1 transitions to 0^-, 1^-, and 2^- states above 2-MeV excitations. The 3^+ states all appear to be members of quasi-rotational bands. The spin sequence of the negative-parity states is quite confused and suggests a more complex structure. About one-half of the negative-parity states appear to be part of a quasi-band. In general the quasi-band structure seen in ^{114}Cd is quite similar to the quasi-band structure observed in the even-Z, even-N Sm isotopes (see Fig. 42).

g. Neutron Capture in Isomeric States in Te Isotopes

R. K. Smither and B. Hamermesh*

The thermal-neutron-capture γ-ray spectrum resulting from neutron capture in the metastable state ($\frac{11}{2}^-$) in ^{123}Te was studied with the Argonne (n, γ) facility using the Ge(Li) γ-ray spectrometer. Primary transitions to states in ^{124}Te with spins 6^+ and 7^- were observed but no transitions to 4^+ states were detected. This suggests that most of the neutron capture is in 6^- states rather than 5^- states. The metastable state was made by neutron capture in the Oak Ridge HF reactor. Further experiments are planned for neutron capture in isomeric states of ^{123}Te, ^{125}Te, and ^{127}Te to study the high-spin states in ^{124}Te, ^{126}Te, and ^{128}Te. This work will complement the more traditional (n, γ) studies where the neutron capture is in the ground state of the odd-Te isotopes with $J^\pi = \frac{1}{2}^+$ and $\frac{3}{2}^+$ and the low-spin states are fed by the primary γ transitions.

---

*Cleveland State University, Cleveland, Ohio.

h. Nuclear Structure in ^{144}Nd and ^{146}Nd

R. K. Smither, D. L. Bushnell, G. Tassotto, S. Ledvina,* and J. Hawkins

The level schemes of ^{144}Nd and ^{146}Nd are being developed through the use of both thermal-neutron capture and average-resonance neutron-capture gamma-ray spectroscopy. This is part of a systematic study of the even-Z, even-N nuclei and is meant to complement the work being done on the Sm isotopes. Isotopically enriched samples of ^{143}Nd and ^{145}Nd have been used in the thermal-capture experiments on the medium- and high-energy parts of the (n, γ) spectrum. Only natural-abundance targets have been used in the average-resonance neutron-capture experiments. A comparison of the (n, γ) spectra obtained with thermal-neutron capture is used to assign the γ transition to the appropriate isotope of Nd. The spin and parity assignments are based on the average-resonance neutron-capture data and the medium-energy (0.5 MeV to 2 MeV) thermal-capture data. A fairly complete level scheme is obtained for ^{146}Nd and the analysis of this data is almost complete. The analysis of the ^{144}Nd level scheme is in progress. In both isotopes positive-parity states are fed by E1 transitions and give rise to strong lines in the average-resonance neutron-capture work. The average-resonance experiment will have to be repeated with separated-isotope samples to complete the investigation of the negative-parity states. Also missing from the data is the low-energy part of the (n, γ) spectrum. A collaboration may be arranged with the (n, γ) group at Grenoble to complete this part of the program.

---

*Northern Illinois University, DeKalb, Illinois.

i. Studies of the Excited States of ^{160}Tb Populated in the Reactions ^{159}Tb(n, γ) and ^{159}Tb($\bar{n}$, γ)^{160}Tb

S. B. Burson, F. J. Zehr,* J. R. Champion, and C. H. Batson

Extensive analysis has been carried out on data taken earlier at the Argonne CP-5 reactor on the reaction ^{159}Tb(n, γ)^{160}Tb. Both thermal and average-resonance-capture experiments were done at the internal-target facility while electron and gamma singles as well as e^--γ coincidence measurements were made with the Argonne superconducting coincidence spectrometer at the external beam facility of the east thermal column. The information obtained about the excited states through these various techniques is of particular theoretical value since little is known about the nuclear structure of deformed odd-odd nuclides.

Over 400 gamma rays are observed in the Ge(Li) spectrum between 23 and 1300 keV. In the high-energy thermal-neutron-capture spectrum observed with the pair spectrometer, approximately 200 components are observed between the energies 4790 and 6375 keV.

A study of the relative intensities of the primary gamma rays in the average-resonance spectra taken with two different thicknesses of boron shielding indicates that the systematic behavior reported to be applicable in a corresponding study of ^{166}Ho does not apply in the case of ^{160}Tb. We have not found an explanation for this observation. The rotational structure is clearly evident with most of the bands expected to accompany the low-lying intrinsic states being identifiable. From 12 to 15 bands have been found below 1.0 MeV. The analysis is continuing.

---

*Westminster College, New Wilmington, Pennsylvania.

j. Nuclear Structure of ^{178}Hf and ^{180}Hf

R. K. Smither, D. L. Bushnell, and D. J. Buss

The Argonne 7.7-m bent-crystal γ-ray diffraction spectrometer and the Ge(Li) γ-ray spectrometer at the CP-5 research reactor were used to measure the ^{179}Hf(n, γ)^{180}Hf and ^{177}Hf(n, γ)^{178}Hf gamma-ray spectrum from 20 keV to 10 MeV. Both thermal neutron capture and average resonance neutron capture experiments were performed. These (n, γ) spectra were used to develop the level schemes of ^{180}Hf and ^{178}Hf. The experimental (n, γ) work on the ^{179}Hf(n, γ)^{180}Hf reaction has been completed and published in a paper.[1] The analysis of the excited state rotational band structure of ^{180}Hf defied analysis for many years. The low-energy portion of the (n, γ) spectrum had to be remeasured with the improved resolution and precision of the present Argonne diffraction spectrometer before the level structure of the excited state bands could be identified. The basic problem faced in ^{180}Hf is that the level density above 1 MeV excitation energy is so great that the level spacings were not well enough defined by the Ge(Li) γ-detector work to allow one to place the low-energy γ rays in the level scheme with any certainty. The energy precision of the low-energy gamma rays had to be increased to the point that one could use the Ritz combination principle to determine the proper placement. A similar analysis for the ^{178}Hf level scheme was started. In both nuclei the levels above 1-MeV excitation can be described as overlapping rotational band base on two-quasiparticle excited states. The level scheme of ^{180}Hf is shown in Fig. 43. The most significant feature of this work is that it shows quite convincingly that the deformation of the excited-state rotational bands is virtually identical to that of the ground-state band. This is expected for nuclei like ^{180}Hf that exhibit a highly stable deformation for the member of its ground-state band but this fact is often quite difficult to demonstrate in very complex level schemes of nuclei in this mass region.

---

[1] D. L. Bushnell, D. J. Buss, and Robert K. Smither, Phys. Rev. C 10, 2483 (December 1974).

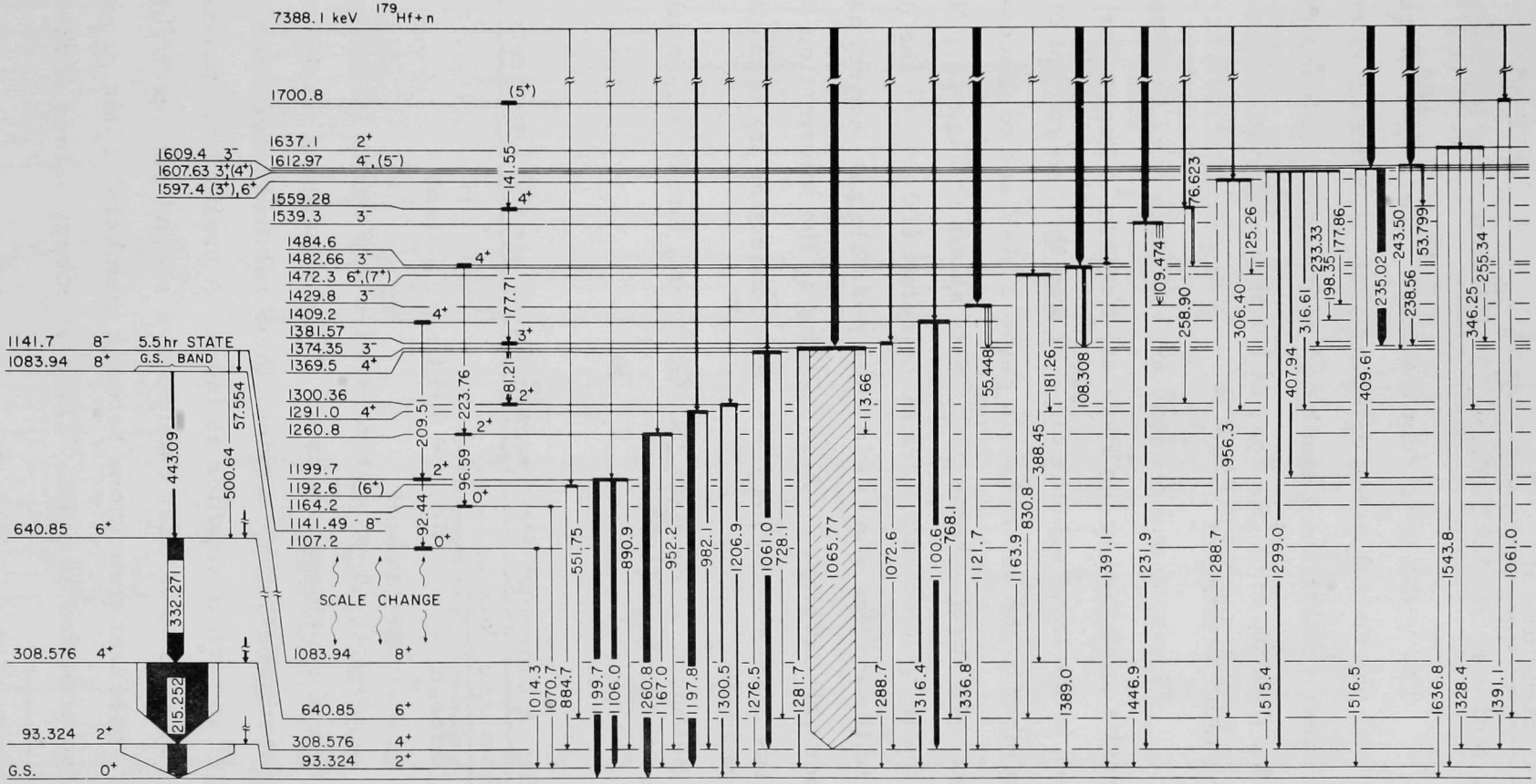

Fig. 43. Level scheme of ^{180}Hf based on (n, γ) experiments. The dark or shaded width of a transition reflects its gamma-ray intensity. The open or unshaded width reflects its conversion-electron intensity. The width shown for the primary gamma transitions reflects the relative gamma-ray intensity observed in the average-resonance neutron-capture spectrum.

k. Nuclear Structure of ^{184}W

R. K. Smither, D. L. Bushnell, J. Hawkins, and R. Goebbert

The γ-ray spectrum from the $^{183}W(n, \gamma)^{184}W$ reaction was measured with the Ge(Li) γ-ray detector system at the CP-5 research reactor. These results were combined with γ-γ coincidence experiments following the β decay of ^{184}Re done at Northern Illinois University to develop the level scheme of ^{184}W.

The (n, γ) and β-decay experiments have been completed and the results published in the Physical Review.[1] The major contribution of this work to the level scheme of ^{184}W was the assignment of spins and parities to most of the known levels below 2 MeV and to discover five new levels. The level scheme of ^{184}W is shown in Fig. 44. No measurements on the (n, γ) spectrum were made below 600 keV so the detailed structure of the excited states and their possible assignment as rotational bands is not well developed. Also missing is the information on the low-energy γ-ray branching ratios for γ rays connecting these excited states.

[1] D. L. Bushnell, J. Hawkins, R. Goebbert, and R. K. Smither, Phys. Rev. C 11, 1401 (1975).

ℓ. Statefit: A Computer Program to Facilitate the Interpretation of Spectroscopic Data

S. B. Burson, G. T. Wood,* and C. H. Batson

Statefit is a program written in Fortran IV to facilitate the interpretation of spectroscopic data. A list containing all the experimentally determined γ-ray energies, their relative intensities, and the uncertainties in each is supplied as input. A preliminary partial decay scheme is assumed to already exist, and a second list specifying the γ rays that represent transitions between members of this group of energy levels is also provided as input. The best energy values of the states

* Cleveland State University, Cleveland, Ohio.

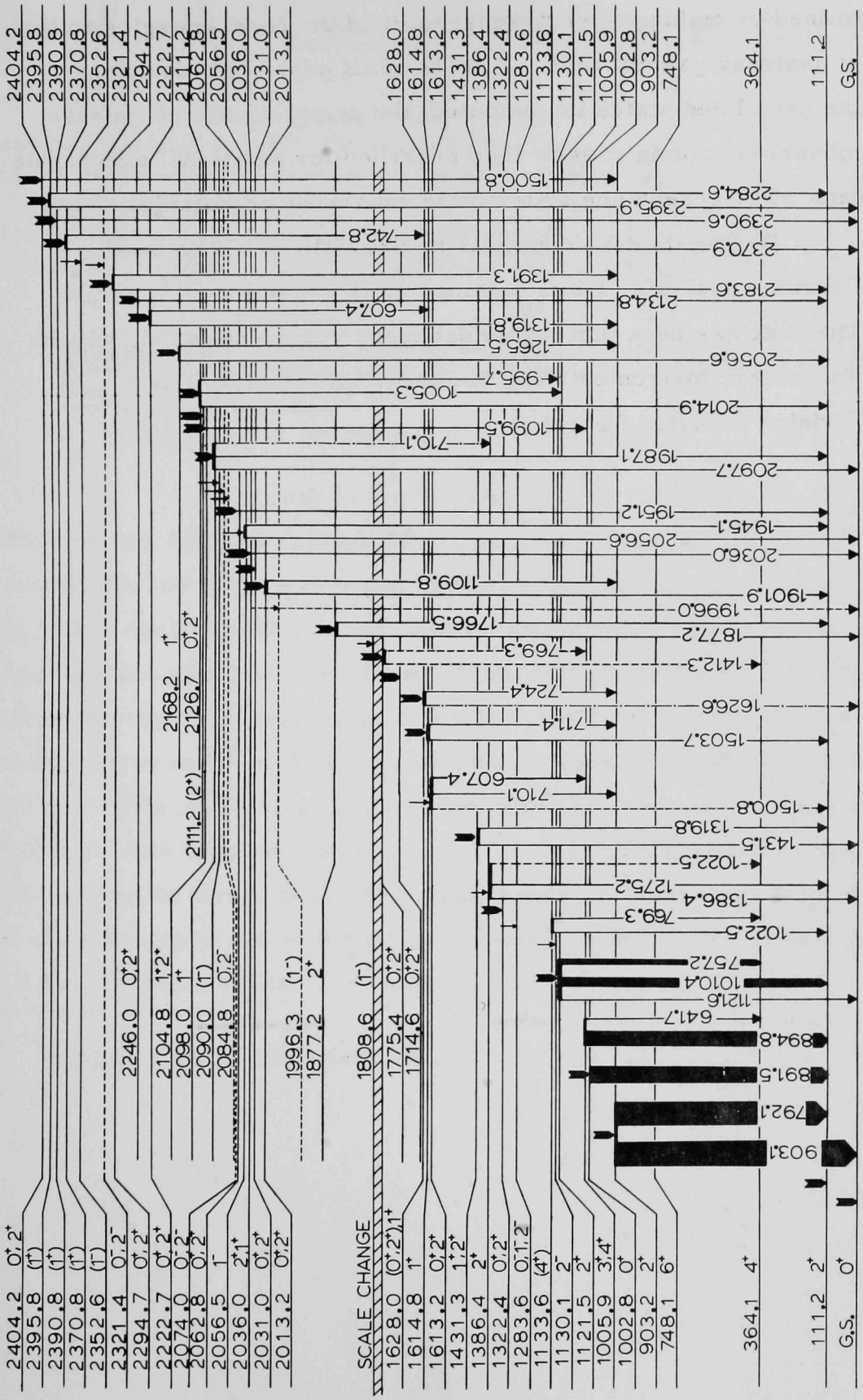

Fig. 44. Level scheme of ^{184}W based on (n,γ) and β-decay experiments with γ-γ coincidence studies. The γ energies and level energies are in keV. The width of the transitions reflects their γ intensity. The width of the short arrows feeding the levels reflects the relative γ intensity observed in the average-resonance neutron-capture spectrum.

are determined by making a least-squares fit of the level energies to the network of assigned gamma rays. A table of all possible transitions between the calculated states is computed; the complete list of experimentally observed gamma rays is then searched for additional acceptable assignments. The acceptance criterion is externally adjustable.

During its development, the program has been used extensively in the analysis of data obtained on the reaction $^{159}Tb(n, \gamma)$ ^{160}Tb. The code has been thoroughly debugged and documented, will be reported in Nuclear Instruments and Methods, and published as a Physics Division Informal Report.

C. FAST-NEUTRON RESEARCH

The program of neutron-physics experiments formally carried out at the 4-MV Dynamitron has been inactive recently because the manpower normally involved in this activity has been diverted to the measurement of low-energy charged-particle cross sections of interest for CTR applications. The one investigation described below was carried out at the tandem Dynamitron operated by the Applied Physics Division.

Experimental and Theoretical Studies of Neutron Elastic Scattering from ^{12}C Below 5 MeV

R. J. Holt, A. B. Smith,* and J. F. Whalen*

This work is the result of a collaboration between the Physics and Applied Physics Divisions. Studies of the $^{12}C(n,n)^{12}C$ reaction in the MeV region are important for reactor applications, neutron flux calibration standards and fundamental nuclear structure information. Angular distributions of neutrons elastically scattered from ^{12}C were measured in the energy range 1.8 to 4.0 MeV and at 20 to 90 reaction angles between 20° and 160°. In addition, total neutron cross sections for the $^{12}C(n,n)^{12}C$ reaction were measured in the energy range 0.1 to 5.0 MeV with high resolution ($\sim$2 keV). These experimental results were interpreted in terms of the R-matrix theory of Wigner and Eisenbud. A self-consistent set of R-matrix parameters was found which describes all observations of the ^{12}C+n system below 5 MeV.

---

*Applied Physics Division, ANL.

VII. THEORETICAL PHYSICS

A. HEAVY-ION REACTION THEORY

The generally accepted view of heavy-ion reaction theories in the past distinguished two main sorts of heavy-ion-reaction processes—peripheral and head-on. Peripheral collisions involve mutual penetration only at the outer fringes of the nuclei involved and lead to "quasi-elastic" processes wherein the amounts of matter, energy, and angular momentum exchanged are small. Head-on collisions lead to transfer of matter and energy on a large scale and the most distinctive known consequence of such collisions is complete fusion; the decay of the resulting compound system is expected to yield products retaining little memory of the original mode of formation.

In the past twelve months this view of heavy-ion processes has been significantly modified by new experimental discoveries. In the first place, work at Orsay, Dubna, and by an Argonne-Rochester collaboration at Berkeley has revealed a third class of heavy-ion reaction—intermediate between quasi-elastic and fusion reactions. These "deep inelastic" reactions yield products close in mass to the incident ions, but are very far from quasi-elastic in that huge amounts of kinetic energy are dissipated and the emerging ions are highly excited. In the second place, experimental work at Argonne has demonstrated conclusively that in quasi-elastic heavy-ion reactions no single channel dominates. This is in contrast to light-ion-induced direct reactions, wherein the elastic channel is overwhelmingly predominant.

These new experimental findings have serious implications for heavy-ion reaction theory.

(1) The deep-inelastic reactions are direct manifestations of dissipative or viscous effects in heavy-ion collisions; the study of viscosity thus acquires greater immediacy.

(2) The experimental results which place many quasi-elastic channels on the same footing impel us towards a many-channel reaction theory wherein a first-order treatment of the interaction inducing transitions is at the very least questionable.

1. PERIPHERAL OR QUASI-ELASTIC COLLISIONS

a. Calculational Techniques and Methods

D. H. Gloeckner, M. H. Macfarlane, and S. C. Pieper

For peripheral heavy-ion collisions, it is now clear that DWBA is adequate only under special circumstances. However, the computational problems involved in a many-channel direct-reaction calculation already appear in DWBA. Thus a first step towards a workable many-channel approach is a highly-efficient DWBA. The computer programs for this work have been made much more efficient both in terms of faster execution and smaller core-storage requirements. This has been done by exploiting the physical characteristics of heavy-ion collisions.

(1) The semiclassical orbit substructure of heavy-ion processes yields information about the regions of configuration space that contribute most significantly to quasi-elastic processes. We use this information to compute quadrature formulae that are specific to each reaction (rather than using general formulae with step-sizes that are externally-supplied parameters).

(2) The simple angular-momentum properties of peripheral heavy-ion reactions are used to reduce numerical labor by about an order of magnitude (see Sec. b, below). DWBA programs incorporating these features are now complete and in use. We view these programs now as way stations on the road to multichannel calculations; it is clear that the methods used to accelerate DWBA apply directly in the many-channel situation.

b. Partial-Wave Structure of Heavy-Ion-Transfer Amplitudes

M. H. Macfarlane and S. C. Pieper

It has been established that quasi-elastic heavy-ion reactions occur predominantly in a few partial waves close to the grazing angular momentum. In this "L window" the reaction amplitudes peak

strongly in magnitude and vary smoothly in phase. This L-space behavior can be parameterized by simple analytic functions of L and the resulting parameterization used (1) to interpolate in L in DWBA (and many-channel) calculations, thereby reducing computational labor by an order of magnitude and (2) to study L-space singularities (Regge poles) of heavy-ion transfer amplitudes. The results of such studies are now being written up for publication.

c. Structure Amplitudes for Three-Nucleon Transfer with 1p-Shell Targets

D. Kurath and D. J. Millener*

Spectroscopic amplitudes have been calculated for transfer of three nucleons whose spatial wave function is symmetric under particle exchange. These amplitudes are needed to calculate magnitudes of cross sections for cluster transfer. The selectivity and distribution in energy of such transfer was investigated for targets in the nuclear 1p shell. Some examples of interference between $(1p)^3$ and $(p1)(2sd)^2$ transfer were treated, and found to be more important in stripping than in pickup reactions. The results are presented in Nucl. Phys. A238, 269 (1975).

*Nuclear Physics Laboratory, Oxford, England.

2. HEAD-ON COLLISIONS, FUSION, AND VISCOSITY

a. Microscopic Calculations of Viscosity in Heavy-Ion Collisions

D. Glas* and U. Mosel

Dynamical calculations have been carried out for the heavy-ion system $^{16}O + ^{16}O$ showing that in a close collision a great deal of kinetic energy is converted into internal excitation energy. The two-center shell model is used to describe the manner in which the individual shell spectra of the separated ions merges into the single-particle

*University of Giessen, Giessen, Germany.

spectrum of the compound nucleus as the distance between the centers of mass decreases. The process of energy conversion is calculated using the Landau-Zener approximation familiar in molecular physics; this approximation assumes that excitations occur only when two single-particle levels in the vicinity of the combined Fermi surface approach each other. These calculations reveal the importance of a critical distance or "point of no return" at which the two shell structures first significantly perturb each other. When the ions approach each other to this point of no return, they stick together due to loss of kinetic energy long enough to form the compound system that leads to fusion. This calculation (the first microscopic description of viscosity in heavy-ion collisions) is described in Phys. Lett. 49B, 301 (1974).

b. Critical Distances in Fusion Reactions

D. Glas* and U. Mosel

The systematics of heavy-ion-fusion cross sections have been interpreted in terms of a critical distance; if ions reach this separation, they are assumed to fuse with near certainty. However, data on fusion cross sections near the Coulomb barrier seem to yield a critical radius R_B significantly larger than that found at higher energies. This two-radius discrepancy has been removed by the new data alluded to above on deep inelastic processes and by the concept of point of no return described in Sec. a. The new data show that, whereas near the Coulomb barrier the total-reaction and total-fusion cross sections are almost identical, far above the barrier the fusion cross section is much less than the reaction cross section. Thus near the Coulomb barrier only the barrier radius R_B matters; at higher energies the colliding ions must approach to the "point of no return" (less than R_B). In Nucl. Phys. A237, 429 (1975) a simple model is presented which shows how the apparent "two-radius" discrepancy can be understood as a change of relative importance of interaction barrier and point of no return as the energy increases.

*University of Giessen, Giessen, Germany.

3. ELECTROMAGNETIC EFFECTS IN HEAVY-ION REACTIONS

Vacuum Polarization- and Molecular-Potential Effects in Heavy-Ion Scattering

Johann Rafelski

Large angle ($\theta_{c.m.} > 10^{\circ}$) heavy-ion scattering is mainly determined by Coulomb, and above the Coulomb barrier by nuclear forces. However, with increasing precision of the experiments it might be possible to measure the deviation from pure Coulomb scattering due to vacuum polarization[1,2] and molecular effects[3] at sub-Coulomb-barrier energies. The effect due to the molecular potential is most important for collisions with $Z = Z_{projectile} + Z_{target} \geqslant 130$. Its origin is from the electrons that are bound to the combined system of projectile and target nucleus. For collisions with $(Z_1 + Z_2) \sim 184$, the molecular potential at R = 15 fm reaches -6.2 MeV, which is about 0.8% of the Coulomb barrier.

We use the classical approximation in our calculations.[4] The heavy ions are assumed to move on classical trajectories in a given potential. In $^{16}O \rightarrow {}^{208}Pb$ at 69.1 MeV (lab) the vacuum polarization effect is dominant. However, in the interval $60^{\circ} - 160^{\circ}$ we have a rise in the cross section of only 0.1% which is easily compatible with the results of Barnett *et al.*[5] This is not the ideal region to measure the vacuum polarization effects. Using lower energy projectiles (30 MeV

---

[1] J. Rafelski and A. Klein, Phys. Rev. C 9, 1756 (1974).

[2] R. Z. Roskies, Phys. Rev. C 10, 1565 (1974).

[3] J. Rafelski, B. Müller, and W. Greiner, Nuovo Cimento Lett. 4, 469 (1972).

[4] J. Rafelski, "Vacuum Polarization- and Molecular-Potential Effects in Heavy-Ion Scattering," Argonne preprint, 1975, to be published.

[5] A. R. Barnett, W. R. Phillips, P. J. A. Buttle, and L. J. B. Goldfarb, Nucl. Phys. A176, 321 (1971).

^{16}O) will help if we measure between 20° and 80°, where the relative effect rises by 0.3%.

The actual measurement of vacuum polarization might be more feasible if one could devise an experiment to measure the difference of the contributions at large and small angles simultaneously. Such an experiment is possible using a detector which would detect both target and projectile ions.[6] Such a detector would measure the scattering cross section at two different angles simultaneously. For example, placing it at 20° (lab) it will measure the scattering at 21.5° (c.m.) (detection of ^{16}O) and at 140° (c.m.) for detection of recoil ^{208}Pb. The ratio of Pb to ^{16}O events should differ by 0.4% from the expected one [for 60—70 MeV (lab) ^{16}O on ^{208}Pb]. In the most extreme case choosing a detector at 10° (lab system) thus measuring at 10.7° (c.m.) and 160° (c.m.), we can expect 0.13% and 0.66% changes which would result in a 0.53% observable difference.

As a characteristic example where molecular potential becomes dominant, we have chosen the scattering of ^{232}Th on ^{238}U at 1600 MeV (lab). Since the molecular potential is negative and has a magnitude larger than the positive vacuum-polarization potential, we will find a net decrease of the cross section. Furthermore, since the molecular potential grows more slowly than the nuclear Coulomb repulsion as a function of R, the correction to Rutherford scattering will become smaller with increasing scattering angle.

We find a change of 2.6% in the cross section as we go from 10° to 110° in scattering angle. This greater change comes because the addition of vacuum polarization and molecular effects enhances the relative effect at chosen scattering angles—a very desirable effect.

In view of the above calculations we feel that both effects can be well established by measuring heavy-ion differential scattering

---

[6] J. Schiffer, private communication.

cross sections at fixed projectile energies. The measurement of the molecular potential might also yield some knowledge of the binding of electrons in very strong external fields.

B. NUCLEAR MATTER AND NUCLEAR FORCES

Nuclear forces are very poorly determined from first principles. The only unambiguous theoretical result is that the one-pion-exchange potential should dominate at large distances. The first step in a phenomenological program to learn more about the nucleon-nucleon force is to require that it reproduce the empirical scattering phase shifts. But this does not by any means determine the potential uniquely. It is therefore desirable to further test potentials that fit the scattering by requiring them to account for the binding energies and density distributions of nuclei. Another aspect of this program is the possibility of unifying nuclear structure calculations and nucleon-nucleon scattering by showing that both can be understood in terms of the same basic nucleon-nucleon potential.

The testing ground for this program is infinite nuclear matter. Conditions in nuclear matter are expected to approximate those in the interior of a nucleus. Thus a two-body potential that can account for the equilibrium energy and density of nuclear matter is expected to also predict accurate binding energies and radii for nuclei. The goals of the work on nuclear matter and nuclear forces are: (1) To improve the present method of solving the many-body problem so that accurate and reliable tests of potentials can be made. (2) To explore effects not included in the usual model of point nucleons interacting through a two-body potential. These include effects due to relativity and to explicit meson degrees of freedom in the nucleus. (3) To use the principles of Lorentz invariance and quantum field theory to put additional theoretical restrictions on the nucleon-nucleon potential.

Reaction-matrix calculations of the equilibrium binding energy and density of nuclear matter are at present in disagreement with the empirical values. Many different two-body potentials, all of which reproduce the nucleon-nucleon scattering data, have been used, but without success. Potentials that give enough binding give too high a density, and potentials that give the right density give too little binding. The Reid potential, for example, underbinds by about 2 MeV and predicts a density 20% too large. A possible reason for the discrepancy is that existing calculations of three-body correlations are inaccurate. The effort to develop an accurate three-body calculation has been continued, and greatly improved calculations are now feasible. Calculations of relativistic corrections and of isobar degrees of freedom were completed and were shown not to resolve the present discrepancy. Details on this and other work are given below.

1. RELATIVISTIC EFFECTS IN PHENOMENOLOGICAL NUCLEON-NUCLEON POTENTIALS AND NUCLEAR MATTER

F. Coester, Steven C. Pieper, and F. J. D. Serduke

For any phenomenological nucleon-nucleon potential the Brueckner theory predicts the energy per nucleon and the density of homogeneous nuclear matter. The predicted values vary widely for different potentials that fit the same scattering data. However, the predicted binding energy and density are always correlated in such a manner that no potential fits the experimental values. It is therefore necessary to examine neglected effects that might remove the discrepancy. There are necessarily relativistic effects due to the center-of-mass motion of correlated nucleon pairs and due to the relativistic momentum dependence of the kinetic energy. We have identified and isolated these effects in such a manner that they can be calculated as unambiguous correction terms to the predictions for any conventional phenomenological nucleon-nucleon potential. Crude estimates indicate that the magnitude of these corrections may be significant. Detailed numerical results have been obtained for the Reid soft-core potential, the Ueda-Green potential and several separable potentials. Due to extensive cancellations of the individual terms the total correction is considerably smaller than the crude estimates. For the Reid potential the total correction to the energy per nucleon is only +0.22 MeV and the change in density is negligible. The energy correction is also positive for all other potentials considered. Our calculations (Fig. 45) are sufficiently representative to conclude in general that the relativistic effects considered in this work are negligible for most purposes. A paper on this work has been published in the Physical Review.[1]

---

[1] F. Coester, Steven C. Pieper, and F. J. D. Serduke, Phys. Rev. C 11, 1 (1975).

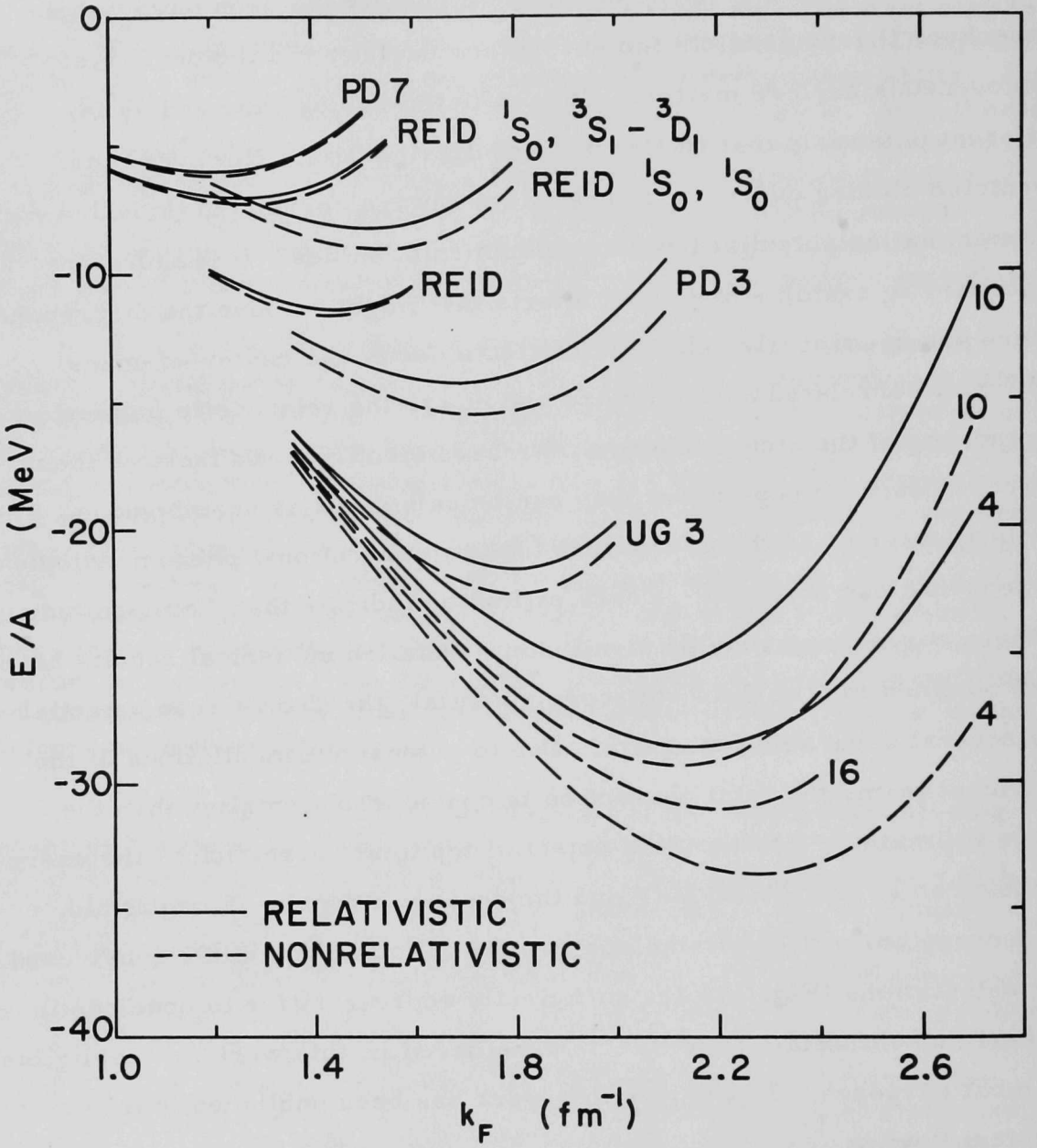

Fig. 45. Relativistic and nonrelativistic nuclear matter saturation curves for several potentials. For details see Phys. Rev. C 11, 1 (1975).

2. THREE-BODY CORRELATIONS IN NUCLEAR MATTER

B. Day and F. Coester

The size of the present discrepancy between theory and experiment in nuclear matter is comparable to the present calculational uncertainty in the three-body correlation energy. To pin down the discrepancy, more accurate three-body calculations are needed. Such calculations have previously been done in momentum space for an S-state force. Computer programs have now been written to apply this method to the full nucleon-nucleon potential, including tensor and spin-orbit forces.

Tests are being carried out using the Reid potential. The main problem in the calculation, as in all three-body calculations, is to prevent the matrices to be inverted from becoming unmanageably large. This problem has been successfully overcome with the aid of an efficient numerical method for representing an arbitrary two-body reaction matrix as a sum of separable terms. The remaining problem is to estimate the errors due to use of an angle-average Pauli operator. If this problem can be resolved, accurate calculations of the binding energy and density of nuclear matter with two-body potentials will become feasible. This will permit us either to resolve the apparent discrepancy or to show convincingly that it really exists.

If the discrepancy does persist, a possible remedy is the inclusion of three-body <u>forces</u>, in addition to three-body <u>correlations</u> produced by two-body forces. Taking three-body forces into account requires an accurate three-body wave function, and the present method, if successful, will produce this wave function.

3. ISOBAR CONFIGURATIONS IN NUCLEAR MATTER

B. Day and F. Coester

Conventional nuclear-matter calculations assume that the two-body potentials can satisfactorily reproduce all important effects of the suppressed meson degrees of freedom. Explicit inclusion of some important meson degrees of freedom into the nuclear matter wave function provides a partial check of the validity of this assumption. We have treated the $\Delta(1236)$ pion-nucleon resonance as an excited state of the nucleon in order to see whether the saturation properties of nuclear matter are changed significantly. In this model the $^1S_0$ two-body potential has components that change a nucleon-nucleon (NN) pair into a nucleon-Δ (NΔ) pair. We obtained an excellent fit to the $^1S_0$ scattering phase shifts by readjusting the parameters of the Haapakoski potential. In all other partial waves we assumed the Reid or Ueda-Green potentials with no coupling to the Δ state.

The effective $^1S_0$ interaction in nuclear matter in this model is weaker than the effective interaction for two free nucleons for two reasons: (1) in nuclear matter the energy denominators are larger than in scattering, and (2) the exclusion principle forbids NΔ states in which the nucleon momentum is below the Fermi level.

The NΔ coupling in the $^1S_0$ state was found to shift the saturation points substantially. But the same correlation persisted between equilibrium binding energy and density as in the conventional calculation. Hence inclusion of the isobar degree of freedom did not improve the saturation properties.

4. APPROXIMATELY RELATIVISTIC PARTICLE INTERACTIONS

F. Coester and P. Havas*

Equations of motion for the world lines of classical particles with direct interactions can be derived from Fokker action principles. A canonical form for such equations of motion exists only approximately to order $1/c^2$. Such action principles have been investigated extensively by Havas and collaborators. Fully relativistic, canonical direct-interaction theories are possible if the requirement of observable invariant world lines is abandoned for the interacting particles. That is reasonable for the quantum mechanical description of strongly interacting particles, for which only scattering amplitudes are actually observable. It is then sufficient to require the existence of an S matrix and the dynamic and kinematic independence of separated clusters. Such theories have been used by Coester et al. to investigate relativistic effects in nuclear structure. In the classical limit, and an expansion to order $1/c^2$, the Hamiltonian can be compared with those derived from Fokker action principles in the same approximation. We are investigating what, if any, restriction the classical world-line condition imposes on phenomenological potentials.

*Temple University, Philadelphia, Pennsylvania.

5. ELASTIC ELECTRON-DEUTERON SCATTERING AS A PROBE OF THE DEUTERON WAVE FUNCTION

F. Coester and A. Ostebee

Nucleon-nucleon scattering data do not determine the potential. Since different phase-shift-equivalent potentials may lead to different deuteron wave functions, an experimental probe of the short-range part of the deuteron wave function may provide additional constraints on acceptable potentials. High-energy electron-deuteron

scattering appears to provide a suitable probe. The differential cross section depends on the deuteron wave function through the electromagnetic form factors of the deuteron. Even at moderate values of the momentum transfer, a nonrelativistic calculation of these form factors is inadequate. Since the nucleon-nucleon interaction modifies the representation of the Lorentz transformations, covariance of the charge-current density requires interaction terms in the charge density as well as the current density. These dynamic effects are substantially larger than the kinematic relativistic effects. For local potentials only, the relativistic corrections are the same as those previously derived from field theory. We have analyzed the relation between the phenomenological theory and the field theoretical derivation of these effects. Detailed calculations for a number of representative deuteron wave functions illustrate the quantitative features.

C. COLLAPSED NUCLEI AND DENSE NUCLEAR MATTER

We have previously discussed, for the first time, the phenomenology of "collapsed nuclei." These were considered to be superstable objects of much smaller size and (possibly much) greater binding energy than ordinary nuclei. In particular we discussed the stability of ordinary nuclei with respect to collapse, the possible properties and production of collapsed nuclei, and also some astrophysical implications, in particular the stability of dense nuclear matter in neutron stars.

Recently, there has been much interest in collapsed nuclear states as a result of a proposal by T. D. Lee and G. C. Wick of a dynamical model involving nonlinear meson interactions. This implies so-called "abnormal" nuclear matter which may also be more strongly bound and of higher density than ordinary nuclear matter. Although the hypothetical abnormal matter is not expected to be as dense as the (totally) collapsed nuclei we considered, the phenomenology of both types of collapsed objects has many common features. An important question for the phenomenology of possible Lee-Wick collapsed nuclei is the question of their stability, in particular the region of mass numbers for which they may be expected to be stable. This is of importance for the possible production and detection of these objects.

Consideration of collapsed nuclei leads naturally to questions of the properties and means of producing dense states of nuclear matter in general. The only conceivable means of production seems to be in the high-energy collision of heavy nuclei. Thus if the relative velocities of the nuclei are greater than the speed of sound in nuclear matter, then there is the possibility of shock-wave phenomena with associated very high densities and temperatures. Whether such conditions can also lead to the production of collapsed nuclear states—even if these should exist—is quite problematical since collapsed states correspond to effectively zero-temperature conditions.

1. PHENOMENOLOGY OF COLLAPSED NUCLEI

A. R. Bodmer

We are continuing our considerations of the phenomenology of collapsed nuclei, in particular as concerns the stability and lifetime of ordinary matter against collapse and the possible production of such objects.

2. SURFACE PROPERTIES OF ABNORMAL NUCLEAR MATTER

A. R. Bodmer and J. Boguta*

The surface properties of abnormal nuclear matter are of critical importance for the understanding of finite nuclei made of Lee-Wick nuclear matter and in particular for their binding energy and therefore stability. We are studying the problem of the surface energy of abnormal nuclear matter for the somewhat idealized semi-infinite case, i.e., of a slab of nuclear matter with a free surface. We have formulated this problem and have made some progress in its solution.

*University of Illinois at Chicago Circle, Chicago, Illinois.

D. NUCLEAR STRUCTURE THEORY

1. NON-NORMAL PARITY STATES IN LIGHT NUCLEI

D. Kurath and D. J. Millener*

In the low-excitation energy spectrum of nuclear levels, there are often states with parity opposite to that of the ground-state configuration. The spectra of such non-normal parity states depend on the nature of the particle-hole interaction, and for mass number $A \leqslant 20$ this is the $(1p)^{-1}(2sd)$ interaction.

A particle-hole interaction has been derived which gives a good account of the non-normal parity states of a number of nuclei between ^{11}Be and ^{16}O. The important features of this interaction are that it remains close in character to a realistic G-matrix interaction and that it reproduces two prominent characteristics of the nuclear-level spectra: (1) the relative separation of the $2s_{1/2}$ and $1d_{5/2}$ single-particle centroids as a function of mass number and (2) the separation of multiplets of differing isospin.

The resulting wave functions give a good description of the recently measured beta decay of ^{14}B, as shown in Table VI. An important feature of these calculations is that the spurious effects of center-of-mass excitation have been eliminated completely. These results are being prepared for publication.

Gamma decays in the A=13 nuclei provide another test for the wave functions. As seen in Table VII, the E1 calculations are much closer to experiment for decays involving the $\frac{5}{2}^+$ state than for decays involving $\frac{1}{2}^+$. There are also large differences observed for some mirror transitions in ^{13}N, and these cannot be accounted for by the Coulomb interaction. It appears that the $\frac{1}{2}^+$ state must be treated more carefully, taking account of its lower binding energy in ^{13}N.

---

*Nuclear Physics Laboratory, Oxford, England.

TABLE VI. Beta decay of ^{14}B ($I = 2^-$) to states of ^{14}C. Log ft values are given for various final states (I_f).

I_f	Log ft (Exp)[a]	Log ft (Calc.)
1^-	4.22 ± 0.05	4.13
2^-	>4.9	4.83
3^-	5.10 ± 0.30	5.33
0^+	–	10.21

[a]D. E. Alburger and D. R. Goosman, Phys. Rev. C 10, 912 (1974).

TABLE VII. Reduced transition probabilities (units of e^2fm^2 for E1, M2; e^2fm^4 for E2) for gamma decays in ^{13}C.

Transition	Exp	Calc
$B(E1)(\frac{1}{2}^+ \rightarrow \frac{1}{2}^-)$	14×10^{-3}	5.9×10^{-3}
$B(E1)(\frac{3}{2}^- \rightarrow \frac{1}{2}^+)$	13×10^{-3}	2.5×10^{-3}
$B(E1)(\frac{5}{2}^+ \rightarrow \frac{3}{2}^-)$	2.8×10^{-3}	2.3×10^{-3}
$B(M2)(\frac{5}{2}^+ \rightarrow \frac{1}{2}^-)$	6.1	5.7
$B(E2)(\frac{5}{2}^+ \rightarrow \frac{1}{2}^+)$	2.4	0.6

2. DIRECT RADIATIVE CAPTURE

J. E. Monahan, A. J. Elwyn, and F. J. D. Serduke

The cross section for the direct radiative capture of alpha particles contains rather unambiguous information about the alpha-particle structure of the final state. This results from the fact that

the capture is from an initial state that does not involve any nuclear interaction to a bound final state. Thus, if the (α, γ) cross section is written as $\sigma = |M|^2 \theta^2$, where θ^2 is the alpha-particle reduced width of the final state, the evaluation of the matrix M is essentially model independent.

Measurements of the direct (α, γ) reaction at the ANL Dynamitron accelerator are being considered. The initial reaction of interest is $^{16}O(\alpha, \gamma)^{20}Ne$ to the 1.63-MeV state in ^{20}Ne. For an incident energy $E_\alpha = 2.5$ MeV, the cross section of this reaction is calculated to be $3.3\ \theta^2$ nb.

3. HARTREE-FOCK CALCULATIONS FOR LIGHT NUCLEI USING THE SKYRME INTERACTION

B. D. Chang, M. H. Macfarlane, U. Mosel, and K.-H. Passler

The Skyrme interaction, with a velocity-dependent two-body and a contact three-body term, has been widely used as a "soft" interaction suitable for Hartree-Fock studies of finite nuclei. It contains six parameters which can be adjusted to provide reasonably accurate descriptions of nuclear binding energies, radii, and fission barriers. Conventional (i.e., one-center) HF studies of odd-A and odd-odd light nuclei have shown that those variants of the Skyrme interaction which best describe the ground-state properties of spherical nuclei are unstable against spin realignment unless time-reversal invariance is imposed as an explicit constraint on the HF ground-state wave function. This spin instability occurs in nuclear matter, for which explicit conditions (in terms of the parameters of the Skyrme interaction) have been derived for spin stability.

Similar results are found in two-center HF studies of deformed, even-even light nuclei. Methods are discussed whereby the Skyrme interaction can be modified to prevent the spin instability

mentioned above and to provide at the same time a reasonably accurate description of the ground-state rotational bands of ^{20}Ne and ^{24}Mg.

4. SPURIOUS CENTER-OF-MASS MOTION

D. H. Gloeckner and R. D. Lawson

A method for removing spurious center-of-mass motion from shell-model calculations has been developed and implemented in the Argonne shell-model codes. The method is to add to the usual shell-model Hamiltonian a term corresponding to the excitation energy of the center of mass and to multiply this added term by a large factor ($\sim 10^5 - 10^7$). Thus any state with spurious motion is forced to lie at high excitation energy and consequently cannot mix into the low-lying states. The method has been applied to study nuclei near A = 16, and it has been shown that when the spurious center-of-mass motion is removed, the energies of certain states are drastically changed. This work has been published in Phys. Lett. 53B, 313 (1974).

5. ISOSPIN-FORBIDDEN E1 TRANSITIONS

D. H. Gloeckner and R. D. Lawson

T=0→T=0 E1 transitions are forbidden if isospin is a good quantum number. In ^{40}Ca the 1^- T=0 state at 6.95 MeV has a lifetime for decay to the T=0 ground state of 1.2×10^{-15} sec. We have used the shell-model programs (modified to remove spurious center-of-mass motion—see preceding report) to calculate this transition rate. Both the Coulomb interaction and the fact that the neutron single-particle levels in ^{39}Ca and ^{41}Ca have slightly different excitation energies than those of the analogous proton states in ^{39}K and ^{41}Sc have been included

in the calculation. When these effects are included, the predicted lifetime for the 1^- state is 1.8×10^{-15} sec. This calculated value is extremely sensitive to small changes in the single-particle energies. For example, a change of only 100 keV in the energy of the $p_{3/2}$ and $p_{1/2}$ proton single-particle energies changes the predicted lifetime by about 30%. Since these energies are uncertain to at least this amount, it is clear that no information on a possible isospin violating part of the residual nucleon-nucleon interaction can be obtained from this type of data.

6. THE E6 GAMMA TRANSITION IN ^{53}Fe

D. H. Gloeckner and R. D. Lawson

A recent measurement of the transition between the 3.0406-MeV $\frac{19}{2}^-$ state and the $\frac{7}{2}^-$ ground state in ^{53}Fe has shown that this transition is inhibited by a factor of four relative to the value deduced by use of the $(f_{7/2})^{13}$ wave functions. The effect of $f_{5/2}$ mixing on this transition has been calculated on the assumption that only terms linear in the $f_{5/2}$ component should be kept. Several interactions have been considered. When the $f_{5/2}$-$f_{7/2}$ single-particle energy splitting is chosen to agree with experiment, the matrix element governing the transition is decreased by about 30% independently of the interaction used. To explain experiment with an isoscalar effective charge ($e_p = 1 + \delta$, $e_n = \delta$), one must choose $\delta \approx -0.4$. This is the only known E6 transition and consequently provides the first information on what the magnitude of core polarization effects are on this multipolarity transition.

7. BETA DECAY OF ^{209}Tl

R. D. Lawson

^{209}Tl, which has a $\frac{1}{2}^+$ ground state, beta decays to the $\frac{1}{2}^-$ 2.13-MeV level in ^{209}Pb but is not observed to decay to the 2.01-MeV $\frac{1}{2}^+$ state. The Gamow-Teller beta-decay operator cannot change the radial wave function of the decaying state and consequently one would expect the matrix element governing the latter transition (in which a $4s_{1/2}$ neutron becomes a $3s_{1/2}$ proton) to vanish provided neutrons and protons move in the same single-particle well. However, it is known that collective effects strongly modify beta-decay matrix elements and consequently this Δn-forbidden transition would be expected to occur due to these effects. A lower limit on the log ft for the transition would therefore allow one to estimate to what degree the collective effect is cancelled by the fact that neutrons and protons move in different single-particle wells. Thus from a study of this decay one can learn about the size difference of the neutron and proton single-particle wells. This work was discussed in an invited paper at the International Conference on Nuclear Structure and Spectroscopy, Amsterdam, September 1974, published by Scholar's Press, Amsterdam, 1974, p. 464.

8. SHELL-MODEL STUDY OF NUCLEI WITH $Z < 38$ AND $N \leq 50$

D. H. Gloeckner and F. J. D. Serduke

The N=50, 49, and 48 isotones of Rb, Kr, and Br have received considerable experimental study in the past few years. As yet, there have been no significant shell-model interpretations of the data that have emerged. Most of the low-lying states of these nuclei can reasonably be described by a model space with $2p_{3/2}$ and $1f_{5/2}$ proton holes and $1g_{9/2}$ and $2p_{1/2}$ neutron holes in the nucleus $^{88}_{38}Sr_{50}$. We are currently determining a shell-model effective interaction that should serve to correlate this body of available experimental data.

9. SHELL-MODEL STUDY OF N=48 NUCLEI

D. H. Gloeckner and F. J. D. Serduke

Nuclear properties of the N=48 isotones with $Z > 38$ have been calculated using the shell-model effective interactions determined from the N=49 and N=50 isotone studies described earlier. There is excellent agreement with the experimental spectra for the known low-lying states of ^{87}Y, ^{88}Zr, ^{89}Nb, and ^{90}Mo. Of particular interest are states in ^{88}Zr that will soon be investigated at the ANL FN tandem with the $^{86}Sr(^{16}O, ^{14}C)^{88}Zr$ reaction. Our model predicts unambiguously that a two-proton transfer reaction should strongly populate the <u>second</u> state of a given spin in this nucleus. This is in contrast to two-neutron pickup on ^{90}Zr which should preferentially excite the <u>first</u> state of a given spin. Our shell model of the neutron-deficient nuclei in the mass-90 region also should prove useful in interpreting the data for other nuclei in the forthcoming heavy-ion studies.

10. SHELL-MODEL STUDY OF N=49 NUCLEI

D. H. Gloeckner, R. D. Lawson, and F. J. D. Serduke

The N=49 isotones with $Z > 38$ are described by a shell model that allows Z-38 protons in the $2p_{1/2}$-$1g_{9/2}$ single-particle levels and a single neutron hole in the same levels. The 20 matrix elements of the proton-neutron hole effective interaction have been determined by a least-squares minimization procedure. There are over 60 known energy levels in the nuclides ^{88}Y, ^{89}Zr, ^{90}Nb, ^{91}Mo, ^{92}Tc, and ^{93}Ru that can reasonably be expected to emerge from our model; their positions are reproduced to an rms deviation of ~65 keV. Our model wave functions yield a satisfactory description of the results for a large variety of transfer reactions leading to states in these N=49 isotones. Antianalog states in ^{90}Nb and ^{92}Tc are predicted. Seniority conservation in the

T=1 effective interaction among $1g_{9/2}$ nucleons is independently substantiated in this study.

11. AN EXTENDED SHELL-MODEL DESCRIPTION OF $^{88}_{39}Y_{49}$

D. H. Gloeckner and F. J. D. Serduke

The nucleus ^{88}Y can be reached experimentally by nearly a dozen different reactions involving "light" particles. As a consequence, there is a wealth of experimental data on its structure. Most of these data have emerged within the last two or three years. The $2p_{1/2}$-$1g_{9/2}$ proton neutron-hole model space used in our previous studies does a respectable job in describing many of the excitations of this nucleus, but there is still a large number of states not describable within that model space. The abundance of high-quality experimental data and the tractability of an extended shell-model calculation that includes $2p_{3/2}$ and $1f_{5/2}$ active nucleons has stimulated our efforts in this direction.

E. OTHER THEORETICAL PHYSICS

1. THE PION-NUCLEUS INTERACTION

J. E. Monahan, L. Meyer-Schützmeister, and F. J. D. Serduke

Measurements of prompt gamma rays resulting from the bombardment of various targets with high-energy pions yield information about the abundances of the final product nuclei. A plausible interpretation of these measurements is the following. The primary interactions of the incoming pion with the target result in the emission of, at most, a few prompt nucleons. The pion may be absorbed or it may be re-emitted in any of its charge states. The emitted particles carry away varying amounts of kinetic energy and thus leave residual nuclei with wide ranges of excitations. These nuclei, in turn, may evaporate additional nucleons. The observed gamma rays are those associated with transitions in the final nuclides with an excitation energy below threshold for further nucleon evaporation.

Evaporation is essentially a statistical process and, for the study of π-nucleus reactions, is of less interest than the primary or pre-equilibrium interactions. Given a model for the calculation of evaporation spectra, it may be possible to abstract from the measurements information about the pre-equilibrium interactions. Preliminary calculations have been made for 200-MeV $\pi^{\pm}$ incident on ^{60}Ni and ^{51}V based on the assumption that the primary π-nucleus interaction is simply inelastic (π, π') scattering with no charge exchange or direct nucleon knockout. The results of these calculations are in qualitative agreement with the corresponding gamma-ray measurements. More extensive calculations are necessary to determine whether this approach gives results which are sufficiently unique to allow an investigation of the primary pion-nucleus interactions from the experimental gamma-ray data.

2. BOUNDARY PERTURBATIONS

J. E. Monahan and Norbert Rosenzweig

The physical properties of an assembly of small metallic particles depend on the (discrete) spectra of electronic energy levels which are determined by the size and shape of each of the particles. Current theory considers the assembly to be a random collection of particles and assumes that the associated energy spectra are also distributed randomly. However, recent measurements of the static magnetic properties of systems of small metal particles have led to the suggestion that this assumption be re-examined. To do this, it is first necessary to develop an expansion for the change in the (degenerate) electronic eigenvalues caused by an arbitrary perturbation of the shape of a particle. Such an expansion has been obtained in a form which seems suitable to the further investigation of this problem.

3. GROUPED-SAMPLE MODIFICATIONS OF THE CRAMÈR-SMIRNOV TEST FOR GOODNESS OF FIT

J. E. Monahan and Norbert Rosenzweig

The utility of a test statistic that would complement Pearson's χ^2 in tests of goodness of fit is generally recognized. The statistic most often suggested for this role is the Cramèr-Smirnov statistic ω_n^2. Since ω_n^2 is defined only for individual observations (i.e., for a nongrouped sample), whereas χ^2 is defined only for a grouped sample, the modifications of ω_n^2 necessary for its application to grouped samples is of interest. For a sample of n events grouped into k disjoint classes, a statistic ω_{nk}^2, which has the property that $\lim_{n\to\infty} \omega_{nk}^2$ approaches $\lim_{n\to\infty} \omega_n^2$ as k increases, can be defined. In addition to its role as an alternative to χ^2, preliminary results indicate that the sampling distribution of ω_{nk}^2 may provide criteria for the design of sampling procedures.

4. A STATISTICAL ANALYSIS OF COUNTING DATA

J. E. Monahan

The analysis of experimental data to test a given theory or to evaluate the free parameters of a particular theoretical model is essentially a statistical problem. Standard procedure is to formulate this problem in terms of a chi-squared statistic. However, in any particular application, it is often difficult to justify the implicit assumption that the statistic actually used is distributed according to the chi-squared law. In the special case of counting data, it is possible to formulate an analysis based on the exact sampling distribution of the experimental results. Given this sampling distribution, it is possible to define explicitly the experimental conditions that must be satisfied in order to justify the analysis. A comparison of the proposed method and the conventional chi-squared procedure shows that, under certain specified conditions, the application to analysis of counting data of a modified version of the latter can be rigorously justified.

5. THE HARTREE-FOCK APPROXIMATION AND QUANTUM ELECTRODYNAMICS

J. Rafelski and Berndt Müller*

We derive a set of self-consistent amplitude equations from the operator equations of motion for coupled electron and photon fields. This set is a generalization of the known Hartree-Fock equations. We confirm the previous work of Reinhard et al.[1]

In the Hartree-Fock approximation we provide a self-consistent scheme to determine bound-state solutions of the Hamiltonian

*University of Washington, Seattle, Washington.

[1] P. A. Reinhard, Nuovo Cimento Lett. 3, 313 (1970); P. B. Reinhard, W. Greiner, and M. Arenhovel, Nucl. Phys. A166, 173 (1971).

treating the real and virtual effects (e.g., vacuum polarization) on the same basis. As the most practical thing, we work in the frame of quantum electrodynamics but the method is applicable to all interacting field theories. Especially, it may be used to justify the procedure of solving classical nonlinear field equations to obtain some insights on quark confinement.

6. SPURIOUS CONTACT DIVERGENCES IN THE S-MATRIX FORMULATION OF FIELD THEORY

Johann Rafelski and Michael Danos*

The most widely used way to obtain approximate solutions in the field theory is the perturbative evaluation of S-matrix elements (Feynman diagrams). This procedure unveils severe divergences, which usually are eliminated in the so-called renormalization procedure. Several such divergences, however, give rise to inconsistencies and there was no cogent way to eliminate them. As an example, consider the quadratic divergence of vacuum polarization, which breaks the gauge invariance of quantum electrodynamics.

It is shown that most such divergences are spurious and pertain to poor mathematical formulation and evaluation of the S-matrix elements in perturbation theory. A Feynman graph has to be analyzed in configuration space (and not in momentum space) for short distance behavior. It is shown that all contact ($\delta^4(x)$) divergences (i.e., $\delta^4(x)\delta(x^2)$) which is the "quadratic" divergence of vacuum polarization) are not present in physical matrix elements.

New mathematical methods to recognize "meta" distributions (products like $\delta^4(x)\delta(x^2)$, $1/(x^2 - i\varepsilon)^3$, etc.) are formulated and used to recognize spurious contact divergences.

*National Bureau of Standards, Washington, D.C.

It is found that all well-known inconsistencies of divergent and finite contributions in field theory (quadratically divergent vacuum polarization, Adler anomaly, $m_{renom} > m_0$, etc.) disappear. Furthermore, the absence of worse divergences suggests that some theories, considered nonrenormalizable so far, might be well behaved.

7. STABILIZATION OF THE CHARGED VACUUM CREATED BY VERY STRONG ELECTRICAL FIELDS IN NUCLEAR MATTER

Johann Rafelski

The behavior of electrons in strong electromagnetic fields gives rise to phenomena outside the range of the usual perturbation theory treatment of quantum electrodynamics (QED). One is forced to give up the usual concept of a neutral ground state (the vacuum) of QED, as the strength of the potential passes through the critical point ($Z_{cr} \approx 172$ for ordinary nuclei). It was shown that the supercritical vacuum is charged.[1] In this work[2] we explored the consequences of the idea of a charged vacuum when applied to the description of extended bulk nuclear matter, e.g., charged domains in neutron stars or abnormal nuclear states.

The expectation value of electrical charge in charged vacuum is calculated utilizing relativistic Thomas-Fermi approximation. We find almost complete screening of the nuclear charge. For any given nuclear density there is an upper bound for the electrical potential. For normal nuclear densities this value is -250 MeV. This suggests that the vacuum is stable against spontaneous formation of heavy,

---

[1] J. Rafelski, B. Müller, and W. Greiner, Nucl. Phys. B68, 585 (1974); B. Müller, H. Peitz, J. Rafelski, and W. Greiner, Phys. Rev. Lett. 28, 1235 (1972); L. Fulcher and A. Klein, Phys. Rev. D 8, 2455 (1973); L. Fulcher and A. Klein, Ann. Phys. (N.Y.) 84, 335 (1974).

[2] B. Müller and J. Rafelski, Phys. Rev. Lett. 34, 349 (1975).

charged particles. Our calculations involve integration of the Coulomb equation

$$\Delta V(\vec{r}) = e\rho_N(\vec{r}) - e\rho_e(V(\vec{r})), \tag{1}$$

where ρ_N is the external "nuclear" charge density (henceforth considered to be ρ_0 for $r < R$ and 0 for $r > R$, $R = 1.2\,A^{1/3}$, $A = 2Z$, $Z = \int \rho_N d^3x$); and the electron's charge density is obtained from the relativistic Thomas-Fermi approach

$$e\rho_e = \frac{e^2}{3\pi^2} p_f^3 \tag{2}$$

$$p_f = ((E_f - V)^2 - M^2)^{1/2}, \tag{3}$$

where p_f and E_f are Fermi momentum and energy of the electron gas. We set $E_f = -m_e$, which restricts the electron density to the bound states that dived into the negative energy continuum states of the Dirac equation. In Fig. 46 we show solutions of the relativistic statistical potential [Eq. (1)] for selected values of the nuclear charge as a function of r. The self-consistent potential V is shown in Fig. 46a, while the corresponding charge distribution of the electrons below $E_\gamma = -m_e$ is shown in Fig. 46b.

The effective charge of the supercritical system is shown in Fig. 47, curve denoted γ, while the number of electrons below the Fermi surface $E_f = -m_e$ is denoted by $Z - \gamma$. Each curve is shown as a function of the "nuclear" charge Z.

The result with the most important consequences is that there is a limit to the electrostatic potential. Depending on the density of the external charge distribution—which is for our purposes independent of electromagnetic interactions—only a finite number of species of charged elementary particles can create a charged vacuum or form a

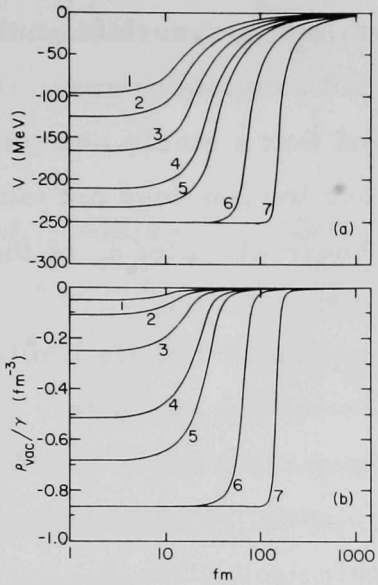

Fig. 46. The solutions of the relativistic statistical potential equation (1) for selected values of the nuclear charge as a function of r. Curve 1, Z = 600; curve 2, 1000; curve 3, 2000; curve 4, 5000; curve 5, 10 000; curve 6, 10^5; curve 7, 10^6. (a) The self-consistent potential; (b) the corresponding charge distribution of the vacuum.

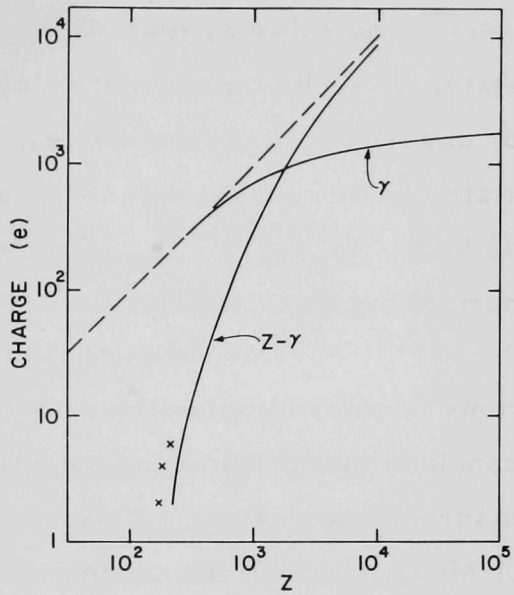

Fig. 47. The unscreened charge γ and the total charge of the vacuum (Z − γ) as a function of Z. The crosses denote points from Hartree-Fock calculations. The dashed line denotes the nuclear charge Z.

Bose condensate.[3] Whether the formation of a pion condensate for $Z \geqslant 2000$, as discussed in Ref. 3, is possible, depends on the details of the pion-nucleus interaction.

In the Lee and Wick[4] theory of abnormal nuclear states, there is a significant gain in the energy (ca. 150—3000 MeV) of the vacuum excitation whenever a baryon is absorbed. Due to the compensation of the repulsive electric forces inside the nucleus by the polarization of the vacuum and the existence of the limiting potential, the Coulomb

[3] A. Klein and J. Rafelski, "Bose Condensation in Supercritical External Fields," Phys. Rev. D, in print.

[4] T. D. Lee and G. C. Wick, Phys. Rev. D 9, 2291 (1974); A. Bodmer has also considered condensed states of nuclear matter [Phys. Rev. D 4, 1601 (1971)].

interaction will not, most likely, stop the growth of the abnormal nuclear state. If such states could be created, they would continue to grow by absorption of normal nuclear matter. We find that a stable abnormal state can be created only if the binding energy per baryon does not exceed $90\ \mathrm{MeV} \cdot (\rho_B/\rho_0)^{1/3}$ (ρ_B is the density of the abnormal state; ρ_0 is the normal nuclear density).

Our time-independent statistical approach has its limitations in macroscopic distances ($r \gg \hbar/mc$). It would be wrong to conclude that the limiting potential described above is an upper bound for macroscopic devices. This is understood for potential barriers $\gtrsim 2m$ (1 MeV); although the channel for spontaneous pair production is already open, the tunneling factor $\exp(-\int V\,dr)$ is too small by hundreds of orders of magnitude. Therefore a macroscopic experiment to determine the value of the limiting potential is not feasible.

Finally, let us say again, that our Eq. (1) is most suitable to calculate the effects of real vacuum polarization in very strong external fields. Similar calculations performed previously in the vicinity of the critical potential,[5] already required a prohibitive numerical effort.

---

[5] B. Müller, J. Rafelski, and W. Greiner, Nuovo Cimento A 18, 551 (1973); M. Gyulassy, Phys. Rev. Lett. 33, 921 (1974).

8. GENERAL FORMULATION OF PIONIC DECAYS IN THE QUARK MODEL

Harry J. Lipkin

Predictions for pionic decays of resonances to states in the low-lying baryon-56 or meson-36 supermultiplets are shown to follow from general model-independent algebraic properties. All models in which transition operators change the state of only a single quark allow only two partial waves for the decay pion and give $SU(6)_W$ relations between decays in each partial wave, while not necessarily

relating different partial waves. A paper on this topic has been published in Phys. Rev. D 9, 1579 (1974).

9. EINSTEIN'S EQUIVALENCE PRINCIPLE. AN EXPLICIT STATEMENT AND ITS DERIVATION FROM SPECIAL RELATIVISTIC PRESYMMETRY

Y. Avishai and H. Ekstein

A statement of the observable implications of the equivalence principle that is precise and general rather than allusive and illustrative is given. This statement is derived from previously formulated principles of special-relativistic presymmetry. The substantial identity of our result with Einstein's curved-space formulation is exhibited. This work has been published in Commun. Math. Phys. 37, 193 (1974).

F. SPEAKEASY DEVELOPMENT

1. THE KAPPA RELEASE OF SPEAKEASY

S. Cohen, Steven C. Pieper, and M. J. Stob

Speakeasy is a user-oriented computer system that has gained widespread acceptance throughout the world. Originally designed to provide effective access to a computer for a research scientist, it has proven to be of use to a much wider community. One of its major design specifications provides for evolutionary enhancements to its capabilities.

The newest release of the processor, called Kappa, represents a significant increase in the development. The wide community of users has required a considerable broadening of the capabilities of Speakeasy. Included in Kappa are many statistical operations, new graphics capabilities, and a general increase in the functional capabilities of the processor for interacting with novice computer users.

Speakeasy is now in active use in some 50 sites. These include universities, government laboratories, and commercial corporations. It is now clear that Speakeasy is becoming a recognized computer system. Speakeasy is a project in the SHARE IBM user group, and sessions dealing with Speakeasy occur in all of its major meetings. Speakeasy has found a home in several major universities. It is now being used in classes as a direct teaching aid.

2. THE SPEAKEASY CENTER

S. Cohen

In order to provide coherence in the distribution of information among the large number of Speakeasy sites and to insure continued

maintenance and development of the processor, a Center has been established at Argonne. This Center is funded primarily by the outside user community by a yearly membership fee in the Speakeasy users group.

VIII. ATOMIC AND MOLECULAR PHYSICS

INTRODUCTION

Research into the properties of matter on the atomic-molecular scale is carried out in many divisions at Argonne. The Physics Division's contribution consists of the following six activities:

A. Photoionization and photoelectron physics and chemistry, primarily at ultraviolet energies.

B. Surface-science studies, primarily the interactions of energetic particles and radiations with material surfaces.

C. Spectroscopy of free atoms and molecules, primarily by atomic-beam and laser absorption techniques.

D. Mössbauer-effect research, applied to diverse scientific problems.

E. Development of a scanning secondary-ion microprobe for biological and other application.

F. Beam-foil spectroscopy, including studies of the dynamics involved in the passage of MeV atoms through matter.

Most of this work is motivated by basic research goals, but there are several applied aspects. In particular, the major part of the surface-science studies is directed mainly toward obtaining information needed for design of the first wall in a thermonuclear reactor, and the ion-microprobe work is a feasibility study motivated by applied applications. The Mössbauer-effect research has a minor component motivated by ecological problems.

Details of the individual activities are given below.

A. PHOTOIONIZATION AND PHOTOELECTRON PHYSICS AND CHEMISTRY

1. PHOTOIONIZATION MASS SPECTROMETRIC STUDY OF SEVERAL MOLECULES IN THE EXTREME ULTRAVIOLET

Paula L. Kronebusch and J. Berkowitz

The vast majority of photoionization mass spectrometric investigations to date cover the wavelength range from ionization threshold to ~600 Å (20 eV). The present work is aimed at extending our knowledge of fragmentation processes deeper into the vacuum ultraviolet to 304 Å (40.8 eV) for two major reasons:

(1) To provide more complete tests for various theories of unimolecular decay and

(2) To map out in more complete detail the interaction of radiation with gaseous matter. The successively higher degrees of sophistication can be outlined as

- (a) Measurement of total absorption cross section as a function of incident-photon energy,
- (b) Determination of the fraction of that absorption which leads to ionization,
- (c) The partition of ionization among the various allowed ionic states, using photoelectron spectroscopy, and
- (d) The fragmentation behavior of each molecular-ion state formed.

We address our attention here to point (2d). Ideally, to attack this problem we would like to have a source of continuum radiation which is monochromatized, and perform a photoion-photoelectron coincidence experiment. For the present, we have found an interim solution—a hollow cathode lamp that generates a number of lines between 16.7 and 40.8 eV is our light source, and ordinary mass-spectrometric analysis provides some of the information that would be forthcoming from coincidence experiments.

The energies of the lines used in this research, and their origins, are given in Table VIII.

The apparatus, in addition to the hollow-cathode lamp, consists of a normal-incidence vacuum-ultraviolet monochromator and a magnetic mass spectrometer. Kinetic-energy discrimination exists, especially for ions with kinetic energy >1 eV. Hence, the results presented below must be interpreted as lower limits for fragment intensity with

suprathermal kinetic energy. However, the examples we have chosen (H_2O and CO_2) can be shown to produce fragments with very little excess kinetic energy, and the results are felt to be significant and useful.

TABLE VIII. Energies of lines available, and their origins.

λ, Å	E, eV	Origin
743.718	16.67	Ne
735.895	16.85	
584.334	21.22	He
537.0296	23.09	He
488—491	25.3	Ne^{++}, several lines
460.725	26.95	Ne^{+}
445—447	27.8	Ne^{+}, several lines
405.852	30.6	Ne^{+}
407.136		
379.308	32.71	Ne^{++}
303.781	40.81	He^{+}
303.786		

a. Photodissociative Ionization of CO_2

In Fig. 48 is shown the photoelectron spectrum of CO_2 produced with 584 Å incident radiation. This figure indicates the states of the molecular ion (CO_2^{+}) formed by 21.2-eV photons and their approximate relative abundance. We know from thermochemical considerations that the X, A, and B states cannot dissociate, and hence will be observed in mass-spectrometric studies as CO_2^{+}. However, the C state and all energetically higher states can dissociate, and our goal is to find the preferred channels and their relative abundance. Eland[1]

[1] J. H. D. Eland, Int. J. Mass Spectry. Ion Phys. 9, 397 (1972).

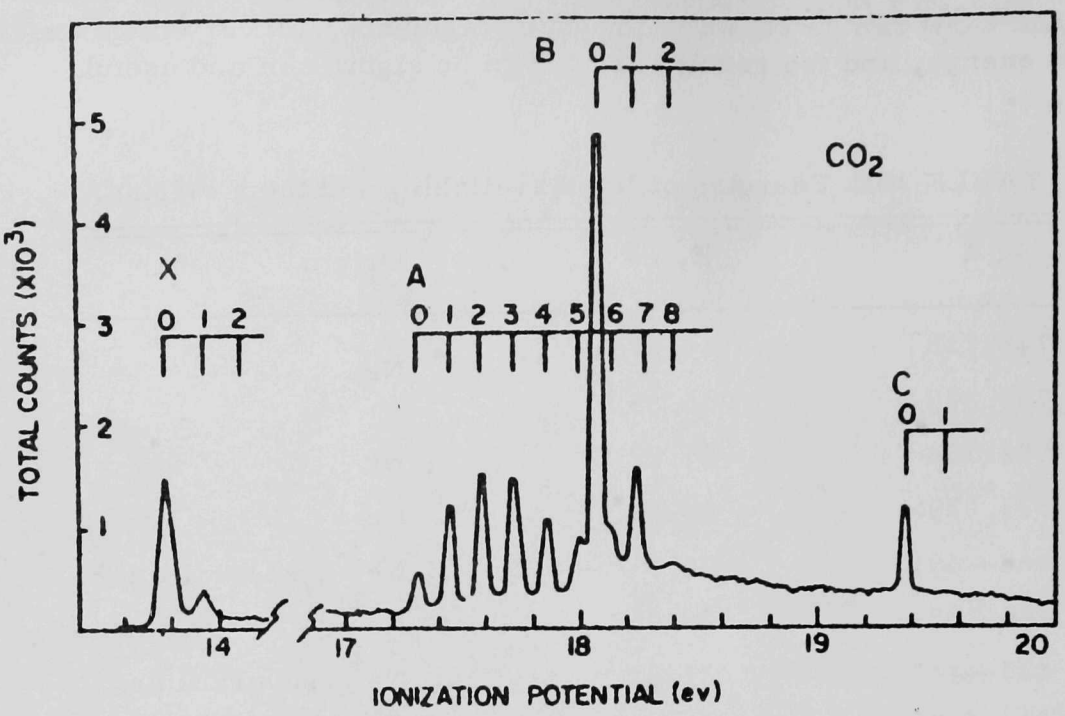

Fig. 48. The 21.2-eV photoelectron spectrum of CO_2. [From J. A. R. Samson, J. L. Gardner, and J. E. Mentall, J. Geophys. Res. 77, 5560 (1972), copyrighted by American Geophysical Union.]

has determined the branching ratio of the C state into O^+ + CO and CO^+ + O, using photoion-photoelectron coincidence measurements.

Some of the relevant higher states can be seen in the 1253.6-eV x-ray photoelectron spectrum of CO_2 (Fig. 49). In particular, there is a rather broad band between 30—40 eV which has been identified with Σ_g and Σ_u states formed by the ejection of electrons from 2s-like molecular orbitals on C and O, respectively. In Table IX, we list our observed relative ion intensities in the CO_2 mass spectrum as the incident photon energy is increased between 16.7 and 40.8 eV. In agreement with Eland,[1] Fryar and Browning,[2] and others,[3] we note that fragmentation does not occur at 16.76 eV, but at 21.2 eV the O^+ + CO and CO^+ + O channels are both open and competitive. The $C^+ + O_2$ channel becomes

[2] J. Fryar and R. Browning, Planet. Space Sci. 21, 709 (1972).

[3] K. E. McCulloh, J. Chem. Phys. 59, 4250 (1973).

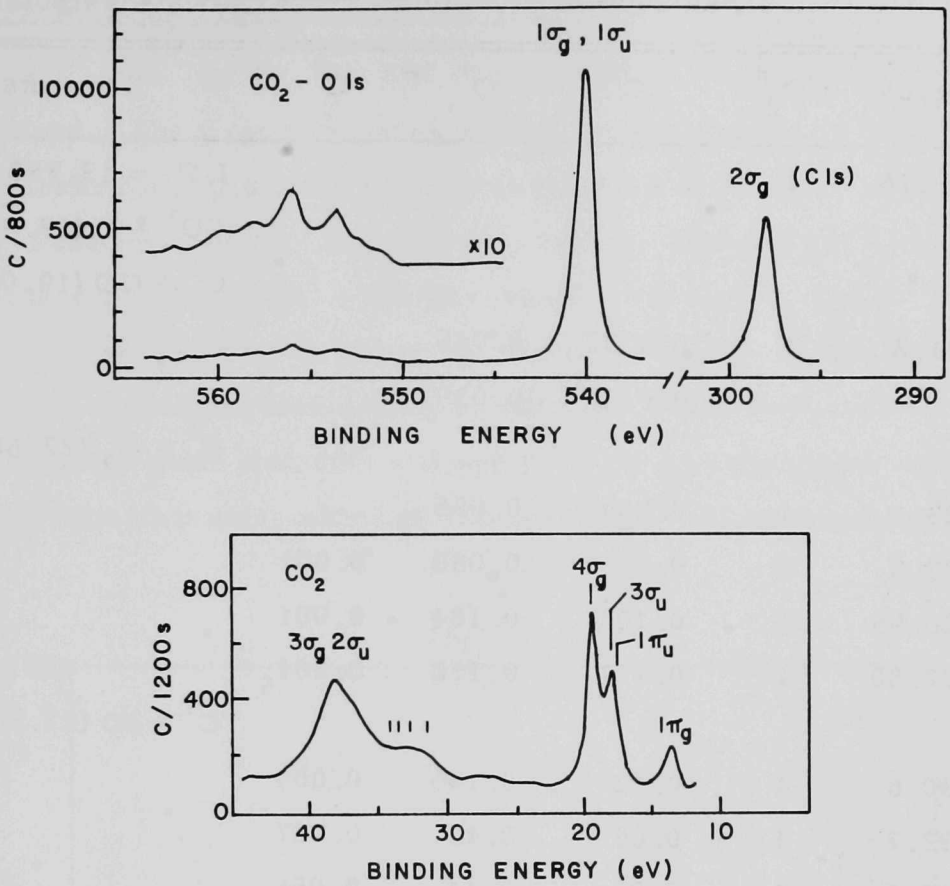

Fig. 49. Composite of the 1253.6-eV photoelectron spectrum of CO_2. [From C. J. Allan, U. Gelius, D. A. Allison, G. Johansson, H. Siegbahn, and K. Siegbahn, J. Electron Spectrosc. 1, 131 (1972) and K. Siegbahn et al., "ESCA Applied to Free Molecules" (North-Holland, Amsterdam, 1969), p. 13.]

accessible at 22.685 eV, but C^+ does not start to become significant until 25.3 eV or higher. At 27.8 eV the C^+ +2O channel opens, and a significant increase in the C^+ intensity occurs at 30.6 eV. It will be recalled that Fig. 49 indicates the onset of the broad band at ~30 eV. The C^+ signal continues to grow, relative to the other ionization modes, between 30.6—40.8 eV, and at 40.8 eV it is almost as intense as O^+ and CO^+. The decomposition of these higher molecular-ion states into C^+ + 2O could give rise to significant excess kinetic energy (which is not true of the C state) and hence the measured C^+ intensity must be regarded as a lower limit. It seems clear from Table IX and Fig. 49

TABLE IX. Fragmentation ratios and energetics for CO_2.

λ, Å	hν, eV	CO_2^+	CO^+	O^+	C^+	Remarks
740	16.76	1	. . .	. . .	. . .	I.P. = 13.788 eV
						CO^+ + O (19.466 eV)
						O^+ + CO (19.067 eV)
584	21.2	1	0.025	0.045	. . .	
			(0.018)[a]	(0.039)[a]		
						C^+ + O_2 (22.685)
537	23.1	1	0.039	0.055	. . .	
490	25.3	1	0.075	0.088	0.001	
460	26.95	1	0.105	0.104	0.001	
446	27.80	1	0.117	0.112	0.001_5	
						C^+ + 2O (27.80 eV)
405	30.6	1	0.123	0.146	0.009	
379	32.7	1	0.09	0.13	0.027	
304	40.8	1	0.08	0.14	0.056	
			(0.14)[a]	(0.22)[a]		

[a]Reference 2.

that the CO_2^+ ions formed in the broad-banded region between 30—40 eV are decomposing predominantly into C^+ + 2O.

Since we know something about the decomposition ensuing when the very deep (K shell) electrons of CO_2 are ejected, from earlier x-ray mass spectrometric studies,[4] CO_2 is perhaps the first triatomic molecule for which all of the relevant decomposition modes produced by photoionization can be traced.

[4]T. A. Carlson and M. O. Krause, J. Chem. Phys. 56, 3206 (1972).

b. Photodissociative Ionization of H_2O

In Fig. 50, the 584 Å photoelectron spectrum of H_2O is displayed. The first two states of H_2O^+ are incapable of fragmenting, on thermochemical grounds. The first fragmentation appears in the middle of the third state. In principle, one can observe $OH^+ + H$ (threshold = 18.11 eV), $H^+ + OH$ (threshold = 18.72 eV), and $O^+ + H_2$ (threshold = 18.65 eV). In Table X, the results of two other groups of workers, and the present data, all obtained at 21.2 eV, are compared. It seems fairly clear that $OH^+ + H$ and $H^+ + OH$ are the major competitive decomposition channels, although Dibeler et al.[1] do not report any H^+.

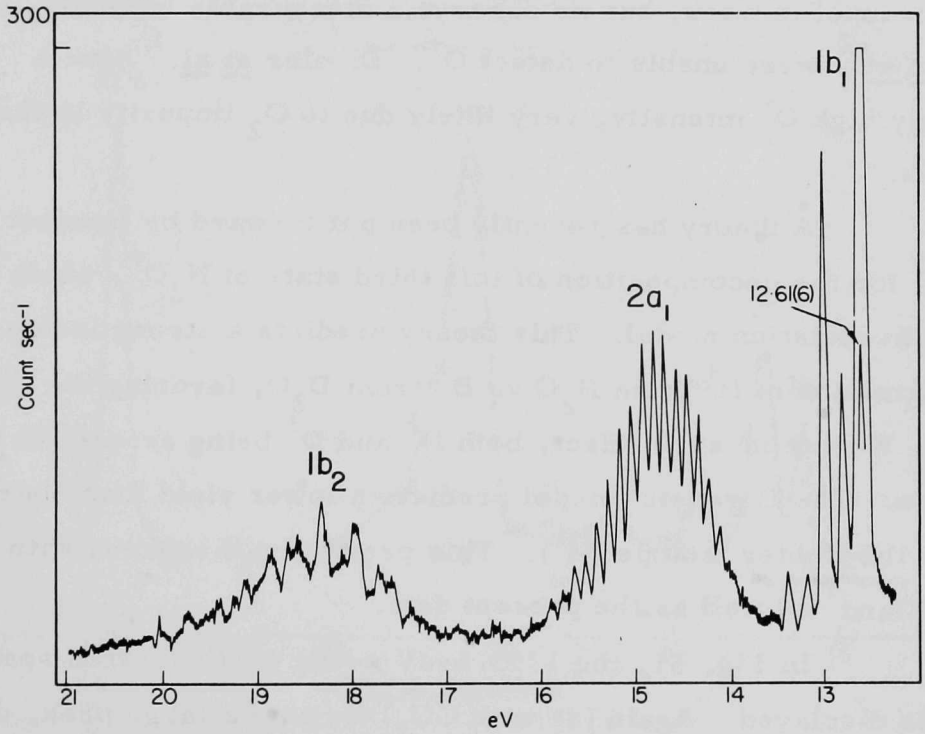

Fig. 50. The 21.2-eV photoelectron spectrum of H_2O. [From D. W. Turner, C. Baker, A. D. Baker, and C. R. Brundle, "Molecular Photoelectron Spectroscopy" (Wiley-Interscience, London, 1970), p. 113.]

[1] V. H. Dibeler, J. A. Walker, and H. M. Rosenstock, J. Res. Natl. Bur. Stand. 70A, 459 (1966).

TABLE X. Relative intensities of mass peaks in photoionization of H_2O at 21.2 eV.

	Dibeler et al.[a]	Cairns et al.[b]	Present
H_2O^+	1	1	1
OH^+	0.4	~0.5	0.4
H^+	Not reported	~0.045	0.07
O^+	0.05	<0.001	0.001

[a]Reference 1.

[b]Reference 2.

The O^+ channel is weak, but we observe a measurable intensity, whereas Cairns et al.[2] were unable to detect O^+. Dibeler et al.[1] have a spuriously high O^+ intensity, very likely due to O_2 impurity in their apparatus.

A theory has recently been put forward by Lorquet and Lorquet[3] for the decomposition of this third state of H_2O^+, which is based on a predissociation model. This theory predicts a strong isotope effect in the formation of H^+ from H_2O vs D^+ from D_2O, favoring the lighter isotope. We see no such effect, both H^+ and D^+ being around 5% of total ionization. The Lorquets' model predicts a lower yield than observed even for the lighter isotope (H^+). This prediction disagrees with recent data of Eland[4] as well as the present data.

In Fig. 51, the 1253.6-eV x-ray photoelectron spectrum of H_2O is displayed. Again (as with CO_2) we note a large peak, designated $1a_1$, in the 30—40-eV region. In Table XI we list our relative

[2]R. B. Cairns, H. Harrison, and R. I. Schoen, J. Chem. Phys. 55, 4886 (1971).

[3]A. J. Lorquet and J. C. Lorquet, Chem. Phys. 4, 353 (1974).

[4]J. H. D. Eland, Adv. in Mass Spectry. 6, 917 (1974); J. H. D. Eland, "The Predissociations of Water Ions," Submitted to Chem. Phys.

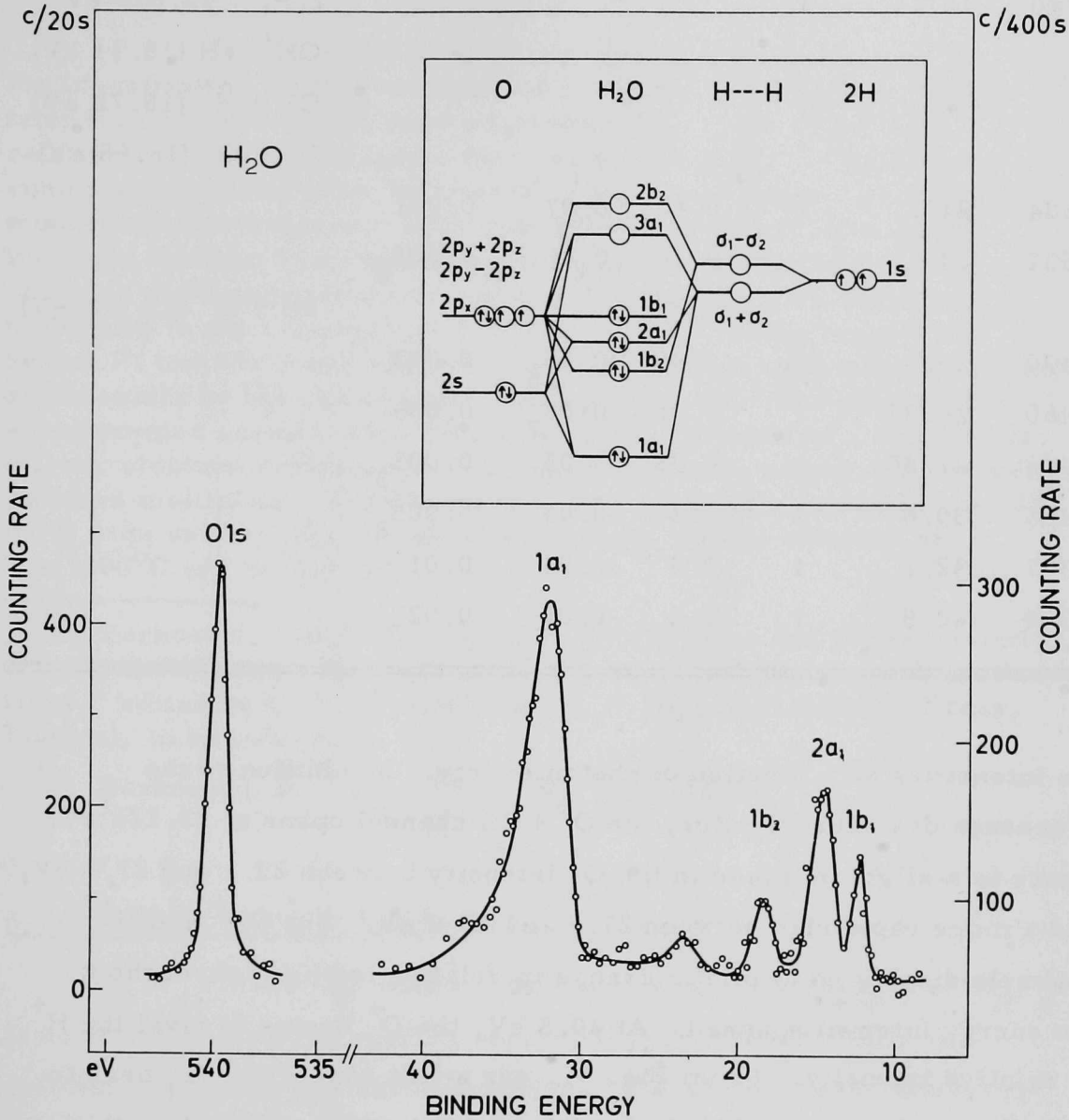

Fig. 51. The 1253.6-eV photoelectron spectrum of H_2O. [From K. Siegbahn et al., "ESCA Applied to Free Molecules" (North-Holland, Amsterdam, 1969), p. 83.]

TABLE XI. Fragmentation ratios and energetics for H_2O.

λ, Å	hν, eV	H_2O^+	OH^+	H^+	O^+	Remarks
740	16.76	1	. . .	. . .	. . .	I.P. = 12.616 eV
						OH^+ + H (18.11 eV)
						OH + H^+ (18.72 eV)
						H_2 + O^+ (18.65 eV)
584	21.2	1	0.4	0.07	0.001	
537	23.1	1	0.35	0.06	0.001_6	
						2H + O^+ (23.126 eV)
490	25.3	1	0.36	0.05_5	0.003	
460	26.95	1	0.37	0.05_7	0.003	
446	27.80	1	0.35	0.05	0.003_3	
405	30.6	1	0.3	0.05	0.005_8	
377	32.7	1	0.3	0.04	0.01	
304	40.8	1	0.3	0.07	0.02_7	

ion intensities as a function of photon energy. In addition to the processes described earlier, the O^+ + 2H channel opens at 23.126 eV. There is a slight increase in the O^+ intensity between 23.1 and 27.8 eV, and a more rapid rise between 27.8 and 40.8 eV. The OH^+ and H^+ channels display no dramatic change in relative intensity throughout the energy interval spanned. At 40.8 eV, the O^+ begins to rival the H^+ in relative intensity. From Fig. 51, one might expect the $1a_1$ peak to contribute a larger fraction to the total ion intensity. However, this is misleading because the 1253.6-eV photoelectron spectrum strongly favors the 1s-like and 2s-like orbitals, the latter being $1a_1$. A 40.8-eV photoelectron spectrum would be the appropriate one for comparison but has heretofore not been reported in satisfactory form. In summary, it seems clear from the data of Table XI that the $1a_1$ state of H_2O^+ decomposes primarily into O^+ + 2H.

2. PHOTOELECTRON SPECTROSCOPY OF HIGH-TEMPERATURE VAPORS

D. G. Streets and J. Berkowitz

Photoelectron spectroscopy is an extremely useful tool for investigating binding energies of electrons in molecules. High-temperature techniques[1] have enabled studies of the vapor from relatively involatile inorganic materials to be made. Heavy-metal compounds can therefore be ionized in the vapor phase by ultraviolet monochromatic sources. This provides much information on the interplay between ionic and covalent bonding and also on the magnitudes of ligand-field and spin-orbit splitting phenomena. We are studying molecules in the temperature range $T < 1000^{\circ}C$ using resistively heated Pt and Mo ovens and are currently attempting to raise this limit significantly by the use of laser-heating methods. The photoelectron spectrometer used for this work essentially consists of a cylindrical mirror electron analyzer[2] with a helium resonance lamp and channeltron electron multiplier. Significant results have been obtained below $1000^{\circ}C$ for a wide variety of molecules, and recent results obtained at $T \sim 1500^{\circ}C$ are encouraging.

---

[1] J. Berkowitz, "High-Temperature UPS Studies and Other Variations," chapter in "Electron Spectroscopy: Theory, Techniques, and Applications," edited by C. R. Brundle and A. D. Baker (Academic Press, London), to be published.

[2] J. Berkowitz, J. Chem. Phys. 56, 2766 (1972).

a. Thallium Fluoride Dimer

Previous work[1,2] on elucidating the structure of Tl_2F_2 from its photoelectron spectra concluded that a linear dimer was favored. A recent gas chromatograph of the sample used, however, showed a high impurity concentration of Tl_2CO_3 which was responsible for spurious peaks in the spectrum and led to an erroneous analysis. The experiment has been repeated under higher resolution and, by

---

[1] J. Berkowitz, J. L. Dehmer, and L. C. Cusachs, Argonne National Laboratory Physics Division Annual Review ANL-8035 (1972-73), p. 158.

[2] J. L. Dehmer, J. Berkowitz, and L. C. Cusachs, J. Chem. Phys. 58, 5681 (1973).

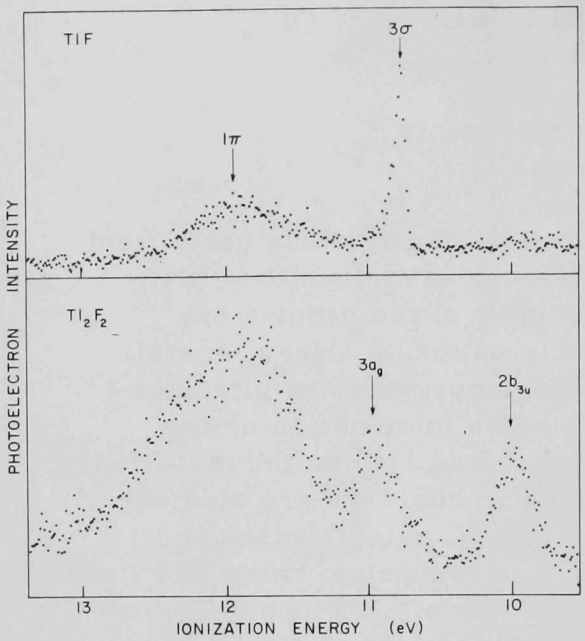

Fig. 52. The 584 Å photoelectron spectra of TlF and Tl_2F_2.

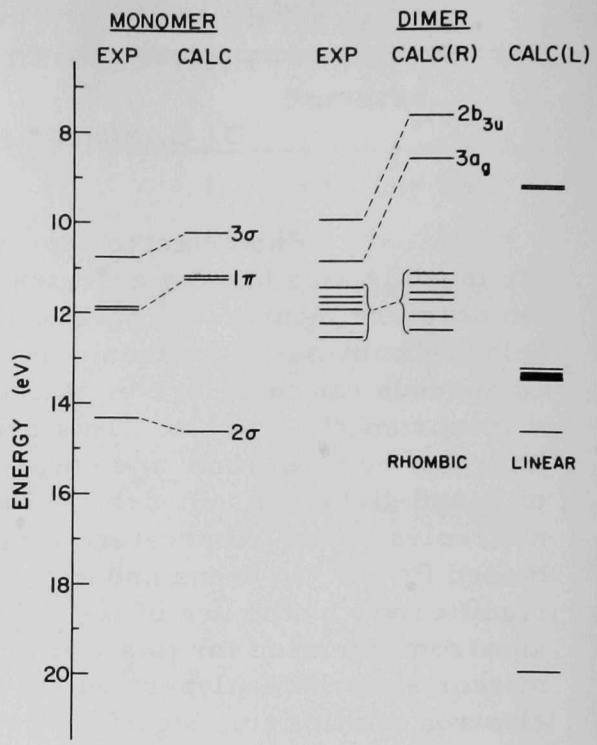

Fig. 53. Experimental and calculated energy levels of TlF and Tl_2F_2.

using different oven techniques, spectra comprising different monomer/dimer ratios were obtained. Separated spectra from monomer and dimer (Fig. 52) were then obtainable by computer subtraction of the data. Comparison of these experimental energy levels with the extended Hückel molecular-orbital calculations of Cusachs[2] showed that the rhombic dimer structure was preferred (Fig. 53).

b. Group VI Homonuclear Diatomic Molecules

The molecules O_2, S_2, Se_2, and Te_2 possess very interesting electronic structures in terms of multiplet and spin-orbit phenomena, and their photoelectron spectra have been studied. The O_2 spectrum is well known and the S_2 spectrum is easy to obtain, from HgS, and to interpret. The Te_2 spectrum has been obtained by

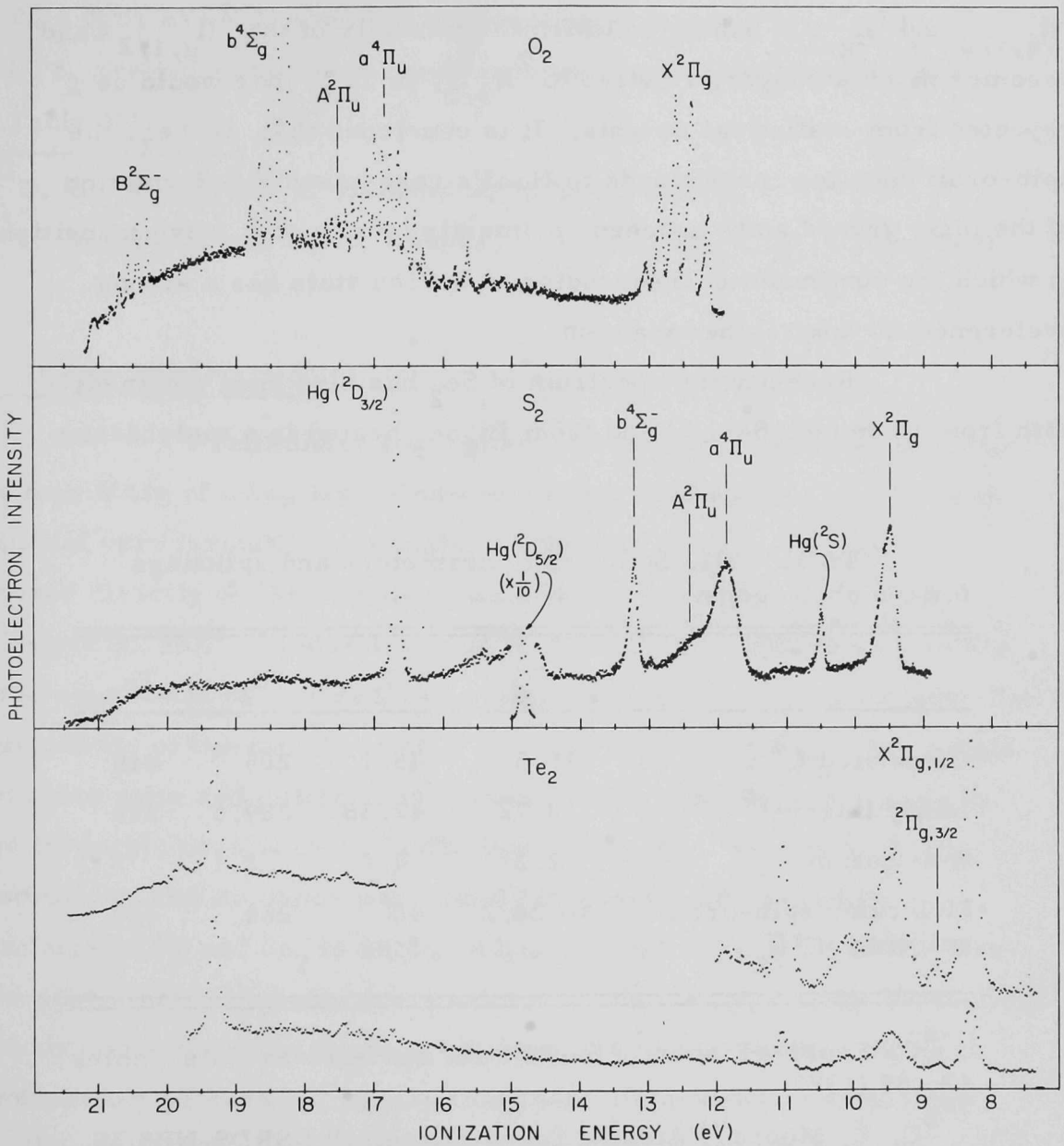

Fig. 54. The 584 Å photoelectron spectra of O_2, S_2, and Te_2.

vaporizing elemental tellurium in a Pt oven. The interpretation[1] of the spectra from these three compounds (Fig. 54) shows characteristic similarities with predictable trends dependent upon the atomic weight of the chalcogen. Very interesting splitting was observed for the $^2\Pi_{g,1/2}$ and $^2\Pi_{g,3/2}$ bands, in which the intensity of the $^2\Pi_{g,1/2}$ band becomes much stronger, relative to $^2\Pi_{3/2}$, in Te_2, than would be expected from statistical weights. It is concluded that, in Te_2, the spin-orbit coupling corresponds to Hund's case-c and that formation of the ionic ground state proceeds primarily by way of a $\Delta\Omega=0$ transition in which the continuum corresponding to the ion state has a strong preference for $tp\sigma$, rather than $tp\pi$.

Recently the spectrum of Se_2 has also been obtained, both from CdSe (see Sec. c) and from Bi_2Se_3 heated in a molybdenum

TABLE XII. Spin-orbit parameters and splittings for the chalcogens.

	O_2	S_2	Se_2	Te_2
Calculated ζ[a]	18.3	45.1	205	419
Landé interval[b]	18.72	47.36	209.5	389
% deviation	2.2	4.8	2.1	7.7
Molecular spin-orbit splitting of $^2\Pi_g$	23—24.2[c]	40	260	470

[a] C. Froese-Fisher, Atomic Data and Nuclear Data Tables 12, 89 (1973).

[b] C. E. Moore, "Atomic Energy Levels," NSRDS-NBS 35, Reprint of National Bur. Std. (U.S.) Circ. 467 (1971).

[c] O. Edqvist, E. Lindholm, L. E. Selin, and L. Åsbrink, Physica Scripta 1, 25 (1970).

[1] J. Berkowitz, J. Chem. Phys. 62, 4074 (1975).

oven.[2] The first ionization potential for Se_2 obtained from these experiments, 8.88 eV (±0.01) is in excellent agreement with the value obtained by photoionization.[3] The experiment with Bi_2Se_3 also produced quantities of Se_5, enabling its ionization potential to be determined (8.04 ± 0.01 eV). The spin-orbit coupling parameter for O_2, S_2, Se_2, and Te_2 are compared with Landé intervals and calculated ζ values in Table XII.

---

[2] D. G. Streets and J. Berkowitz, to be published.

[3] J. Berkowitz and W. A. Chupka, J. Chem. Phys. 50, 4245 (1969).

c. Laser Vaporization

Preliminary experiments have been undertaken to study the feasibility of using laser-induced heating methods for producing the vapor of very involatile materials. A 50 watt CO_2 laser beam is focused directly on the sample contained in a boron nitride sample holder (Fig. 55). Temperatures up to 2000°C have been measured for some compounds but the success of this technique is dependent upon the absorptivity of the sample at 10.6 μ. This is low in general for metals and some salts and difficulty is encountered in obtaining good spectra. One favorable case is that of CdSe (mp > 1350°C). This has a high absorptivity and its vapor was readily obtained. The resulting spectrum of Cd and Se_2 is shown in Fig. 56 and is the highest temperature photoelectron spectrum yet obtained. The Se_2 spectrum is identical with that obtained from Bi_2Se_3, although at lower resolution owing to condensation problems. Experiments with other substances such as Bi, UO_2, and MgF_2 have produced melting or vaporization but no spectra have been obtained from them to date. Various technical improvements, including better focusing, Q switching, and sample mixing, are under way to improve this promising new technique.

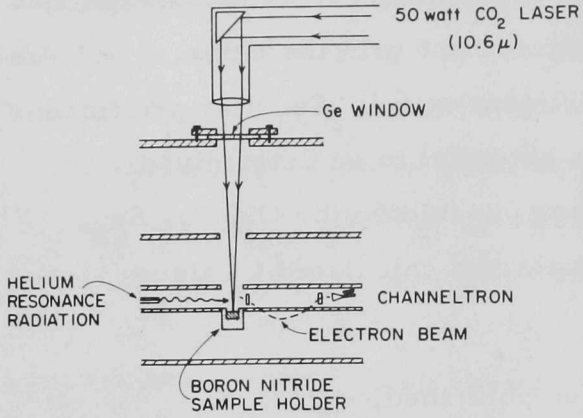

Fig. 55. Experimental apparatus for laser-induced vaporization.

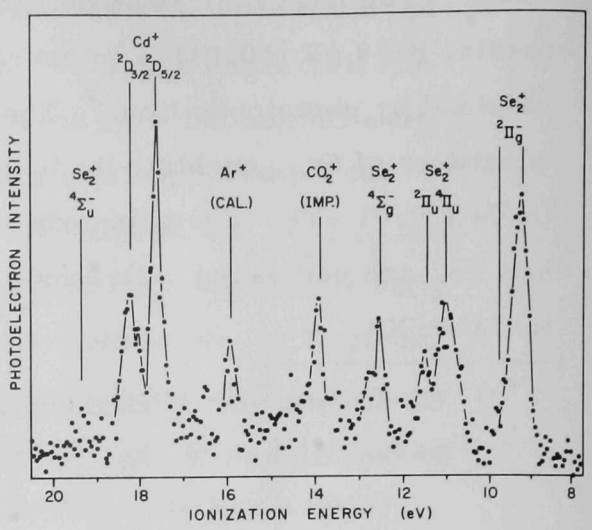

Fig. 56. The 584 Å photoelectron spectrum of CdSe.

3. HIGH-RESOLUTION PHOTOIONIZATION STUDIES

a. High-Resolution Study of Photoionization in H_2, HD, and D_2

W. A. Chupka, P. M. Dehmer, and W. T. Jivery

Relative absorption and photoionization efficiency curves were measured for ordinary H_2 and D_2, para-H_2, and HD at 78°K from the ionization threshold to approximately 700 Å, with a wavelength resolution of 0.017 Å (FWHM). The apparatus used consists of a 3-meter near-normal incidence vacuum monochromator with a quadrupole mass filter for mass analysis of photoions. Differential pumping of the variable temperature photoionization chamber permits operation with sample gas pressures up to the onset of viscous flow out of the chamber. Design improvements in the gas discharge lamp and the lamp power supply resulted in an intensity increase (at comparable resolution) of about two orders of magnitude over that of earlier work.

The absorption spectrum of para-H_2 at 78°K from the v=0 ionization threshold to the v=3 convergence limit of H_2^+ was extensively

analyzed by Herzberg and Jungen.[1] The present data supplement their photographic data by providing accurate relative intensities and peak shapes in ionization and in absorption. Three short sections of the relative photoionization efficiency curve for para-H_2 in the regions of the v=1, v=2, and v=3 thresholds are shown in Fig. 57. The spectra in these regions consist predominantly of strongly autoionized Rydberg series converging to the N=0 and N=2 states of the H_2^+ ion, with the members of the latter series appearing as "window resonances" in the N=0 continuum. The assignments shown are those of Herzberg and Jungen.

A large number of peaks of the entire spectrum have widths greater than the resolution width, and thus accurate autoionization lifetimes can be determined. The widths as well as the absolute value and sign of the Fano q parameter of those lines which are reliably identified are determined by the relative σ and π character of the mutually perturbed states, as is implied by the analysis of Herzberg and Jungen. The selection rule ($\Delta v = -1$) for vibrational autoionization is seen to play a strong role in determining autoionization lifetimes. The apparent exceptions to this selection rule are exemplified by the $7p\pi$ v=2 peak at 790.15 Å. In this case the anomalously large width of the peak is a result of the strong interaction (characterized by $\Delta v = 1$) with the dense manifold of members of a Rydberg series which can autoionize according to the $\Delta v=-1$ selection rule. Thus, such cases might be described as "accidental preionization" by analogy with the phenomenon of accidental predissociation.

---

[1] G. Herzberg and Ch. Jungen, J. Mol. Spectrosc. 41, 425 (1972).

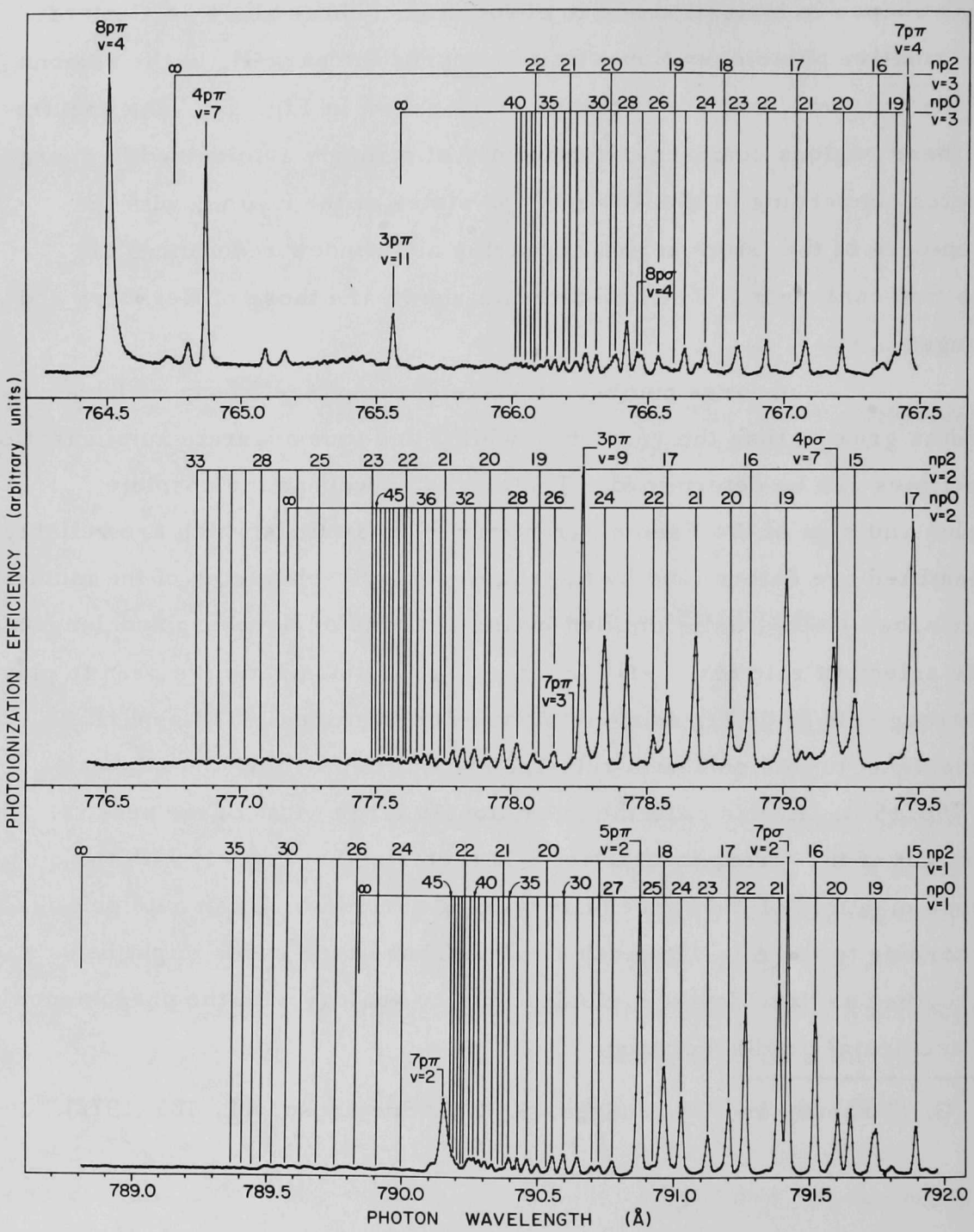

Fig. 57. Relative photoionization efficiency curves for para-H_2 (78°K) in the region of the v=1, v=2, and v=3 convergence limits of H_2^+.

b. High-Resolution Photoionization Study of Ion-Pair Formation in H_2, HD, and D_2

W. A. Chupka, P. M. Dehmer, and W. T. Jivery

The new photoionization mass spectrometer which is significantly superior to previous instruments in both wavelength resolution and ion intensity has been used in the study of photon-induced ion-pair formation at 78°K in para-H_2, ordinary H_2 and D_2 (the ortho-para equilibrium mixtures), and HD in the wavelength region from 718 Å to 700 Å at a wavelength resolution (FWHM) of 0.035 Å for para-H_2, 0.07 Å for ordinary H_2 and D_2, and 0.15 Å for HD. The photoionization efficiency curves for the parent ion H_2^+ and the fragment H^- ion from para-H_2 are shown in Fig. 58. The top two curves were taken at a wavelength resolution of 0.07 Å and the bottom curve was taken at a resolution of 0.035 Å. The threshold region taken at the higher resolution is shown in Fig. 59.

The threshold for formation of ion pairs from para-H_2 occurs at 715.753 ± 0.008 Å (17.3223 ± 0.0002 eV) and this value, together with the accurately known values of the dissociation energy of H_2 and the ionization potential of atomic hydrogen, yields a value of the electron affinity of the hydrogen atom of 0.754_2 ± 0.001 eV in excellent agreement with the theoretical value of 0.75421 eV calculated by Pekeris.[1] (The observed thresholds for ion-pair formation in D_2 and HD are also in excellent agreement with the calculated positions.) For para-H_2 the region within 0.5 Å of the threshold (Fig. 59) has a continuum-like appearance and contains window resonances which are interpreted as predissociating members of a Rydberg series converging to H_2^+ (v = 9, N = 2). The continuum results from closely spaced predissociating Rydberg states converging to H_2^+ (v = 9, N = 0) which were not resolved in the present experiment. A number of other tentative Rydberg state assignments were made for para-H_2 based on the results of

[1] C. L. Pekeris, Phys. Rev. 126, 1470 (1962).

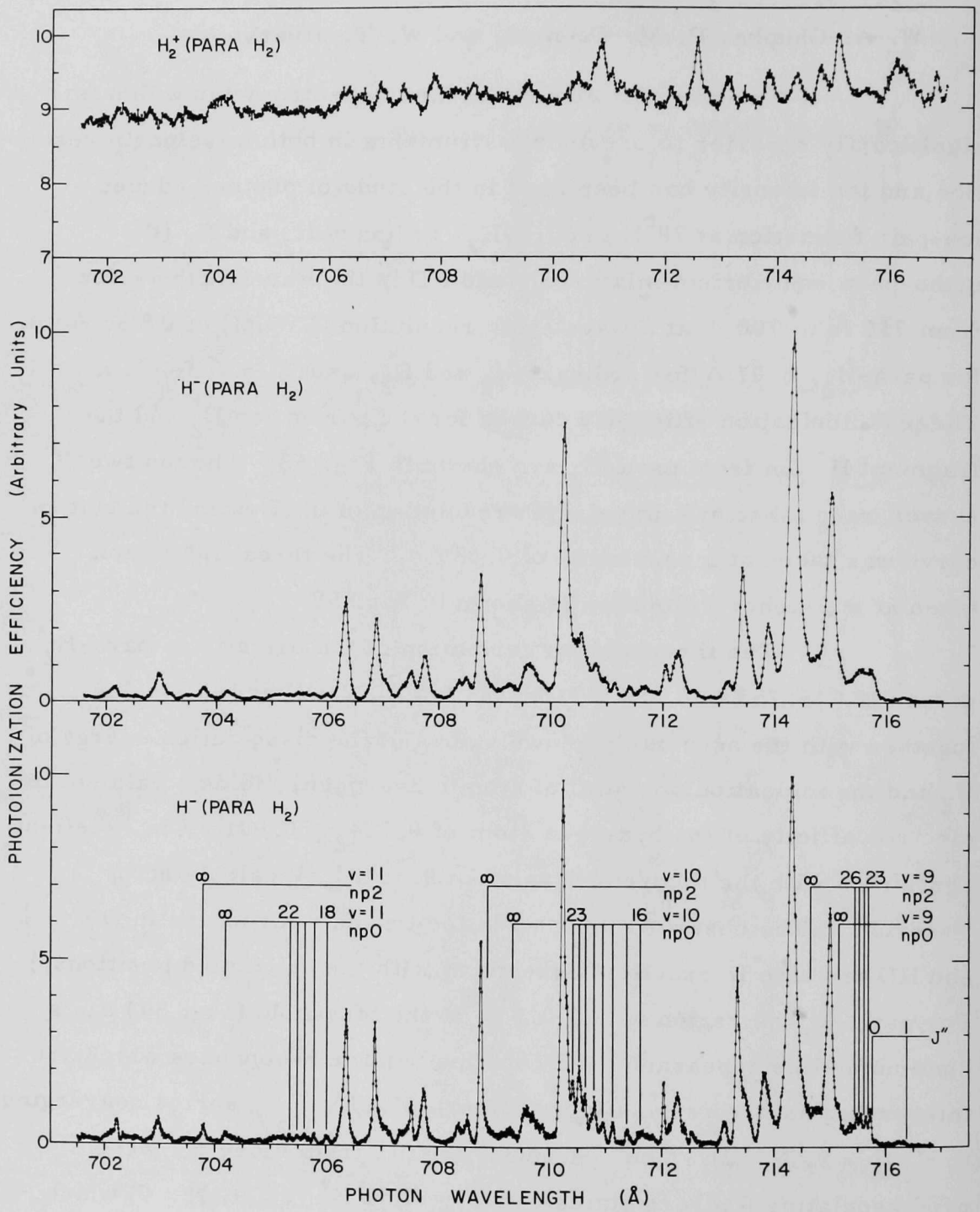

Fig. 58. Photoionization efficiency curves for H_2^+ and H^- from para-H_2 taken at 78°K and a wavelength resolution of 0.07 Å (top two curves) and 0.035 Å (bottom curve).

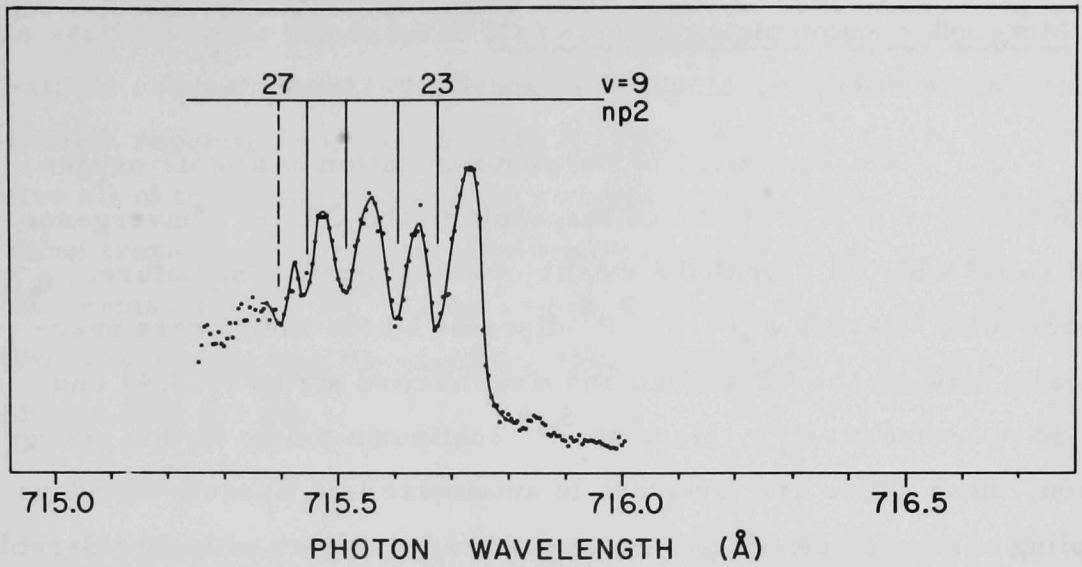

Fig. 59. Threshold region of the photoionization efficiency curve for H^- from para-H_2 taken at 78°K and at a wavelength resolution of 0.035 Å. The absolute counting rate on the first small peak (at 715.73 Å) was approximately 3.5 counts/sec.

an analysis using multichannel quantum defect theory.[2] Some of these assignments are shown in Fig. 58. The prominent peaks in the PIE curve are generally low n ($n \cong 6-12$) Rydberg members of series converging to high vibrational states of H_2^+ ($v \cong 10-16$). No Rydberg state identifications were attempted for the other systems due to the greatly increased complexity of their spectra. For HD which can dissociate to either $H^+ + D^-$ or $H^- + D^+$ the wavelength dependence of the H^-/D^- ratio appears to decrease with decreasing wavelength; however, this is at least in part due to discrimination by the detection system against the more energetic H^- ions. Some conclusions regarding the mechanism for predissociation in H_2 are deduced, particularly the importance of the $4f\sigma\ ^1\Sigma_u^+$ state.

---

[2] (a) U. Fano, Phys. Rev. 124, 1866 (1961); (b) U. Fano, Phys. Rev. A 2, 353 (1970); (c) K. T. Lu and U. Fano, Phys. Rev. A 2, 81 (1970).

c. High-Resolution Study of Photoionization and Photoemission from Metastable Autoionizing States of OI

P. M. Dehmer, W. A. Chupka, and W. T. Jivery

A recent study of the photoionization of atomic oxygen in the energy region from the OI threshold to the OII $^2P^0$ convergence limit (~920—650 Å) revealed a wealth of autoionization structure.[1] Of particular interest were the $^3P^0$ discrete states which were energetically between the OII ground and first excited states (910.44 and 731.82 Å, respectively). Since no $^3P^0$ continuum exists in this energy region, these states are forbidden to autoionize in a Russell-Saunders coupling scheme,[2] yet all were observed to autoionize with considerable intensity. In the breakdown of LS coupling, these states may autoionize via interactions with continua of different L and/or S; however, this process is expected to be slower than Russell-Saunders allowed autoionization.

It was found that autoionization intensities from certain excited $^3P^0$ states are nonstatistical, i.e., the observed intensities for components of the multiplets do not correspond to the theoretical absorption intensities predicted by a Russell-Saunders coupling scheme. The autoionization lifetimes of these states are comparable to their emission lifetimes, and it was believed that competition by photon emission was responsible for the nonstatistical autoionization intensities. Measurements of the emission intensities of these multiplets confirmed this hypothesis. It was found that when the autoionization and emission lifetimes are comparable, both decay channels show nonstatistical behavior, and that the branching ratios vary substantially for the different total angular momentum components of the decaying state. These results were tentatively interpreted in terms of preferential autoionization of certain total angular momentum levels.[2]

---

[1] P. M. Dehmer, W. A. Chupka, and J. Berkowitz, J. Chem. Phys. 59, 5777 (1973).

[2] P. M. Dehmer and W. A. Chupka, J. Chem. Phys. 62, 584 (1975).

In order to quantify these results, the photoionization cross sections were remeasured for these metastable autoionizing transitions using the new 3-meter photoionization apparatus. Using wavelength resolutions of up to 0.035 Å (FWHM), we were able to resolve all of the components of the autoionizing multiplets. Lifetimes for those transitions for which autoionization is allowed (i.e., $^3S^0$ or $^3D^0$ terms, but not $^3P^0$ terms) are of the order of 10^{-12} sec and lifetime broadening was observed for these transitions (taken at a resolution of 0.035 Å).

d. Photoionization Study of the Reaction of $O_2^+(a\,^4\Pi_u)$ with O_2

P. M. Dehmer, W. A. Chupka, and W. T. Jivery

The reaction of $O_2^+ + O_2$ to form $O_3^+ + O$ is an example of an ion-molecule reaction which is endothermic for the ground state of the ion, but exothermic for certain excited electronic states. The present high-resolution photoionization study of the production of O_3^+ from the reaction of $O_2^+(a\,^4\Pi_u)$ with O_2 determined that the reaction proceeds primarily through the v' = 5 to 10 vibrational levels of the $O_2^+(a\,^4\Pi_u)$ state. The relative photoionization efficiency curve for the formation of O_3^+ is shown in Fig. 60. The data were taken at a wavelength resolution (FWHM) of 0.14 Å and a temperature of 78°K. The main autoionization structure corresponds to Rydberg series in O_2 converging to the ground and first few excited vibrational levels of the $b\,^4\Sigma_g^-$ state of O_2^+. This structure, which is also prominent in the photoionization spectrum of O_2,[1] is labeled according to the identifications of Yoshino and Tanaka.[2] The calculated thermodynamic threshold for O_3^+ production corresponds to a wavelength of 747.2 ± 1.4 Å, which nearly coincides with the $O_2^+(a\,^4\Pi_u$, v' = 4) convergence limit at 747.25 Å. A very small amount of reaction is observed at this vibrational convergence limit;

---

[1] P. M. Dehmer and W. A. Chupka, J. Chem. Phys. 62, 4525 (1975).

[2] K. Yoshino and Y. Tanaka, J. Chem. Phys. 48, 4859 (1968).

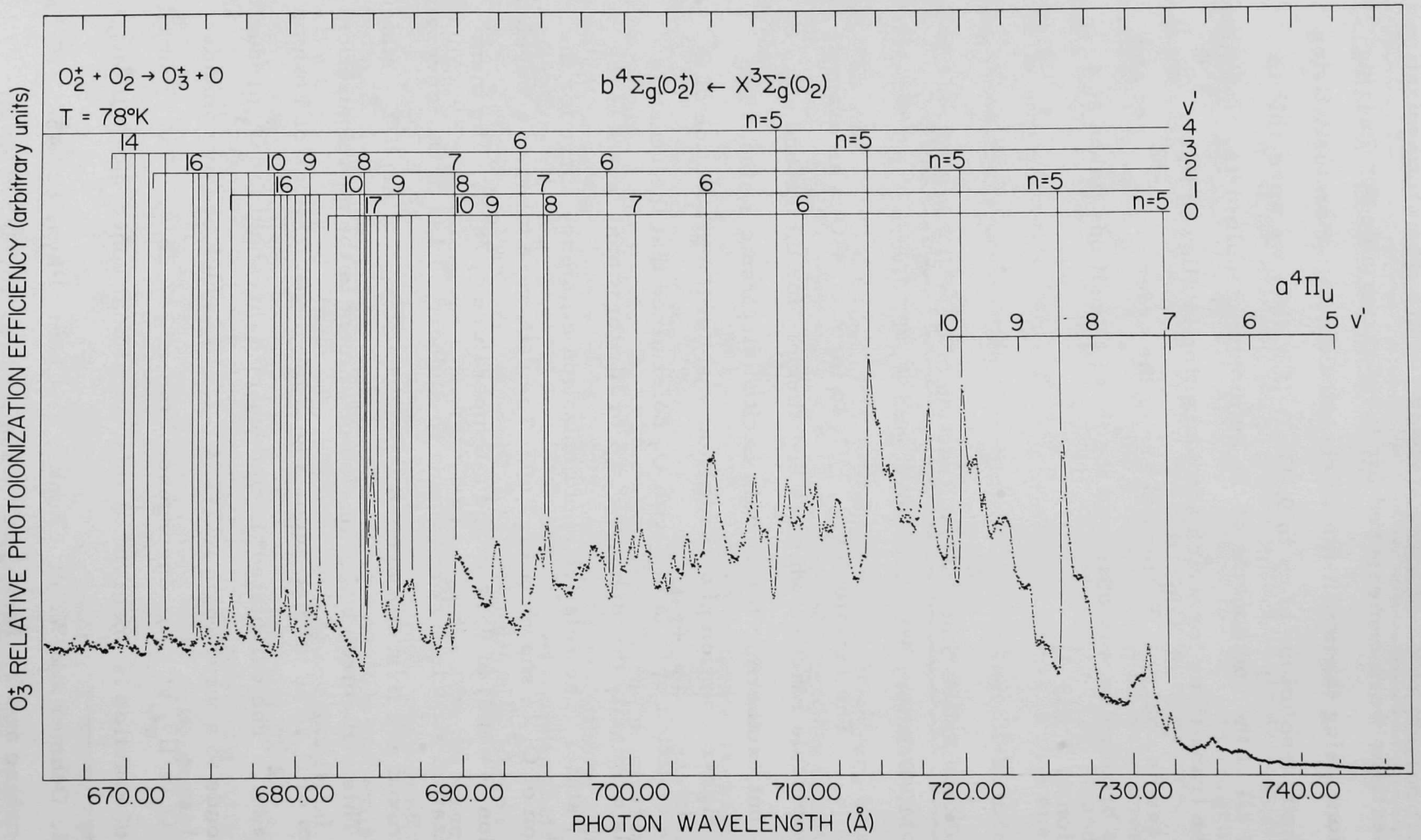

Fig. 60. Relative photoionization efficiency for O_3^+ production. The data were taken at 78°K and at a wavelength resolution (FWHM) of 0.14 Å.

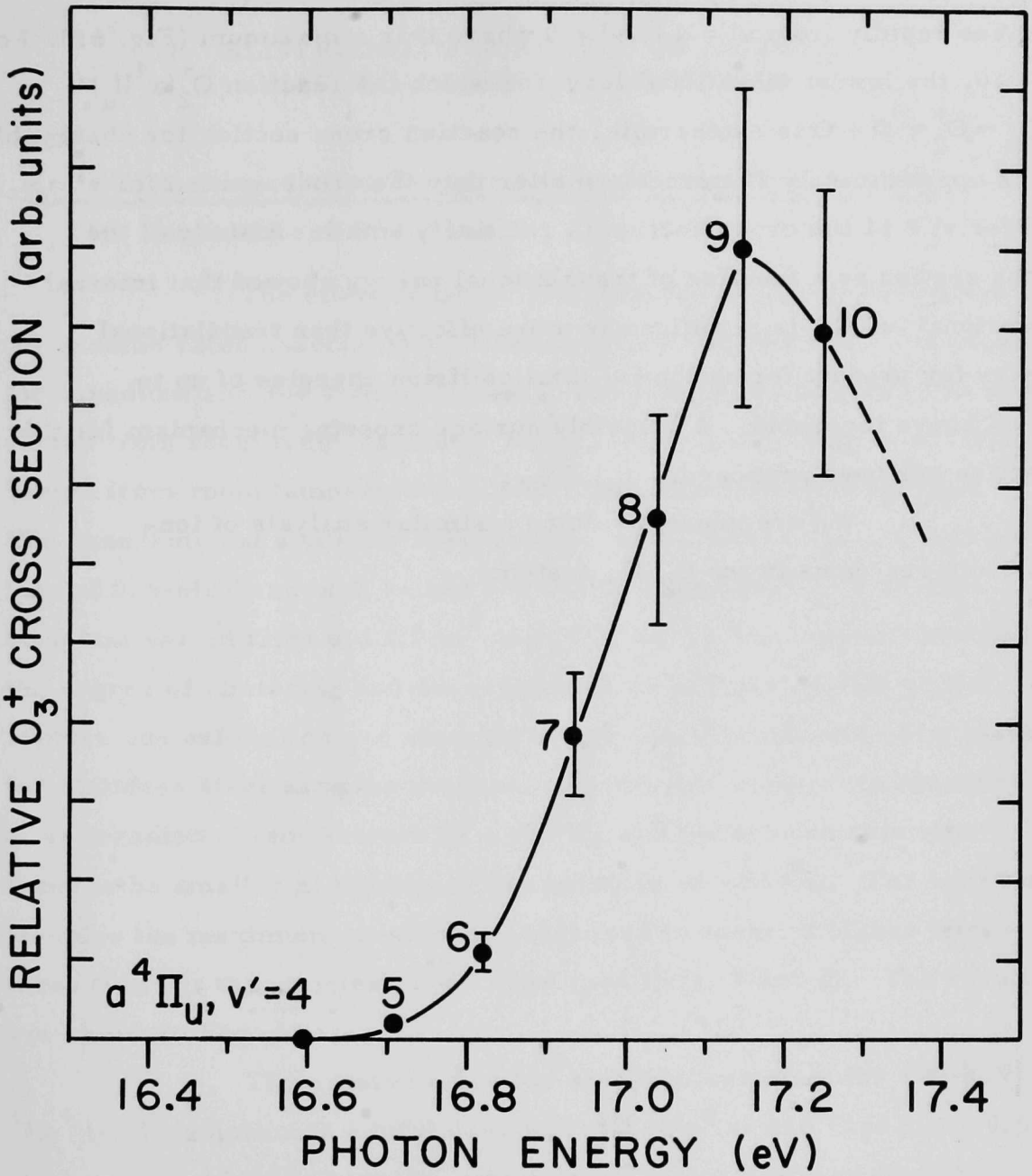

Fig. 61. Relative cross sections for O_3^+ production as a function of the $O_2^+(a^4\Pi_u)$ vibrational level at a thermal translational energy corresponding to 78°K.

however, this is due at least in part to the thermal rotational and translational energy of the reactants.

The relative reaction cross section for O_3^+ formation increases rapidly from v' = 4 to v' = 9 where it is a maximum (Fig. 61). For v' = 10, the lowest vibrational level for which the reaction $O_2^+(a\,^4\Pi_u) + O_2 \rightarrow O_2^+ + O + O$ is exothermic, the reaction cross section for observable O_3^+ is approximately 10 percent smaller than the cross section for v' = 9, and for v' $\geqslant$ 11 the cross section is relatively small. A study of the cross section as a function of translational energy showed that internal vibrational energy is significantly more effective than translational energy for product formation for total collision energies of up to $\sim$1 eV above threshold. A plausible surface crossing mechanism for the reaction has been proposed.

We are presently doing a similar analysis of ion-molecule reactions in the O_2-N_2 system.

B. INTERACTIONS OF ENERGETIC PARTICLES AND PHOTONS WITH SURFACES OF SOLIDS

1. BLISTERING OF SURFACES OF SOLIDS BY CHARGED-PARTICLE IRRADIATION

a. Effect of Irradiation Temperature on Erosion by Blistering

M. Kaminsky and S. K. Das

The effect of target temperature on blister formation and the erosion rates associated with helium blistering has been investigated for vanadium and 304 stainless steel. The irradiation temperature was varied from room temperature to 900°C for vanadium targets and was varied from room temperature to 550°C for stainless steel targets. The vanadium and stainless steel targets were bombarded with helium ions of 0.5-MeV and of 0.1- and 0.5-MeV, respectively. The total dose was varied from 0.1 C/cm^2 to 1.0 C/cm^2. The results show that the degree of blistering and the erosion rates associated with blister rupture and exfoliation are strongly temperature dependent. For example, for stainless steel samples the maximum erosion rates were observed at an irradiation temperature of ~450°C, and the erosion rate was found to be smaller at the higher temperature of ~550°C. For vanadium samples the maximum erosion was observed to occur at higher temperatures than for the stainless steel case (see Refs. 1 and 2). The results are shown in Fig. 62.

The erosion rates for 304 stainless steel for 100-keV $^4He^+$ ion irradiation to a total dose of 0.5 C/cm^2 at 450°C is 3.0 ± 0.5 atoms per incident helium ion, which is ~300 times higher than the erosion rate due to sputtering under similar conditions. Such a high

---

[1] M. Kaminsky and S. K. Das, Nuclear Technology 22, 373-378 (1974).

[2] S. K. Das and M. Kaminsky, Journal of Nuclear Materials 53, 115-126 (1974).

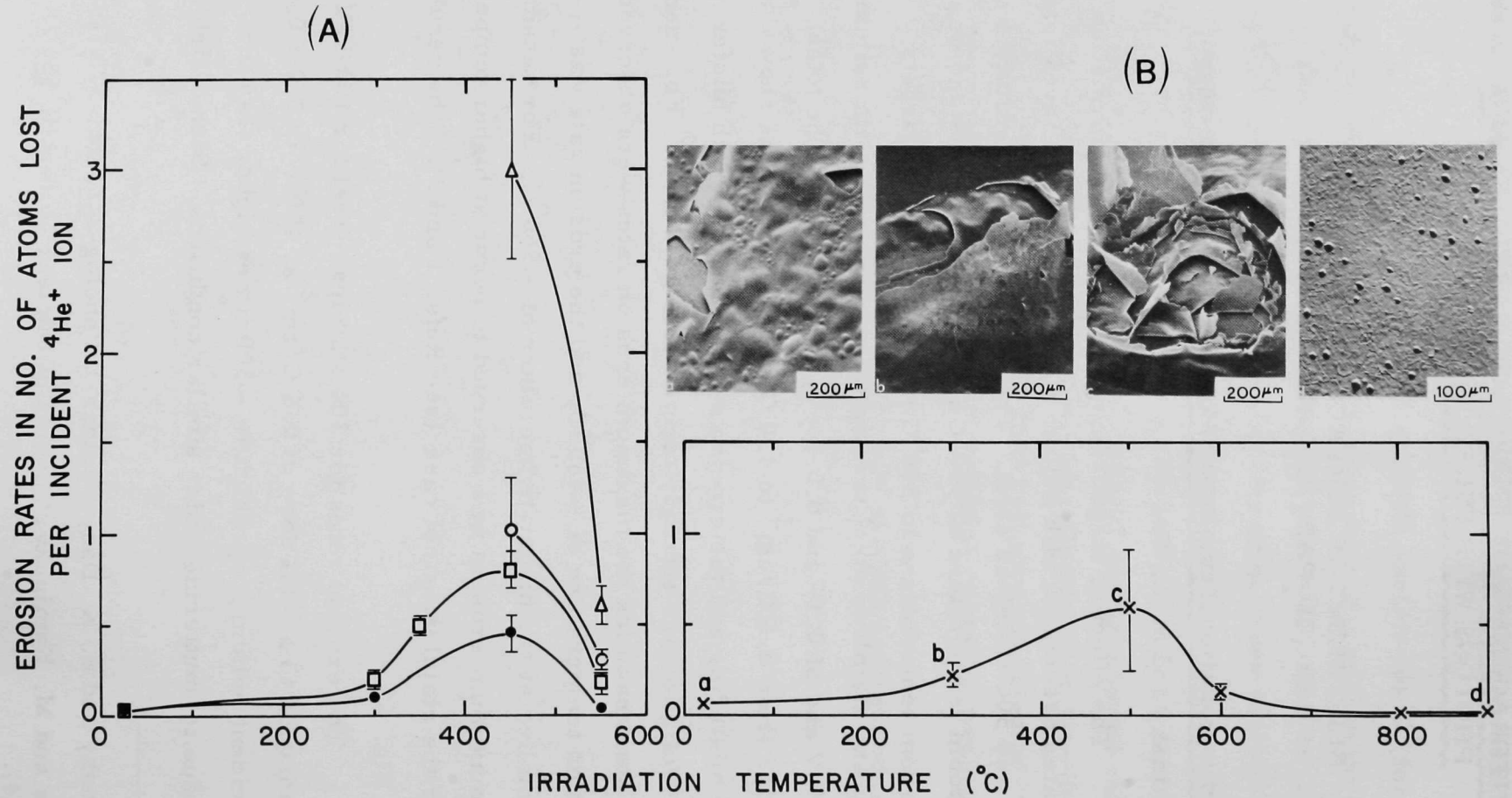

Fig. 62. (A) Erosion rates for annealed Type 304 stainless steel as a function of irradiation temperature for different projectile energies and total doses; ●: 0.5 C/cm² with 0.5-MeV $^4He^+$, □: 1.0 C/cm² with 0.5-MeV $^4He^+$, O: 0.1 C/cm² with 100-keV $^4He^+$, Δ: 0.5 C/cm² with 100-keV $^4He^+$. (B) Erosion rates for annealed polycrystalline vanadium as a function of irradiation temperature for 0.5-MeV $^4He^+$ ions and for a total dose of 1.0 C/cm². The figures a—d at the top of (B) show SEMs of irradiated surfaces for the temperatures indicated on the lower rate curve.

erosion rate would lead to an annual thickness loss [assuming a helium flux of 1×10^{13} projectiles/(cm^2-sec)] of about 0.09 mm per year. An estimate of the annual thickness loss for 0.5-MeV $^4He^+$ ion irradiation at 450°C for 304 stainless steel for a helium flux of 1×10^{13} projectiles/(cm^2-sec) gives a value of ~0.02 mm per year. The annual thickness loss for vanadium at 600°C is ~0.005 mm for the same helium flux. Thus the erosion rate for stainless steel at 450°C is a factor of four higher than for vanadium (at 600°C) for otherwise identical irradiation conditions. Such erosion rates may be enhanced by the vaporization of the blister skin due to heating by energetic photon absorption (e.g., photons from bremsstrahlung, synchrotron radiation, line radiation).

The low wall temperatures suggested recently for the operation of a toroidal fusion reactor (e.g., 466°C at the front of the niobium blanket cell) will very likely lead to more serious erosion due to blistering than a wall temperature of about 900°C. A possible solution for reduction of erosion due to helium blistering is to operate the first wall at high temperatures. These types of measurements will be extended to other materials of CTR interest. The reports on these studies have appeared in Nuclear Technology[1] and Journal of Nuclear Materials.[2]

b. Irradiation of Nb by He^+ Ions of Different Energies

M. Kaminsky and S. K. Das

The radiation blistering of polycrystalline-niobium surfaces at room temperature has been investigated for different doses of helium ions implanted at 0.5 MeV and for different amounts of initial defect structure in the samples. The cold-worked samples show large blisters. In samples annealed before irradiation (at a dose of 1.0 C/cm^2), the blistering was observed to be even greater. Not only was the skin ruptured at many different places, but in one area the first skin had already peeled off and the second skin had started to rupture in

many places. These first results indicate that the surface erosion of annealed polycrystalline niobium by 0.5-MeV helium blistering is approximately three orders of magnitude faster than the combined erosion by sputtering by 20.0-keV deuterons and tritons and 3.5-MeV helium ions.

c. Effect of He^+ and D^+ Ion Beam Flux on Blister Formation in Niobium and Vanadium

S. K. Das and M. Kaminsky

The effect of incident ion-beam flux on the blister formation in annealed polycrystalline niobium and vanadium has been investigated for 0.5-MeV He^+ and 0.25-MeV D^+ projectiles. For the He^+ ions the flux was varied from 1×10^{13} ions/(cm^2-sec) to 1×10^{15} ions/(cm^2-sec), the targets were held at 900°C, and the total dose was varied from 0.1 to 1.0 C/cm^2. For the D^+ ion irradiation the flux was varied from 1×10^{14} to 1×10^{15} ions/(cm^2-sec), the niobium targets were held at 700°C, and the total dose was 2.0 C/cm^2. For both the helium implanted vanadium and niobium the blister density shows a stronger flux dependence than does the average blister diameter. For deuteron-implanted niobium the blister size increased as the flux was increased from 1×10^{14} to 1×10^{15} ions/(cm^2-sec). These results have appeared in Ref. 1. Representative scanning electron micrographs (SEMs) are shown in Fig. 63.

---

[1] S. K. Das and M. Kaminsky, Applications of Ion Beams to Metals (Proceedings of the International Conference, Albuquerque, New Mexico, 2-4 October 1973), edited by S. T. Picraux, E. P. EerNisse, and F. L. Vook (Plenum, New York, 1974), pp. 543-555.

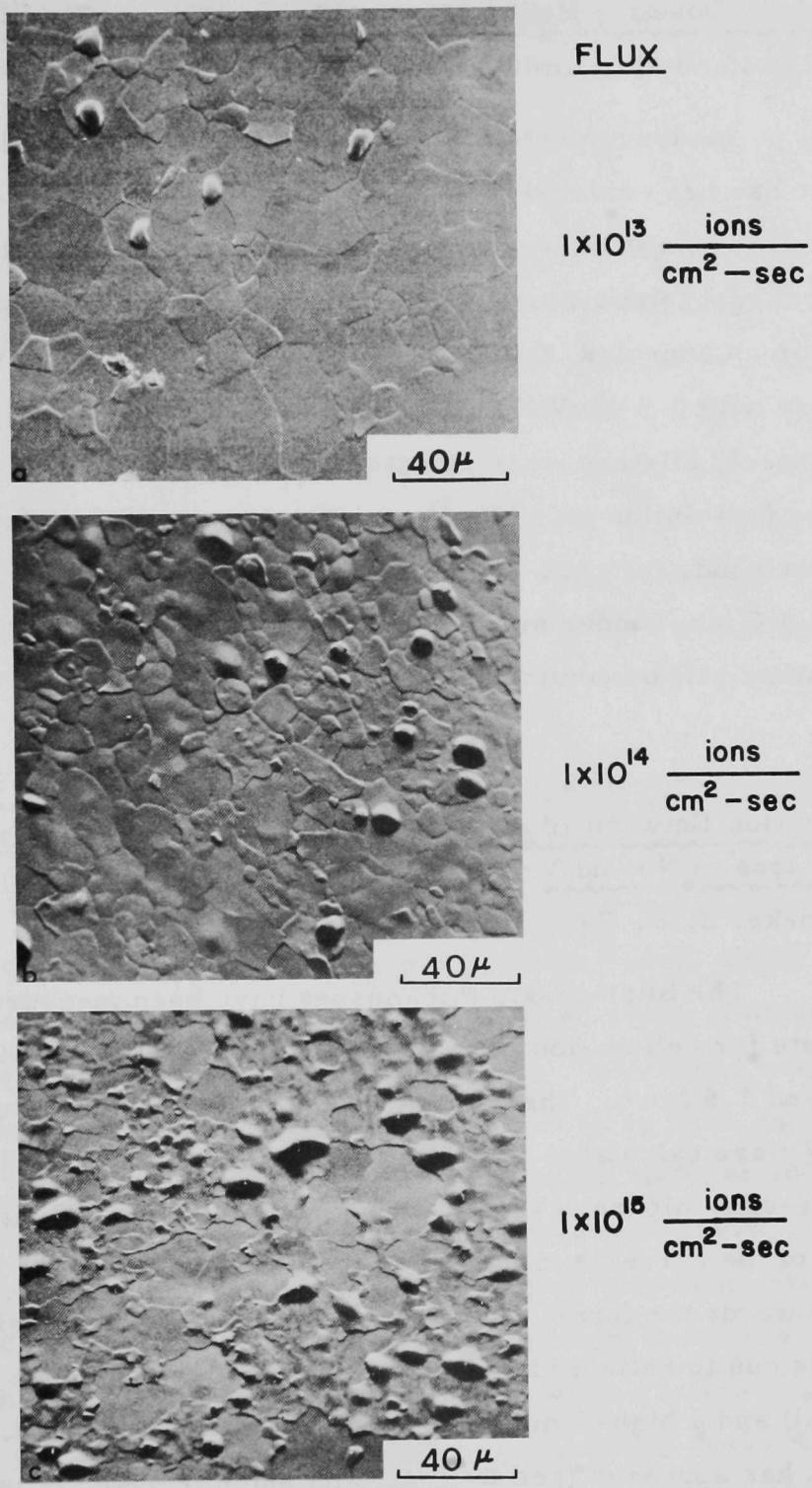

Fig. 63. SEMs of surfaces of annealed polycrystalline vanadium after irradiation at 900°C with 0.5-MeV $^4He^+$ for a total dose of 0.1 C/cm^2 at fluxes of (a) 1×10^{13} ions/(cm^2-sec), (b) 1×10^{14} ions/(cm^2-sec), and (c) 1×10^{15} ions/(cm^2-sec).

d. Threshold Dose for Helium Blister Appearance in Nb

S. K. Das and M. Kaminsky

Measurements of threshold dose for helium-blister appearance has been started for Nb at room temperature and at 900°C. Threshold dose was found to be strongly dependent on projectile energy, dose rate, target temperature and initial defect concentration in the target. For an annealed, polycrystalline-Nb target, irradiated at room temperature with 0.5-MeV He^+ ions at a dose rate of 1×10^{14} ions/(cm^2-sec), blisters were detected with a scanning electron microscope (resolution of ~100 Å) at doses between 0.3 to 0.4 C/cm^2. On the other hand, for cold-rolled Nb, blisters were observed at doses of 0.1 C/cm^2 under similar irradiation conditions. These measurements will be continued for other irradiation parameters.

e. Correlation Between Blister-Skin Thickness and Projected Ranges of He^+ Ions in Nb and V

G. Fenske, S. K. Das, and M. Kaminsky

The blister-skin thicknesses have been measured for Nb and V targets for helium-ion energies of 100 keV, 250 keV, 500 keV, 1.0 MeV, and 1.5 MeV. Theoretical projected ranges of helium ions in Nb and V were calculated according to Brice and Schiott. The measured blister-skin thickness values for different projectile energies fall within 20% of the corresponding calculated projected ranges. This is the first step towards the formulation of a semiempirical expression for the erosion rate due to helium blistering. Similar measurements for a low-Z material (Al) and a high-Z material (Au) have been completed. A paper on the work has appeared (see Ref. 1), and another paper is in preparation.

---

[1] S. K. Das and M. Kaminsky, Journal of Nuclear Materials 53, 115-126 (1974).

f. Helium Blistering in Nb Damaged by 14-MeV Neutron Irradiation

M. Kaminsky and S. K. Das

Cold-rolled polycrystalline Nb targets were irradiated at room temperature with 14-MeV neutrons at the RTNS at Lawrence Livermore Laboratory in the same irradiation chamber used for the neutron sputtering experiments to a total fluence of 4.6×10^{15} neutrons/cm^2. These targets were subsequently irradiated at room temperature with 0.5-MeV He^+ ions to a dose of 1.0 C/cm^2. Preliminary results show no significant difference between these blisters and those formed on cold-rolled Nb targets without pre-irradiation with 14-MeV neutrons. These experiments will be continued for different types of Nb targets and for different neutron irradiation conditions.

g. Effect of Irradiation Temperature on Blister Morphology in Nickel

M. K. Sinha, S. K. Das, and M. Kaminsky

Previous helium blistering studies of bcc metals such as Nb and V were extended to a fcc metal such as nickel, which is closest to austenitic stainless steel. The (110) surfaces of nickel monocrystals were irradiated with 0.5-MeV He^+ ions under initial channeling conditions for target temperatures ranging from room temperature to 950°C. In contrast with the results on Nb at 900°C where crowfoot shape blisters with threefold symmetry were observed on (111) surface, the nickel monocrystals showed only dome shaped blisters at 900°C. However, faceting of the blisters was observed at 850°C, but the detailed crystallography of the blister facets has not been worked out. A report on this work was presented at the APS meeting in Anaheim, California, January 29 to February 1, 1975 and is being prepared for publication.

h. Helium Blistering of Silicon Carbide

M. Kaminsky and S. K. Das

The erosion of silicon carbide surfaces was investigated for irradiation at room temperature with 100-keV and 250-keV He^+ ions. The silicon carbide used for this study was a mixture of high-density pyrolytic carbon and silicon carbide, which had been co-vapordeposited on a graphite substrate. The erosion rate for this material under 100-keV He^+-ion irradiation ($\sim 0.2 \pm 0.1$ atoms/ion) was found to be approximately two orders of magnitude larger than the corresponding sputtering yields for silicon or carbon. The erosion rate for 250-keV He^+ irradiation was $\sim 0.5 \pm 0.3$ atoms/ion, a value which is higher than the erosion rate for niobium ($\sim 0.2 \pm 0.1$ atoms/ion) under similar irradiation conditions. A report on these studies has appeared in proceedings of the First Topical Meeting on the Technology of Controlled Fusion.[1]

---

[1] M. Kaminsky and S. K. Das, in Proceedings of the First Topical Meeting on the Technology of Controlled Nuclear Fusion, San Diego, California, 16-18 April 1974, edited by G. R. Hopkins (National Technical Information Service, U.S. Dept. of Commerce, Springfield, Va., 1974), CONF-740402-P2, Vol. II, pp. 508-516.

i. Studies of the Reduction of Surface Erosion Due to Helium Blistering

S. K. Das, M. Kaminsky, and T. Rossing

As pointed out earlier in Sec. 1a, one way to reduce the erosion rate due to helium blistering is to irradiate the wall at high temperatures (e.g., $\geqslant 900^{\circ}C$ for Nb). However, the maximum operating wall temperature may be limited by other design criteria. Therefore, another solution should be searched for by the choice of a suitable microstructure for a particular wall material which will reduce helium buildup in near surface regions. Preliminary results on sintered aluminum powder compact (SAP) at room temperature irradiated with

100-keV He^+ to a dose of 1.0 C/cm^2 show an astonishingly high reduction in the erosion rate by about four orders of magnitude as compared to pure Al for similar irradiation conditions. These measurements on SAP will be continued for different irradiation temperatures.

2. 14-MeV NEUTRON SPUTTERING

a. 14-MeV Neutron Sputtering of Nb

M. Kaminsky and S. K. Das

The particle release from niobium surfaces under 14-MeV neutron impact to total fluences ranging between $4.2-4.8 \times 10^{15}$ neutrons/cm^2 was investigated under ultrahigh vacuum conditions. Two types of deposits were observed on the collector surfaces, one in the form of large chunks (Fig. 64), the other in atomic form covering the surface as a fractional atomic layer. The number of chunks, their size and shape was found to depend very strongly on the degree of microstructure of the irradiated surface (e.g., microprotrusions, microcracks) and on the tensile stresses in the near surface regions (e.g., due to cold-rolling). The chunk densities were 30—1000 chunks/cm^2 for 45% cold-rolled polycrystalline Nb (microfinish ~5 μm after 1 min electropolish), 10—250 chunks/cm^2 for 45% cold-rolled poly Nb (microfinish ~5 μm after 1 sec etch), 2—100 chunks/cm^2 for annealed Nb (microfinish ~2 μm after electropolishing), 0—40 chunks/cm^2 for annealed Nb (microfinish ~0.5 μm), but no chunks were observed for monocrystalline Nb (111) surface. The chunk density values quoted above indicate the smallest and the largest number of chunks which can be found on a contiguous surface area of 1 cm^2 within the total collector area of ~4.4 cm^2. The chunk density values for the repeat runs fall within the ranges listed. The report of these studies

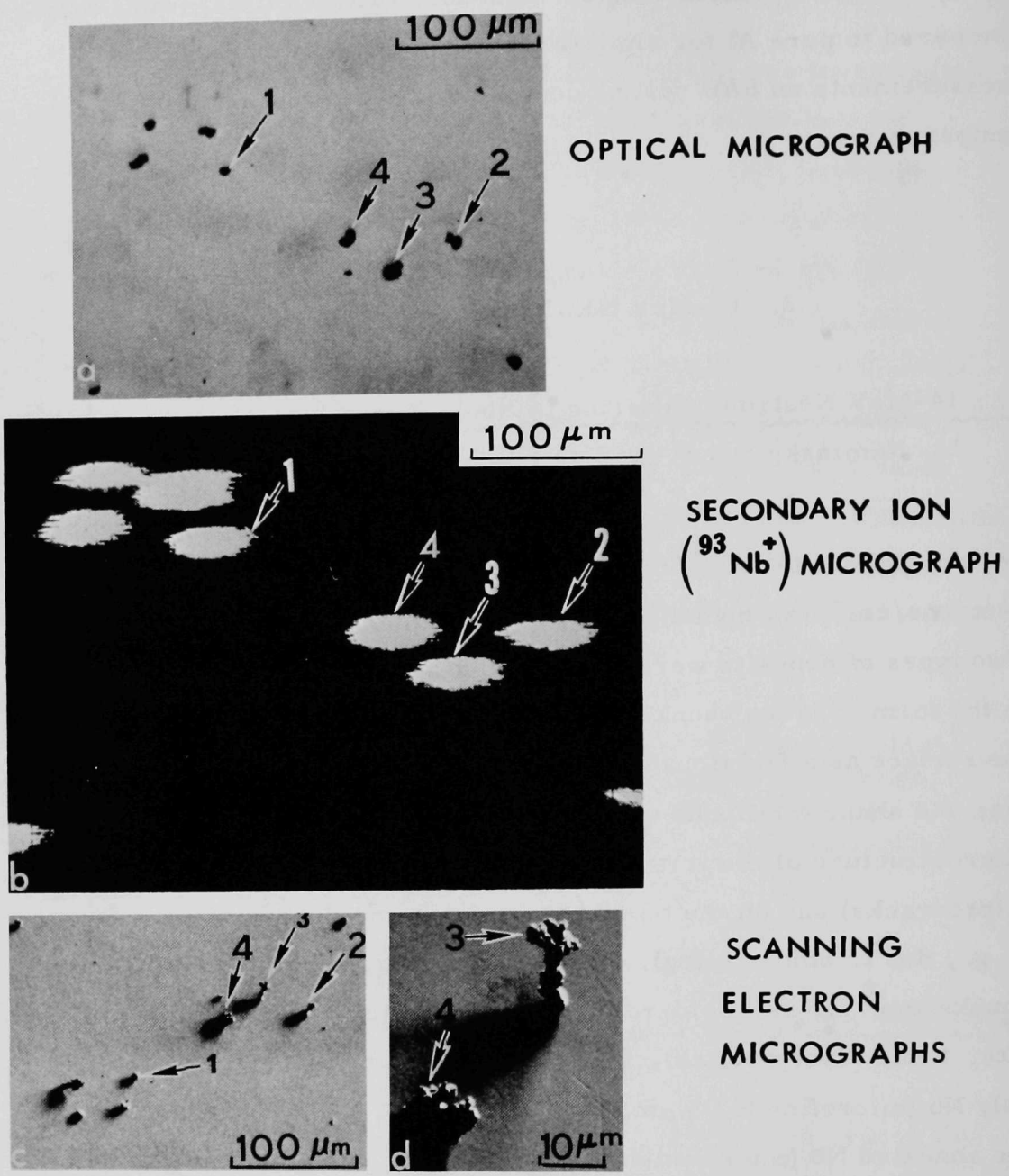

Fig. 64. Niobium deposited on a silicon (111) substrate when a niobium target at ambient temperature (estimated to be near room temperature) was irradiated with 14-MeV neutrons to a total dose of 4.6×10^{15} neutrons/cm^2. (a) Optical micrograph of niobium chunks deposited on a Si(111) surface. (b) Secondary ion ($^{93}Nb^+$) micrograph of the same area as in (a). (c) Scanning electron micrograph (backscattered electron image) of the same area as in (a), showing the size and shape of the deposited chunks of Nb. (d) An enlarged view of some chunks shown in (c).

has appeared in Phys. Rev. Lett.,[1] Proceedings of Fifth Symposium on Engineering Problems of Fusion Research,[2] J. Nucl. Materials,[3] and some parts will appear in the proceedings of the IAEA Conference on Plasma Physics and Controlled Nuclear Fusion Research.[4]

---

[1] M. Kaminsky, J. H. Peavey, and S. K. Das, Phys. Rev. Lett. 32, 599-602 (1974).

[2] M. Kaminsky and S. K. Das, in Proceedings of the Fifth Symposium on Engineering Problems of Fusion Research, Princeton University, November 5-9, 1973 (IEEE Nuclear and Plasma Science Society, 1974), IEEE Pub. No. 73CH0843-3-NPS, pp. 37-40.

[3] M. Kaminsky and S. K. Das, Journal of Nuclear Materials 53, 162-170 (1974).

[4] M. Kaminsky, IAEA Conference on Plasma Physics and Controlled Nuclear Fusion Research, Tokyo, Japan, November 11-15, 1974, ANL-PHY/CTR/TM-30 (in press).

b. 14-MeV Neutron Sputtering of Silicon Carbide

M. Kaminsky and S. K. Das

Two types of silicon carbide samples were irradiated with 14-MeV neutrons. One sample was a high-density, high-purity silicon carbide which had been vapor deposited on a graphite substrate and was irradiated to an estimated dose of $\sim 5.0 \times 10^{14}$ neutrons/cm^2. Another sample was a hot pressed and sintered powder compact of silicon carbide and was irradiated to an estimated neutron fluence of $\sim 6.0 \times 10^{14}$ neutrons/cm^2. For both types of targets, plate-like chunks were observed on the collector surface and their average diameter ranged from 3 to 10 μm. The results of these studies have appeared in the Proceedings of the First Topical Meeting on the Technology of Controlled Nuclear Fusion.

c. Effect of Irradiation Temperature on 14-MeV Neutron Sputtering of Nb

M. Kaminsky and S. K. Das

A polycrystalline niobium target was irradiated at 700°C to a total fluence of $\sim 4.3 \times 10^{15}$ neutrons/cm^2. Preliminary results show chunk deposits of Nb on the Si(111) collector surface. In contrast with the room temperature irradiated cold-rolled Nb samples, where some cylindrical type chunks were observed, only quasi-spherical chunks were detected for 700°C irradiation.

d. Chunk Emission from V, Stainless Steel, Monocrystalline Si

M. Kaminsky and S. K. Das

Chunk emission has also been observed for 14-MeV neutron impact on materials such as cold-rolled polycrystalline V, Type 304 stainless steel and monocrystalline Si. For monocrystalline silicon the chunk density was very small ($\sim$3—5 chunks/cm^2). Detailed evaluation of erosion rates for vanadium are underway.

e. Neutron Sputtering of Surfaces Prestressed with Helium-Ion Implantation

M. Kaminsky and S. K. Das

The studies on neutron sputtering of surfaces, which have been previously prestressed by helium-ion implantation, have been started. Preliminary results on 14-MeV neutron irradiation of annealed Nb surfaces, implanted with helium ions of energies larger than 0.5 MeV, do not show any marked change of the blisters. The data on lower helium-ion energies are being evaluated.

f. Dependence of Neutron Sputtering on Incident Neutron Energy

M. Kaminsky and S. K. Das

In order to establish the threshold energy of neutrons for initiation of chunk emission, experiments were done at different

neutron energies. The variable energy cyclotron at Davis was used in conjunction with (d,n) reaction on a beryllium target to obtain neutrons with different energy spectra. At a mean neutron energy of 5 MeV no chunk emission was observed for Nb. The results on higher mean neutron energy are being analyzed.

3. ION SPUTTERING

P. Dusza and M. Kaminsky

When energetic projectiles penetrate into solids with sufficient energy, they can displace lattice particles from their sites and become implanted in the lattice at the end of their range. A fraction of the displaced lattice particles can escape from the bombarded surface as atoms, molecules, molecular clusters, and particulate matter in a neutral or charged state. This sputtering process causes not only the release of gaseous species into the vacuum space but also the erosion of the bombarded surface area. There is another competing process which causes surface erosion and the release of gases—radiation blistering, as mentioned in Secs. 1a—i. Studies were started to determine the relative contributions of sputtering and blistering to the erosion of surfaces and the release of gas. In a first set of experiments the surfaces of V and Nb were bombarded with He ions with energies ranging from ~0.1—1.5 MeV for a range of dose values and for different target temperatures. The observed total surface erosion rates show a strong dependence on the primary particle energy, the target temperature, the dose rate, and the total dose. In order to determine the relative contributions of sputtering and blistering to the total erosion rate, additional information is required. We have started measurements of the sputtering yield (total yield, partial yields for both charged and neutral species) for helium ions in the energy range of interest for V and Nb targets. There has previously been a

complete lack of such experimental data, and theoretical predictions for yield values differ by more than 300%. With the aid of experimentally determined yield values and from the measured total erosion rates (which includes a correlation between measured blister-skin thickness and the projected ranges of He ions in the target), the blistering contribution to the total erosion rate can be determined.

4. SURFACE PHENOMENA INDUCED BY PHOTON IMPACT

S. Brumbach, M. Kaminsky, and S. K. Das

The interaction of energetic photons (e.g., bremsstrahlung x rays, and γ rays) with such components of plasma devices and fusion reactors as limiters, liners, divertors, and walls can cause gas released and lead to plasma contamination. Such processes as photodesorption, photodecomposition (e.g., of insulator surfaces), photocatalysis, photoelectron induced desorption, and sputtering by energetic γ rays ($>$1 MeV) can contribute to the gas release. In addition, the photon impact can cause changes in the chemical composition of surface layers, in the electrical conductivity of insulators and in the surface microstructure.

An apparatus has been designed and constructed for preliminary studies of photon-impact phenomena. The apparatus consists of an ultrahigh-vacuum chamber and pumping system, a target holding assembly (including target heating device), a beryllium window and a quadrupole mass spectrometer for the detection of released gas species. The chamber has been tested to pressures of $\sim 2 \times 10^{-10}$ Torr. Tests have been completed to determine the detection sensitivity of the mass spectrometer for various gas species with the aid of calibrated leaks.

Measurements of the gas released from surfaces under x-ray irradiation have begun with the recently constructed ultrahigh vacuum apparatus. At the present, stainless steel and alumina surfaces

are under investigation using x rays in the energy range 15—50 keV. With the aid of a quadrupole mass spectrometer, it has been determined that such species as M = 44 [CO_2], M = 28 [CO], M = 16 [CH_4 and O], and M = 2 [H_2] are the predominant gases released under photon impact. Measurements are in progress to determine more quantitatively the quantum yields for each gas species for the types of surfaces discussed. In addition, measurements of the dependence of the quantum yields on the photon energy and photon intensity are in progress. These measurements are normally conducted at a total pressure of about 1×10^{-9} Torr.

The alumina surfaces before and after irradiation have been characterized by Auger electron spectroscopy. This characterization will be expanded to include scanning electron microscopy in conjunction with energy dispersive x-ray spectrometry.

5. DEVELOPMENT OF TECHNIQUES FOR MEASURING SURFACE CONTAMINATION IN VERY SMALL CONCENTRATIONS (10^{-1}—10^{-4} MONOLAYERS)

M. Kaminsky and P. Dusza

In order to measure the sputtering yield from 14-MeV neutrons, it was necessary to develop independent techniques for measuring the small amounts of sputtered material deposited on highly cleaned substrates. After careful calibration, the Rutherford-backscattering technique and the ion-microprobe method yielded the most reliable and self-consistent results for surface contaminants in concentrations equivalent to a small fraction of a monolayer. An Auger spectrometric technique is being developed and further work will continue.

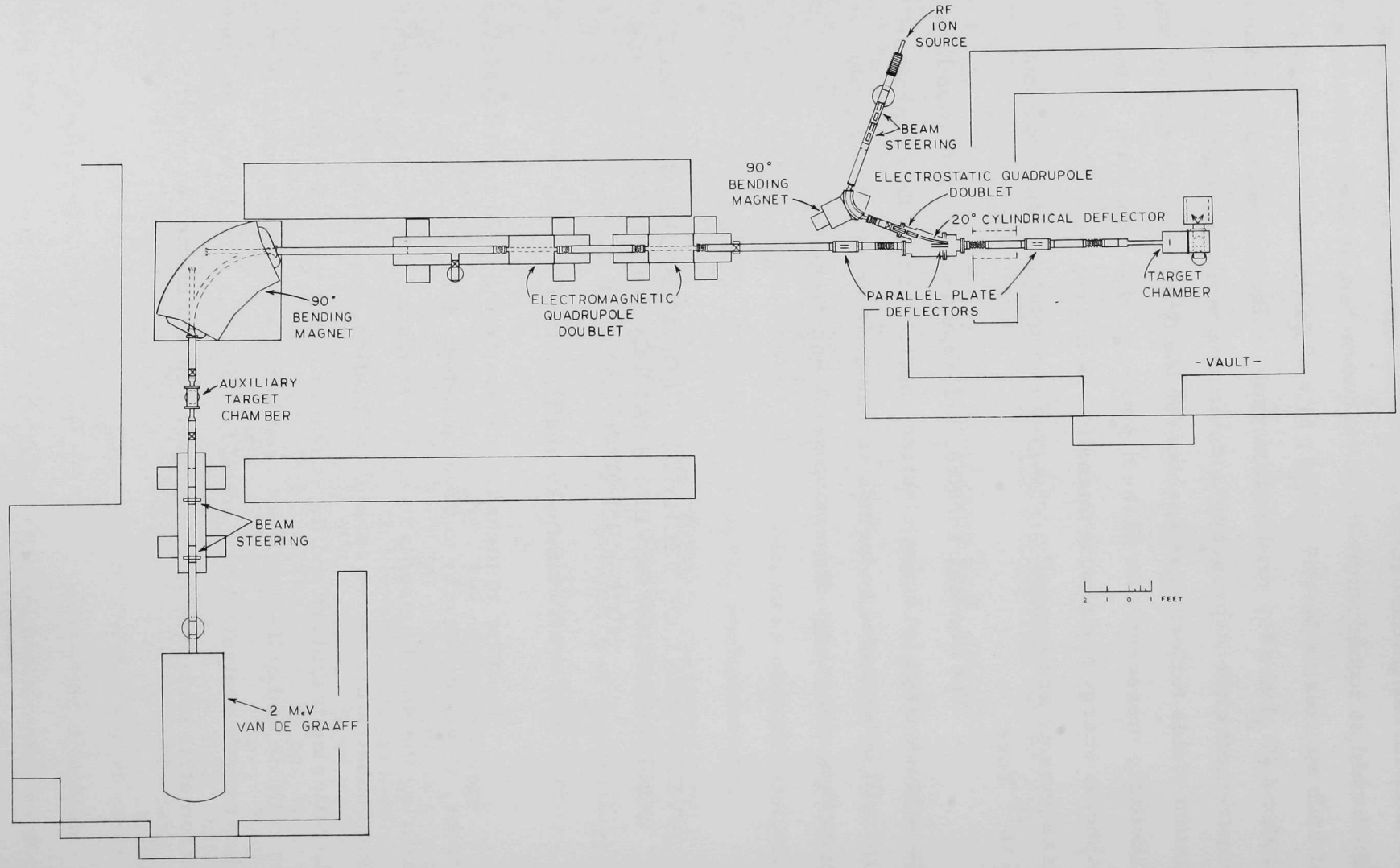

Fig. 65. Two-component ion-accelerator system.

6. DESIGN OF A TWO-COMPONENT ION-ACCELERATOR SYSTEM

R. Ekern, D. C. Hess, and M. Kaminsky

The design of major components of a low-energy ion accelerator (5—50 keV) has been completed. This accelerator will be used as an injector into the beam line of an existing 2-MeV Van de Graaff, so that targets can be bombarded by ions of the same species at two different energies or by ions of different species (e.g., D^+ and He^+) at specified energies. This two-component ion-accelerator system allows studies of synergistic effects due to simultaneous bombardment of target surfaces with two different ion-beam components. The low-energy ion accelerator (see Fig. 65) consists of an RF ion source, beam steerer, analyzing magnet, insulated slits, electrostatic quadrupole doublet, electrostatic cylindrical deflector, and parallel-plate beam deflectors. The construction of the ion source and the electrostatic cylindrical deflector has been started.

C. OPTICAL AND RADIOFREQUENCY SPECTROMETRY OF FREE ATOMS AND MOLECULES

1. ATOMIC-BEAM MAGNETIC RESONANCE OF THE ACTINIDES

W. J. Childs, H. Diamond,* L. S. Goodman, and T. Waech

The atomic structure of the actinides is generally much more complex than that of the lighter atoms, and it cannot be inferred by extrapolation from them nor calculated ab initio with any accuracy. The two principal sources of theoretical difficulty are the much greater importance of relativistic and configuration-interaction effects. Studies of the hyperfine structure (hfs) can be particularly revealing because of the importance of relativistic effects near the nucleus. The atomic-beam technique is ideal for such atomic studies, and carries the bonus of providing nuclear spin and moment data for these heavy nuclides. The program is a joint undertaking with the Chemistry Division and relies heavily on its special facilities and expertise in heavy element chemistry.

Extensive measurements were made of the hfs of ^{253}Es and ^{254m}Es. No method was found to produce an atomic beam free of substantial (nonrandom) fluctuations even over time scales as short as seconds. The problem was solved by a novel detection scheme in which the deposition targets were cycled synchronously with the programming of the radiofrequency sweep. The composition of the Es atomic ground state deduced from the few known levels was confirmed by the experimentally measured g_J value. The agreement between the directly measured nuclear dipole moment of ^{253}Es with that predicted from the measured dipole hfs and recently calculated relativistic $\langle r^{-3} \rangle$ values[1] shows that configuration interaction is relatively unimportant in the Es

*Chemistry Division, ANL.

[1] W. B. Lewis, J. B. Mann, D. A. Liberman, and D. T. Croner, J. Chem. Phys. 53, 809 (1970); and private communication.

ground state, in sharp contrast to the case of Pu. Analysis of the experimental results gives convincing evidence that the relativistic Dirac-Slater technique[1] for calculating $\langle r^{-3} \rangle$ values appears to be satisfactory for atomic states for which configuration interaction is not severe. A paper describing the results in detail has been published in Physical Review.[2]

A hot-wire ionizer mass-spectrometer detector has been built and installed on the atomic-beam apparatus. Test runs with Sm and Tb, for which the ease of detection can be expected to be similar to that of most actinides, were encouraging and experiments are now being started to measure directly the nuclear dipole moment of ^{237}Np. This measurement was requested by both optical and Mössbauer spectroscopists, since the moment value is essential to further interpretation of their experimental results.

[2] L. S. Goodman, H. Diamond, and H. E. Stanton, Phys. Rev. A 11, 499 (1975).

2. EXPERIMENTS WITH ^{221}Fr

W. J. Childs, H. Diamond,* L. S. Goodman, and B. Greenebaum

A paper reporting on our successful efforts to see absorption in ^{133}Cs using laser-quenching spectroscopy with fewer than 10^8 atoms was published in Applied Optics.[1] Figure 66 shows densitometer traces through the $6^2S_{1/2} \rightarrow 7^2P_{3/2}$ 4556 Å absorption line in ^{133}Cs. The 9192 MHz hyperfine splitting of the ground state is clearly resolved. For the upper trace, the number of atoms in the vapor was $\sim 4 \times 10^9$; the line can still be seen when only $\sim 9 \times 10^7$ atoms are present (lower trace). The paper stirred considerable interest and gives us real hope that the corresponding experiment can be done on Fr.

*Chemistry Division, ANL.

[1] W. J. Childs, M. S. Fred, and L. S. Goodman, Appl. Optics 13, 2297 (1974).

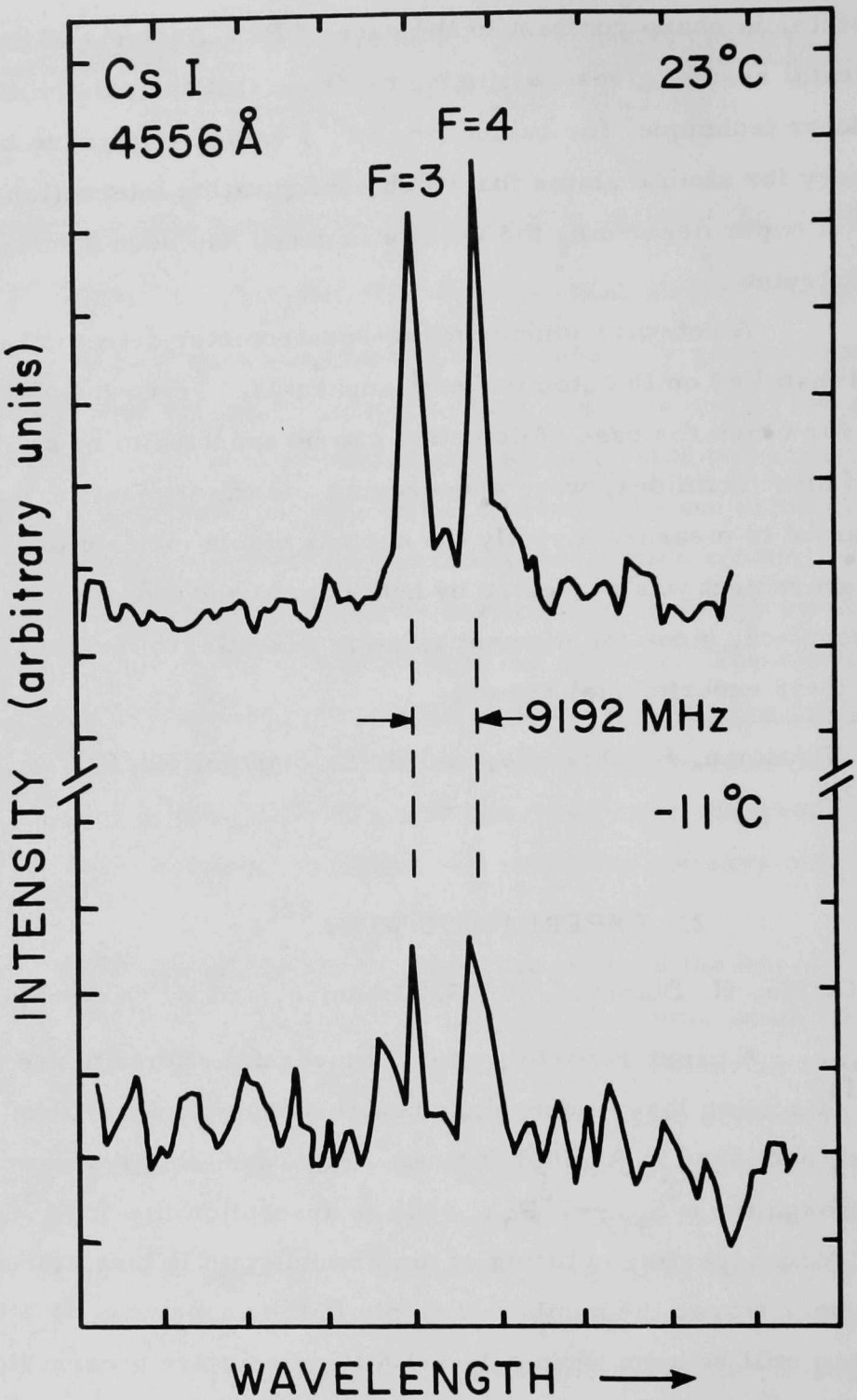

Fig. 66. Densitometer scans through the $6^2S_{1/2} \rightarrow 7^2P_{3/2}$ absorption line in Cs vapor observed with an intracavity absorption cell at the temperatures shown. The 9192-MHz hyperfine splitting of the $^2S_{1/2}$ ground state is well resolved. As may be seen from the lower tracing, it is difficult to see the line below about -11°C; fewer than 10^8 atoms of Cs were in the vapor at this temperature.

If the effort is successful, it would provide the first experimental information on the atomic structure of Fr, the heaviest alkali atom. Theoretical calculations of the excitation energies to be measured vary widely because of the different approximations used for including relativistic effects.

3. LASER SPECTROSCOPY OF ACTINIDE MOLECULES

W. J. Childs and L. S. Goodman

This project is intended to explore the usefulness of tunable dye lasers for studying the spectroscopy of actinide molecules in the visible, and is a joint effort with the Chemistry Division. It is hoped that it will be feasible to demonstrate isotope shifts and to apply them to understanding the molecular structure. The initial studies have been made with a flash-lamp-pumped broad-band dye laser in conjunction with the Argonne 30-foot high-resolution grating spectrograph. The sample is placed between the mirrors of the dye laser (the intracavity position), so that not only is absorption increased by multiple passage, but in addition each photon absorbed is no longer free to stimulate emission. The laser light is thereby selectively quenched at the wavelengths characteristic of the absorber. We have demonstrated using Cs that the sensitivity is typically 2—3 orders of magnitude greater than with the conventional, single-pass (extracavity) configuration, and the resolution is that of the analyzing spectrograph, in our case, about 0.05 Å. The experimental setup is shown in Fig. 67.

We found early in our studies that because of the high sensitivity of the technique, one often observed absorption lines in the visible due to airborne water vapor even though the room is dehumidified. These lines are normally observed only by absorption in the solar spectrum on damp days, and can be seen in the laboratory with conventional techniques only with extremely long (multiple-pass) absorption

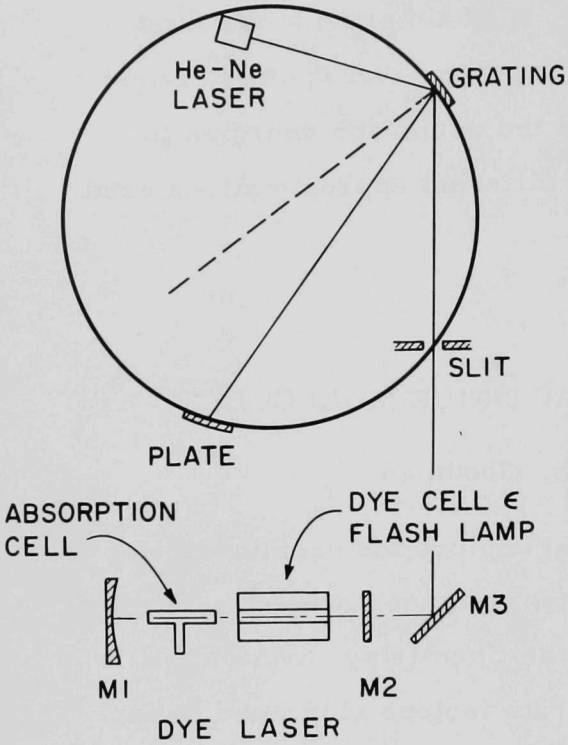

Fig. 67. Schematic diagram of apparatus. The 70-cm laser cavity (M1, M2) is greatly exaggerated relative to the 30-foot diameter of the grating circle. The absorption cell is shown in the intracavity position; it can also be used externally between the slit and the mirror M3. The He-Ne laser is used to facilitate alignment.

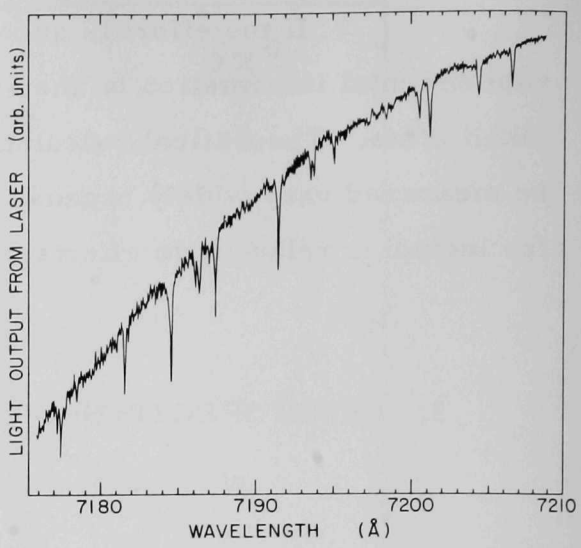

Fig. 68. Absorption lines due to airborne H_2O in the light output from a pulsed dye laser. The laser is selectively quenched at the characteristic rotation-vibration lines of water. These lines are extremely difficult to observe with conventional laboratory techniques, but do appear in absorption in solar spectra taken on damp days.

cells. Figure 68 shows some of these H_2O absorption lines in the output of the laser using Nile Blue dye. All of the lines shown are associated with the rotation-vibration bands of water.

The first actinide molecule investigated was $NpCl_4$, and hundreds of sharp molecular lines were seen in the region 6200—6700 Å. Although the chemists who prepared the absorption cell feel the likelihood of impurities is very small, the ease with which the lines were seen was surprising in view of previous studies of the vapor pressure of

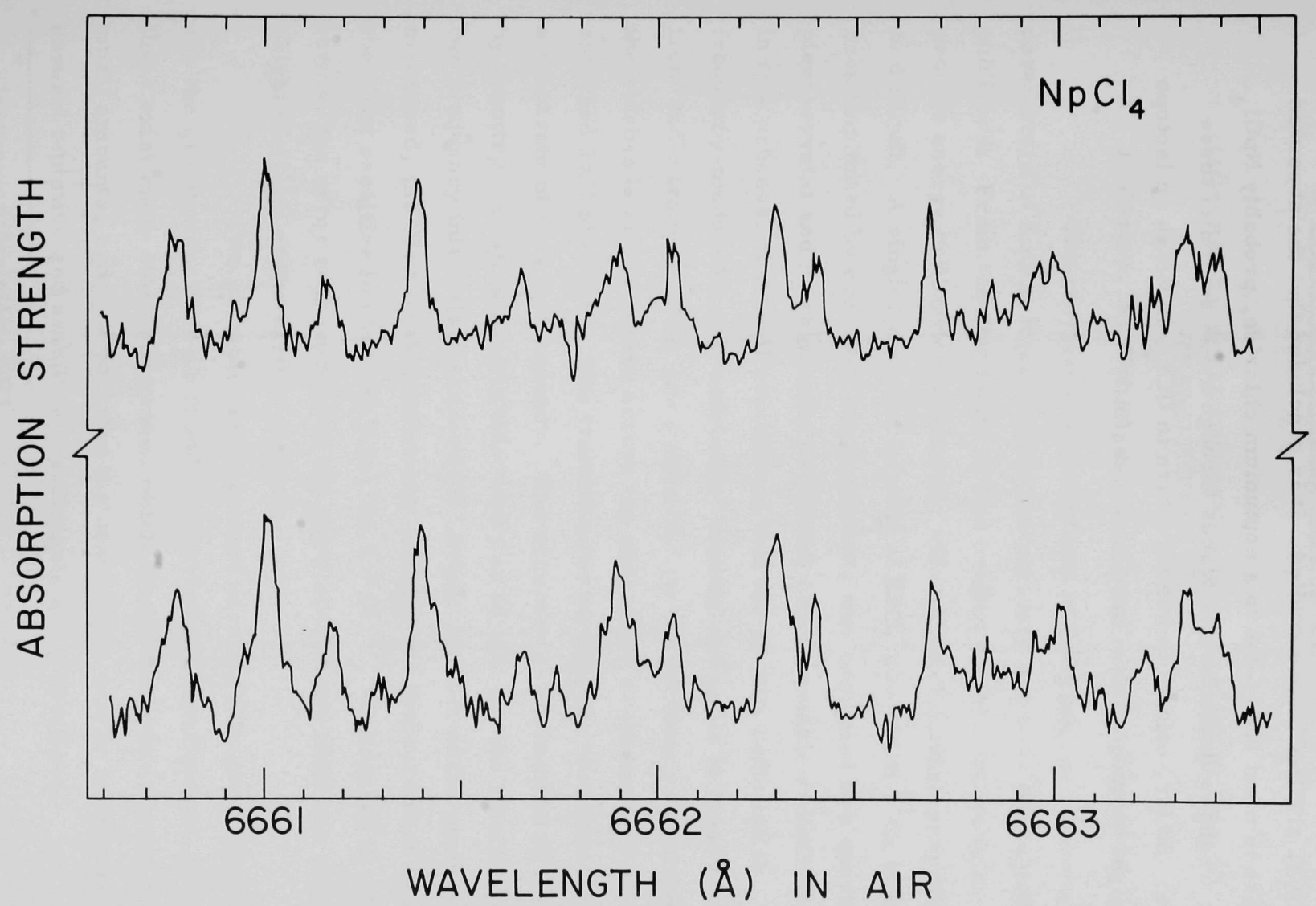

Fig. 69. Densitometer traces of photographic plates obtained on the Argonne 30-foot high-resolution grating spectrograph. The intracavity absorption cell contained $NpCl_4$ at about 225°C; no lines were observed at room temperature. The region shown is only about 3 Å wide.

$NpCl_4$. For this reason, samples of the most likely contaminants (Cl_2, HCl, and H_2O) were studied. It is concluded that the observed structure is most likely due to a neptunium chloride, probably $NpCl_4$. Figure 69 shows densitometer traces through a 3 Å region of these spectra. So far, efforts to see structure in UCl_4, in which an isotope shift might be sought, have been unsuccessful.

D. MÖSSBAUER EFFECT RESEARCH

1. MÖSSBAUER MEASUREMENTS WITH THE 93.26-keV TRANSITION IN ^{67}Zn

G. J. Perlow, W. Potzel, R. M. Kash,* and H. DeWaard

The precision measurement of the quadrupole-interaction parameters of ZnO at liquid helium temperature has been completed and published. From the standpoint of this project its importance is to provide energy calibration standards, without which further progress is difficult. A single, oriented crystal of ZnO, into which ^{67}Ga had been implanted by cyclotron bombardment, was cemented to a quartz piezo-crystal and mechanically oscillated with a variable radiofrequency. In this process, it is well established that the gamma radiation is frequency-modulated and "sidebands" exactly analogous to those familiar from radio transmission, are produced. As the frequency is varied, the sidebands sweep in turn across the absorption resonances of an enriched ZnO absorber. The transmission through the absorber displays a spectrum of dips vs frequency. The accuracy of the method is limited by counting statistics, and in this case was ±1 kHz for the smaller of the two frequency intervals measured (361 kHz). In units of the quantity measured, the 93.26-keV gamma-ray energy, the measurement is among the most sensitive in physics, i.e., $\pm 4.4 \times 10^{-17}$. Expressed in other terms, the error corresponds to the gravitational red shift in a change of height of 41 cm at the earth's surface.

Two possible and important uses for this great accuracy are the gravitational red-shift and the ether-drift experiments. However, there exist many other phenomena which change the γ-ray energy by small amounts, and it seems that the next efforts will be to explore several tentative and sensitive experiments along new lines.

---

*Electronics Division, ANL.

2. STUDY OF LAKE MICHIGAN SEDIMENTS BY ^{57}Fe MÖSSBAUER SPECTROSCOPY

G. J. Perlow, W. Potzel, and D. Edgington*

Mössbauer spectroscopy can be used for nondestructive analysis of iron compounds in a sample. The various valence states, condition of magnetic ordering, and in favorable cases specific chemical form, produce different spectra. When done with care, one may obtain reliable quantitative analyses that are obtained only with great difficulty by other methods. We have studied the variation with depth of various components of lake bottom sediments in a region of high sedimentation. The sediment had been collected by coring techniques on shipboard.

The results of the first investigation have been published. They are interesting because they clearly show the variation with time of a ferric-oxide component which can be attributed to air pollution from the extensive steel-mill complex along the southern shores of Lake Michigan. The component is magnetically ordered. It displays a maximum in the recent past (about 1960) and is indistinguishable from natural background before about 1915. The increase with time during the period of rapid change is exponential, with a doubling time of 18 years.

A series of samples from other regions of the lakes has been prepared and is being studied at the Technische Universität München with partial support from the Alexander von Humboldt foundation. This work is to be resumed at Argonne after June 1, 1975. It is now quite apparent that the Mössbauer effect is a very useful tool in the study of lake ecology.

---

*Radiological and Environmental Research Division, ANL.

3. ATOMIC MOTIONS IN LIQUIDS AND GLASSES

S. L. Ruby, B. J. Zabransky, J. C. Love, and P. A. Flinn*

The Mössbauer effect is able to give information about local structure, and its changes with time, of ions in liquids if they are viscous enough. We have found a model system (H_3PO_4 in water—with Fe^{2+} ions dissolved as probes) which can be supercooled to requisite viscosities. Most of our measurements have been detailed studies of the γ-ray absorption line shape of the ^{57}Fe nuclei, from which we can deduce information on both rotary and diffusive motions.

Until now, our best theory of the process was not quite able to explain the data at all temperatures. Recently a new treatment (created elsewhere) appears to improve the treatment of simultaneous rotary and diffusive motions and is now being tested against our data. Also this year we added a new kind of measurement (macroscopic diffusion). This has already resulted in the first experimental determination of the inapplicability of "jump" diffusion to liquids, in contrast to crystals. The combination of new measurement with better theory encourages our belief that we will finish the explanation of the present model system this year.

*Carnegie-Mellon University, Pittsburgh, Pennsylvania.

4. RADIATION DAMAGE EFFECTS

R. S. Preston* and B. J. Zabransky

Study of the radiation damage produced in solids by energetic particles, not only improves our understanding of solids, but also is necessary for the development of structural materials for fission and fusion reactors. It may be possible to use the Mössbauer effect to study details of the radiation damage in micro-regions as small as

*Northern Illinois University, DeKalb, Illinois.

~10 atoms. We have a modest project to explore this possibility by using energetic ^{57}Mn atoms to produce radiation damage and then to become a Mössbauer source through decay to the excited state of ^{57}Fe. As a first effort, we have studied radiation damage in Cr_2O_3 caused by ^{57}Mn atoms produced in the bombardment of ^{54}Cr with α particles from the tandem.

5. x-RAY MIRRORS

S. L. Ruby

Scattering by nuclei is nearly always incoherent among the numerous nuclei of the scattering body. Coherent nuclear scattering will have new and useful properties. For certain very precise energies, there are certain nuclei which have very large (resonant) scattering amplitudes, even much larger than the total scattering amplitude from all that atom's electrons. For these energies, a Bragg x-ray scattering geometry would have a coherent nuclear component, as well as the usual coherent electronic one. We are endeavoring to find conditions where this scattering could indeed be mirror-like.

Our work so far has indicated that certain isotopically enriched, single, "perfect" (in the dynamical theory of x-rays sense) crystals (such as FeCo, GeSe, SnTe, KCl, CsI, InSb, etc.) will reflect the appropriate Mössbauer γ ray at the mirror angle and with nearly perfect efficiency. This overcomes a dissipative process, internal conversion, which usually "wastes" a large fraction of the scattered radiation. And the Bragg or mirror angle can be chosen quite large, approaching perpendicular reflection. A major problem is to obtain such unique and difficult crystals.

These properties may be demonstrable using radioactive sources. Such sources are too weak to put much intensity into the very finely-beamed solid angles required. Synchrotron radiation from the

electron storage rings at SLAC do have adequate intensities, but are not monochromatic. We have published a description of a method to overcome this problem using the temporal dispersion associated with nuclear scattering, which is an additional effect to the well-known dispersion in energy and angle of electronic Bragg scattering.

The implications of these ideas are quite far reaching. In particular, consider the considerable efforts to create a gamma-ray laser, "gaser." They are motivated basically by the desire for very monochromatic beams, and the laser coherence is only a technique to get that. The mirrors discussed here can be used as filters to select such a narrow band. The long-range aims include such ideas as x-ray holography and microscopy.

6. MÖSSBAUER SPECTROSCOPY OF ^{129}I IN THYROXIN-LIKE COMPOUNDS

S. L. Ruby, R. S. Preston,* and B. J. Zabransky

We had found earlier that Mössbauer studies of ^{129}I in thyroxin and di-iodino-tyrosine (a precursor form) give very similar spectra. This disappointment (it argues against the potential use of such methods to study iodine metabolism) surprised us since other work had shown that the various iodomethanes did have dissimilar (enough) such spectra. Since thyroxin is built from benzene rings, it was pertinent to examine iodobenzenes. Having done so, we see that there is indeed very little change made in the spectrum from two iodines attached to the same ring, whatever their spacings from each other on the six carbons. The work is being concluded by preparation of a paper on local environmental effects as seen in this kind of spectrometry.

*Northern Illinois University, DeKalb, Illinois.

7. CARBONIC ANHYDRASE STUDIES USING MÖSSBAUER SPECTROSCOPY

A. M. Friedman* and S. L. Ruby

Carbonic anhydrase is an enzyme which plays an important role in the expiration of CO_2 in mammals. Crystal structure studies had indicated a single "active" site in the large ($M \cong 30\ 000$) molecule where a Zn atom is bonded. Information about the bonding at that site is strongly desired. The perturbed angular correlation (PAC) method could give useful information. An attempt has been made (unfortunately for technical reasons substituting ^{111}Cd for the Zn); the results indicate that there are two binding sites for the metal in the enzyme.

We suspected that even this limited conclusion gave the wrong impression. Our concern was that either or all of (a) chemical aftereffects from radioactive decay, (b) concentration effects upsetting macroscopic preparative techniques when using radioactive materials, and (c) possibility of several microsites which could give rise to spectra similar enough not to be distinguished, could confuse the interpretation of the Cd experiment. The Mössbauer technique, which is normally a finer tool than PAC, was utilized. Here, again unfortunately, ^{57}Fe had to be substituted for the Zn.

Our methods included extremely careful sample preparation and analyses which measured biological efficiency, as well as Mössbauer spectroscopy. The results identify the active site as one which binds a divalent iron atom of low spin. Also we find that both the (a) and (c) problems definitely confuse the PAC work. There is no reason to suspect the crystallographic conclusions.

---

*Chemistry Division, ANL.

E. SCANNING SECONDARY-ION MICROPROBE

MICROSCOPIC LOCATION OF STABLE TRACER ISOTOPES

V. E. Krohn, W. E. Kisieleski,* and G. R. Ringo

The aim of this project is to improve the present ion-microprobe analyzer very significantly in two respects—(1) space resolution and (2) mass resolution—to make it a much more useful instrument, particularly in biology. The ion-microprobe analyzer generally uses a beam of primary ions focused to a point whose diameter determines the space resolution of the instrument and is at present 1 to 2 μm. The primary beam is scanned over the specimen and a map of the distribution of an element or isotope of interest in the specimen is built up by detection of the secondary ions produced in the specimen and analyzed by a mass spectrometer of appropriate resolution, usually around 300.

We believe this instrument could be very useful in biology to map stable isotopes such as ^{13}C, ^{17}O, etc. used as tracers. However, for full usefulness it will be necessary to have enough mass resolution to distinguish ion pairs such as ^{17}O and ^{16}OH—about 5000—and the best practical space resolution—which might be as good as 100 Å. In the first phase of this project we devised an extraction system for efficient collection of the secondary ions and their injection into the small phase space accepted by a high-resolution (25 000) mass spectrometer.[1] The present phase is the production of a reasonably intense ion beam of 1000 Å or so diameter. We are trying to do this with a field evaporation (EHD) source using a liquid metal point formed by the applied electric field.

---

*Biological and Medical Research Division, ANL.

[1] V. E. Krohn and G. R. Ringo, Rev. Sci. Instr. 43, 1771 (1972).

We have made some progress toward understanding the operation of this type of source[2,3] and have built an optical bench for ions on which we can test sources and optical elements such as lenses. With its aid, we have studied an EHD source using cesium and gallium as these appeared to be the most interesting working fluids. We studied the effect of various electrode configurations near the source, methods of stabilizing the power supply, methods of starting the beam and variations of other parameters of the source such as temperature and hydrostatic pressure and have established operating conditions that give an effective brightness of about 10^4 A cm^{-2} str^{-1}.

The next phase of the project would be a study of the secondary ion spectra emitted by various biochemicals with various bombarding ions and with and without neutral cesium added to the organic surfaces in an attempt to increase the yield of negative ions. This is obviously important to the tracer scheme mentioned earlier but it may suggest a useful mode of microscopy itself if the spectra prove to be sufficiently distinctive. The final phase would be the construction of an instrument suitable for use in these new forms of microscopy.

In a somewhat separate effort[4] we have found with the aid of the Argonne's Applied Research Laboratory Ion-Microprobe Analyzer that with an oxygen-ion primary beam, at least, organic materials give very few H_2 ions (of either sign). This means that ^2H can be detected with little background with existing commercial ion microprobes and could be located with a resolution of a few micrometers in the plane of the specimen and, what is somewhat more interesting, with a resolution of roughly 20 Å in depth. Since the depth of focus of the microprobe beam is many μm, it would be possible to peel off successive layers with an ion beam and determine the depth beneath the surface of some

---

[2] V. E. Krohn, Appl. Phys. Lett. 23, 220 (1973).

[3] V. E. Krohn, J. Appl. Phys. 45, 1144 (1974).

[4] W. E. Kisieleski and G. R. Ringo, J. Microscopy, to be published.

labeled material even with a very irregular object—an isolated cell for example. While this technique is very limited in resolution, sensitivity and range of usable isotopes compared with the one we are hoping to develop, it is available immediately in at least 30 laboratories.

F. RADIATIVE SPECTRA, DECAY TIMES, AND COLLISION DYNAMICS OF HEAVY IONS

1. OKOROKOV EFFECT IN CHANNELING

D. S. Gemmell, R. E. Holland, J. M. Remillieux, and H. G. Berry

A fast ion beam channeled in a thin gold crystal sees a periodic interaction of the successive lattice planes. If the resonant frequency matches an atomic energy separation, resonant excitation might occur. We searched without success for the reported He^{+} ($n = 1 \rightarrow 4$) excitation, for N^{3+} ($2s \rightarrow 3p$) excitations, and also for possible charge-state resonances.

2. LIGHT POLARIZATION OF CHANNELED IONS

H. G. Berry and J. M. Remillieux

When 1.0-MeV Ne ions from the Dynamitron accelerator were allowed to pass through a thin gold crystal, the polarization of the emitted light from the emerging Ne^{2+} ions showed a dependence on channeling direction—a 4±1% effect for channeling versus nonchanneling directions. This result suggests that channeled ions are aligned along the channel direction and maintain this alignment on exiting the crystal. The selective alignment disappears as the surface becomes coated with carbon layers. Further experiments are in progress.

3. ORIENTATION OF FAST HEAVY-ION BEAMS

H. G. Berry and C. H. Batson

If a fast ion beam is excited by a thin carbon foil tilted at an angle other than 90° to the beam axis, then orientation of the ions can occur. Thus, excited Ne^{1+} and Ne^{2+} ions exciting such foils were

found to emit circularly polarized light. The degree of circular polarization which is directly proportional to the atomic orientation was investigated as a function of tilt angle and ion beam energy (1—4 MeV from the Dynamitron accelerator). In particular, we found that different excited states may emit photons that have opposing signs of circular polarization—i. e., that the angular momentum of the ions have different projections on directions along an axis perpendicular to the plane of the beam and foil normal.

Further experiments are proposed to test various possible theories of these surface interactions, and we hope eventually to investigate different crystalline, metallic, and nonmetallic surfaces.

4. CIRCULARLY POLARIZED QUANTUM BEATS

H. G. Berry, R. M. Schectman,* and L. J. Curtis*

Using tilted-foil excitation of $^{14}N^{+}$ beams at 2—3-MeV beam energies, a search was made for circularly-polarized zero-field quantum beats in the $3s\,^3S$-$3p\,^3P$ transition of N IV. Such quantum beats between the hyperfine levels F = 0 and F = 1 of the J = 1 fine structure level would give direct evidence of the tilted-foil surface interaction. First results show a very weak effect. With a perpendicular foil, linearly-polarized quantum beats have been observed between other hyperfine levels of the same transition resulting in the first measurement of a hyperfine interaction constant in nitrogen, other than for the neutral ground state.

*University of Toledo, Toledo, Ohio.

5. ELECTRIC FIELD QUANTUM BEATS

H. G. Berry, G. Gabrielse,* R. M. Schectman,† and L. J. Curtis†

Application of a longitudinal electric field to close-lying hydrogenic states of opposite parity induces quantum beats in the time-resolved radiative decay of the states. We have used the beam-foil technique to observe such quantum beats in n = 1—2, 1—3, 2—3, 2—4 in H I and n = 3—4 in He II. On reversing the field direction, the phases and amplitude of the beats may change. This indicates a coherence of the opposite parity states produced in the foil excitation. Thus, it has been shown that in all the above examples, the excited electron leaves the foil traveling faster, and slightly ahead of the nucleus.

We are searching for a theoretical model of the surface interaction which will explain both this effect and the orientation of atoms produced by the tilted foils.

---

*University of Chicago, Chicago, Illinois.

†University of Toledo, Toledo, Ohio.

6. HEAVY-ION SPECTROSCOPY AND LIFETIMES

H. G. Berry and C. H. Batson

The analysis of beam-foil spectra of chlorine (from the Dynamitron accelerator) in the visible region was completed, and radiative lifetimes measured in ions from Cl IV to Cl IX. The hydrogenic transitions n = 6—7, 7—8 of Cl VII were studied in relatively high resolution (5 in 10^4) to separate transitions from states of different angular momentum. From these observations, relative populations of excited states were obtained by use of our measured lifetimes, and additional transitions from excited core states were found.

Similar work has continued in vanadium and nickel and has been extended to the vacuum-ultraviolet region (500—2000 Å) with the

aid of a 1-meter near-normal incidence spectrometer. The vanadium V spectrum has been analyzed and lifetime measurements completed for many of the known terms. This alkali-like spectrum is of particular interest because of the already identified doubly-excited states of the $2p^5 3d$ core.

IX. PUBLICATIONS FROM 1 APRIL 1974 THROUGH 31 MARCH 1975

The papers listed here are those whose publication was noted by the reporting unit of the Laboratory in the 1-year period stated above. The dates on the journals therefore often precede this period, and some dated within the period will be listed subsequently. The list of "journal articles and book chapters," which also includes letters and notes, is classified by topic; the arrangement is approximately that followed in the Table of Contents of this Annual Review. The "reports at meetings" include abstracts, summaries, and full texts in volumes of proceedings; they are listed chronologically.

A. BOOK

1. SURFACE EFFECTS IN CONTROLLED FUSION (Proceedings of the Conference on Surface Effects in Controlled Thermonuclear Fusion Devices and Reactors, Argonne, Illinois, 10-12 January 1974) edited by H. Wiedersich,* M. S. Kaminsky, and K. M. Zwilsky† North-Holland, Amsterdam, 1974 [Reprinted from J. Nucl. Mater. 53 (1974)]

---

*Materials Science Division, ANL.

†USAEC, Washington, D.C.

B. PUBLISHED JOURNAL ARTICLES AND BOOK CHAPTERS

1. MEASUREMENT OF KAONIC x RAYS FROM Al, Si, Ni AND Cu
   P. D. Barnes,* R. A. Eisenstein,* W. C. Lam,* J. Miller,* R. B. Sutton,* M. Eckhause,† J. R. Kane,† R. E. Welsh,† D. A. Jenkins,‡ R. J. Powers,‡ A. R. Kunselman,§ R. P. Redwine, and R. E. Segel
   Nucl. Phys. A231, 477-492 (1974)

2. OBSERVATION OF ANTIPROTONIC x RAYS IN ^{6}Li AND ^{4}He
   M. Eckhause,† J. R. Kane,† B. L. Roberts,† R. E. Welsh,† R. P. Redwine, R. E. Segel, P. D. Barnes,* R. A. Eisenstein,* W. C. Lam,* J. Miller,* R. B. Sutton,* D. A. Jenkins,‡ R. J. Powers,‡ and A. R. Kunselman§
   Phys. Rev. C 11, 1056-1058 (March 1975)

3. DIP IN THE ^{12}C(^{12}C,α)^{20}Ne CROSS SECTION AT $E_{c.m.}$ = 19.2 MeV
   L. R. Greenwood, H. T. Fortune, R. E. Segel, and J. R. Erskine
   Phys. Rev. C 10, 1211-1212 (September 1974)

4. NONPECULIAR BEHAVIOR OF THE (^{16}O,^{12}C) TRANSFER REACTION IN THE s-d SHELL
   J. R. Erskine, W. Henning, D. G. Kovar, L. R. Greenwood, and R. M. DeVries‖
   Phys. Rev. Lett. 34, 680-683 (17 March 1975)

5. ELASTIC AND INELASTIC SCATTERING OF HEAVY IONS
   R. H. Siemssen
   Chap. IV.C.1 in Nuclear Spectroscopy and Reactions, Part B, edited by Joseph Cerny (Academic, New York, 1974), pp. 233-278

6. MEASUREMENT OF THE REACTION ^{48}Ca(^{16}O,^{15}C)^{49}Ti
   D. G. Kovar, W. Henning, B. Zeidman, Y. Eisen, and H. T. Fortune
   Phys. Rev. Lett. 33, 1611-1614 (30 December 1974)

---

*Carnegie-Mellon University, Pittsburgh, Pennsylvania.

†College of William and Mary, Williamsburg, Virginia.

‡Virginia Polytechnic Institute and State University, Blacksburg, Virginia.

§University of Wyoming, Laramie, Wyoming.

‖University of Rochester, Rochester, New York.

7. L DEPENDENCE IN ANGULAR DISTRIBUTIONS OF THE TWO-PROTON TRANSFER REACTION $^{48}Ca(^{16}O,^{14}C)^{50}Ti$
W. Henning, D. G. Kovar, B. Zeidman, and J. R. Erskine
Phys. Rev. Lett. 32, 1015-1019 (6 May 1974)

8. SPIN DETERMINATION FROM ANGULAR STRUCTURE OF $p_{1/2}$ PROTON TRANSFER IN THE $^{48}Ca(^{15}N,^{14}C)^{49}Sc$ REACTION
W. Henning, D. G. Kovar, J. R. Erskine, and L. R. Greenwood
Phys. Lett. 55B, 49-52 (20 January 1975)

9. CROSS SECTIONS FOR THE $^{7}Li(d,p)^{8}Li$, $^{6}Li(^{3}He,n)^{8}B$, $^{6}Li(d,\alpha)^{4}He$, $^{6}Li(d,p)^{7}Li$, AND $^{6}Li(d,n)^{7}Be$ REACTIONS
Charles R. McClenahan and Ralph E. Segel
Phys. Rev. C 11, 370-382 (February 1975)

10. RADIATIVE PROTON CAPTURE STUDY OF THE GIANT DIPOLE RESONANCE IN $^{55,57}Co$
J. V. Maher, L. Meyer-Schützmeister, E. L. Sprenkel-Segel, D. von Ehrenstein, R. J. Nemanich, G. C. Kiang, J. F. Tonn,* and R. E. Segel
Phys. Rev. C 9, 1440-1445 (April 1974)

11. LEVEL STRUCTURE OF ^{76}As
J. F. Lemming,† J. Rapaport,† and A. J. Elwyn
Nucl. Phys. A239, 412-426 (3 March 1975)

12. SYSTEMATICS OF THE $(^{3}He,p)$ REACTION ON SOME f-SHELL NUCLEI
Gerald Hardie, David Gloeckner, L. Meyer-Schützmeister, and T. H. Braid
Phys. Rev. C 10, 1829-1845 (November 1974)

13. NEUTRON STRENGTH OF THE 5.08-MeV $\frac{3}{2}^{+}$ STATE OF ^{17}O
H. T. Fortune and C. M. Vincent‡
Phys. Rev. C 10, 1233-1235 (September 1974)

14. SPIN AND PARITY OF THE 3.52-MeV STATE OF ^{16}N
H. T. Fortune, L. R. Medsker,§ J. N. Bishop,§ and S. C. Headley§
Phys. Rev. C 11, 304-307 (February 1975)

---

*Northwestern University, Evanston, Illinois.

†Ohio University, Athens, Ohio.

‡University of Pittsburgh, Pittsburgh, Pennsylvania.

§University of Pennsylvania, Philadelphia, Pennsylvania.

15. STRUCTURE OF 0^+ STATES IN ^{18}O
H. T. Fortune and S. C. Headley*
Phys. Lett. 51B, 136-138 (22 July 1974)

16. 4^+ AND 6^+ CORE-EXCITED STATES IN ^{20}Ne
H. T. Fortune, L. R. Greenwood, R. E. Segel, and J. R. Erskine
Phys. Lett. 52B, 51-53 (16 September 1974)

17. MATRIX ELEMENTS FOR THE $1d_{3/2}$-$1f_{7/2}$ INTERACTION AND THE $^{37}Cl(d,p)^{38}Cl$ AND $^{39}K(d,p)^{40}K$ REACTIONS
C. L. Fink and J. P. Schiffer
Nucl. Phys. A225, 93-108 (1974)

18. STUDY OF ^{249}Bk, ^{241}Am, AND ^{231}Pa WITH PROTON TRANSFER REACTIONS
J. R. Erskine, G. Kyle,† R. R. Chasman,‡ and A. M. Friedman‡
Phys. Rev. C 11, 561-579 (February 1975)

19. ANOMALIES IN THE $^{72}Ge(\alpha,n)^{75}Se$ REACTION NEAR ISOBARIC ANALOG RESONANCES IN ^{76}Se
A. J. Elwyn, J. E. Monahan, J. F. Lemming,§ J. Rapaport,§ and M. Sample§
Phys. Rev. C 10, 1939-1947 (November 1974)

20. ANOMALOUS POPULATION OF TWO 4^+ STATES IN $^{12}C(^6Li,d)^{16}O$
P. T. Debevec, H. T. Fortune, R. E. Segel, and J. F. Tonn
Phys. Rev. C 9, 2451-2453 (June 1974)

21. $^{92,98}Mo(d,\alpha)^{90,96}Nb$ REACTIONS AND PARTICLE-HOLE MULTIPLETS
J. R. Comfort, H. T. Fortune, G. C. Morrison, and J. V. Maher
Phys. Rev. C 10, 2399-2415 (December 1974)

22. MASSES OF TECHNETIUM ISOTOPES
J. R. Comfort,§ R. W. Finlay,§ C. M. McKenna,§ and P. T. Debevec
Phys. Rev. C 10, 1236-1238 (September 1974)

23. UNBOUND STATES IN ^{29}Si WITH THE $^{28}Si(d,p)$ REACTION
L. R. Medsker, H. E. Jackson, and J. L. Yntema
Phys. Rev. C 9, 1851-1856 (May 1974)

---

*University of Pennsylvania, Philadelphia, Pennsylvania.

†University of Minnesota, Minneapolis, Minnesota.

‡Chemistry Division, ANL.

§Ohio University, Athens, Ohio.

24. DECAY OF THE 22-μs ISOMERIC STATE OF ^{38}K
S. W. Yates,* F. J. Lynch, R. E. Holland, I. Ahmad,* and A. M. Friedman*
Phys. Rev. C 9, 1857-1860 (May 1974)

25. LIFETIMES OF THE $\frac{1}{2}+[631] \rightarrow \frac{5}{2}+[622]$ E2 TRANSITIONS IN SOME ACTINIDE NUCLEI
S. W. Yates,* I. Ahmad,* A. M. Friedman,* F. J. Lynch, and R. E. Holland
Phys. Rev. C 11, 599-606 (February 1975)

26. MICROSCOPIC FORM FACTOR CALCULATIONS FOR THE QUASI-ELASTIC (^{6}Li,^{6}He) REACTIONS
W. R. Wharton and P. T. Debevec
Phys. Lett. 51B, 447-450 (2 September 1974)

27. CORRESPONDENCE BETWEEN ZERO ANGULAR MOMENTUM TRANSFER CROSS SECTIONS OF (^{6}Li,^{6}He) REACTIONS AND THE GAMOW-TELLER STRENGTH
W. R. Wharton and P. T. Debevec
Phys. Lett. 51B, 451-453 (2 September 1974)

28. A HIGH-RESOLUTION MASS-IDENTIFICATION SYSTEM FOR HEAVY IONS
B. Zeidman, W. Henning, and D. G. Kovar
Nucl. Instrum. Methods 118, 361-365 (1974)

29. HEAVY ION STRIPPING IN TANDEM ACCELERATOR TERMINALS
J. L. Yntema
Nucl. Instrum. Methods 122, 45-52 (1974)

30. CHARACTERISTICS OF A HIGH-PURITY GERMANIUM DETECTOR
George E. Thomas and Richard H. Pehl†
Nucl. Instrum. Methods 121, 65-67 (1974)

31. CORRECTION FOR A RESONANCE-CAPTURE COMPONENT IN THERMAL-NEUTRON-CAPTURE GAMMA-RAY SPECTRA
Gerald D. Loper, George E. Thomas, and Lowell M. Bollinger
Nucl. Instrum. Methods 121, 581-587 (1 November 1974)

32. G_A/G_V MEASURED IN THE DECAY OF POLARIZED NEUTRONS
V. E. Krohn and G. R. Ringo
Phys. Lett. 55B, 175-177 (3 February 1975)

---

*Chemistry Division, ANL.

†Lawrence Berkeley Laboratory, University of California, Berkeley, California.

33. CAPTURE GAMMA RAYS FROM HIGH-SPIN STATES EXCITED BY THERMAL-NEUTRON CAPTURE IN NUCLEAR ISOMERS
Bernard Hamermesh* and Robert K. Smither
Phys. Rev. C 11, 827-828 (March 1975)

34. ^{180}Hf ENERGY LEVELS DEDUCED FROM THERMAL AND AVERAGE RESONANCE NEUTRON-CAPTURE γ-RAY SPECTRA
D. L. Bushnell, D. J. Buss, and Robert K. Smither
Phys. Rev. C 10, 2483-2511 (December 1974)

35. ALPHA-PARTICLE SPECTROSCOPIC AMPLITUDES IN THE j-j COUPLED SHELL MODEL
D. Kurath and I. S. Towner†
Nucl. Phys. A222, 1-12 (1 April 1974)

36. THREE-NUCLEON TRANSFER FOR THE 1p SHELL
D. Kurath and D. J. Millener‡
Nucl. Phys. A238, 269-286 (3 February 1975)

37. NEUTRON-RICH ARGON NUCLEI
D. H. Gloeckner, R. D. Lawson, and F. J. D. Serduke
Phys. Rev. C 9, 2071-2073 (May 1974)

38. SPURIOUS CENTER-OF-MASS MOTION
D. H. Gloeckner and R. D. Lawson
Phys. Lett. 53B, 313-318 (23 December 1974)

39. VISCOSITY IN HEAVY ION REACTIONS DEMONSTRATED FOR $^{16}O + ^{16}O$
D. Glas§ and U. Mosel
Phys. Lett. 49B, 301-304 (29 April 1974)

40. LIMITATION ON COMPLETE FUSION DURING HEAVY-ION COLLISIONS
D. Glas§ and U. Mosel
Phys. Rev. C 10, 2620-2622 (December 1974)

---

*Cleveland State University, Cleveland, Ohio.

†Chalk River Nuclear Laboratories, Atomic Energy of Canada Limited, Chalk River, Ontario, Canada.

‡Nuclear Physics Laboratory, Oxford, England.

§University of Giessen, Giessen, Germany.

41. RELATIVISTIC EFFECTS IN PHENOMENOLOGICAL NUCLEON-NUCLEON POTENTIALS AND NUCLEAR MATTER
F. Coester, Steven C. Pieper, and F. J. D. Serduke
Phys. Rev. C 11, 1-18 (January 1975)

42. CROSS SECTIONS IN THE QUANTUM THEORY OF SCATTERING
F. Coester
Physical Reality and Mathematical Description, edited by C. P. Enz and J. Mehra (Reidel Publishing Co., 1974), pp. 313-320

43. EINSTEIN'S EQUIVALENCE PRINCIPLE. AN EXPLICIT STATEMENT AND ITS DERIVATION FROM SPECIAL RELATIVISTIC PRE-SYMMETRY
Y. Avishai and H. Ekstein
Commun. Math. Phys. 37, 193-220 (1974)

44. NUCLEAR STRUCTURE OF LIGHT NUCLEI USING THE SELECTIVITY OF HIGH ENERGY TRANSFER REACTIONS WITH HEAVY IONS
N. Anyas-Weiss,* J. C. Cornell,* P. S. Fisher,* P. N. Hudson,* A. Menchaca-Rocha,* D. J. Millener,* A. D. Panagiotou,* D. K. Scott,* D. Strottman,* D. M. Brink,† B. Buck,† P. J. Ellis, and T. Engeland‡
Phys. Lett. 12C, 201-272 (1974)

45. TRANSFER REACTIONS
M. H. Macfarlane and J. P. Schiffer
Chap. IV. B. 2 in Nuclear Spectroscopy and Reactions, Part B, edited by Joseph Cerny (Academic, New York, 1974), pp. 169-194

46. SELF-CONSISTENT CALCULATIONS FOR HIGHLY EXCITED COMPOUND NUCLEI
U. Mosel, P.-G. Zint, and K. H. Passler§
Nucl. Phys. A236, 252-268 (23 December 1974)

---

*Nuclear Physics Laboratory, Oxford, England.

†Department of Theoretical Physics, Oxford, England.

‡University of Oslo, Norway.

§University of Giessen, Giessen, Germany.

47. STABILIZATION OF THE CHARGED VACUUM CREATED BY VERY STRONG ELECTRICAL FIELDS IN NUCLEAR MATTER
Berndt Müller,* and Johann Rafelski
Phys. Rev. Lett. 34, 349-352 (10 February 1975)

48. MEASUREMENT OF RESONANCES IN ATOMIC OXYGEN BY ELECTRON TRANSMISSION SPECTROSCOPY
D. Spence,† and W. A. Chupka
Phys. Rev. A 10, 71-73 (July 1974)

49. PHOTOIONIZATION STUDY OF THE REACTION $O_2^+(a^4\Pi_u)$ WITH O_2
P. M. Dehmer and W. A. Chupka
J. Chem. Phys. 62, 2228-2234 (15 March 1975)

50. PHOTOIONIZATION OF ATOMIC NITROGEN
P. M. Dehmer, J. Berkowitz, and W. A. Chupka
J. Chem. Phys. 60, 2676-2679 (1 April 1974)

51. NONSTATISTICAL EMISSION FROM METASTABLE AUTOIONIZING STATES OF OI
P. M. Dehmer and W. A. Chupka
J. Chem. Phys. 62, 584-591 (15 January 1975)

52. PHOTOELECTRON SPECTROSCOPY OF HIGH TEMPERATURE VAPORS. V. HeI SPECTRA OF GaX_3 AND InX_3 (X = Cl, Br, I)
J. L. Dehmer,† J. Berkowitz, L. C. Cusachs,‡ and H. S. Aldrich§
J. Chem. Phys. 61, 594-599 (15 July 1974)

53. PARTIAL PHOTOIONIZATION CROSS SECTIONS FOR Hg BETWEEN 600 AND 250 Å. EFFECT OF SPIN-ORBIT COUPLING ON THE $^2D_{5/2}/^2D_{3/2}$ BRANCHING RATIO OF Hg
J. L. Dehmer† and J. Berkowitz
Phys. Rev. A 10, 484-490 (August 1974)

54. ON THE PHOTOELECTRON SPECTRA OF ALKALI HALIDE VAPORS
J. Berkowitz, J. L. Dehmer,† and T. E. H. Walker
J. Electron Spectrosc. 3, 323-325 (1974)

---

*University of Washington, Seattle, Washington.

†Radiological and Environmental Research Division, ANL.

‡Loyola University, Chicago, Illinois.

§St. Mary's Dominican College, New Orleans, Louisiana.

55. VALENCE SHELL EXCITATION ACCOMPANYING PHOTOIONIZATION IN MERCURY
J. Berkowitz, J. L. Dehmer,* Y.-K. Kim,* and J. P. Desclaux†
J. Chem. Phys. 61, 2556-2559 (1 October 1974)

56. PES OF HIGH-TEMPERATURE VAPORS. VI. 304 Å AND 584 Å PES OF Zn, Cd, AND Hg HALIDES AND THE ELECTRONEGATIVITY SCALE
J. Berkowitz
J. Chem. Phys. 61, 407-413 (1 July 1974)

57. EFFECT OF TEMPERATURE ON FIRST WALL EROSION BY RADIATION BLISTERING
M. Kaminsky and S. K. Das
Nuclear Technology 22, 373-378 (June 1974)

58. NUCLEAR AND ATOMIC MOMENTS AND HYPERFINE-STRUCTURE PARAMETERS OF ^{253}Es AND ^{254m}Es
L. S. Goodman, H. Diamond,‡ and H. E. Stanton
Phys. Rev. A 11, 499-504 (February 1975)

59. COMPOSITION OF THE Ir I ATOMIC GROUND STATE, AND NUCLEAR ELECTRIC-QUADRUPOLE MOMENTS OF ^{191}Ir AND ^{193}Ir
W. J. Childs, M. Fred,‡ E. Schrödl,§ and Th. A. M. van Kleef‖
Phys. Rev. A 10, 1028-1033 (October 1974)

60. ULTRASENSITIVE DETECTION OF Cs VAPOR BY INTRACAVITY LASER QUENCHING
W. J. Childs, M. S. Fred,‡ and L. S. Goodman
Applied Optics 13, 2297 (1974)

61. HYPERFINE STRUCTURE MEASUREMENTS IN THE GROUND STATES $^5F_5$, $^5F_4$, $^5F_3$, AND $^5F_2$ OF ^{99}Ru AND ^{101}Ru WITH THE ATOMIC-BEAM MAGNETIC-RESONANCE METHOD
S. Büttgenbach,§ M. Herschel,§ G. Meisel,§ E. Schrödl,§ W. Witte,§ and W. J. Childs
Z. Phys. 269, 189 (1974)

---

*Radiological and Environmental Research Division, ANL.

†Institut Max von Laue—Paul Langevin, Grenoble, France.

‡Chemistry Division, ANL.

§University of Bonn, Bonn, Germany.

‖Zeeman Laboratory, Amsterdam, The Netherlands.

62. GROUND STATE HYPERFINE STRUCTURE OF ^{95}Mo AND ^{97}Mo
S. Büttgenbach,* M. Herschel,* G. Meisel,* E. Schrödl,* W. Witte,* and W. J. Childs
Z. Phys. 266, 271 (1974)

63. HYPERFINE INTERACTIONS AND NUCLEAR MOMENTS IN EVEN URANIUM ISOTOPES FROM MÖSSBAUER SPECTROSCOPY
R. D. Meeker,† G. M. Kalvius,† B. D. Dunlap,† S. L. Ruby, and D. Cohen‡
Nucl. Phys. A224, 429-436 (27 May 1974)

64. EQUILIBRIUM POSITIONS OF Au ATOMS IN Sn CRYSTALS AS DETERMINED BY A CHANNELING TECHNIQUE
J. W. Miller,§ D. S. Gemmell, R. E. Holland, J. C. Poizat, J. N. Worthington, and R. E. Loess§
Phys. Rev. B 11, 990-994 (1 February 1975)

65. LAMB SHIFT AND FINE STRUCTURE OF 3s ^{3}S-3p ^{3}P IN N VI
H. G. Berry‖ and R. M. Schectman
Phys. Rev. A 9, 2345-2349 (June 1974)

66. BEAM-FOIL OBSERVATIONS OF Na I DOUBLY-EXCITED STATES
H. G. Berry, R. Hallin,¶ R. Sjödin,¶ and M. Gaillard**
Phys. Lett. 50A, 191-192 (2 December 1974)

67. FAILURE TO OBSERVE COHERENT EFFECTS IN THE EXCITATION OF CHANNELED IONS
H. G. Berry,‖ D. S. Gemmell, R. E. Holland, J.-C. Poizat, J. Remillieux, and J. N. Worthington
Phys. Lett. 49A, 123-124 (26 August 1974)

68. TESTS OF THE FINAL SURFACE ELECTROSTATIC INTERACTION IN BEAM—TILTED-FOIL EXPERIMENTS
H. G. Berry, L. J. Curtis,†† and R. M. Schectman††
Phys. Rev. Lett. 34, 509-512 (3 March 1975)

---

*University of Bonn, Bonn, Germany.

†Solid State Science Division, ANL.

‡Chemistry Division, ANL.

§Materials Science Division, ANL.

‖University of Chicago, Chicago, Illinois.

¶University of Uppsala, Uppsala, Sweden.

**Université de Lyon, Lyon, France.

††University of Toledo, Toledo, Ohio.

69. COMPUTER SIMULATION OF RADIOFREQUENCY CONFINEMENT OF A PLASMA
Albert J. Hatch and J. L. Shohet
Physics of Fluids 17, 232-239 (January 1974)

70. MULTIPLE RING DISCHARGES IN A CYLINDRICAL RESONANT CAVITY
J. R. Hamann, A. J. Hatch, and J. L. Shohet,*
IEEE Trans. Plasma Sci. PS-2, 241-249 (December 1974)

71. USE OF ^{244}Cm AND ^{145}Pm AS SOURCES FOR BONE MINERALIZATION STUDIES
A. M. Friedman,† B. G. Oltman,‡ J. Kastner,‡ K. F. Eckerman,‡ and L. S. Goodman
J. of Nuclear Medicine 15, 335-337 (May 1974)

72. THE JUSTIFICATION OF SCIENCE TO SCIENTISTS—A REMINDER OF WHY THE ENTERPRISE WAS LAUNCHED
Roy Ringo
Bull. Atomic Scientists 31(3), 29-33 (March 1975)

73. COMMENTS ON PAPERS BY RYCE ET AL. ON THE ELECTROSTATIC DISPERSION OF LIQUIDS
V. E. Krohn
Can. J. Phys. 52, 1046-1047 (1974)

C. PUBLISHED REPORTS AT MEETINGS

International Meeting on Perspectives of Neutron Spectroscopy, Dubna, USSR, 13-16 October 1970

1. NEUTRON-CAPTURE GAMMA RAYS
L. M. Bollinger
Problems of Elementary Particles and Atomic Nucleus Physics, Vol. 2, Part 4 (Joint Institute for Nuclear Research, Dubna, 1972), pp. 885-916

---

*University of Wisconsin, Madison, Wisconsin.

†Chemistry Division, ANL.

‡Radiological and Environmental Research Division, ANL.

Nuclear Structure Study with Neutrons (Proceedings of the International Conference, Budapest, Hungary, 31 July-5 August 1972), edited by J. Erő and J. Szűcs (Plenum Press, 1974)

2. THE (n, γ) SPECTROSCOPY
Lowell M. Bollinger
pp. 347-370

The Nuclear Many-Body Problem (Proceedings of the International Symposium on "Present Status and Novel Developments in the Nuclear Many-Body Problem," Roma, 19-23 September 1972, edited by F. Calogero and C. Ciofi Degli Atti (Editrice Compositori, Bologna, 1973)

3. COLLAPSED NUCLEI AND NUCLEAR COLLAPSE
A. R. Bodmer
Vol. 2, pp. 505-532 + discussion on pp. 533-534

4. Λ-PARTICLE BINDING IN NUCLEAR MATTER
A. R. Bodmer and D. M. Rote*
Vol. 2, pp. 567-583 + discussion on p. 584

Scattering Theory in Mathematical Physics (Proceedings of the NATO Advanced Study Institute, Denver, Colorado, 11-29 June 1973), edited by J. A. LaVita and J.-P. Marchand (Reidel Publishing Co., 1974)

5. HISTORY AND PERSPECTIVES IN SCATTERING THEORY. A STRICTLY PERSONAL VIEW
Hans Ekstein
pp. 383-389

Fifth Conference of the European Group for Atomic Spectroscopy (EGAS), Lund, Sweden, 10-13 July 1973, edited by K. Bockasten (University of Lund, 1973), Summaries of Contributions

6. CONFIGURATION INTERACTION IN THE ATOMIC GROUND STATE MULTIPLETS OF ^{11}B AND ^{45}Sc. ZEEMAN EFFECT MEASUREMENTS IN THE $^3P_2$ METASTABLE STATE OF ^{88}Sr
R. Aldenhoven,† R. Aydin,† W. Dankwort,† L. Degener,† J. Ferch,† H. Gebauer,† G. Meisel,† S. Penselin,† H. Walther,† and W. J. Childs
No. 37

7. HYPERFINE STRUCTURE INVESTIGATIONS OF HIGHLY REFRACTORY ELEMENTS WITH THE ATOMIC-BEAM MAGNETIC-RESONANCE METHOD
S. Büttgenbach,† M. Herschel,† G. Meisel,† E. Schrödl,† W. Witte,† and W. J. Childs
No. 38

---

*Energy and Environmental Systems Division, ANL.

†University of Bonn, Bonn, Germany.

Proceedings of the International Conference on Nuclear Physics, Munich, 27 August-1 September 1973, edited by J. de Boer and H. J. Mang (North-Holland, Amsterdam, 1973)

8. TRANSFER REACTIONS WITH ^{19}F
   C. L. Fink, G. C. Morrison, and J. L. Yntema
   Vol. 1, Contributed Papers, p. 460

9. EXPERIMENTAL STUDIES OF MEDIUM AND HEAVY K^- ATOMS
   J. Fox,* W. C. Lam,* P. D. Barnes,† R. A. Eisenstein,† J. Miller,† R. Sutton,† M. Eckhause,‡ J. Kane,‡ B. L. Roberts,‡ R. E. Welsh,‡ R. P. Redwine, R. E. Segel, D. A. Jenkins,§ R. J. Powers,§ and R. Kunselman‖
   Vol. 1, Contributed Papers, p. 316

10. (^{6}Li,d) REACTION ON ^{40}Ca
    H. W. Fulbright,¶ R. G. Markham,¶ R. N. Horoshko,¶ U. Strohbusch, C. L. Fink, and B. Zeidman
    Vol. 1, Contributed Papers, p. 480

11. $^{12}C(^{12}C,\alpha)^{20}Ne$ EXCITATION FUNCTIONS AND STATISTICAL ANALYSIS
    L. R. Greenwood, R. E. Segel, and J. R. Erskine
    Vol. 1, Contributed Papers, p. 543

12. INTERACTION OF FAST NEGATIVE PIONS WITH ^{60}Ni
    H. E. Jackson, L. Meyer-Schützmeister, T. P. Wangler, R. P. Redwine, R. E. Segel, J. P. Schiffer, and J. Tonn**
    Vol. 1, Contributed Papers, p. 679

13. CONFERENCE SUMMARY
    J. P. Schiffer
    Vol. 2, Invited Papers, pp. 813-836

---

*Brookhaven National Laboratory, Upton, L.I., New York.

†Carnegie-Mellon University, Pittsburgh, Pennsylvania.

‡College of William and Mary, Williamsburg, Virginia.

§Virginia Polytechnic Institute, Blacksburg, Virginia.

‖University of Wyoming, Laramie, Wyoming.

¶Nuclear Structure Research Laboratory, Rochester, New York.

**Northwestern University, Evanston, Illinois.

Nuclear Physics, Munich (Contd.)

14. HIGH SPIN STATES IN ^{41}Ca: $K=\frac{3}{2}^+$ AND $K=\frac{3}{2}^-$ ROTATIONAL BANDS?
Kamal K. Seth,* A. Saha,* and L. Greenwood
Vol. 1, Contributed Papers, p. 143

15. SEARCH FOR STATES OF THE ^{16}O-^{12}C CONFIGURATION IN ^{28}Si
W. R. Wharton, P. T. Debevec, and J. P. Schiffer
Vol. 1, Contributed Papers, p. 541

Order-Disorder Transformations in Alloys (Proceedings of the International Symposium, Tübingen, Germany, 3-6 September 1973), edited by H. Warlimont (Springer-Verlag, 1974)

16. ON STRUCTURAL INTERPRETATION OF SHORT RANGE ORDER
S. K. Das and G. Thomas†
pp. 332-343

Proceedings of the Conference on Surface Effects in Controlled Thermonuclear Fusion Devices and Reactors, Argonne, Illinois, 10-12 January 1974

17. RADIATION BLISTERING OF STRUCTURAL MATERIALS FOR FUSION DEVICES AND REACTORS
S. K. Das and M. Kaminsky
J. Nucl. Mater. 53, 115-126 (1974)
+ Surface Effects in Controlled Fusion (Proceedings of the Conference), edited by H. Wiedersich, M. S. Kaminsky, and K. M. Zwilsky (North-Holland, Amsterdam, 1974), pp. 115-126 [Reprinted from J. Nucl. Mater. 53, 115-126 (1974)]

18. PARTICLE EMISSION FROM SOLIDS UNDER 14-MeV NEUTRON IMPACT
M. Kaminsky and S. K. Das
J. Nucl. Mater. 53, 162-170 (1974)
+ Surface Effects in Controlled Fusion, pp. 162-170 [Reprinted from J. Nucl. Mater. 53, 162-170 (1974)]

---

*Northwestern University, Evanston, Illinois.

†Lawrence Berkeley Laboratory and University of California, Berkeley, California.

Mössbauer Effect Methodology, Vol. 9 (Proceedings of the Ninth Symposium, Chicago, 3 February 1974), edited by I. J. Gruverman, C. W. Seidel, and D. K. Dieterly (Plenum, New York, 1974)

19. CURVE FITTING AND THE TRANSMISSION INTEGRAL: WARNINGS AND SUGGESTIONS
G. K. Shenoy,* J. M. Friedt,* H. Maletta,† and S. L. Ruby
pp. 277-305

Electrostatic and Electromagnetic Confinement of Plasmas and the Phenomenology of Relativistic Electron Beams, Proceedings of the Conference, New York, 4-7 March 1974 (Ann. N.Y. Acad. Sci., Vol. 251), edited by L. C. Marshall and H. L. Sahlin (New York Academy of Sciences, 1975)

20. PROPERTIES OF RADIOFREQUENCY-CONFINED PLASMAS
Albert J. Hatch
pp. 394-406

Proceedings of the EANDC Topical Discussion on "Critique of Nuclear Models and Their Validity in the Evaluation of Nuclear Data," Tokyo, Japan, 27 March 1974, edited by T. Fuketa (Japan Atomic Energy Research Institute, February 1975), Report No. NEANDC(J)38L

21. STATUS OF PREDICTIONS OF PHOTON STRENGTH FUNCTIONS BY GIANT DIPOLE RESONANCE AND VALENCE MODELS
H. E. Jackson
p. 119

Proceedings of a Symposium on Very High Level Languages, Santa Monica, California, 28-29 March 1974

22. SPEAKEASY—AN EVOLUTIONARY SYSTEM
S. Cohen
SIGPLAN Notices 9(4), 118-126 (April 1974)

Proceedings of the First Topical Meeting on the Technology of Controlled Nuclear Fusion, San Diego, California, 16-18 April 1974, edited by G. R. Hopkins (National Technical Information Service, U.S. Department of Commerce, Springfield, Virginia, 1974), CONF-740402-P2

23. EROSION OF SILICON CARBIDE SURFACES UNDER HELIUM ION AND 14 MeV NEUTRON IRRADIATIONS
M. Kaminsky and S. K. Das
Vol. II, pp. 508-516

---

*Centre de Recherches Nucléaires, Strasbourg, France.

†Institut für Festkorperforschung der Kernforschungsanlage, Julich, Germany.

American Physical Society, Washington, D.C., 22-25 April 1974

24. EXCITATION OF OUTGOING PARTICLES IN HEAVY-ION-INDUCED REACTIONS
H. T. Fortune, W. Henning, D. G. Kovar, and B. Zeidman
Bull. Am. Phys. Soc. 19, 504 (1974)

25. STATISTICAL MODEL CALCULATIONS FOR THE $^{12}C(^{12}C,\alpha)^{20}Ne$ REACTION
L. R. Greenwood
Bull. Am. Phys. Soc. 19, 548 (1974)

26. SENSITIVITY OF TRANSFER ANGULAR DISTRIBUTIONS TO THE DISTORTING POTENTIAL
W. Henning, D. G. Kovar, B. Zeidman, J. R. Erskine, and H. T. Fortune
Bull. Am. Phys. Soc. 19, 504 (1974)

27. THE $Ti^{48}(He^3,t)V^{48}$ REACTION
J. C. Manthuruthil,* C. P. Poirier,* and L. Meyer-Schützmeister
Bull. Am. Phys. Soc. 19, 545 (1974)

28. MEASUREMENT OF g FACTOR OF 10-μsec ISOMERIC STATE OF ^{115}Te
R. J. Mitchell,† T. V. Ragland,† R. P. Scharenberg,† F. J. Lynch, and R. E. Holland
Bull. Am. Phys. Soc. 19, 474 (1974)

29. $^{12}C(^{12}C,\alpha)^{20}Ne$ ANGULAR DISTRIBUTIONS
R. E. Segel, L. R. Greenwood, M. A. Lee, and K. Raghunathan
Bull. Am. Phys. Soc. 19, 548 (1974)

30. ABSOLUTE CAPTURE CROSS SECTIONS AND γ-RAY INTENSITIES FOR $^{113}Cd(n,\gamma)^{114}Cd$ AND $^{149}Sm(n,\gamma)^{150}Sm$
R. K. Smither and G. E. Thomas
Bull. Am. Phys. Soc. 19, 525 (1974)

31. A SENSITIVE TEST OF THE $(^6Li,^6He)$ REACTION MECHANISM USING THE $^{30}Si(^6Li,^6He)^{30}P$ REACTION
W. R. Wharton, P. T. Debevec, and L. Meyer-Schützmeister
Bull. Am. Phys. Soc. 19, 499 (1974)

---

*Aerospace Research Laboratories, Wright-Patterson Air Force Base, Ohio.

†Purdue University, Lafayette, Indiana.

9th International Conference on High Energy Accelerators, SLAC, Stanford University, Stanford, California, 2-7 May 1974 (U.S. Atomic Energy Commission, 1974), CONF-740522

32. DEVELOPMENT OF THE SUPERCONDUCTING HELIX FOR HEAVY-ION ACCELERATION
J. Aron,* R. Benaroya,* L. M. Bollinger, B. E. Clifft,* O. Despe,† A. H. Jaffey,* K. W. Johnson,* T. K. Khoe,‡ J. J. Livingood, P. J. Markovich,* J. M. Nixon,* G. W. Parker,* and W. A. Wesolowski*
pp. 159-163

Proceedings of the International Conference on Reactions Between Complex Nuclei, Vanderbilt University, Nashville, Tennessee, 10-14 June 1974, edited by R. L. Robinson, F. K. McGowan, J. B. Ball, and J. H. Hamilton (North-Holland, 1974)

33. MULTISTEP PROCESSES IN TRANSFER REACTIONS WITH ^{19}F
C. L. Fink, G. C. Morrison, and J. L. Yntema
Supplement to Vol. 1, Contributed Papers, p. 11

34. TRANSFER REACTION ON HEAVY NUCLEI ($A \geqslant 40$)
Dennis G. Kovar
Reactions Between Complex Nuclei, Vol. 2, Invited Papers, pp. 235-256

1974 NATO Advanced Study Institute on Ion-Molecule Interactions, Biarritz, France, 24 June-6 July 1974

35. EFFECTS OF INTERNAL ENERGY ON ION-MOLECULE REACTIONS
William A. Chupka
Interaction Between Ions and Molecules (Lectures presented at the Institute), edited by P. Ausloos (Plenum, New York, 1975), Series B: Vol. 6, pp. 249-262

---

*Chemistry Division, ANL.

†Electronics Division, ANL.

‡Accelerator Research Facilities Division, ANL.

4th International Conference on Atomic Physics, Heidelberg, Germany, 22-26 July 1974

36. STRUCTURE INFORMATION FROM ATOMIC-BEAM MAGNETIC-RESONANCE STUDIES OF MANY-ELECTRON ATOMS
William J. Childs
Atomic Physics 4 (Proceedings of the Conference), edited by G. zu Putlitz, E. W. Weber, and A. Winnacker (Plenum Press, New York, 1975), pp. 731-745

37. INTRACAVITY DYE LASER SPECTROSCOPY IN CONJUNCTION WITH THE ARGONNE 10 METER SPECTROGRAPH
L. S. Goodman and W. J. Childs
Abstracts of Contributed Papers, edited by J. Kowalski and H. G. Weber (University of Heidelberg, 1974), pp. 321-322

Proceedings of SHARE XLIII Conference, Chicago, 26-30 August 1974 (SHARE, Inc., 1974)

38. THE KAPPA RELEASE OF SPEAKEASY
Sai-Pak Chan,* Jane Clifford, Kathleen Gallagher, and Michael Stob
pp. 1532-1544

International Conference on the Applications of the Mössbauer Effect, Bendor, France, 2-6 September 1974

39. SERIAL STUDY OF LAKE MICHIGAN SEDIMENTS BY ^{57}Fe MÖSSBAUER SPECTROSCOPY
G. J. Perlow, W. Potzel, and D. Edgington†
Scientific Program Abstracts (International Union of Pure and Applied Physics, Imperial College, London SW7, U.K., 1974), pp. 230-231
+ Suppl. J. Phys. (Paris) 35, C6-547—548 (1974)

40. APPLICATION OF A METHOD OF FREQUENCY MODULATION MÖSSBAUER SPECTROSCOPY IN ^{67}Zn TO THE PRECISE DETERMINATION OF THE ELECTRIC QUADRUPOLE INTERACTION OF ^{67}ZnO
G. J. Perlow, W. Potzel, R. M. Kash,‡ and H. DeWaard
Scientific Program Abstracts, pp. 32-33
+ Suppl. J. Phys. (Paris) 35, C6-197—201 (1974)

---

*Applied Mathematics Division, ANL.

†Radiological and Environmental Research Division, ANL.

‡Electronics Division, ANL.

Applications of the Mössbauer Effect, Bendor, France (Contd.)

41. MÖSSBAUER EXPERIMENTS WITHOUT CONVENTIONAL SOURCES
S. L. Ruby
Scientific Program Abstracts, pp. 36-37
+ Suppl. J. Phys. (Paris) 35, C6-209—211 (1974)

Second International Symposium on Neutron Capture Gamma Ray Spectroscopy and Related Topics, Petten, The Netherlands, 2-6 September 1974

42. THRESHOLD PHOTONEUTRON SPECTRA
H. E. Jackson
Neutron Capture Gamma-Ray Spectroscopy (Proceedings of the Conference), edited by K. Abrahams, F. Stecher-Rasmussen and P. Van Assche (Reactor Centrum Nederland, Petten, The Netherlands, March 1975), pp. 437-458

43. ENERGY LEVELS IN THE ODD-N Sm ISOTOPES
R. K. Smither
Preprints of Papers, edited by P. M. Endt (State University, Utrecht) et al. (Dutch Ministry of Science and other organizations, 1974), pp. 133-137
+ Neutron Capture Gamma-Ray Spectroscopy, pp. 358-363

Proceedings of the International Conference on Nuclear Structure and Spectroscopy, Amsterdam, 9-13 September 1974, edited by H. P. Blok and A. E. L. Dieperink (Scholar's Press, Amsterdam, 1974)

44. SINGLE AND MULTI-NUCLEON TRANSFER REACTIONS
H. T. Fortune
Vol. 2, Invited Papers, pp. 341-387

45. NUCLEAR GAMMA AND BETA DECAY
R. D. Lawson
Vol. 2, Invited Papers, pp. 464-484

146th Meeting of The Electrochemical Society, New York, 13-17 October 1974

46. RADIATION BLISTERING IN SOLIDS
S. K. Das and M. Kaminsky
Abstract No. 161, p. 30
+ Extended Abstracts, Vol. 74-2 (Electrochemical Society, 1974), Abstract No. 161, pp. 388-389

Proceedings of the Third Conference on Application of Small Accelerators, North Texas State University, Denton, Texas, 21-23 October 1974, edited by J. L. Duggan and I. L. Morgan (National Technical Information Service, U.S. Department of Commerce, Springfield, Virginia, 1975), CONF-741040-P1

47. CTR RELATED SURFACE DAMAGE STUDIES USING SMALL ACCELERATORS
S. K. Das and M. Kaminsky
Vol. I, pp. 278-286

48. SITES OF Au ATOMS IN Sn CRYSTALS AS DETERMINED BY CHANNELING
J. W. Miller,* D. S. Gemmell, R. E. Holland, J.-C. Poizat, J. N. Worthington, and R. E. Loess*
Vol. I, pp. 132-138

MATCON '74 Conference and Materials Science Symposium '74 Abstracts, Detroit, Michigan, 21-24 October 1974 (American Society for Metals, 1974)

49. EFFECT OF VARIABLE ENERGY IMPLANTATION OF HELIUM PROJECTILES IN NIOBIUM ON BLISTER FORMATION
S. K. Das and M. Kaminsky
Abstract 68, p. 20

American Physical Society, Division of Plasma Physics, Albuquerque, New Mexico, 28-31 October 1974

50. NUMERICAL SIMULATION OF RF CONFINEMENT
A. J. Hatch, J. L. Shohet,† and S. J. Gitomer‡
Bull. Am. Phys. Soc. 19, 968 (October 1974)

American Physical Society, Division of Nuclear Physics, Pittsburgh, Pennsylvania, 31 October-2 November 1974

51. THE DISTRIBUTION OF GAMOW-TELLER STRENGTH IN ^{48}Sc FROM THE ^{48}Ca(^{6}Li,^{6}He)^{48}Sc REACTION
P. T. Debevec and W. R. Wharton
Bull. Am. Phys. Soc. 19, 989 (October 1974)

52. ANGULAR DISTRIBUTIONS OF THE ^{42}Ca(^{16}O,^{12}C)^{46}Ti AND ^{42}Ca(^{16}O,^{14}C)^{44}Ti REACTIONS
Y. Eisen, H. T. Fortune, W. Henning, D. G. Kovar, and B. Zeidman
Bull. Am. Phys. Soc. 19, 1024 (October 1974)

---

*Materials Science Division, ANL.

†University of Wisconsin, Madison, Wisconsin.

‡Los Alamos Scientific Laboratory, Los Alamos, New Mexico.

APS, Pittsburgh (Contd.)

53. AN INVESTIGATION OF THE $^{40}Ca(^{16}O,^{12}C)^{44}Ti$ REACTION
J. R. Erskine, W. Henning, and D. G. Kovar
Bull. Am. Phys. Soc. 19, 1024 (October 1974)

54. AN INVESTIGATION OF RECOIL EFFECTS IN THE $^{40}Ca(^{7}Li,^{6}Li)^{41}Ca$ REACTION
D. S. Gale, B. Zeidman, C. L. Fink, and K. Katori
Bull. Am. Phys. Soc. 19, 1024 (October 1974)

55. ONE- AND TWO-NEUTRON TRANSFER REACTIONS ON ^{48}Ca AND ^{42}Ca
W. Henning, Y. Eisen, H. T. Fortune, D. G. Kovar, and B. Zeidman
Bull. Am. Phys. Soc. 19, 1024 (October 1974)

56. STUDY OF THE $^{42}Ca(^{16}O,^{13,14,15}N)^{45,44,43}Sc$ REACTIONS
D. G. Kovar, Y. Eisen, H. T. Fortune, W. Henning, and B. Zeidman
Bull. Am. Phys. Soc. 19, 1024 (October 1974)

57. LEVEL STRUCTURE OF ^{76}As
J. F. Lemming,* J. Rapaport,* and A. J. Elwyn
Bull. Am. Phys. Soc. 19, 1002 (October 1974)

58. CORRESPONDENCE BETWEEN ZERO ANGULAR MOMENTUM TRANSFER CROSS SECTIONS OF $(^{6}Li,^{6}He)$ REACTIONS AND THE GAMOW-TELLER STRENGTH
W. R. Wharton and P. T. Debevec
Bull. Am. Phys. Soc. 19, 989 (October 1974)

59. MODIFICATION OF THE ARGONNE FN TANDEM
J. L. Yntema
Bull. Am. Phys. Soc. 19, 1026 (October 1974)

60. MASS, ENERGY AND ANGULAR DISTRIBUTIONS FROM HEAVY ION INTERACTIONS WITH Ca ISOTOPES
B. Zeidman
Bull. Am. Phys. Soc. 19, 1005 (October 1974)

---

*Ohio University, Athens, Ohio.

American Physical Society, Division of Electron and Atomic Physics, Chicago, 2-4 December 1974

61. DETERMINATION OF THE ELECTRON AFFINITY OF ATOMIC OXYGEN FROM ION-PAIR FORMATION IN O_2
P. M. Dehmer and W. A. Chupka
Bull. Am. Phys. Soc. 19, 1195 (1974)

62. NONSTATISTICAL EMISSION FROM METASTABLE AUTO-IONIZING STATES OF OI
P. M. Dehmer and W. A. Chupka
Bull. Am. Phys. Soc. 19, 1203 (1974)

1974 Nuclear Science Symposium and 14th Scintillation and Semiconductor Counter Symposium, Washington, D.C., 11-13 December 1974

63. BASIC LIMITATION OF SCINTILLATION COUNTERS IN TIME MEASUREMENTS
F. J. Lynch
IEEE Trans. Nucl. Sci. NS-22, 58 (February 1975)

American Physical Society, Anaheim, 29 January-1 February 1975

64. ^{180}Hf ENERGY LEVELS DEDUCED FROM THERMAL AND AVERAGE RESONANCE NEUTRON-CAPTURE γ-RAY SPECTRA
D. L. Bushnell, D. J. Buss, and R. K. Smither
Bull. Am. Phys. Soc. 20, 96 (1975)

65. ENERGY LEVEL STRUCTURE OF ^{245}Pu AS OBSERVED BY (d,p) REACTIONS
D. S. Gale, J. R. Erskine, and A. M. Friedman*
Bull. Am. Phys. Soc. 20, 97 (1975)

66. DELBRÜCK AND NUCLEAR RAMAN SCATTERING OF 9—12 MeV PHOTONS
H. E. Jackson
Bull. Am. Phys. Soc. 20, 81 (1975)

67. SURFACE RADIATION EFFECTS IN CONTROLLED FUSION
M. Kaminsky
Bull. Am. Phys. Soc. 20, 36 (1975)

68. ENERGY LEVELS OF $^{89}_{41}Nb_{48}$
F. J. D. Serduke and W. Henning
Bull. Am. Phys. Soc. 20, 73 (1975)

---

*Chemistry Division, ANL.

APS, Anaheim (Contd.)

69. HELIUM BLISTERING OF NICKEL MONOCRYSTALS
M. K. Sinha, S. K. Das, and M. Kaminsky
Bull. Am. Phys. Soc. 20, 45 (1975)

70. ENERGY LEVELS AND GAMMA RAY BRANCHING RATIOS IN ^{152}Sm
Robert K. Smither
Bull. Am. Phys. Soc. 20, 96 (1975)

1975 Neutron Sputtering Workshop, Battelle Memorial Institute, Richland, Washington, 18-19 February 1975

71. NEUTRON SPUTTERING EXPERIMENTS AT THE ARGONNE PHYSICS DIVISION
M. S. Kaminsky
Proceedings of the Workshop, prepared by O. K. Harling, M. T. Thomas, and D. L. Styris (1975)

American Physical Society, Denver, Colorado, 31 March-3 April 1975

72. DETERMINATION OF EQUILIBRIUM SITES OF Au ATOMS IN Sn SINGLE CRYSTALS, BY A CHANNELING TECHNIQUE
J. W. Miller,* D. S. Gemmell, R. E. Holland, J. C. Poizat, J. N. Worthington, and R. E. Loess*
Bull. Am. Phys. Soc. 20, 352 (1975)

D. TOPICAL REPORTS

1. GSPEAK: A DATA MANAGEMENT FACILITY FOR SPEAKEASY
S. Cohen and D. H. Gloeckner
Argonne National Laboratory Topical Report ANL-8097 (May 1974)

2. THE KAPPA LEVEL OF SPEAKEASY
Stanley Cohen, Steven C. Pieper, and Michael Stob
Argonne National Laboratory Topical Report ANL-8137 (November 1974)

---

*Materials Science Division, ANL.

3. THE ARGONNE NUCLEAR SHELL-MODEL SYSTEM
David H. Gloeckner
Argonne National Laboratory Topical Report ANL-8113 (September 1974)

4. MEASUREMENT OF THE TOTAL CROSS SECTIONS FOR THE $^{7}Li(d,p)^{8}Li$, $^{6}Li(^{3}He,n)^{8}B$, $^{6}Li(d,\alpha)^{4}He$, $^{6}Li(d,p)^{7}Li$, AND $^{6}Li(d,n)^{7}Be$ REACTIONS
Charles R. McClenahan
Argonne National Laboratory Topical Report ANL-8088 (March 1974)
Ph. D. Thesis, Northwestern University (June 1974)

5. AN ENGINEERING DESIGN STUDY OF A REFERENCE THETA-PINCH REACTOR (RTPR), edited by R. A. Krakowski,* F. L. Ribe,* T. A. Coultas,† and A. J. Hatch, Argonne National Laboratory Topical Report ANL-8019 and Los Alamos Scientific Laboratory Report LA-5336 (March 1974)

INTRODUCTION
R. A. Krakowski,* F. L. Ribe,* T. A. Coultas,† and A. J. Hatch
pp. 1-4

SUMMARY PLANT DESCRIPTION
T. A. Coultas,† P. Dauzvardis,† and A. J. Hatch
pp. 17-26

FUEL SUPPLY AND REMOVAL SYSTEM
D. C. Hess
pp. 78-82

APPENDIX B: COMPUTER OUTPUT SUMMARY OF RTPR PARAMETER DESIGN VALUES
C. B. Dennis† and A. J. Hatch
pp. 114-127

---

*Los Alamos Scientific Laboratory, Los Alamos, New Mexico.

†Engineering Division, ANL.

E. PATENT

1. METHOD AND MEANS OF EFFECTING CHARGE EXCHANGE IN PARTICLE BEAMS
   Jan L. Yntema
   U.S. Patent No. 3,806,749 (23 April 1974)

X. STAFF MEMBERS OF THE PHYSICS DIVISION

The Physics Division staff for the year ending 31 March 1975 is listed below. Although the members are classified by programs, it must be understood that many of them work in two or more of the areas. In such cases, the classification indicates only the current primary interest.

In the period from 1 April 1974 through 31 March 1975, there were 37 temporary staff members and visitors (including 12 postdoctoral fellows), 14 graduate students, and 22 undergraduates. In these lists, the Temporary Scientific Staff are those with appointments for ≥9 months, while Visitors are on shorter appointments. Research Participants come to Argonne part-time for research while continuing their work at their own institutions.

EXPERIMENTAL NUCLEAR PHYSICS

Permanent Scientific Staff

[†] Lowell M. Bollinger, Ph. D., Cornell University, 1951

[‡] Thomas H. Braid, Ph. D., Edinburgh University, 1950

S. Bradley Burson, Ph. D., University of Illinois, 1946

Cary N. Davids, Ph. D., California Institute of Technology, 1967

Alexander J. Elwyn, Ph. D., Washington University, 1956

John R. Erskine, Ph. D., University of Notre Dame, 1960

[§] Donald S. Gemmell, Ph. D., Australian National University, 1960

[†] Director of the Physics Division; on leave from that office to manage the Superconducting Linac Project June 1972—September 1974.

[‡] Joint appointment as Associate Editor of the Applied Physics Letters; Acting Editor October 1974—June 1975.

[§] Acting Associate Director of the Physics Division until August 1974. Temporarily at University of Munich (September 1974—September 1975).

Robert E. Holland, Ph. D., University of Iowa, 1950

Roy J. Holt, Ph. D., Yale University, 1972

†Harold E. Jackson, Jr., Ph. D., Cornell University, 1959

Dennis G. Kovar, Ph. D., Yale University, 1970

Alexander Langsdorf, Jr., Ph. D., Massachusetts Institute of Technology, 1937

‡John J. Livingood, Ph. D., Princeton University, 1929

Frank J. Lynch, B.S., University of Chicago, 1944

Luise Meyer-Schützmeister, Ph. D., Technical University of Berlin, 1943

§F. P. Mooring, Ph. D., University of Wisconsin, 1951

‖John P. Schiffer, Ph. D., Yale University, 1954

¶Ralph E. Segel, Ph. D., Johns Hopkins University, 1955

Robert K. Smither, Ph. D., Yale University, 1956

††Thomas P. Wangler, Ph. D., University of Wisconsin, 1964

‡‡J. L. Yntema, Ph. D., Free University of Amsterdam, 1952

Benjamin Zeidman, Ph. D., Washington University, 1957

Temporary Scientific Staff

*Paul T. Debevec, Ph. D., Princeton University, 1972

Yossi Eisen, Ph. D., Weizmann Institute of Science, 1974

*H. Terry Fortune, Ph. D., Florida State University, 1967 (From University of Pennsylvania)

---

*No longer at Argonne as of 31 March 1975.

†Acting Associate Director of the Physics Division until September 1974.

‡Emeritus.

§In charge of Dynamitron accelerator operations.

‖Associate Director of the Physics Division. Joint appointment with the University of Chicago. Temporarily at Technical University, Munich (July 1973—July 1974).

¶Joint appointment with Northwestern University.

††Assigned to work at the Los Alamos Meson Physics Facility as part of the Medium Energy activity.

‡‡In charge of Tandem accelerator operations.

Walter Henning, Ph. D., Technische Hochschule München, 1968
(From Technische Universität München, Germany)

Trevor R. Ophel, Ph. D., Australian National University, 1959
(From Australian National University)

*Joseph M. Remillieux, Ph. D., University of Lyon, 1972
(From Institut de Physique Nucleaire, Lyon, France)

Peter Sperr, Dr. rer. nat., Technical University, Munich, 1973
(From Technical University, Munich)

Steven E. Vigdor, Ph. D., University of Wisconsin, 1973

*William R. Wharton, Ph. D., University of Washington, 1972

William M. Wilson, Ph. D., Duke University, 1973

Visitors

*David L. Bushnell, Ph. D., Virginia Polytechnic Institute, 1961
(From Northern Illinois University)

Duane J. Buss, Ph. D., University of Notre Dame, 1966
(Research participant from Illinois Benedictine College)

*Douglas S. Gale, Ph. D., Kansas State University, 1972
(Research participant from East Texas State University)

*Margaret Stautberg Greenwood, Ph. D., University of Colorado, 1966
(Research participant from DePaul University)

*Gerald Hardie, Ph. D., University of Wisconsin, 1962
(Research participant from Western Michigan University)

*Hans-Joachim Körner, Ph. D., University of Hamburg, 1963
(From Technische Universität München, Germany)

Esther L. Segel, Ph. D., University of Rochester, 1960
(Research participant from Illinois Institute of Technology)

Supporting Staff

Charles H. Batson

John J. Bicek

William F. Evans

Linda R. Gritter

Joseph E. Kulaga

James R. Specht

---

*No longer at Argonne as of 31 March 1975.

*Elizabeth A. Sutter

George E. Thomas, Jr.

James N. Worthington

Graduate Students

Richard L. Boudrie (University of Kansas)

William C. Corwin (Illinois Institute of Technology)

*Jonnie K. Hawkins (Northern Illinois University)

Michael A. Lee (Northwestern University)

Richard C. Pardo (University of Texas)

Lewis A. Parks (University of Texas)

Krishnaswamy Raghunathan (Northwestern University)

Timothy R. Renner (University of Chicago)

*Gianni R. Tassotto (Northern Illinois University)

Jeffrey F. Tonn (Northwestern University)

THEORETICAL PHYSICS

Permanent Scientific Staff

†Arnold R. Bodmer, Ph. D., Manchester University, 1953

‡Fritz Coester, Ph. D., University of Zurich, 1944

Stanley Cohen, Ph. D., Cornell University, 1955

Benjamin Day, Ph. D., Cornell University, 1963

§Dieter Kurath, Ph. D., University of Chicago, 1951

Robert D. Lawson, Ph. D., Stanford University, 1953

---

*No longer at Argonne as of 31 March 1975.

†Joint appointment with the University of Illinois, Chicago Circle Campus.

‡Temporary joint appointment with the University of Iowa, Iowa City, Iowa until May 1974.

§Temporarily at Oxford University (August 1973—August 1974).

†Malcolm H. Macfarlane, Ph. D., University of Rochester, 1959

James E. Monahan, Ph. D., St. Louis University, 1953

‡Murray Peshkin, Ph. D., Cornell University, 1951

Steven C. Pieper, Ph. D., University of Illinois, 1970

Franklin J. D. Serduke, Ph. D., University of California, Davis, 1970

Temporary Scientific Staff

Bei-dwo Chang, Ph. D., University of Chicago, 1975

*David H. Gloeckner, Ph. D., University of Chicago, 1972

Johann Rafelski, Ph. D., Johann Wolfgang Goethe University, 1973

Visitors

Francesco Iachello, Ph. D., Massachusetts Institute of Technology, 1969
(From Kernfysisch Versneller Instituut, Groningen, Netherlands)

*§Harry J. Lipkin, Ph. D., Princeton University, 1950
(From Weizmann Institute of Science, Rehovot, Israel)

*Ulrich B. Mosel, Dr. Phil. Nat., University of Frankfurt, 1968
(From University of Giessen, Germany)

*Norbert Rosenzweig, Ph. D., Cornell University, 1951
(From State University of New York, Albany)

Graduate Student

*Karl-Heinz Passler (Justus Liebig-Universität, Giessen, Germany)

EXPERIMENTAL ATOMIC AND MOLECULAR PHYSICS

Permanent Scientific Staff

Joseph Berkowitz, Ph. D., Harvard University, 1955

†H. Gordon Berry, Ph. D., University of Wisconsin, 1967

Stephen B. Brumbach, Ph. D., Pennsylvania State University, 1971

*No longer at Argonne as of 31 March 1975.

†Joint appointment with the University of Chicago.

‡Associate Director of the Physics Division; Acting Director June 1972—September 1974.

§Joint appointment with the Fermi National Accelerator Laboratory.

William J. Childs, Ph. D., University of Michigan, 1956

William A. Chupka, Ph. D., University of Chicago, 1951

Santosh K. Das, Ph. D., University of California, Berkeley, 1971

†Leonard S. Goodman, Ph. D., University of Chicago, 1952

‡David C. Hess, Ph. D., University of Chicago, 1949

Manfred S. Kaminsky, Ph. D., University of Marburg, Germany, 1957

Victor E. Krohn, Ph. D., Case Western Reserve University, 1952

§Gilbert J. Perlow, Ph. D., University of Chicago, 1940

G. R. Ringo, Ph. D., University of Chicago, 1940

Stanley L. Ruby, B. A., Columbia University, 1947

Henry E. Stanton, Ph. D., University of Chicago, 1944

Temporary Scientific Staff

Patricia M. Dehmer, Ph. D., University of Chicago, 1972

Ronald J. Ekern, Ph. D., Clarkson College of Technology, 1975

*Jer-shen Maa, Ph. D., University of Minnesota, 1974

Karl Radler, Ph. D., University of Hamburg, 1974

Thomas D. Rossing, Ph. D., Iowa State University, 1954
(From Northern Illinois University)

David G. Streets, Ph. D., University of London, 1971

Visitors

Ben Greenebaum, Ph. D., Harvard University, 1965
(Research participant from University of Wisconsin—Parkside)

*Arnold V. Lesikar, Ph. D., California Institute of Technology, 1965
(Research participant from St. Cloud State College)

---

*No longer at Argonne as of 31 March 1975.

†Assistant Director of the Physics Division.

‡Joint appointment as Associate Editor of the Journal of Applied Physics and Applied Physics Letters.

§Joint appointment as Editor of the Applied Physics Letters. Temporarily at Technical University of Munich, Germany (October 1974—June 1975).

*John C. Love, Ph. D., Ohio State University, 1969
(Research participant from Florida Institute of Technology)

*Adam B. Ritchie, Ph. D., University of Virginia, 1968
(Research participant from University of Alabama)

*Mahendra K. Sinha, Ph. D., Pennsylvania State University, 1961
(Research participant from North Dakota State University)

*Theodore G. Waech, Ph. D., University of Wisconsin, 1968
(Research participant from Condordia College)

Supporting Staff

John A. Dalman

Peter J. Dusza

Warren T. Jivery

Marvin J. Kral

Peter D. Schnur

Bruce J. Zabransky

Graduate Students

*George R. Fenske (University of Illinois)

*Kenneth V. Smith (University of Cincinnati)

ADMINISTRATIVE STAFF

*†Charles Eggler, B.S., Virginia Polytechnic Institute, 1944

‡Albert J. Hatch, M.S., University of Illinois, 1947

---

*No longer at Argonne as of 31 March 1975.

†Special Assistant to the Director of the Physics Division.

‡Assistant Director of the Physics Division.

ARGONNE NATIONAL LAB WEST
3 4444 00007227 2